

Abstract

KULKARNI, MORESHWAR BALAKRISHNA. Effect of Tack and Prime Coats, and Baghouse Fines on Composite Asphalt Pavements. (Under the direction of Dr. Akhtarhusein A. Tayebali.)

This investigation was undertaken to develop a mechanistic design procedure to minimize the interfacial delamination distress, and to evaluate the contribution of baghouse fines to delamination in composite pavements. The need for this research was based on extensive occurrence of delamination problems in Division 13 of NCDOT. Pavements in Buncombe County, where emulsions were used as tack coat, had higher occurrence of such distresses compared to Rutherford County where PG64-22 binder was used as tack coat. In addition to use of tack coats, the asphalt mixes in these counties were prepared by an intermittent purging of baghouse fines.

Results from particle analyzer indicated similar gradations for baghouse fines and regular mineral fillers. DSR testing of mastics indicated a similar performance of mastics prepared with regular fillers and baghouses. SST (FSCH and RSCH) and APA tests results on the mixtures with and without baghouse fines did not indicate a significant difference between the two mixes. However, AASHTO T283 test indicated that mixes with baghouse fines were moisture sensitive than mixes without baghouse fines. It could be possible that dosage of anti-strip additive might not have been adequate to counteract moisture damage.

Composite AC-AC, AC-PCC and AC-CTB samples were fabricated in the laboratory and the interfacial bond strength was measured using the SST. For tack coats, it was observed that PG64-22 performed better on AC-AC interfaces, whereas CMS-2 performed

better on AC-PCC interface. CSS-1h performed better than EA-P and EPR-1 as a prime coat. Non-bonded surfaces could not resist any interfacial shear.

Using a 3-D computer program, the interfacial shear stresses were computed at various thickness, loading and temperature conditions. The results indicated that delamination will not be a problem at lower temperature (20 °C), but at elevated temperatures a minimum AC layer thickness is necessary to reduce the interfacial shear stress to laboratory measured values. For thin pavement sections, the use of prime coat was recommended to increase the bond between the AC and underlying layers.

**EFFECT OF TACK AND PRIME COATS, AND BAGHOUSE
FINES ON COMPOSITE ASPHALT PAVEMENTS**

by

MORESHWAR BALAKRISHNA KULKARNI

A dissertation submitted to the Graduate Faculty of
North Carolina State University
in partial fulfillment of the requirements for the Degree of
Doctor of Philosophy

CIVIL ENGINEERING

Raleigh, North Carolina

April, 2004

Approved by:

Dr. Y. Richard Kim

Dr. Tasnim Hassan

Dr. John W. Baugh, Jr.

Dr. Akhtarhusein A. Tayebali
(Chair of Advisory Committee)

Dedicated to my parents,

Mr. Balakrishna A. Kulkarni

And

Mrs. Swati B. Kulkarni,

And my sister,

Ms. Ratnamala B. Kulkarni

Biography

Moreshwar Kulkarni, son of Mr. Balakrishna Kulkarni and Ms. Swati Kulkarni, was born on July 2, 1976, in Bombay, India. After finishing his high school education in 1993, he joined the Indian Institute of Technology, Bombay (IIT Bombay) for Bachelors in Civil Engineering. In fall 1997, after graduating from IIT Bombay, he joined the Master's program in Transportation Materials at North Carolina State University. During his MS at NC State, he worked on pavement analysis, asphalt mix design, and performance evaluation of binders and mixes. He graduated with a MS degree in summer 1999 and enrolled in the PhD program in fall 1999. He served as a Departmental Ambassador for international students for academic years from 2000-03. After graduation from NC State, he intends to pursue a career in field of transportation engineering.

Acknowledgments

The author expresses his thanks to everyone that has been of assistance in the experimental work and writing of this dissertation. Special thanks are due to Dr A. A. Tayebali, graduate advisor, and Chairman of the advisory committee, for his guidance, patience, help, and relentless support during my pursuit of doctoral degree. He has been a mentor, an excellent teacher, and constant source of encouragement always eager to help. He has been a great advisor, and his patience in going through versions of this dissertation, various research reports, and several quarterly progress reports, is appreciated.

I am thankful to my committee members, Dr. Tasnim Hassan, Dr. Y. Richard Kim, Dr. John W. Baugh, and Dr. R. Michael Young for their time, and evaluation of my work. Thanks are also due to Dr. David W. Johnston, Director of Graduate Programs, for his help and consideration. Dr. Michael Leming's help in regard to design of PCC mixes and CTB bases is appreciated. Dr. M. S. Rahman and Ms. Qingxia Xu's assistance in the research work related to this thesis is acknowledged.

Thanks are due to North Carolina Department of Transportation for their sponsorship of this project. Mr. Christopher Bacchi, M&T unit NCDOT, has been of immense help answering our queries and helping us with material procurement.

It was fun rolling and coring slabs with Kevin Fischer, my fellow graduate student. I truly enjoyed your company while working and appreciate your help. Thanks are due to Yuanxiong Huang and Prasad Kollipara for their assistance in fabricating samples. Steven Wade, departmental mechanic, has been helpful in fabrication of molds for slab construction, and repairing of the rolling wheel compactor.

During my assignment to the Graduate Programs office, interaction with Renee Howard and Edna White was enjoyable. I relished working on those 'orange folders' very much. I wish to mention Ms. Barbara Nicholson from Civil Engineering main office for her help in administrative matters. I would take this opportunity to say hello to my current and former colleagues from room 401 and asphalt lab: Priya Nimbole, Suriyan Sadasivam, Dr. Glen Malpass, Hazim Dwairi, Dr. Bing Xu, Dr. Jo Daniel, Dr. Yanqing Zhao, Dr. Haifang

Wen, Dr. Sungho Mun, Mark King, Shane Underwood, Mostafa Momen, and Dr. Ghassan Chehab. Thanks are due to Balaji Iyengar for his help in troubleshooting computers and printers, as well as keeping the systems up to date.

It was an excellent six and half year sojourn in the US. I truly enjoyed the time spent on and off campus. Dr. Gajanan Natu and his wife, Vijaya, have been supportive and helpful during some of my most trying times. I am grateful to them for their support. These acknowledgements would not be complete without a mention of my friends from my alma mater, IIT Bombay, responsible for maxing out my cellular night and weekend minutes. I enjoyed having conversations with you all – Dr. Atul Karve, Amitkumar Rao, Anupkumar Rao, Babu Mamidipally, Nagendra Jain, Manish Goyal, Anurag Pareek, and Dr. Durgaprasad Shamain – and thanks for your support. I would like to mention Anuja Shukla for her encouragement, advice and interesting conversations.

Thank you to Amit Kulkarni, Ajit Moghe, Chirag Modi, Sirish Somanchi, Devarajan Balaraman, Kesava Narasimhan, Rahul Vallabh, and Pankaj Agrawal for putting up with me as a roommate. Thanks are due to Dibyendu Sengupta for his continuous insight and encouragement in my ongoing job search. I would like to take this opportunity to thank my physicians Drs. Michael Dewitt, Laura Pratt, and Shawn Phelan.

Last but not the least, I would like to express my indebtedness to my parents and my sister for pushing me to undertake and complete this mission; without your unwavering support this would not have been possible. It has been a dream comes true for all of us.

Table of Contents

LIST OF TABLES.....	ix
LIST OF FIGURES.....	xi
LIST OF ABBREVIATIONS AND SYMBOLS.....	xv
1 INTRODUCTION AND LITERATURE SURVEY	1
1.1 INTRODUCTION.....	1
1.2 LITERATURE SURVEY	3
1.2.1 Study by Mohammad et al [18]	3
1.2.2 Study by Shahin et al [21]	4
1.2.3 Study by Uzan et al [30, 31]	5
1.2.4 Study by Tschegg et al [29]	7
1.2.5 Study by Ameri-Gaznon et al [6]	8
1.2.6 Study by Ishai et al [15].....	10
1.2.7 Study by Hachiya et al [12].....	11
1.2.8 Study by Mukhtar et al [19].....	13
1.2.9 Study by Sholar et al [24]	13
1.2.10 Prime Coats	14
1.2.11 Tack Coats	15
1.3 RESEARCH NEED	16
1.3.1 Prior Work.....	16
2 RESEARCH APPROACH AND METHODOLOGY	19
2.1 OBJECTIVE	19
2.2 RESEARCH METHODOLOGY	19
2.2.1 Literature Review and Survey.....	19
2.2.2 Asphalt and Mastics Testing.....	20
2.2.3 SST Testing of SGC Specimens, TSR and APA Tests.....	20
2.2.4 Material Characterization	21
2.2.5 Fabrication of Slabs and Test Specimens	21
2.2.6 Bond Strength Determination using Shear Testing.....	21
2.2.7 Mechanistic Analysis	22
3 SURVEY RESULTS.....	24
3.1 DEVELOPMENT OF QUESTIONNAIRE	24
3.2 SURVEY RESPONSES.....	24
4 RHEOLOGICAL EVALUATION.....	28
4.1 INTRODUCTION.....	28
4.2 SELECTION OF FINES	28
4.3 GRADATION ANALYSIS OF FINES USING FHWA PARTICLE ANALYZER.....	29
4.3.1 Method Description	29
4.3.2 Results and Discussion	29
4.4 ANALYSIS OF ASPHALT-FINES MASTICS USING DSR	30
4.4.1 Specimen Preparation	31
4.4.2 Test Parameters.....	31
4.4.3 Test Results and Discussion.....	32
4.5 DSR TESTING OF EMULSIONS	33

4.5.1	<i>Test Results and Discussion</i>	34
4.6	BROOKFIELD VISCOSITY	35
4.7	CONCLUSIONS	35
5	PERFORMANCE TESTING OF SGC SPECIMENS.....	45
5.1	INTRODUCTION.....	45
5.2	TEST PARAMETERS	45
5.3	TEST TEMPERATURE	46
5.3.1	<i>Selection of Testing Temperature</i>	46
5.3.2	<i>Temperature Zones</i>	46
5.3.3	<i>Selection of Depth for Computation of Testing Temperature</i>	47
5.3.4	<i>Reliability Factors</i>	47
5.3.5	<i>Temperature Selection Method</i>	47
5.4	PERFORMANCE TEST RESULTS OF LAB MIXES WITH BAGHOUSE FINES	48
5.4.1	<i>Specimen Fabrication</i>	48
5.4.2	<i>FSCH Test</i>	49
5.4.3	<i>RSCH Test</i>	50
5.5	ASPHALT PAVEMENT ANALYZER TESTS	51
5.5.1	<i>APA Test Results</i>	52
5.6	EFFECT OF BAGHOUSE FINES ON MOISTURE SENSITIVITY.....	53
5.7	SUMMARY AND CONCLUSION	53
6	SPECIMEN FABRICATION USING ROLLING WHEEL COMPACTOR	64
6.1	INTRODUCTION.....	64
6.2	FABRICATION OF STEEL MOLDS.....	64
6.3	SPECIMEN FABRICATION	65
6.3.1	<i>Asphalt Concrete Slabs</i>	65
6.3.2	<i>Portland Cement Concrete Slabs</i>	66
6.3.3	<i>Cement Treated Base Slab</i>	66
6.4	TACK / PRIME COAT APPLICATION.....	67
6.5	CORING AND CUTTING SAMPLES.....	68
7	MATERIAL CHARACTERIZATION.....	76
7.1	INTRODUCTION.....	76
7.2	ASPHALT MIX CHARACTERIZATION.....	76
7.2.1	<i>Frequency Sweep Test at Constant Height (FSCH)</i>	77
7.2.2	<i>Repeated Shear Test at Constant Height (RSCH)</i>	78
7.2.3	<i>Axial Frequency Sweep Test (AFST)</i>	78
7.2.4	<i>Repeated Axial Test</i>	79
7.3	PORTLAND CEMENT CONCRETE (PCC) CHARACTERIZATION.....	80
7.3.1	<i>Mixing, Casting and Curing of Specimens</i>	80
7.3.2	<i>Compressive Strength of Cylindrical Concrete Specimens</i>	82
7.3.3	<i>Modulus of Rupture for Concrete Specimens</i>	83
7.3.4	<i>Splitting Tension Test for Concrete Specimens</i>	83
7.3.5	<i>Elastic Modulus Test for Concrete Specimens</i>	83
7.4	CEMENT TREATED BASE (CTB) CHARACTERIZATION	84
7.4.1	<i>CTB Composition</i>	84
7.4.2	<i>Atterberg Limits for CTB Aggregates</i>	85
7.4.3	<i>Modified Proctor Density Test</i>	85
8	BOND STRENGTH DETERMINATION.....	107
8.1	INTRODUCTION.....	107
8.1.1	<i>Shear Test Description</i>	107
8.2	BOND STRENGTH USING METAL PLATENS	108
8.3	BOND STRENGTH OF AC-AC SPECIMENS	109
8.3.1	<i>Axial and Shear Ramp Test</i>	109

8.3.2	<i>Axial Test Results</i>	110
8.3.3	<i>Shear Test Results</i>	110
8.4	BOND STRENGTH OF PCC-AC SPECIMENS	112
8.5	BOND STRENGTH OF CTB-AC SPECIMENS	114
8.6	SUMMARY AND CONCLUSIONS.....	116
9	DEVELOPMENT OF DESIGN GUIDELINES FOR USE OF TACK AND PRIME COATS	136
9.1	3-D LAYERED ELASTIC PROGRAM DESCRIPTION	136
9.2	LOAD CONDITIONS.....	137
9.3	TEMPERATURE EFFECTS.....	138
9.4	ANALYSIS OF AC-AC BONDING.....	139
9.5	ANALYSIS OF PCC-AC BONDING.....	140
9.6	ANALYSIS OF CTB-AC BONDING	141
9.7	OUTLINE OF GUIDELINE DEVELOPMENT FOR USE OF TACK OR PRIME COAT	142
9.8	SUMMARY AND CONCLUSIONS.....	143
10	SUMMARY, CONCLUSIONS AND RECOMMENDATIONS	151
10.1	SUMMARY AND CONCLUSIONS.....	151
10.2	FUTURE SCOPE.....	156
11	REFERENCES.....	158
	APPENDIX A.....	162
	APPENDIX B.....	164
	APPENDIX C.....	170
	APPENDIX D.....	174
	APPENDIX E.....	179
	APPENDIX F.....	189

List of Tables

TABLE 4-1 PROPERTIES OF FINES FROM PARTICLE SIZE ANALYSIS (SET 2) [13].....	36
TABLE 4-2 TEMPERATURES FOR RESIDUAL BINDERS WHEN $ G^* /\sin\delta \geq 1.0$ kPA	36
TABLE 5-1 AIR VOIDS AND G_{MM} OF 150-MM DIAMETER LABORATORY MIX SPECIMENS	54
TABLE 5-2 NATIONWIDE PAVEMENT TEMPERATURES, [23]	54
TABLE 5-3 AVERAGE DEPTHS AND TEST TEMPERATURES	55
TABLE 5-4 $ G^* $ (PA) VERSUS FREQUENCY (HZ) FOR LAB MIXES, 50.2 °C, BUNCOMBE COUNTY	55
TABLE 5-5 δ (DEGREES) VERSUS FREQUENCY (HZ) FOR LAB MIXES, 50.2 °C, BUNCOMBE COUNTY	55
TABLE 5-6 AVERAGE $ G^* $, δ , AND $ G^* /\sin \delta$ VALUES, 50.2 °C, LAB MIXES BUNCOMBE COUNTY	56
TABLE 5-7 $ G^* $ (PA) VERSUS FREQUENCY (HZ) FOR LAB MIXES, 50.2 °C, RUTHERFORD COUNTY	56
TABLE 5-8 δ (DEGREES) VERSUS FREQUENCY (HZ) FOR LAB MIXES, 50.2 °C, RUTHERFORD COUNTY	56
TABLE 5-9 AVERAGE $ G^* $, δ , AND $ G^* /\sin \delta$ VALUES, 50.2 °C, LAB MIXES RUTHERFORD COUNTY	57
TABLE 5-10 STRAIN AT THE END OF RSCH TEST, 50.2 °C, LAB MIXES	57
TABLE 5-11 AIR VOIDS AND HEIGHTS OF 6-INCH DIAMETER LABORATORY SPECIMENS FOR APA TEST	57
TABLE 5-12 BUNCOMBE COUNTY (WITH BAGHOUSE FINES) TSR RESULTS (4-INCH SPECIMENS).....	57
TABLE 5-13 BUNCOMBE COUNTY (W/OUT BAGHOUSE FINES) TSR RESULTS (4-INCH SPECIMENS)	58
TABLE 5-14 RUTHERFORD COUNTY (WITH BAGHOUSE FINES) TSR RESULTS (4-INCH SPECIMENS)	58
TABLE 5-15 RUTHERFORD COUNTY (W/OUT BAGHOUSE FINES) TSR RESULTS (4-INCH SPECIMENS)	58
TABLE 5-16 SUMMARY OF TSR RESULTS	58
TABLE 7-1 AIR VOIDS OF AC MIX SAMPLES	86
TABLE 7-2 $ G^* $ VS. FREQUENCY FOR AC MIX, 20 °C, IN PA.....	86
TABLE 7-3 SHEAR PHASE ANGLE (DEGREES) VS. FREQUENCY FOR AC MIX, 20 °C.....	87
TABLE 7-4 $ G^* $ VS. FREQUENCY FOR AC MIX, 30 °C, IN PA.....	87
TABLE 7-5 SHEAR PHASE ANGLE (DEGREES) VS. FREQUENCY FOR AC MIX, 30 °C.....	87
TABLE 7-6 $ G^* $ VS. FREQUENCY FOR AC MIX, 40 °C, IN PA.....	88
TABLE 7-7 SHEAR PHASE ANGLE (DEGREES) VS. FREQUENCY FOR AC MIX, 40 °C.....	88
TABLE 7-8 $ G^* $ VS. FREQUENCY FOR AC MIX, 60 °C, IN PA.....	88
TABLE 7-9 SHEAR PHASE ANGLE (DEGREES) VS. FREQUENCY FOR AC MIX, 60 °C.....	89
TABLE 7-10 RSCH CYCLES, AT 40 AND 60 °C.....	89
TABLE 7-11 AIR VOIDS OF AXIAL TEST SAMPLES.....	89
TABLE 7-12 $ E^* $ VS. FREQUENCY FOR AC MIX, 20 AND 30 °C, IN PA.....	89
TABLE 7-13 AXIAL PHASE ANGLE (DEGREES) VS. FREQUENCY FOR AC MIX, 20 AND 30 °C.....	90
TABLE 7-14 $ E^* $ VS. FREQUENCY FOR AC MIX, 40 AND 60 °C, IN PA.....	90

TABLE 7-15 AXIAL PHASE ANGLE (DEGREES) VS. FREQUENCY FOR AC MIX, 40 AND 60 °C.....	90
TABLE 7-16 REPEATED AXIAL TEST CYCLES, AT 40 AND 60 °C	90
TABLE 7-17 AGGREGATE MOISTURE CONTENTS AND SPECIFIC GRAVITIES	91
TABLE 7-18 BATCH WEIGHTS FOR PCC.....	91
TABLE 7-19 PROPERTIES OF CONCRETE.....	91
TABLE 7-20 ELASTIC MODULUS FOR PCC	91
TABLE 7-21 GRADATION (% PASSING) FOR AGGREGATE PILES USED FOR CTB	92
TABLE 7-22 GRADATION CRITERIA FOR MATERIAL PASSING #10 SIEVE (SOIL MORTAR).....	92
TABLE 7-23 MOISTURE DENSITY DETERMINATION FOR CTB	92
TABLE 7-24 LIQUID LIMIT PROPERTY FOR CTB USING DOT MODIFIED METHOD.....	92
TABLE 8-1 RESULTS FOR AC-AC AXIAL RAMP TESTS (TENSILE), 40 °C	117
TABLE 8-2 RESULTS FOR AC-AC AXIAL RAMP TESTS (TENSILE), 60 °C	117
TABLE 8-3 RESULTS FOR AC-AC SHEAR RAMP TESTS, 20 °C	117
TABLE 8-4 RESULTS FOR AC-AC SHEAR RAMP TESTS, 40 °C	118
TABLE 8-5 RESULTS FOR AC-AC SHEAR RAMP TESTS, 60 °C	118
TABLE 8-6 SUMMARY OF SHEAR STRENGTHS FROM SHOLAR ET AL, [24]	118
TABLE 8-7 RESULTS FOR PCC-AC SHEAR RAMP TESTS, 20 °C	119
TABLE 8-8 RESULTS FOR PCC-AC SHEAR RAMP TESTS, 40 °C	119
TABLE 8-9 RESULTS FOR PCC-AC SHEAR RAMP TESTS, 60 °C	119
TABLE 8-10 SUMMARY OF PCC-AC BOND STRENGTHS, [19]	120
TABLE 8-11 RESULTS FOR CTB-AC SHEAR RAMP TESTS, 40 °C.....	120
TABLE 8-12 RESULTS FOR CTB-AC SHEAR RAMP TESTS, 60 °C.....	120
TABLE 9-1 RECOMMENDED MINIMUM SKID NUMBERS FOR RURAL HIGHWAYS [16].....	144
TABLE 9-2 INTERFACIAL SHEAR BOND STRENGTH SUMMARY FOR PG64-22 AND CMS-2	144
TABLE 9-3 AC-CTB SHEAR BOND STRENGTH SUMMARY FOR CSS-1H, EA-P, AND EPR-1	144

List of Figures

FIGURE 1-1 DELAMINATION OF SURFACE COURSE (SOURCE: HTTP://WWW.KOCHPAVEMENTSOLUTIONS.COM/DISTRESSES/PUSHING.HTM).....	2
FIGURE 1-2 DELAMINATION, EXPOSURE OF UNDERLYING LAYER (SRC: HTTP://WWW.DEFENCE.GOV.AU/DEMG/7TECHNICAL_GUIDANCE/AIRCRAFT_PAVEMENT_MANUAL/PART_A/A 4.HTM).....	2
FIGURE 1-3 DISTORTION AND SHOVING, DEFORMATION OF SURFACE LAYER UNDER LOAD (SRC: HTTP://WWW.DEFENCE.GOV.AU/DEMG/7TECHNICAL_GUIDANCE/AIRCRAFT_PAVEMENT_MANUAL/PART_A/A 4.HTM).....	2
FIGURE 1-4 TYPICAL SLIPPAGE FAILURE [11, 19].....	3
FIGURE 1-5 COLLARS DESIGNED FOR TESTING SAMPLES IN SHEAR, [18].....	4
FIGURE 1-6 SCHEMATIC OF SPECIMEN DEFORMATION DURING SHEAR TESTING, [31].....	7
FIGURE 1-7 SPECIMEN SHAPES FOR WEDGE SPLITTING TESTS, [29].....	9
FIGURE 1-8 SETUP OF WEDGE SPLITTING TEST, [29].....	9
FIGURE 1-9 SPECIMEN SHAPES AND TESTING METHOD, [12].....	12
FIGURE 1-10 SHEAR TEST ON EMULSIONS, [12].....	12
FIGURE 1-11 SPECIMENS WITH TACK COAT AT INTERFACE, [19].....	13
FIGURE 1-12 SHEARING DEVICE DEVELOPED BY SHOLAR ET AL [24].....	14
FIGURE 2-1 SUMMARY OF RESEARCH OUTLINE AND METHODOLOGY.....	23
FIGURE 4-1 GRADATION ANALYSIS OF FINES USING FHWA PARTICLE ANALYZER, SET 2.....	37
FIGURE 4-2 GRADATION ANALYSIS OF FINES USING FHWA PARTICLE ANALYZER, SET 1.....	37
FIGURE 4-3 MASTER CURVES ($ G^* $) FOR BUNCOMBE COUNTY, 64 °C.....	38
FIGURE 4-4 MASTER CURVES ($ G^* $) FOR RUTHERFORD COUNTY, 64 °C.....	38
FIGURE 4-5 MASTER CURVES ($ G^* /\sin \delta$) FOR BUNCOMBE COUNTY, UNAGED, 64 °C.....	39
FIGURE 4-6 MASTER CURVES ($ G^* /\sin \delta$) FOR BUNCOMBE COUNTY, AGED, 64 °C.....	39
FIGURE 4-7 MASTER CURVES ($ G^* /\sin \delta$) FOR RUTHERFORD COUNTY, UNAGED, 64 °C.....	40
FIGURE 4-8 MASTER CURVES ($ G^* /\sin \delta$) FOR RUTHERFORD COUNTY, AGED, 64 °C.....	40
FIGURE 4-9 COMPARISON OF $ G^* /\sin \delta$ AT VARIOUS TEMPERATURES FOR RESIDUAL BINDERS.....	41
FIGURE 4-10 COMPARISON OF $ G^* $ AT VARIOUS TEMPERATURES FOR RESIDUAL BINDERS.....	41
FIGURE 4-11 COMPARISON OF δ AT VARIOUS TEMPERATURES FOR RESIDUAL BINDERS.....	42
FIGURE 4-12 VISCOSITY VS. RPM, 150 °C.....	42
FIGURE 4-13 PERCENT TORQUE VS. RPM, 150 °C.....	43
FIGURE 4-14 VISCOSITY VS. RPM, 135 °C.....	43

FIGURE 4-15 PERCENT TORQUE VS. RPM, 135 °C	44
FIGURE 5-1 NINE CLIMATIC REGIONS IN US	59
FIGURE 5-2 DYNAMIC SHEAR MODULUS ($ G^* $) VS. FREQ., 50.2 °C, BUNCOMBE, LAB MIXES	59
FIGURE 5-3 PHASE ANGLE (δ) VERSUS FREQUENCY, 50.2 °C, BUNCOMBE, LAB MIXES	60
FIGURE 5-4 AVERAGE $ G^* $ AND δ VALUES VS. FREQ., 50.2 °C, BUNCOMBE, LAB MIXES	60
FIGURE 5-5 DYNAMIC SHEAR MODULUS ($ G^* $) VS. FREQ., 50.2 °C, RUTHERFORD, LAB MIXES	61
FIGURE 5-6 PHASE ANGLE (δ) VS. FREQUENCY, 50.2 °C, RUTHERFORD, LAB MIXES	61
FIGURE 5-7 AVERAGE $ G^* $ AND δ VALUES VS. FREQ., 50.2 °C, RUTHERFORD, LAB MIXES	62
FIGURE 5-8 PLASTIC SHEAR STRAIN VS. RSCH CYCLES, 50.2 °C, BUNCOMBE COUNTY, LAB MIXES	62
FIGURE 5-9 PLASTIC SHEAR STRAIN VS. RSCH CYCLES, 50.2 °C, RUTHERFORD COUNTY, LAB MIXES	63
FIGURE 6-1 VIEW OF MOLD WITH ADJUSTABLE RAMPS (ON LEFT)	69
FIGURE 6-2 MOLD WITH ROLLER	69
FIGURE 6-3 FRESHLY CAST PCC SLAB	70
FIGURE 6-4 SIDE VIEW WITH ROLLER ON THE MOLD	70
FIGURE 6-5 PHOTO OF A 1-INCH THICK CTB ‘DISK’	71
FIGURE 6-6 CTB ‘DISKS’ COATED WITH EMULSION	71
FIGURE 6-7 MOLD TOP – PART I	72
FIGURE 6-8 MOLD BOTTOM – PART I	73
FIGURE 6-9 MOLD TOP – PART II	74
FIGURE 6-10 MOLD BOTTOM – PART II	75
FIGURE 7-1 DYNAMIC SHEAR MODULUS ($ G^* $) VS. FREQUENCY FOR AC MIX, 20 °C	93
FIGURE 7-2 SHEAR PHASE ANGLE (δ) VS. FREQUENCY FOR AC MIX, 20 °C	93
FIGURE 7-3 DYNAMIC SHEAR MODULUS ($ G^* $) VS. FREQUENCY FOR AC MIX, 30 °C	94
FIGURE 7-4 SHEAR PHASE ANGLE (δ) VS. FREQUENCY FOR AC MIX, 30 °C	94
FIGURE 7-5 DYNAMIC SHEAR MODULUS ($ G^* $) VS. FREQUENCY FOR AC MIX, 40 °C	95
FIGURE 7-6 SHEAR PHASE ANGLE (δ) VS. FREQUENCY FOR AC MIX, 40 °C	95
FIGURE 7-7 DYNAMIC SHEAR MODULUS ($ G^* $) VS. FREQUENCY FOR AC MIX, 60 °C	96
FIGURE 7-8 SHEAR PHASE ANGLE (δ) VS. FREQUENCY FOR AC MIX, 60 °C	96
FIGURE 7-9 AVERAGE DYNAMIC SHEAR MODULUS ($ G^* $) VS. FREQUENCY FOR AC MIX	97
FIGURE 7-10 AVERAGE SHEAR PHASE ANGLE (δ) VS. FREQUENCY FOR AC MIX	97
FIGURE 7-11 $ G^* $ MASTER CURVE FOR AC MIX, 30 °C	98
FIGURE 7-12 SHEAR PHASE ANGLE (δ) MASTER CURVE FOR AC MIX, 30 °C	98
FIGURE 7-13 $ G^* $ MASTER CURVE FOR AC MIX, 40 °C	99
FIGURE 7-14 SHEAR PHASE ANGLE (δ) MASTER CURVE FOR AC MIX, 40 °C	99
FIGURE 7-15 $ G^* $ MASTER CURVE FOR AC MIX, 30 AND 40 °C	100
FIGURE 7-16 SHEAR PHASE ANGLE (δ) MASTER CURVE FOR AC MIX, 30 AND 40 °C	100

FIGURE 7-17 PLASTIC SHEAR STRAIN VS. RSCH CYCLES, 40 AND 60 °C FOR AC MIXES	101
FIGURE 7-18 DYNAMIC AXIAL MODULUS ($ E^* $) VS. FREQUENCY FOR AC MIX.....	101
FIGURE 7-19 AVERAGE DYNAMIC AXIAL MODULUS ($ E^* $) VS. FREQUENCY FOR AC MIX.....	102
FIGURE 7-20 AVERAGE AXIAL PHASE ANGLE (δ) VS. FREQUENCY FOR AC MIX.....	102
FIGURE 7-21 PLASTIC AXIAL STRAIN VS. CYCLES, 40 AND 60 °C FOR AC MIXES.....	103
FIGURE 7-22 RELATIONSHIP BETWEEN $ G^* $ AND $ E^* $ FOR AC MIXES	103
FIGURE 7-23 RELATIONSHIP BETWEEN SHEAR AND AXIAL PHASE ANGLE FOR AC MIXES.....	104
FIGURE 7-24 SET UP FOR ELASTIC MODULUS OF CONCRETE USING A 6×12 CYLINDER.....	104
FIGURE 7-25 AXIAL STRESS VS. STRAIN AT 7 DAYS FOR PCC.....	105
FIGURE 7-26 GRADATION OF MATERIALS USED FOR CTB	105
FIGURE 7-27 MOISTURE DENSITY CURVE FOR CTB.....	106
FIGURE 7-28 RESILIENT MODULUS OF CEMENT TREATED BASES (CTB), [1, 14].....	106
FIGURE 8-1 DEBONDED COMPOSITE AC-AC SLAB WITHOUT TACK COAT.....	121
FIGURE 8-2 AXIAL FAILURE OF CMS-2 SPECIMEN (C4 6-3-2) AT 2.5 MM/MIN, 40 °C.....	121
FIGURE 8-3 AXIAL FAILURE OF CMS-2 SPECIMEN (C4 6-3-2) AT 2.5 MM/MIN, 40 °C.....	122
FIGURE 8-4 AXIAL FAILURE OF PG64-22 SPECIMEN (M1 5-16-2) AT 2.5 MM/MIN, 40 °C	122
FIGURE 8-5 AXIAL FAILURE OF PG64-22 SPECIMEN (M1 5-16-2) AT 2.5 MM/MIN, 40 °C	123
FIGURE 8-6 AVERAGE SHEAR STRESS VS. TIME FOR AC-AC INTERFACE TACKED WITH CMS-2.....	123
FIGURE 8-7 AVERAGE SHEAR STRESS VS. TIME FOR AC-AC INTERFACE TACKED WITH PG64-22	124
FIGURE 8-8 SUMMARY OF BOND STRENGTHS FOR AC-AC INTERFACE	124
FIGURE 8-9 SHEAR FAILURE OF CMS-2 SPECIMEN (M1 6-16-2) AT 1.0MM/MIN, 40 °C.....	125
FIGURE 8-10 SHEAR FAILURE OF CMS-2 SPECIMEN (M3 6-3-2) AT 1.0MM/MIN, 40 °C.....	125
FIGURE 8-11 SHEAR FAILURE OF CMS-2 SPECIMEN (C1 6-3-2) AT 2.5MM/MIN, 40 °C.....	126
FIGURE 8-12 SHEAR FAILURE OF PG64-22 SPECIMEN (M1 5-7-2) AT 2.5 MM/MIN, 40 °C.....	126
FIGURE 8-13 SHEAR FAILURE OF PG64-22 SPECIMEN (1MMC2_1) AT 1.0 MM/MIN, 20 °C	127
FIGURE 8-14 SHEAR FAILURE OF PG64-22 SPECIMEN (25MMM3) AT 2.5 MM/MIN, 20 °C	127
FIGURE 8-15 DEBONDING OF COMPOSITE PCC-AC SPECIMEN WITHOUT TACK COAT.....	128
FIGURE 8-16 DEBONDED COMPOSITE PCC-AC SLABS WITHOUT TACK COAT.....	128
FIGURE 8-17 AVERAGE SHEAR STRESS VS. TIME FOR PCC-AC INTERFACE TACKED WITH CMS-2.....	129
FIGURE 8-18 AVERAGE SHEAR STRESS VS. TIME FOR PCC-AC INTERFACE TACKED WITH PG64-22	129
FIGURE 8-19 SUMMARY OF BOND STRENGTHS FOR PCC-AC INTERFACE	130
FIGURE 8-20 PCC-AC SPECIMEN TACKED WITH PG64-22 (CRACKS HIGHLIGHTED IN WHITE).....	130
FIGURE 8-21 PCC-AC SPECIMEN TACKED WITH CMS-2.....	131
FIGURE 8-22 SUMMARY OF PCC-AC SHEAR BOND STRENGTHS, [19].....	131
FIGURE 8-23 COMPOSITE CTB-AC SPECIMEN.....	132
FIGURE 8-24 AVERAGE SHEAR STRESS VS. TIME FOR CTB-AC INTERFACE PRIMED WITH CSS-1H.....	132
FIGURE 8-25 AVERAGE SHEAR STRESS VS. TIME FOR CTB-AC INTERFACE PRIMED WITH EAP.....	133

FIGURE 8-26 AVERAGE SHEAR STRESS VS. TIME FOR CTB-AC INTERFACE PRIMED WITH EPR-1	133
FIGURE 8-27 SUMMARY OF BOND STRENGTHS FOR CTB-AC INTERFACE	134
FIGURE 8-28 CTB-AC SPECIMEN PRIMED WITH CSS-1H, SHEARED AT 1MM/MIN (40 °C)	134
FIGURE 8-29 CTB-AC SPECIMEN PRIMED WITH EPR-1, SHEARED AT 1MM/MIN (60 °C)	135
FIGURE 8-30 DEBONDED CTB-AC SPECIMEN PRIMED WITH EA-P, 60 °C	135
FIGURE 9-1 TIRE LAYOUT, TRAVEL DIRECTION, AND AXES ORIENTATION	145
FIGURE 9-2 AC AVERAGE 7-DAY MAXIMUM HIGH PAVEMENT TEMP. VS. DEPTH	145
FIGURE 9-3 DYNAMIC AXIAL MODULUS FOR ASPHALT MIXES VS. TEMPERATURE	146
FIGURE 9-4 PAVEMENT STRUCTURE AND LAYER PROPERTIES, AC OVER AC	146
FIGURE 9-5 MOBILIZED INTERFACIAL SHEAR VS. OVERLAY THICKNESS, AC-AC, 20 °C	147
FIGURE 9-6 MOBILIZED INTERFACIAL SHEAR VS. OVERLAY THICKNESS, AC-AC, 7-D MAX TEMP.	147
FIGURE 9-7 PAVEMENT STRUCTURE AND LAYER PROPERTIES, AC OVER PCC	148
FIGURE 9-8 MOBILIZED INTERFACIAL SHEAR VS. OVERLAY THICKNESS, PCC-AC, 20 °C	148
FIGURE 9-9 MOBILIZED INTERFACIAL SHEAR VS. OVERLAY THICKNESS, PCC-AC, 7-D MAX TEMP.	149
FIGURE 9-10 PAVEMENT STRUCTURE AND LAYER PROPERTIES, AC OVER CTB	149
FIGURE 9-11 MOBILIZED INTERFACIAL SHEAR VS. OVERLAY THICKNESS, CTB-AC, 40 °C	150
FIGURE 9-12 MOBILIZED INTERFACIAL SHEAR VS. OVERLAY THICKNESS, CTB-AC, 7-D MAX TEMP.	150

List of Abbreviations and Symbols

$ E^* $	magnitude of dynamic axial modulus
$ G^* $	magnitude of complex shear modulus
δ	phase angle
d/a	Distance Ratio, distance from the center of wheel divided by contact radius
AC	Asphalt Concrete
AEA	Air Entraining Admixture
AFST	Axial Frequency Sweep Test
APA	Asphalt Pavement Analyzer
ASTM	American Society of Testing and Materials
BISAR	Bituminous Structural Analysis in Roads
CMS	Cationic Medium Setting emulsion
CRS	Cationic Rapid Setting emulsion
CSS	Cationic Slow Setting emulsion
CTB	Cement Treated Base
DSR	Dynamic Shear Rheometer
FSCH	Frequency Sweep test at Constant Height
G_{mm}	Theoretical Maximum Specific Gravity (ASTM D2041)
HDS	High Density Surface course
HF-	High Float
MC	Medium Curing cutback
MTS	Material Test System

MS	anionic Medium Setting emulsion
NCDOT	North Carolina Department of Transportation
PCC	Portland Cement Concrete
PG	Performance Graded
RC	Rapid Curing cutback
RS	anionic Rapid Setting emulsion
RSCH	Repeated Shear test at Constant Height
RV	Rotational Viscometer
SGC	Superpave Gyrotory Compactor
SN	Skid Number
SS	anionic Slow Setting emulsion
SST	Simple Shear Testing machine
SUPERPAVE™	SUperior PERforming PAVEMENTs
TSR	Tensile Strength Ratio
UTM	Universal Testing Machine

1 Introduction and Literature Survey

1.1 Introduction

Asphalt pavements constitute 96 percent of the hard surfaced roads in the US. In terms of distance, approximately 2.2 million miles of roads have asphalt surfaces and approximately 91 percent of the 2 trillion annual vehicular miles of travel occur on these pavements. With ever increasing number of vehicles on the roads, the need for proper maintenance of the existing infrastructure cannot be overemphasized.

Typically for thicker asphalt pavements, construction is done in stages. This is for ease of construction and economic reasons. Before paving a rehabilitation asphalt layer, the top surface of the existing layer is cleaned and a tack coat is applied to bond the new surface being paved and the underlying layer. The tack coat consists of a light application of asphalt binder, usually in the form of asphalt emulsion or liquid asphalt. For optimal performance, it is important that the tack coat be thin and uniform, and ‘breaks’ just before the new asphalt concrete layer is paved [20]. The process of breaking of an emulsion is characterized by the separation of liquid asphalt and water into two separate phases; after evaporation of water the residual asphalt forms a bond with the underlying surface. Similarly, prime coat is used between the aggregate base and the overlying layer. Functionally, it is similar to the tack coat. For the pavement to be structurally and functionally sound there should be proper bonding between the structural layers. Lack of interface bonding may lead to several premature distresses of which slippage cracking, delamination and distortion are most prominent. Slippage cracks (Figure 1-4), formed in the surface course, are crescent shaped and are generally formed in the opposite direction of horizontal force on the pavement. Delamination (Figure 1-1 and Figure 1-2) involves loss of bond between various lifts of asphalt concrete and distortion (Figure 1-3) is the deformation occurring predominantly in the surface course. The loss of bond leads to increased subgrade deformation due to higher vertical compressive stresses. In the literature available so far, assumptions of either full friction or no friction between interlayer surfaces have been made while designing pavements with the exception of BISAR which allows variable amounts of interfacial friction. Although

a lot of progress has been made in the field of polymer composites in modeling the interlayer bond behavior, similar research is lacking in the field of pavements.



Figure 1-1 Delamination of surface course

(Source: <http://www.kochpavementsolutions.com/Distresses/pushing.htm>)



Figure 1-2 Delamination, exposure of underlying layer

(Src: http://www.defence.gov.au/demg/7technical_guidance/aircraft_pavement_manual/part_a/a4.htm)



Figure 1-3 Distortion and shoving, deformation of surface layer under load

(Src: http://www.defence.gov.au/demg/7technical_guidance/aircraft_pavement_manual/part_a/a4.htm)

1.2 Literature Survey

Currently, the design and evaluation of flexible pavements is based on an elastic multi-layered analysis. For the design of pavements, the interfaces are assumed rough with no slippage occurring between the two layers. This, however, is not the case in practice. The state of adhesion at the interfaces between various layers affects the performance of flexible pavements by influencing the stressing level of materials. The stress distribution is more influenced by the interfacial condition of the upper layers than the lower ones. Hence, the knowledge of the interfacial conditions in the upper layers is important. Pertinent research conducted in the area of delamination and shoving is briefly described in the following section.

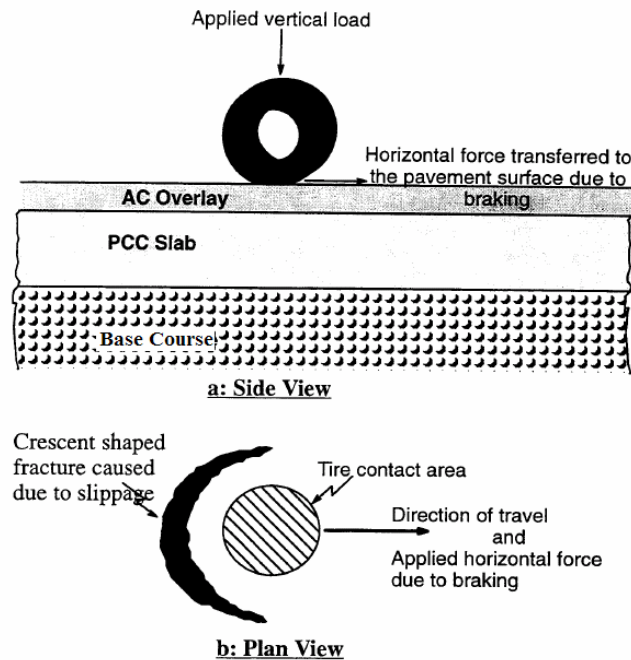


Figure 1-4 Typical slippage failure [11, 19]

1.2.1 Study by Mohammad et al [18]

Mohammad, et al [18] have measured the influence of different tack coats on interface shear strength. They conducted a load-controlled, simple shear test by shearing the specimens

at interface. Lateral confinement was provided by a collar (Figure 1-5) that ensured the failure was at interface and nowhere else. The specimens were manufactured in three steps:

- Compact the ‘bottom’ part of the specimen in a Superpave gyratory compactor
- After cooling, apply the tack coat at the specified rate
- Insert the ‘bottom’ specimen in the gyratory mold, pour loose asphalt mix over the tack coat, and compact.

The target air void content for each of the bottom and top specimens was 6%. Each of those specimens was tested in a SST machine at a loading rate of 50 lb/min until failure. The testing was conducted at temperatures of 25 and 55 °C. It was observed that CRS-2P emulsion performed better than PG64-22, PG76-22M, SS-1, SS-1H, and CSS-1h. In addition, for each of the tack coats, an optimum rate of application that gave the highest shear strength was determined. The study demonstrated that even under the most optimal performance of tack coat, the maximum strength attained is only 83% of monolithic mixture strength, implying that interfaces potentially cause slip planes.

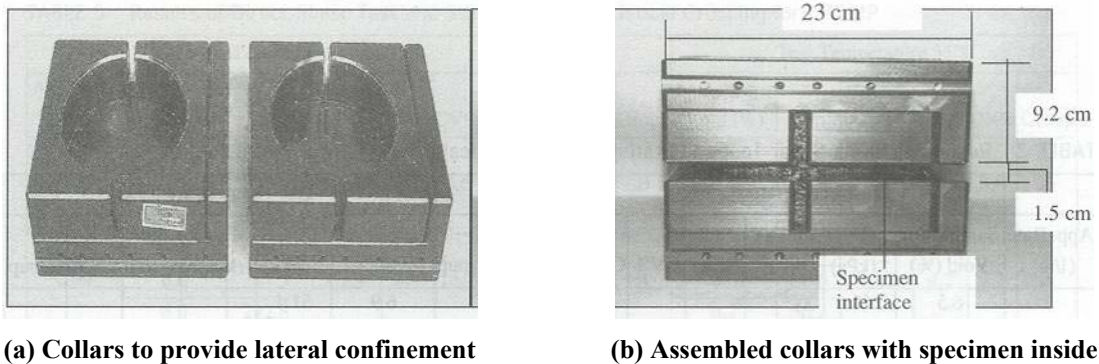


Figure 1-5 Collars designed for testing samples in shear, [18]

1.2.2 Study by Shahin et al [21]

Shahin et al [21] have discussed the effect of layer slippage on the performance of asphalt pavements. Using an example of an airfield pavement and with BISAR (Bituminous Structures Analysis in Roads) and the French Shell model [9] for analysis, various scenarios were evaluated about the fatigue life of the pavement. The pavement section analyzed had a 2-inch thick overlay over a 4-inch thick asphalt cement (AC) surface course. The base course

was 25-inch thick with elastic modulus of 75000 psi and a CBR value of 80. The subgrade was very weak with California Bearing Ratio (CBR) of 5 and stiffness of 7500 psi. The tensile stress at the bottom of the asphalt layers (overlay and the original surface course) and the vertical compressive strain on the subgrade were the criteria for failure. It was found that for full friction between the interfaces, the maximum tensile strain in the section is located at the bottom surface of the original asphalt layer. If the slippage was allowed below the uppermost layer, the tensile strain also existed at the bottom of the overlay. In addition, the following observations were made:

- Only a small amount of slippage is sufficient to produce strains in the pavement that approach those of the free slippage case.
- The tensile stress at the bottom of the overlay causes a compressive stress to develop on the upper surface of the asphalt surface layer. This causes a relative movement of points on the either side of the interface. This distortion further weakens the bond between the asphalt layers, allowing more slippage leading to higher strains.
- The subgrade strains increase with increasing slippage. Because two thinner layers are not as stiff as a single layer of the same overall thickness, the compressive vertical strain on the subgrade increases.
- Further, under the action of horizontal loads, the study found that for no friction, the horizontal strains are much higher than those with full friction.

The principal normal tensile strains, developed by the horizontal loads along the back edge of the contact area, are of the same magnitude and cause progressive failure along the rear edge. This tensile failure would cause slippage cracks in the overlay. If the overlay is not properly bonded to the underlying layers, the overlay moves resulting in opening of the cracks. These cracks are crescent shaped. In order to fix these cracks, either the existing layer needs to be removed and re-paved or a thicker well-bonded overlay be placed on the existing overlay. In addition to strong interlayer bonding, the authors suggested an overlay stiffness of at least 500,000 psi.

1.2.3 Study by Uzan et al [30, 31]

A research to evaluate the adhesion between asphalt mixes was conducted by Uzan, et al. [30, 31] using the Goodman's constitutive law:

$$\tau = K \times \Delta u \quad \text{(Equation 1-1)}$$

where:

τ is the shear stress at interface,

Δu the relative horizontal displacement of the two faces at the interface, and

K is the horizontal interface reaction modulus.

The interface behavior was described, which formerly was restricted only to perfectly rough or perfectly smooth conditions. The analysis was carried out using the BISAR program for a test section at different levels of adhesion. It was observed that for a perfectly smooth interface ($K=0$) the tensile radial strain at the bottom of the uppermost layer was higher than for the perfectly rough interface. The top of the second layer also changed to compressive strain when K approached zero. Further, it has been shown that even an adherence of 90% was very close to a smooth condition as described in Shahin et al [21]. Direct shear tests were performed on the layered asphalt concrete specimens with shearing along the tack coat and the variables were temperature, vertical pressure and rate of application of tack coat (Figure 1-6). It was concluded that the components of the interface shear strength were:

- Adhesion, represented by the tensile properties of the slip plane.
- Interlocking, from the penetration of aggregates into the voids of the other layer. The interlocking component depends on the texture of the surfaces in contact and properties of the asphalt mix.
- Friction, from rugosity of the two faces. Further, the friction component was included in the other two components. It was suggested that measurement of the adhesion component, which is indicated by rupture of the bond between layers in the bitumen or mastic phase, could be done by a tensile test. (The interlocking effect would be absent for pure tension.)

The following factors largely influenced the interface shear strength:

- Temperature: It is known that temperature affects the asphalt properties. The stiffness decreases with increase in the temperature and vice versa. The effect of higher temperatures is more dominant while testing in tension than in compression. In order to offset the effect of increased temperature, higher vertical pressures are applied. With

increasing vertical pressures, the interlocking component gets more dominant than the adhesion component.

- Tack Coat Rate: The tack coat bonding the two layers usually functions in two ways:
 - (a) Fill voids on the surface.
 - (b) Increase the interface film thickness or get absorbed in the adjacent layers.The filling of voids on the surface of the mixes increases the contact area and consequently the adhesion. However, excessive film thickness decreases the adhesion and aggregate interlock. Very low tack coat rate could mean loss of adhesion component. Hence, it is required that the tack coat be applied at optimum rate.
- Rate of Deformation: The rate of shear deformation is an important factor in controlling the strength and deformation ability of the interface. Generally, with increasing rate of deformation, the magnitude of stress developed increases.

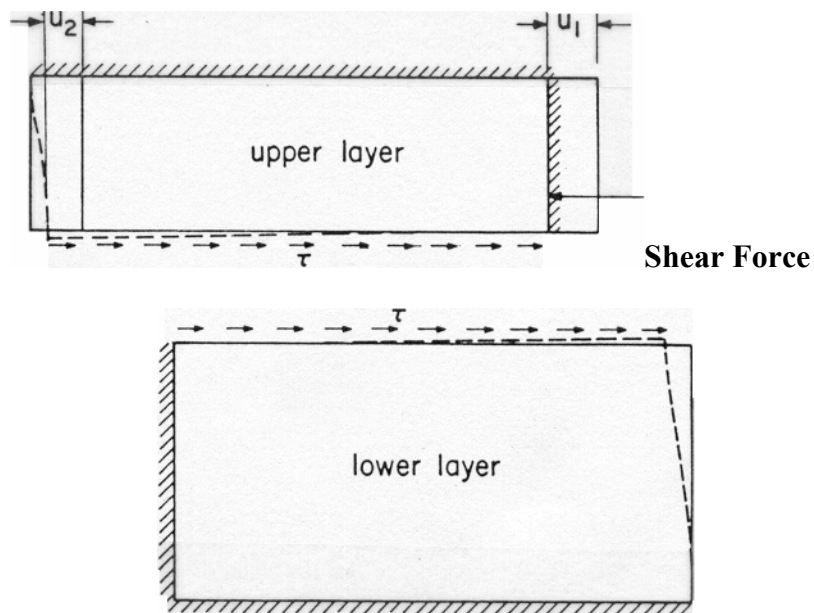


Figure 1-6 Schematic of specimen deformation during shear testing, [31]

1.2.4 Study by Tschegg et al [29]

A common method for measuring the bond strength of asphalt cores is the pull-off test [29]. For this test, cores with a diameter of 100 mm were drilled from the top surface

down through the overlay, through the interface, and about 50 mm into the base layer. Steel plates were glued to the top surface of the cores. Then the drill core was pulled off with a tension machine in axial direction of the base layer. The maximum load is registered during the pull-off test. This is a simple test method but gave only the adhesive tensile strength and showed extensive scattering of results. The reasons for wide scattering of results were: eccentricity of load, small core diameter and large aggregate size, notches at the surface of the cores by drilling or burst out aggregates, stress concentrations, uncontrolled temperature, and indentation effects owing to rough surfaces. In addition, the test was useless if the tensile strength of the mix was lower than the interface bond strength.

For avoiding such drawbacks, a ‘Wedge Splitting Test’ was developed. In this test, a block of asphalt concrete was made to crack along a predetermined joint at steady rate. The splitting was done by a wedge that was located in a groove between the two blocks of asphalt. The force and the displacements were recorded during stable crack propagation until complete separation of the specimen took place. Based on the shape of the force-displacement curve, a differentiation between brittle and ductile behavior is possible. Figure 1-7 and Figure 1-8 show the test setup and the specimens used for testing purposes. It was found that with increasing temperature, the plastic behavior of the asphalt increased. There was a decrease in the peak load values with an increase in the temperature. At low temperatures, it was found that the relationship between the force and the crack opening displacement was linear. However, this test could not distinguish between the two different types of tack coats used for that study.

1.2.5 Study by Ameri-Gaznon et al [6]

Ameri-Gaznon et al [6] evaluated the octahedral shear stress (OSS) and the octahedral shear stress ratio (OSR) for different pavement sections. In particular, the OSR and the rut resistance in an asphalt concrete pavement (ACP) overlay is evaluated based on the overlay thickness, interlayer bonding, effect of stiffness, and horizontal surface shear. The material properties of the bituminous materials were evaluated using the tri-axial test and cohesion, c , and angle of internal friction, ϕ , values were determined at 104 °F at a loading rate of 4-inch per minute. The modified ILLIPAVE finite element computer program was used to calculate the OSRs within ACP layers.

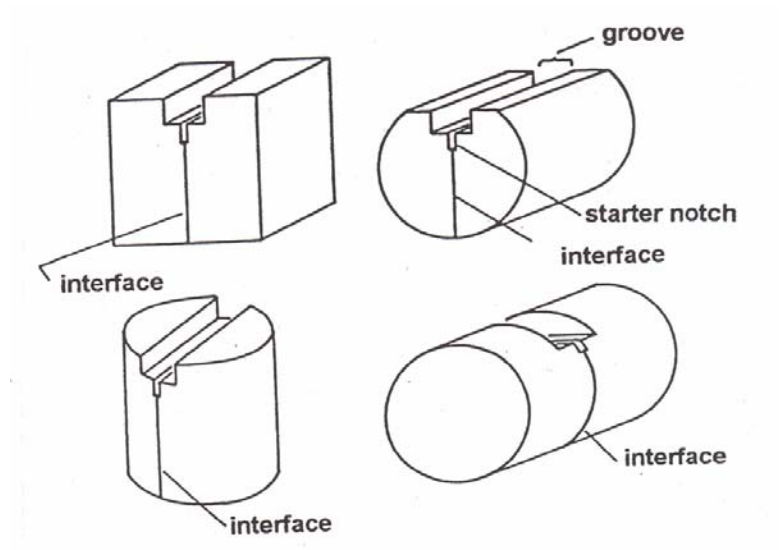


Figure 1-7 Specimen shapes for wedge splitting tests, [29]

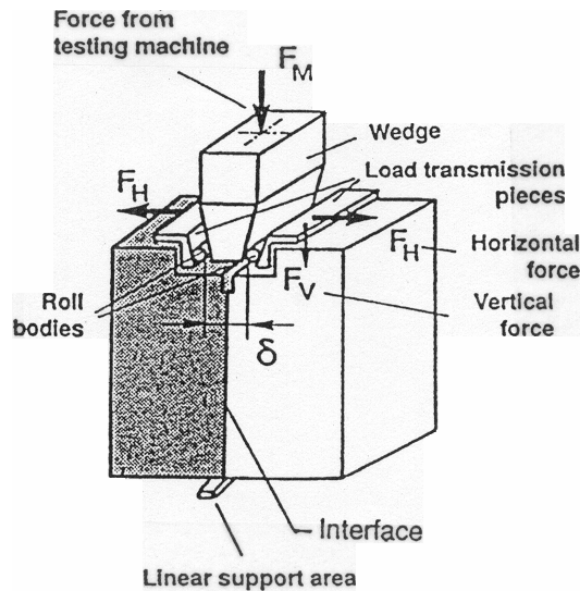


Figure 1-8 Setup of wedge splitting test, [29]

In absence of interlayer bond, the overlay acts independently of the rest of the pavement system allowing greater relative movement in between two asphalt layers. This reduces the confining stress causing larger OSS in the overlay. Pavements of various

thicknesses have been analyzed and the 4-inch thick overlay is the most critical one when there is free slippage.

With increase in the bonding, the critical thickness increases to 6 inches for ACP overlays. For a complete bond, the stress levels are critical at the mid height of the ACP overlay. With loss of bond, the critical stress shifts to the bottom of the surface layer. Also, the stress levels are far more critical than when a complete bond exists. Typically, with increasing stiffness, it is expected that the shear stresses would decrease but it works otherwise if there is a poor interlayer bond. The authors have also considered the effect of horizontal surface shear on pavements. It has been shown that presence of horizontal surface shear force doubles the OSS induced in the ACP overlay for full bond and no-bond conditions.

1.2.6 Study by Ishai et al [15]

The authors have carried out an investigation on the functional and structural role of prime coat in flexible pavements. The areas of investigation were the contribution of prime coat to pavement performance and evaluation of emulsions as an alternative source of prime coats. The experimental program consisted of following:

- Evaluation of the rate of increase of viscosity and evaporation characteristics of the prime coat material;
- Measurement of absorption of prime coat material into the base course;
- Quantification of change in the hardness of the base layer with time;
- And adhesion between the base course and the asphalt layer;

The conclusions drawn from the tests were:

1. Cutbacks had higher viscosity than the emulsions. Hence, it was necessary to heat the cutbacks whereas there was no such problem with emulsions.
2. Rate of loss of liquid for emulsions is much higher than for cutbacks. This translates into faster construction of the overlying pavement structure. Also retention of organic vapors from cutbacks in the base layers could be detrimental to the overlying ACP, if paved immediately. In addition to this, cutback residues have lower viscosity than the emulsion residue, which translates to poorer interlayer bond for cutbacks.

3. The penetration of cutback was higher than that of the emulsions for granular material but for sandy material the values were comparable.
4. The surface hardness of the base layer was measured using a pocket penetrometer. It was found that for cutbacks there was not a significant gain of strength in the first ten days of curing, however, for emulsions, the strength gain was much faster. The accelerated rate of strength gain can be attributed to harder asphalt in the emulsions and faster curing.
5. The interfacial adhesion was measured using the direct shear test performed on composite samples of base and asphalt concrete layers. For unprimed surfaces, the failure was observed along the geometric interface between two layers. For a cutback prime coat, a little bonding was observed due to the interlocking effect created by absorption of the asphalt. The highest interface adhesion was observed when priming was done with emulsions. This could be because of deep penetration and strong adhesive bonds. Also, the failure shear stress was observed to be dependent on the vertical load due to more efficient interlocking and greater adhesion.

It can, therefore, be concluded that emulsion based prime coats enhance the shear strength of the interface at base and asphalt concrete layers.

1.2.7 Study by Hachiya et al [12]

The study consisted of mainly three steps. The first step consisted of analyzing the airport runway and taxiway using BISAR to calculate the interface shear stresses and strains. The results showed that shear stresses at interfaces depended on surface layer thickness (lower thickness producing higher shear stresses) and horizontal force on the surface. An increase in the horizontal force, in form of acceleration and braking, caused an increase in the interfacial shear stresses. The pavement failure was caused by interlayer separation due to increased shear and tensile cracking at the bottom of the top layer. Construction of thicker lifts can help reduce the interlayer shear stresses. In the second step, laboratory tests were conducted on asphalt concrete specimens (Figure 1-9) and emulsions (Figure 1-10) in the laboratory. Asphalt specimens were tested in shear and tension at various temperatures in a strain-controlled mode. The interfaces (Figure 1-9) were hot jointed, cold jointed, tack coated (0.088 gal/yd²) and monolithic. Tack coated joints performed better than cold joints but not

as well as hot joints or monolithic construction. The interlayer shear strength was dependent on type of tack coat used (modified emulsions worked best), rate of application, curing time, and temperature. In the third part, three sections were constructed and subjected to loading by an assembly similar to aircraft landing gear. The top layer in each of the sections was of the same thickness but constructed differently: for the first section it was constructed in three lifts, for the second it was in two lift, and for the third it was a single lift. It was observed that the section constructed in a single lift rutted more than the other two. The section least likely to rut was the one with three lifts. Overall, it was suggested to use higher lift thicknesses and modified emulsions to reduce the interlayer slippage on airport pavements.

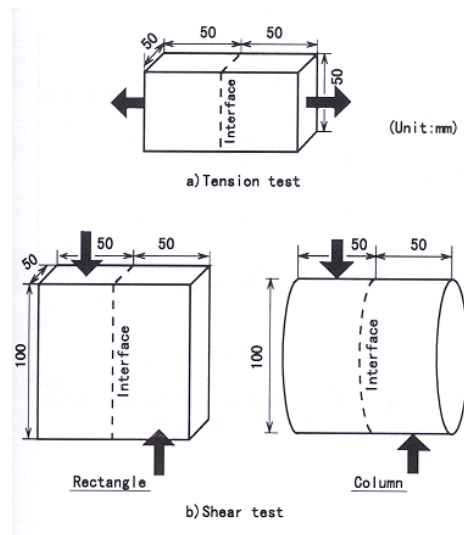


Figure 1-9 Specimen shapes and testing method, [12]

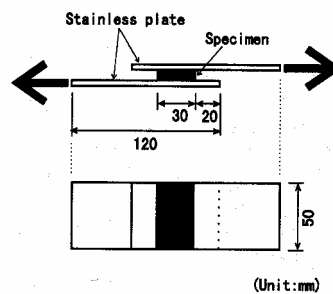


Figure 1-10 Shear test on emulsions, [12]

1.2.8 Study by Mukhtar et al [19]

Tests similar to the current study were conducted by Mukhtar et al [19] to evaluate the shear strength of AC-PCC interface. PCC specimens of dimensions shown in Figure 1-11 were cast and cured for a period of 28 days. Subsequently, a tack coat was applied at one of the surfaces and the PCC specimen was inserted in the mold having 2-inch internal diameter. Loose asphalt mix was compacted to a density of 147 pcf in three lifts each with 1-inch thickness. A vertical confining load of 79 psi was applied to simulate the field condition of having a 2.5-inch thick AC overlay over PCC. The specimens were then sheared at interface in a strain-controlled mode at the rate of 1.0, 30 and 300 inch per min. The testing was carried out at of 0, 20, 40, 60, 80 and 100 °F. It was observed that, regardless of the testing temperature and shearing rate, monolithic AC specimens had higher shear strength than specimens jointed at the interface. The shear strength of the interface increased with higher rate of shear and lowering of temperature. Analysis performed by the authors indicated maximum shear stresses below the wheel.

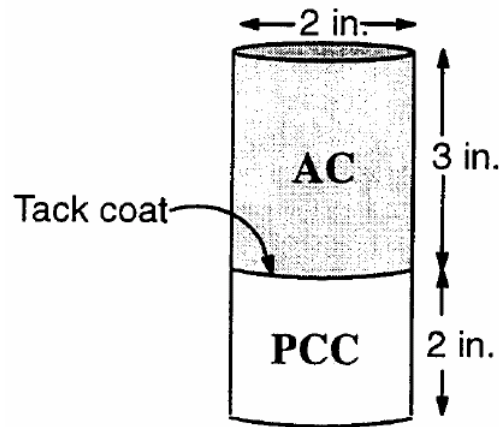


Figure 1-11 Specimens with tack coat at interface, [19]

1.2.9 Study by Sholar et al [24]

The authors have investigated the effect of different tack coat application rates, curing time, types of aggregates, rates of shear and moisture on the interfacial bond strength of composite asphalt specimens. A device, shown in Figure 1-12, was developed to test the

specimens in shear. The device was mounted in a temperature controlled MTS test chamber. The shear strengths of composite samples were measured at constant strain rates. The shear strength of the interface was directly related to the rate of shear and inversely to the test temperature. It was observed that exposure of tack coat to moisture, prior to paving a new overlay, caused reduction in the interfacial shear strength. This emphasizes the need to have proper curing of tack coats before paving a new layer. Further, coarser gradations (19.0 mm) performed significantly better than finer (12.5 mm) gradations in terms of shear strengths. In addition, milling of the existing pavement surface before applying tack coat significantly increased the bond strength of the interface in shear. Increasing the rate of application of tack coat caused a marginal increase in the shear strength of the interface.

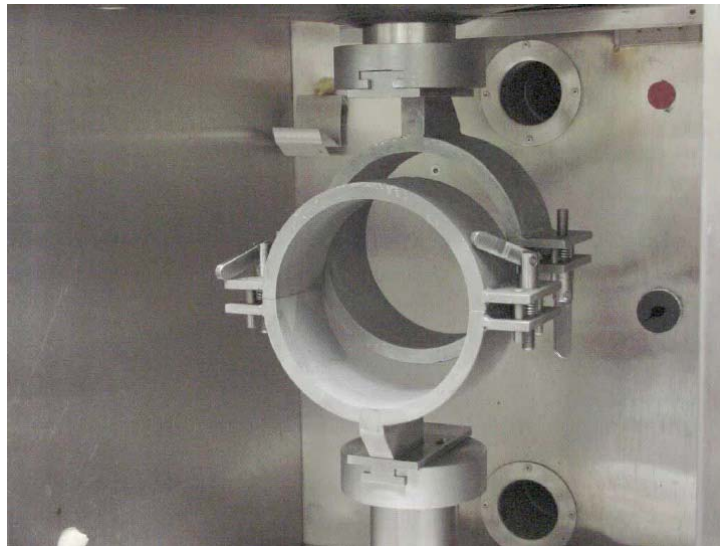


Figure 1-12 Shearing device developed by Sholar et al [24]

1.2.10 Prime Coats

Prime coating is the spray application of asphalt on the surface of a non-asphalt base course. Usually untreated materials are primed with cutback asphalt that helps waterproof the surface of the base, plug capillary voids, coats and bound loose mineral particles, and provide adhesion between the base and asphalt concrete. Although, emulsion based primes have been used as an alternative to cutback, HMA industry experience suggests that emulsions are not

as effective as cutbacks. Due to this reason, for many asphalt pavement constructions, priming is completely eliminated.

Asphalt Institute suggests that prime coats be used for asphalt layers less than 3-4 inches thick. This issue is particularly important for thick pavements placed directly on sub-base or base materials, especially in case of low-volume roads. During construction of pavement sections, asphalt concrete mats are usually placed in 1.5-2 inch lift thicknesses. Construction equipment such as rollers and heavy truck traffic can induce slippage distress in the first AC layer placed over the base even before the pavement is open to traffic. It is, therefore, critical to understand the contribution of prime coat in dissipating the induced shear stresses. Prior studies on the subject of prime coats have investigated the effectiveness of emulsions versus cutbacks, effectiveness of different emulsions, and construction techniques to improve prime coat performance. The current study measures the interlayer bond strength for various prime coats and attempts to correlate them to the mobilized interlayer shear stresses in typical pavement sections.

1.2.11 Tack Coats

In composite asphalt concrete pavements, tack coat provides the interface bond between two AC layers or between AC-PCC layers so that they form a monolithic structure to withstand traffic and environment. A strong tack coat is essential to dissipate the shear stress within the pavement structure. Factors such as traffic level, interface bond strength and surface-layer thickness directly affect the performance and life of the pavement. The study outlined in the next section compares the bond strength of field cores tacked with PG64-22 and CRS-2.5. Certain types of tack coat (e.g. PG 64-22) have been found to perform better than others (e.g. CRS-2.5 emulsion). The efficient use of tack coat is critical for asphalt overlay construction, especially for overlay of the rigid concrete pavement surfaces that need to be opened to traffic within 12 to 24 hours. In many cases contractors preferably use PG64-22 asphalt cement as a tack coat over CRS-2.5 emulsion because the former does not require any curing before traffic can be applied.

For overlay as well as new construction of AC pavements, asphalt concrete mats are usually placed in 1.5-2 inch lift thicknesses. As discussed earlier for prime coats,

construction equipment and heavy truck traffic can induce slippage distresses during construction that can propagate to the surface. It is, therefore, necessary, to understand the relationship between tack coat bond strength and pavement layer thickness for dissipation of traffic induced shear stresses.

1.3 Research Need

The extensive network of highways and interstates add up to very high maintenance costs. The delamination distresses are due to traffic acceleration and deceleration. Poor tack coat undermines the pavement condition at these locations by increasing the shear stresses significantly. A study, that evaluates the material properties as well as their suitability, would enhance the quality of ride and extend the life of pavements thereby reducing the associated direct and indirect costs.

1.3.1 Prior Work

The motivation for this study was from an investigation launched in Division 13 of North Carolina Department of Transportation (NCDOT), by Tayebali et al [28] to examine the severe distresses manifested in the form of asphalt concrete layer delamination and distortion. The goal was to evaluate and identify the causes of delamination and distortion of asphalt concrete mat. The methodology adopted for investigation consisted of evaluating the field cores and testing of laboratory prepared specimens. In the first stage a survey was conducted across plants in Division 13 of NCDOT to acquire information about the use of different tack coats and type of material used in the field. Based on the questionnaire responses, two sections were chosen, each with a different type of tack coat. Enka, Buncombe County and Rutherfordton, Rutherford County had CRS-2.5 emulsion and PG64-22 binder, respectively used as a tack coat.

After the selecting the section, cores of 4-inch and 6-inch diameter were drilled from distressed and non-distressed areas from two counties. The 4-inch specimens were used to determine whether the mixes conformed to the NCDOT job mix formula specifications based on air voids and Marshall mix design criteria. It was found that the mixes indeed conformed with the NCDOT specifications and the only possible cause of distress could be improper

interlayer bonding or construction technique. An on-site inspection and initial survey indicated no such construction abnormalities and the focus was to evaluate the interlayer bonding. The 6-inch diameter cores were tested on the Simple Shear Test (SST) machine.

A frequency sweep test at constant height (FSCH) was conducted on the cores from distressed and non-distressed sections. The test measures the shear viscoelastic properties (dynamic shear modulus, $|G^*|$, and the phase shift, δ) over a range of testing frequencies and at different temperatures. It should be noted that the measured dynamic response of the core is a composite response of the two asphalt layers separated by a thin film of tack coat. It was concluded from the FSCH test that cores from non-distressed sections had higher $|G^*|$ and $G^*/\sin \delta$ values over the cores from distressed sections. This implied that the non-distressed mixes had a higher stiffness and a lower propensity to rut justifying their better performance.

The repeated shear test at constant height (RSCH) was used to measure the rutting potential of the mix over a range of temperatures. This test is performed in a controlled stress mode in accordance with AASHTO TP-7, Procedure F [5]. The RSCH gave results similar to FSCH. It was found that non-distressed cores withstood higher number of cycles than the distressed cores. Also, for cores from Buncombe County (CRS-2.5) there was a distinct difference between the 'good' and 'bad' (i.e., non-distressed and distressed) cores. Examination of the failed core samples showed a distinct pattern of cracking with diagonal cracks in both upper and lower asphalt concrete layers with a horizontal crack joining the diagonal cracks at interface. It should be noted that CRS-2.5 was used as a bonding (tacking) agent. For Rutherford County (where PG64-22 binder was used as tack coat) the difference in the number of cycles to failure was relatively smaller and the failure pattern was consistent with that observed in a monolithic single layer specimen. In addition to this, no interlayer separation or horizontal crack was evident at the interface. It should be noted that Rutherford County cores used PG64-22 as a tack coat. Thus, it was shown that the type of tack coat contributes significantly to the performance and the interface failure pattern.

An axial frequency sweep test (AFST), similar to the FSCH, was performed on the 6-inch diameter specimens. A dynamic axial load is applied and the dynamic axial stiffness modulus ($|E^*|$) along with the phase shift, δ , of an asphalt mix are measured. Ideally, taller specimens would have been preferable but the test was conducted on samples of 50-mm height. The trend in $|E^*|$ values was very much similar to that of $|G^*|$ for both the counties

and $|E^*|$ was found to be higher for non-distressed specimens. Thus, the results were found in agreement with the FSCH and it also proved that this test was robust to detect the difference between ‘good’ and ‘bad’ cores. In the ramp test, the specimens were pulled apart at a rate of 2.5-mm/minute after gluing them to metal platens. This test was used to measure the tensile strength of asphalt mixtures and, in particular, for layered specimens it represented the (tensile) strength of the interfacial joint. It was found that bond strength of the CRS-2.5 emulsion was 46% lower compared to cores from Rutherford County. The failure of Rutherford County cores was in the mix whereas for the Buncombe County cores, the failure was at the interface. Based on the field core test results, it was concluded that sections tacked using PG64-22 binder performed better when compared to sections tacked with CRS-2.5 emulsion. However, it may be noted that based on field core test results it was not possible to conclude whether PG64-22 was a better tacking material than CRS-2.5. This was because the rate of tack coat application could have been different and/or a construction problem such as uniform application, emulsion curing time before construction, and environmental issues. Therefore it became imperative to investigate, in a controlled laboratory test program, whether PG64-22 was indeed superior to the use of emulsions as a tacking material.

2 Research Approach and Methodology

2.1 Objective

The goal of this investigation was to mechanistically evaluate the contribution of prime and tack coat in composite asphalt concrete pavements. The current work undertaken for this study was based on the work conducted earlier [28]. In order to comprehend the contribution of prime and tack coats, it was necessary to understand and quantify the distribution of interlayer shear stresses, and their effect on the interface bonding. The project has two main components: experimental and analytical. The experimental part involves determination of material properties; and the analytical portion involves mechanistic analysis using the developed software that will enable the selection of appropriate pavement thickness and/or the choice of tack coat given an input of material properties, structural thicknesses and loading conditions. The result of this study will also enable designers to choose appropriate tacking materials for specific application. At the same time, with regard to prime coats, the use of emulsions has not been very popular in comparison to cutbacks. Specifically, many highway agencies (AZ, KS, NE, NH, NY and RI) do not use prime coats (emulsion based) any more.

2.2 Research Methodology

In order to achieve the objectives stated above, this investigation was conducted using the following tasks described below and as shown in Figure 2-1.

2.2.1 Literature Review and Survey

In this task, a review (§1.2) on the contribution of prime and tack coats to pavement performance was conducted. A survey questionnaire (Appendix A) was designed and sent to all state highway agencies to gather data on their experience for pavement construction with and without the use of prime and tack coats.

2.2.2 Asphalt and Mastics Testing

The Asphalt Institute Manual Series MS-16 [7] recognizes the detrimental effect of rounded particles and its contribution to mixture instability. Although the present mix in NCDOT Division 13 may not contain high sand content, it was hypothesized that the variable amount of baghouse fines purged intermittently into the asphalt mixture may account for the mix instability and significant changes in volumetric properties.

Therefore, the objective of this (§2.2.2) and the next task (§2.2.3) was to evaluate contribution of baghouse fines. The objective of this task was to evaluate the rheological properties of the binder in presence of baghouse fines using a Dynamic Shear Rheometer (DSR). This task consists of three subtasks:

- evaluate the properties of aged and virgin binders,
- rheological properties of mastics (aged and unaged), and
- viscosity of virgin asphalts and emulsion residues using rotational viscometer.

2.2.3 SST Testing of SGC Specimens, TSR and APA Tests

The objective of this subtask was to evaluate the effect of baghouse fines on mix characteristics using controlled mixes, and investigate their sensitivity to moisture exposure. Raw materials including baghouse fines and job-mix were obtained from NCDOT Division 13. Two mixes were prepared in the laboratory based on the job mix formula with materials passing #200 sieve (mineral filler) containing:

- zero percent baghouse fines; and
- 100 percent baghouse fines.

All other mix parameters such as asphalt content, and aggregate gradation were kept constant. These two mixes were subjected to the following laboratory testing:

- Laboratory FSCH and RSCH test on 6-inch diameter specimens compacted using SGC;
- Georgia wheel rutting test at NCDOT M&T Unit on 6-inch diameter specimens prepared using SGC; and
- Moisture sensitivity testing using the modified AASHTO T283 procedure.

2.2.4 Material Characterization

The objective of this task was to obtain material characteristics that would be needed for mechanistic analysis of the pavement sections elaborated in Chapter 9. The compressive strength and the elastic modulus of the PCC specimens were evaluated using cylindrical specimens. The CTB properties were also determined in the lab. For the asphalt concrete mix, the axial and shear stiffness were characterized at different temperatures and frequencies. Stiffness versus frequency master curves were prepared from the data obtained. These results would enable the selection of the appropriate stiffness and moduli values required for the mechanistic evaluation.

2.2.5 Fabrication of Slabs and Test Specimens

In this task, composite specimens – AC over AC, AC over PCC and AC over CTB – were fabricated using rolling wheel compaction. Approximate size of the slab was 24-inches by 24-inches. To cast the slabs, steel molds were fabricated. The lower layer of the slab was either be 2-inch thick CTB layer or PCC layer for the evaluation of prime and tack coats, respectively. The CTB and PCC layers were allowed to cure for 7-days. Appropriate prime and tack coat was applied (to CTB and PCC, respectively) and allowed to cure according to manufacturer’s recommendation.

For prime coat evaluation, slabs were prepared without any prime coating, and using three prime coats that are on NCDOT’s approved product list. These were EPR-1, CSS-1h and EA-P. Similarly for tack coat evaluation, slabs were prepared without any tack coating, and using a CMS-2 emulsions and PG64-22 asphalt cement. A dense mix asphalt concrete layer was then be rolled using a rolling wheel compactor. After the mix cooled down, the slabs were cored to produce 6-inch diameter specimens, which were tested in shear for bond strength properties.

2.2.6 Bond Strength Determination using Shear Testing

The objective of this task was to evaluate the CTB-AC, AC-AC and PCC-AC layer interface bond strength for various prime and tack coats used. In this study, the bond

strength was proposed to be evaluated using the simple shear test at constant height. Testing was conducted at 40 and 60 °C. For AC-AC and PCC-AC interfaces the testing was conducted at 20 °C as well. Two different shear strain rates were applied. Two replicates were tested at each strain level. For a given shear strain rate, the shear and axial stresses were monitored and the bond strength determined for each prime and tack coat being evaluated. In addition to the testing of composite core specimens, an attempt was also made to test prime and tack coat using two metal platens.

2.2.7 Mechanistic Analysis

Three dimensional stress analysis software based on semi-analytic method was developed as part of the overall project. The pavement was modeled primarily as a layered system of linear elastic materials with surface asphalt layer as a elastic material. Using the software, a detailed parametric study was conducted to investigate the effect of system parameters including layer thickness and stiffness on the stress-strain-displacement fields induced in the pavement. The effect of vehicle load characteristics on the response was also examined.

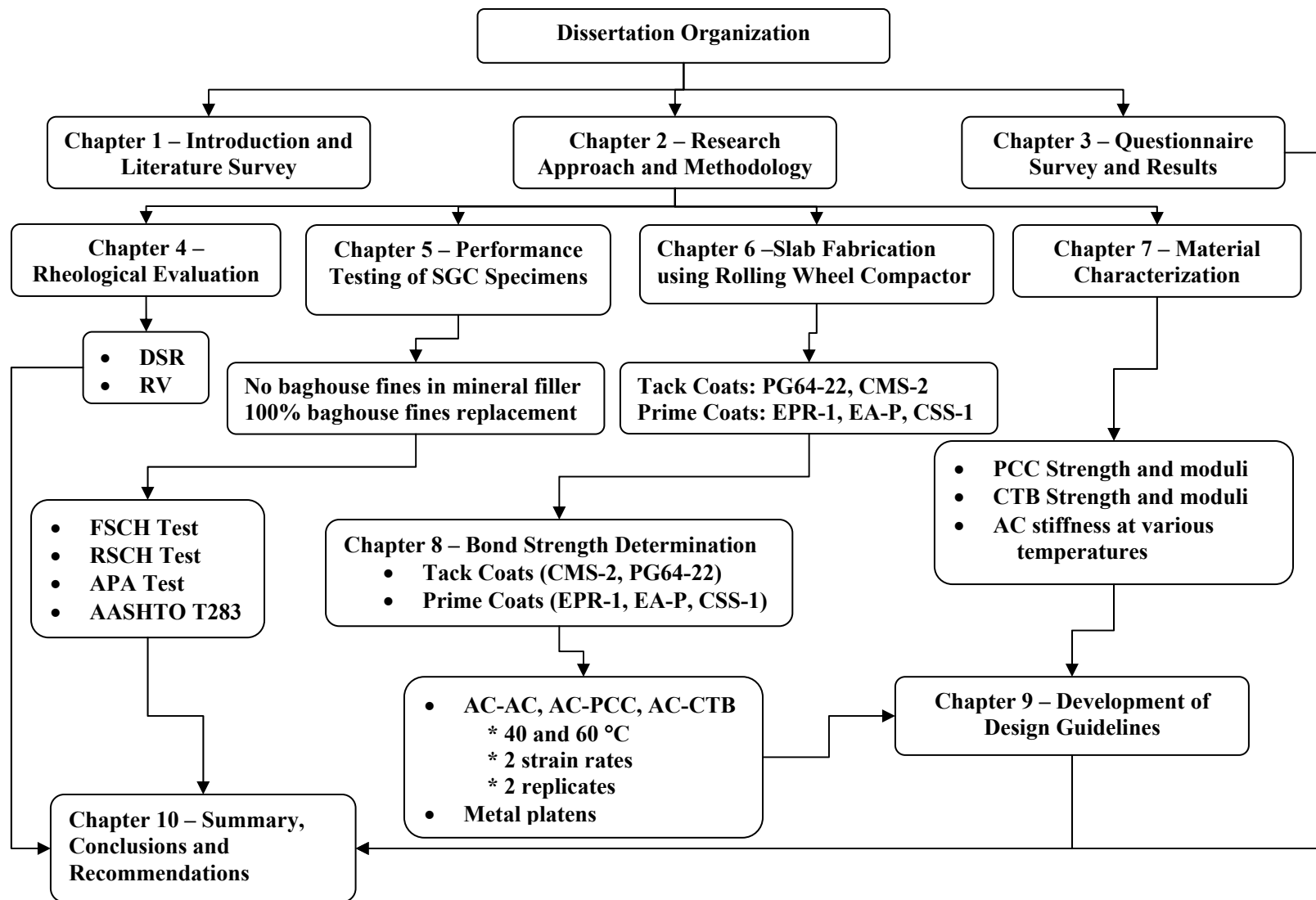


Figure 2-1 Summary of research outline and methodology

3 Survey Results

3.1 Development of Questionnaire

The goal of the current investigation was to examine the effect of various tack and prime coats on interface strength. In order to acquire the information regarding the use of different tack coats and prime coats in the field, it was necessary to conduct a survey of highway agencies. The expected outcome from the survey was to identify overall trends in prime and tack coating, and evaluate the scope for potential improvement.

The developed questionnaire (Appendix A) was sent to various state highway departments and agencies for their responses. Information collected was:

- whether prime coat was required for new construction,
- rate of its application,
- relation of prime coat to asphalt pavement thickness,
- curing time,
- laboratory tests for prime coats,
- field performance tests
- difference between pavements with and without prime coats,
- merits of emulsified asphalts versus cutback asphalts
- types of materials used for tack coats and their application rates, and
- provisions for emulsion breaking under nighttime paving conditions.

3.2 Survey Responses

In all more than 50 questionnaires were sent out and 26 replies have been received to date. The responses of the survey are summarized in Appendix B, and the observations are summarized below:

1. The following states responded to the questionnaire: Alabama, Alaska, Arkansas, Arizona, Connecticut, Florida, Georgia, Idaho, Illinois, Kansas, Kentucky, Maine, Minnesota, Mississippi, Missouri, Nebraska, New Hampshire, New Jersey, New York,

Oklahoma, Rhode Island, South Carolina, Tennessee, Texas, West Virginia, and Wyoming.

2. Ten of the 26 states reported that there is no requirement of prime coat for new construction of the pavement. Two highway agencies Oklahoma and Alaska leave it to the individual designers and mention that it depends on the location in the state.
3. Of the remaining sixteen states using prime coats, seven (AL, AR, NJ, WY, OK, and IL) reported using only cutbacks for prime coat as opposed to emulsions. For the remaining nine states, most of them used a combination of emulsions (diluted or undiluted) and cutbacks; there were states that preferred only emulsions, e.g. WV, CT, KY and TN.
4. For prime coats,
 - (a) Cutbacks that are currently used in practice are: MC-30, MC-70, MC-250, RC-30, RC-70, and RC-250; and
 - (b) The emulsions used are: AE-90, AE-150, AE-200, AE-P, CAE-P, CMS-2h, CSS-1, CSS-1h, EA-1, EAP-1, EAP&T, EP, EPR-1, MS-2h, PCE, SS-1, SS-1h and Primer-L.
5. In most of the cases, it was reported that cutbacks penetrated better than emulsions. The coverage offered by cutbacks was greater than emulsions. However, there were states that have noted the following in preference to emulsion over cutbacks as prime coats:
 - MS (emulsions, when applied properly, are easier to work with),
 - MO (emulsions have more pickup versus cutback),
 - IL (emulsions for resurfacing projects) and
 - TX (emulsions good for open bases)

The cutbacks did not have any curing problems and hence were preferred where it was not possible to wait for the emulsions to break.

6. The rates of application of the prime coat range from 0.03 to 3.44 gal/yd². In some cases, emulsions were diluted before applying thus reducing the concentration of the emulsion e.g. Florida. The rates of application depended on the type of base, as was the case with Mississippi and Alabama. For Maine, the rate was 0.02 gal/yd² for overlays, 0.04 gal/yd² for milled, and 0.01 gal/yd² for new mixes.
7. No specific basis was reported for the curing time of prime coats. In most of the cases, the states did not consider curing time. For those states that required curing, the criteria were subjective such as “tacky to touch” or duration ranging from 1 hour to 3 days. For

Oklahoma the condition was stated as “sufficient to allow proper penetration and hardening of prime coat,” which is quite difficult to assess without testing. Texas requires that the emulsions be worked into the top one inch of the layer and the layer re-compacted.

8. The thickness of the pavement layer has relatively no relevance to the required use of prime coat. Georgia and New Jersey require it if the AC thickness is 125-mm (5-inch) or less whereas the limit for Missouri is 100-mm (4-inch). Illinois requires prime coat only for full depth pavements. In spite of variation in the prime coat requirement, all agencies require it where either the thickness is too low or there are lot of horizontal shearing forces on the surface or where interlayer bond failure is likely to occur.
9. The laboratory tests needed to be performed on the emulsions and cutbacks are the viscosity tests (kinematic), distillation, solubility in trichloroethylene, residue test and float test. Most of the agencies do not have any field performance testing procedures or requirements.
10. While most of the agencies admitted that prime coat does improve performance, there were quite a few (50%) who did not see any difference in performance. Some of the reasons cited for better performance were:
 - (a) Water proofing and creating an impervious barrier to moisture.
 - (b) Erosion control of the base.
 - (c) Reduction in shearing and tearing of thinner pavements – less than 2-inch thick - on curves and on grades (Idaho). Less delamination and inability to separate the layers without a saw. In Oklahoma, absence of prime coat had lead to significant plane slippage problems.
 - (d) Ease of densification of SUPERPAVE™ mixes (New Jersey).
 - (e) Maintenance of optimal moisture content levels in the base thus maintaining the base strength at a constant level.
11. The materials used as tack coat are: AC, AE-60, CMS-1, C-70, C-250, C-800, CMS-2, CRS-1, CRS-2, CRS-2h, CSS-1, CSS-1h, HFE-60, HFE-90, HFMS-1, HFMS-2, HFMS-2h, HFMS-2s, MC-250, MC-800, MS-1, MS-2, MS-2h, PG58-22, PG64-22, PG67-22, RC-70, RC-T, RS-1, RS-2, SS-1, and SS-1h. Thus, a larger variety of materials can be

used as tack coats than prime coats. To reduce the concentration of asphalt, the emulsions used for tack coats were diluted with water before application.

12. Tack coats are applied at the rate of 0.03 - 0.2 gal/yd². In cases, where there was dilution with water, the effective rate of application is within the above range. In South Carolina, the rate of application is based on residual asphalt.
13. Nighttime paving: Most states require that the emulsion should break before the placement of new layer, there has been no concrete method to verify such condition. For a few states, the verification of the breaking of emulsion is done based either on touch - tacky touch - or by observation of the inspector. Some states (OK) disallow use of emulsions after sunset whereas states like Alabama are eliminating the use of emulsions because of difficulty in determining the state of the emulsion (broken or not).

In summary, more than 38% of the responding highway agencies do not require prime coats to be used, and some agencies only use it for relatively thin pavement sections (less than 4 to 5 inches). The current practice of using tack coat in the form of emulsion varies widely depending on the highway agencies. Clearly, there is a vast possibility of error in construction technique that may result in poor performance, especially for night time paving operations. Some of these difficulties have been mitigated by various highway agencies by substituting PG64-22 as a tacking agent over emulsion tack coats.

4 Rheological Evaluation

4.1 Introduction

One of the concerns with respect to asphalt mixtures in NCDOT Division 13 was with regards to the variable amount of baghouse fines purged intermittently in the production of the field mixtures. This chapter deals with:

- the evaluation of the gradation of baghouse fines using the state-of-the-art particle analyzer at FHWA Turner Fairbank Highway Research Center;
- the influence of fines on the rheological properties of asphalt cement using mastics was also evaluated using the DSR; and
- the properties of residual asphalts and emulsions

4.2 Selection of Fines

For this study, the mineral filler and baghouse fines with materials passing #200 sieve were obtained from Buncombe and Rutherford counties. The fines selected for analysis were:

- Buncombe County:
 - passing #200 sieve fraction from wet screenings
 - baghouse fines
- Rutherford County
 - Passing #200 sieve fraction from dry screenings
 - 'fine' baghouse fines
 - 'coarse' baghouse fines.

In all, five different types of fines were analyzed using the particle analyzer.

4.3 Gradation Analysis of Fines using FHWA Particle Analyzer

4.3.1 Method Description

The gradation analysis of mineral fillers was carried out at the Turner Fairbank Highway Research Center, McLean, Virginia. The material was separated using a small splitter, then further separated using a micro splitter, to obtain a representative sample. To run the test, a small amount of material was mixed in a medium to create a suspension. For baghouse fines, distilled water with 1-percent sodium hexametaphosphate was used.

The testing process consisted of taking a ‘blank’ measurement of the medium to establish a baseline. The material was then slowly introduced and mixed with the medium until an ‘optimum’ intensity was found. In order to prevent particle agglomeration, agitation by cavitation was induced by a high intensity ultrasonic processor for 2 minutes. The particle analyzer automatically converted different light intensity measurements into particle size distribution. The average of three different samples was obtained and the results were found to be consistent with each other. The results, however, necessarily need not match with the sieve analysis. The main reason for this is the fact that the gradation obtained from the laser particle analyzer is a volume gradation based on the projection of particles. The device showed the differences that were otherwise difficult to capture.

4.3.2 Results and Discussion

In all two sets of analyses were performed within the duration of this study. Figure 4-1 and Figure 4-2 show the gradations of the mineral fillers and bag-house fines obtained from the two counties. Figure 4-2 presents the particle analysis performed on the first set of fines received before the entire set of materials was requested so that a decision could be made about the further analysis to be performed. Figure 4-1 presents the particle size analysis that was carried out on fines received in the latter batch of materials from which the samples for laboratory testing were actually fabricated.

For Rutherford County, the ‘coarse’ baghouse fines appeared to be ‘sandy’ and hence their size distribution was measured using a slightly more viscous medium. The two media used for Rutherford County ‘coarse’ bag-house fines were distilled water (W) and 90-percent

distilled water plus 10-percent glycerin (G). In Figure 4-2, the particle analysis results using the two different media are fairly different. However, both media show that this sample is the coarsest.

Figure 4-1 and Figure 4-2 show that the ‘coarse’ baghouse fines from Rutherford County is the coarsest material passing #200 sieve. Although it was anticipated that the baghouse fines, in general, would be finer than the regular fines passing #200 sieve, the particle size analysis indicated for both set of materials that the baghouse fines from both counties had more or less similar particle size distribution as the regular fines. Table 4-1 shows the properties of the fines based on the second set of materials which was used for mixture performance testing in this study. The mean particle size of regular fines from Buncombe and Rutherford counties are both 30.5- μm . The baghouse fines from Buncombe County has the mean particle size 40- μm and the Rutherford County ‘fine’ baghouse fines has a mean particle size of 31- μm . The ‘coarse’ baghouse fines from Rutherford County have a mean particle size of 88- μm , more than twice the mean size of any other regular or baghouse fines.

The particle size analysis suggests that based on gradation, the mixture performance should not be affected whether the mineral filler used is regular fines or from baghouses. However, as the particle shape and/or perhaps the mineral content distribution may be different for the baghouse fines, it may have different effect on the rheological behavior of the asphalt cement and mixtures in general. This effect is investigated in the following section where the performance of baghouse and regular fines are studied using asphalt-fines mastics in an aged and unaged condition. In Chapter 5, this effect is also evaluated based on the performance of the asphalt mixtures.

4.4 Analysis of Asphalt-Fines Mastics using DSR

The objective of this task was to evaluate the rheological properties of the binders and mastics containing baghouse fines at intermediate to high temperatures. Testing was conducted in accordance with AASHTO TP5-93 [4].

4.4.1 Specimen Preparation

The asphalt cement used for the preparation of mastics was a PG64-22 supplied by NCDOT. Four mastics were prepared using the fines received from Buncombe and Rutherford counties. The asphalt cements and each of the mastics were tested in an unaged and aged condition with at least three replicates. The following asphalt and mastic combinations were used:

- PG64-22 binder (virgin and RTFO-aged) for both counties
- Mastic (virgin and aged) from the baghouse fines. Only the ‘fine’ baghouse fines was used from Rutherford County.
- Mastic (virgin and aged) from the regular mineral filler (fraction passing #200 sieve) from both counties.

The prepared mastic was a mixture of the filler/fines with asphalt from the corresponding county. The proportion of asphalt was 50-percent by weight of the total mastic. For preparation of mastics, the fines and the asphalt binder were pre-heated to a temperature of 160 °C. The fines were then added slowly to the heated binder with constant stirring until uniform, consistent agglomerate free ‘batter’ was obtained.

The asphalt binders were aged in an RTFO oven, while the mastics were aged in an air draft oven due to the higher consistency of the mastics. Due to high consistency of mastics, problems were encountered in recovery from the RTFO bottles. The mastics, therefore, were poured in a PAV dish and were kept in an oven for a period of 85 minutes at 163 °C for aging to simulate the RTFO aging effect. One problem encountered with handling the mastics was segregation of fines. Hence while pouring into the molds; it was necessary to stir vigorously so as to have a uniform consistency for the DSR specimens.

4.4.2 Test Parameters

The asphalt cement and mastics were evaluated at three temperatures – 58, 64, and 70 °C. For the asphalt binder, the DSR spindle diameter of 25-mm with 1-mm gap was used. As the mastics were more viscous, a spindle diameter of 8-mm with 2-mm gap was used.

Testing at 10 rad/s frequency and at different strain levels (strain sweep) was conducted to establish for each asphalt binder and mastic, the linear viscoelastic region in the strain domain (defined by AASHTO TP5 to be a range of strain values where the test measurement $|G^*|$ does not vary more than 95-percent of the $|G^*|$ estimated at zero strain). Based on the strain sweep test, the strain level for unaged and aged binders selected was 12 and 10-percent, respectively. For the mastics, the strain levels selected were typically in the range of 1 to 2-percent for both aged and unaged binders.

Frequency sweep tests were conducted on the asphalt binders and mastics at the frequencies of 0.01, 0.05, 0.1, 0.15, 0.5, 1.0, 1.59, 5.0, 10.0 and 20.0 Hz. The measured parameters from the test results were the dynamic shear modulus $|G^*|$ and phase angle δ . These results were then used to generate master curves at 64°C for dynamic shear modulus $|G^*|$ and $|G^*|/\sin\delta$.

4.4.3 Test Results and Discussion

Figure 4-3 and Figure 4-4 show the dynamic shear modulus as function of reduced frequency at 64 °C for Buncombe and Rutherford counties. The raw DSR testing data is presented in Appendix E. These figures show that in general:

- 1) aging tends to increase the $|G^*|$ values for both the asphalt binder and the mastics as compared to the unaged condition;
- 2) $|G^*|$ values for the mastics are much higher than the asphalt binder (this trend is expected as the mastics contain 50-percent fines);
- 3) in case of Buncombe County, the mastic containing baghouse fines have higher $|G^*|$ values over the range in frequency as compared to the mastic containing regular mineral filler material;
- 4) in case of Rutherford County, the mastic containing baghouse fines show similar $|G^*|$ values over the range in frequency as compared to the mastic containing regular mineral filler material.

Figure 4-5 through Figure 4-8 show the Superpave rutting parameter, $|G^*|/\sin\delta$, as function of reduced frequency at 64°C. For Buncombe County, mastic containing baghouse fines shows higher $|G^*|/\sin\delta$ values both in aged and unaged condition as compared to the mastic containing regular fines. For Rutherford County, the mastic containing baghouse fines shows higher $|G^*|/\sin\delta$ values in unaged condition but about similar values in aged condition compared to the mastic containing regular fines.

In summary, therefore, it appears that Buncombe County baghouse fines show different effect on aging of asphalt as compared to the Rutherford County baghouse fines.

4.5 DSR Testing of Emulsions

In order to evaluate the properties of the residual binders in the emulsions, DSR testing was conducted. As emulsions contain a large amount of water, they were broken prior to being tested in the DSR. The following two approaches were used to break the emulsions:

- *Rolling Thin Film Oven:*

The rolling thin film oven, commonly referred to as RTFO, is commonly used to simulate the short term aging of asphalt in laboratory. Although the oven uses a temperature of 163 °C for testing purposes, the emulsions were broken in RTFO at lower temperature of 85 °C to prevent excessive aging of AC. At the end of the 85 minute test it was found that there was substantial presence of moisture indicated by soft and fluid nature of residual asphalt as well as by presence of typical brown coloration on the inner walls of the RTFO bottles. In the second round, the RTFO temperatures were increased to 105 °C, however there was not a significant improvement in the results.

- *Open heating:*

Due to non-conclusive outcome of the earlier approach, it was decided to break the emulsions using the shallow, flat pressure aging vessel (PAV) pans. The heating temperature was raised to 135 °C (to ensure complete evaporation of water component) with constant stirring at regular intervals (roughly 15 minutes). The total heating period was 85 minutes, same as the duration of the RTFO test. The temperature of 135 °C was chosen because it is the highest temperature that asphalt can be subjected to without a

significant risk of aging. Most of the emulsions broke satisfactorily using this approach. The emulsion EA-P, however, did not break because of its polymeric nature. This emulsion, therefore, was heated to a temperature of 155 °C and it broke after extensive heating for 2 hours.

The DSR testing was carried out on the residual binders at the following temperatures: 52, 58, 64 and 70 °C. Using a 25-mm diameter spindle and 1-mm thick specimens, the testing was carried out at a frequency of 1.592 Hz. Two tests were performed: a stress sweep test to determine the linear range of the binder and an oscillation test at 1.592 Hz.

4.5.1 Test Results and Discussion

The results are summarized in Figure 4-9 through Figure 4-11 and Table 4-2. The following conclusions can be drawn:

1. It can be seen that with increase in temperature, there is a continuous fall in $|G^*|/\sin\delta$ values. The results yield a straight line when plotted on a log-linear scale. All the curves had an R^2 value of one indicating a very good fit.
2. The CRS-1H is the hardest (stiffest) residual binder and the CMS-2 has the softest residual binder of all. These results are as expected.
3. The testing of CRS-1H binder posed problems at a temperature of 52 °C because the binder was too stiff. The deformation caused by the applied stresses was too small to be accurately recorded by the DSR.
4. The residual binders of CRS-1H, EA-P and I.A.S. emulsions have a ‘reported’ high temperature PG rating of PG70 but their actual PG ratings are PG73.7, PG74.7 and PG70.7 respectively. Similarly, CRS-Koch has a ‘reported PG rating’ of PG64 but the actual PG rating is PG65.1 and CMS-2 has a ‘reported PG rating’ of PG52 but the actual PG rating is PG57.1. The DSR testing, therefore, provides a more accurate classification of the emulsions. Thus, the emulsions can be listed in the following order (of decreasing stiffness):
 - CRS-1H
 - EA-P
 - I.A.S.

- CRS-Koch, and
 - CMS-2.
5. The polymeric nature of the EA-P emulsion, combined with the high ‘actual PG grade’ of residual binder, explains the stability of the emulsion at elevated temperatures.
 6. Based on the DSR results, it can be hypothesized that the tacking strength of the emulsions would be directly proportional to their respective PG temperatures.

4.6 Brookfield Viscosity

A rotational viscometer determines the flow characteristics of the asphalt binder and its ability to be pumped and handled at the hot mix plant. Testing of binders was conducted in accordance with ASTM D4402 (Standard Method for Viscosity Determinations of Unfilled Asphalts using the Brookfield Thermosel Apparatus). It measures the amount of torque required to maintain a constant speed of a cylindrical spindle immersed in liquid binder at a given temperature. The number of replicates for Brookfield Viscometer testing was three. The testing was carried out at two temperatures of 150 and 135 °C.

From Figure 4-12 through Figure 4-14, it can be seen that the EA-P emulsion exhibits a rapid decrease in viscosity compared to other emulsions. Further, CRS-1 and CMS-2 emulsions have relatively similar consistency at 150 and 135 °C whereas for all other emulsions under consideration, there is a rapid drop in viscosity with increase in temperature. This could suggest that CRS-1 and CMS-2 are preferable compared to their counterparts. This is further reinforced by the fact that their viscosities are relatively independent of the spindle RPM. The CRS-1H and IAS emulsions have comparable values however, IAS seems more temperature susceptible than CRS-1H. Based on the test results, the acceptability in the order of preference is CMS-2, CRS-1, CRS-1H, IAS and EA-P.

4.7 Conclusions

It was originally hypothesized that the one of the contributory factor to the delamination and shoving distress observed in Buncombe County was the intermittent purging of the baghouse fines in the field asphalt mixes. Results of the gradation analysis show that the baghouse fines have similar, or in some cases coarser, gradation as compared

to the regular mineral filler used in these respective counties. The dynamic mechanical analysis of the mastics using the DSR suggests that inclusion of baghouse fines in asphalt mixtures may not have any detrimental effect. On the contrary, for Buncombe County, the inclusion of baghouse fines appears to enhance the rut resistance of the asphalt mixture as will be shown to be the case in Chapter 5. However, the effect of moisture sensitivity on the mixtures containing baghouse fines needs to be evaluated before any final conclusion can be made.

Table 4-1 Properties of fines from particle size analysis (set 2) [13]

Particle Property	Buncombe Baghouses	Buncombe Passing #200	Rutherford 'Coarse' Fines	Rutherford 'Fine' Fines	Rutherford Passing #200
Fineness Modulus (F.M.)	5.72	5.40	7.10	5.43	5.31
Coefficient of Uniformity (C_U)	10.20	7.60	4.00	9.11	8.67
Coefficient of Curvature (C_C)	1.73	2.15	1.72	1.96	2.28
Skewness Indicator (σ_1)	2.25	2.31	1.14	2.60	2.30
Skewness Indicator (σ_2)	4.40	2.90	2.75	3.88	3.59
Mean Particle Size (μm)	40.0	30.5	88.0	31.0	30.5

Table 4-2 Temperatures for residual binders when $|G^*|/\sin\delta \geq 1.0$ kPa

Emulsion	Temp. (°C)	PG rating
CRS-1H	73.7	PG70
EA-P	74.7	PG70
IAS ¹	70.7	PG70
CRS-Koch	65.1	PG64
CMS-2	57.1	PG52

¹ The testing was performed at **four** temperatures and the results were extrapolated to determine the appropriate 1-kPa temperature. Extra testing was not felt necessary because the results were almost a straight line when graphed.

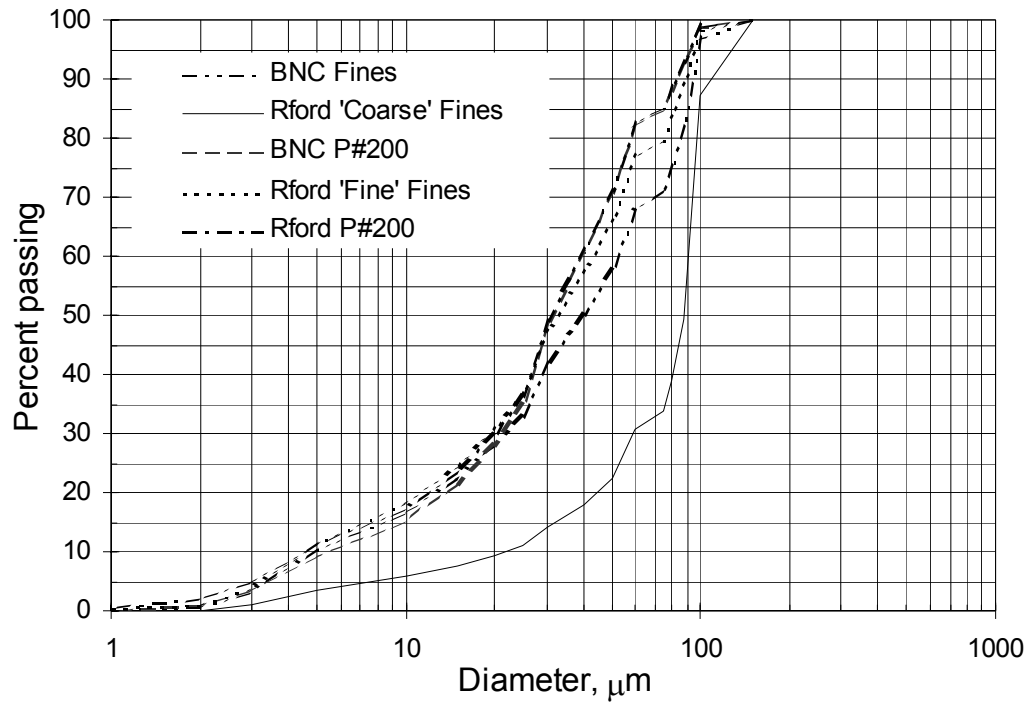


Figure 4-1 Gradation analysis of fines using FHWA particle analyzer, set 2

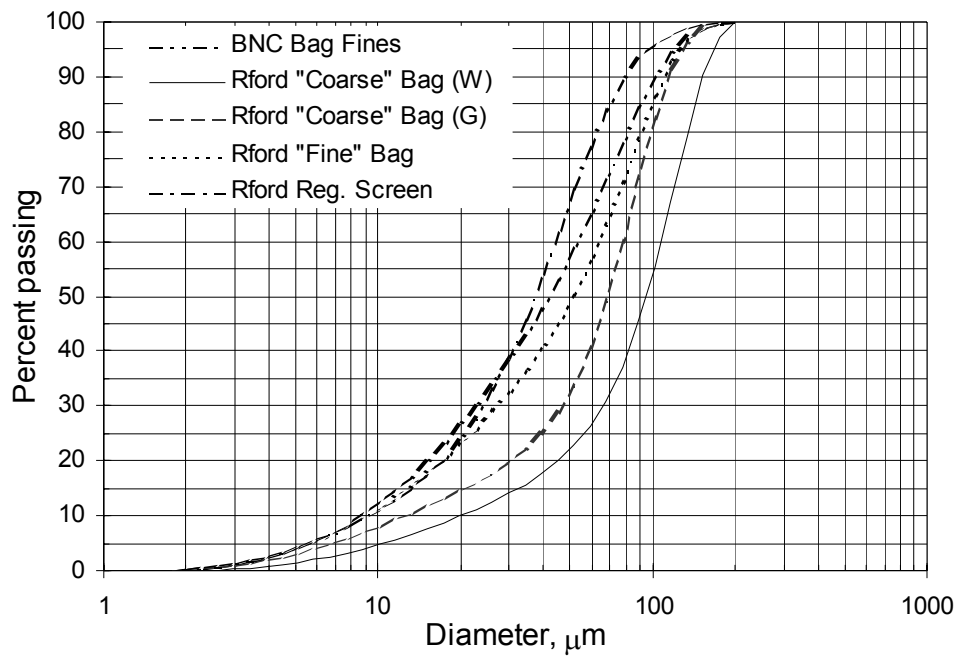


Figure 4-2 Gradation analysis of fines using FHWA particle analyzer, set 1

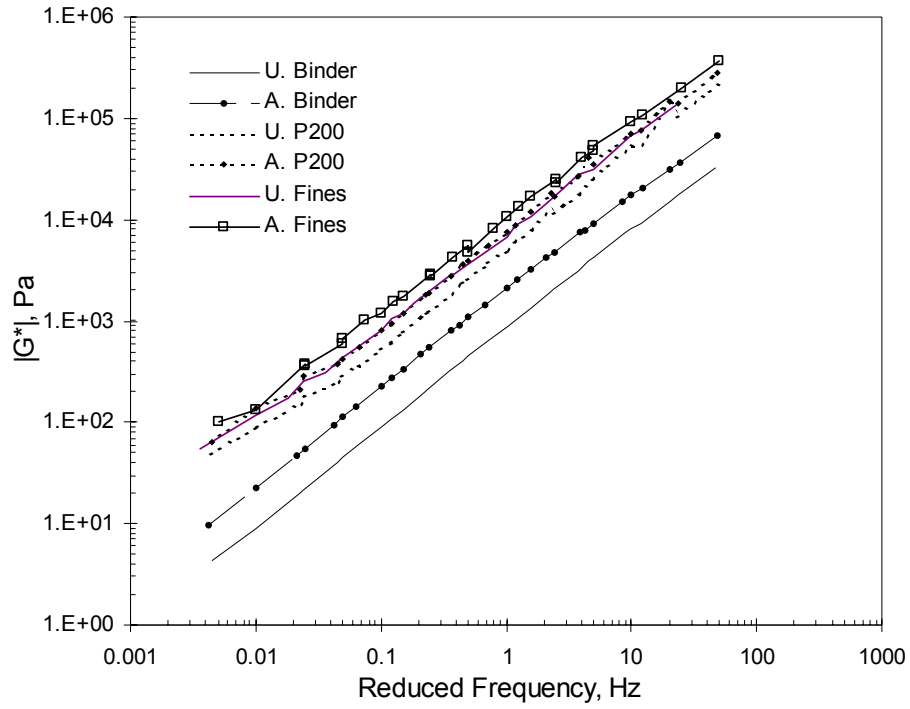


Figure 4-3 Master curves ($|G^*|$) for Buncombe County, 64 °C

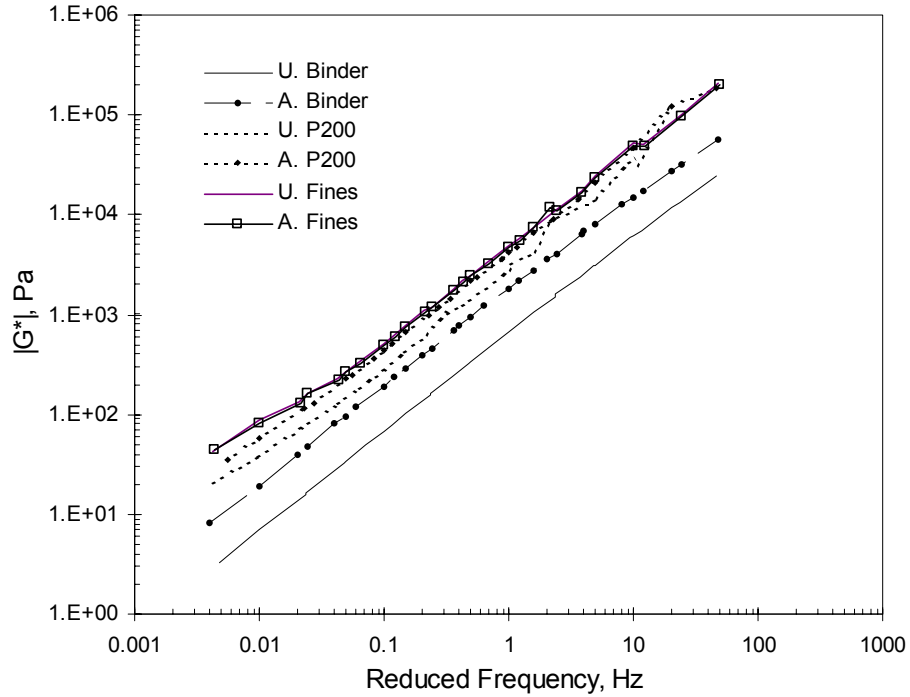


Figure 4-4 Master curves ($|G^*|$) for Rutherford County, 64 °C

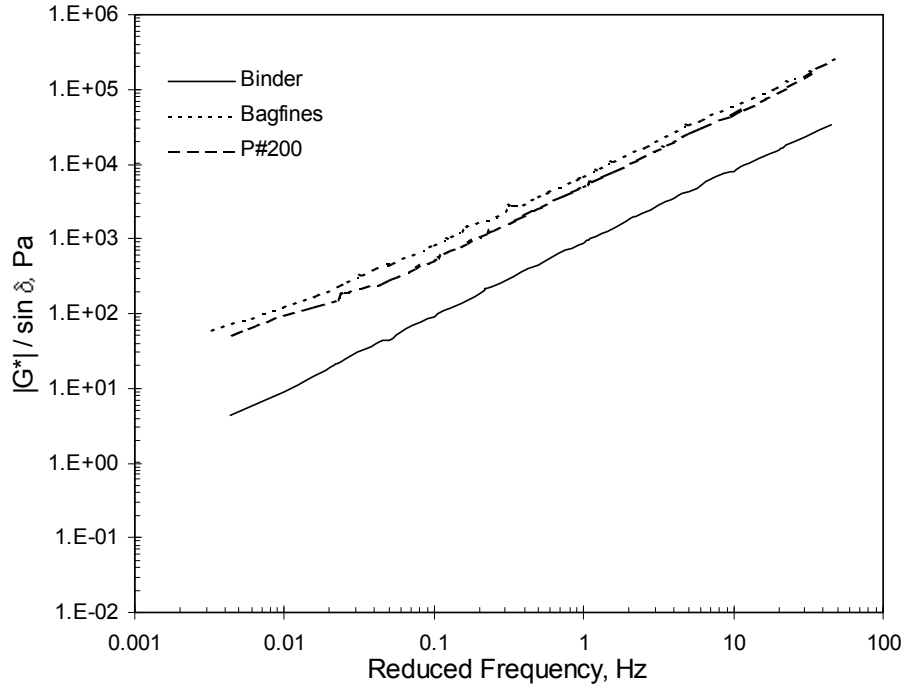


Figure 4-5 Master curves ($|G^*|/\sin \delta$) for Buncombe County, unaged, 64 °C

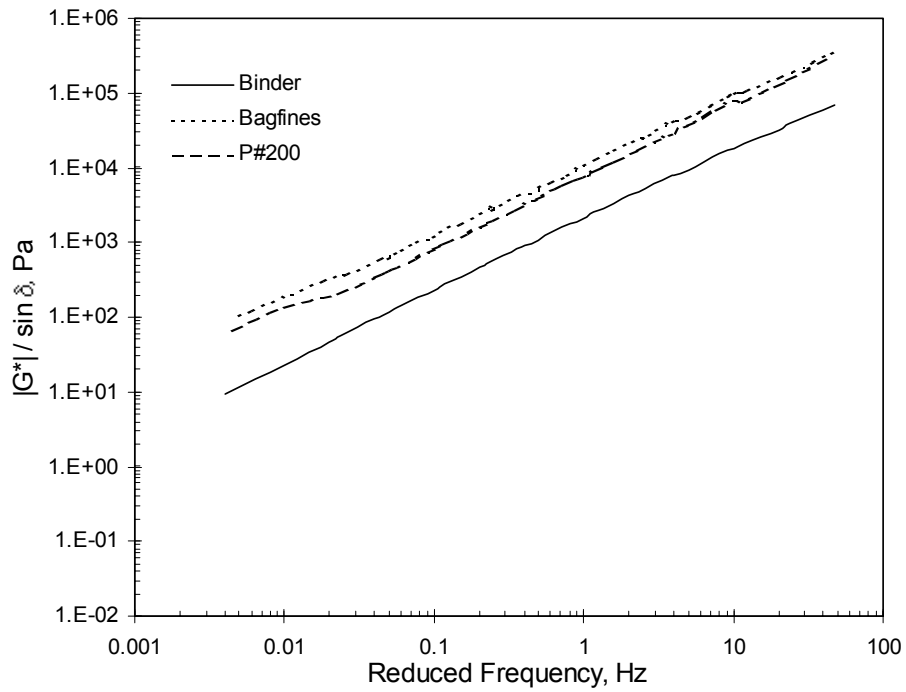


Figure 4-6 Master curves ($|G^*|/\sin \delta$) for Buncombe County, aged, 64 °C

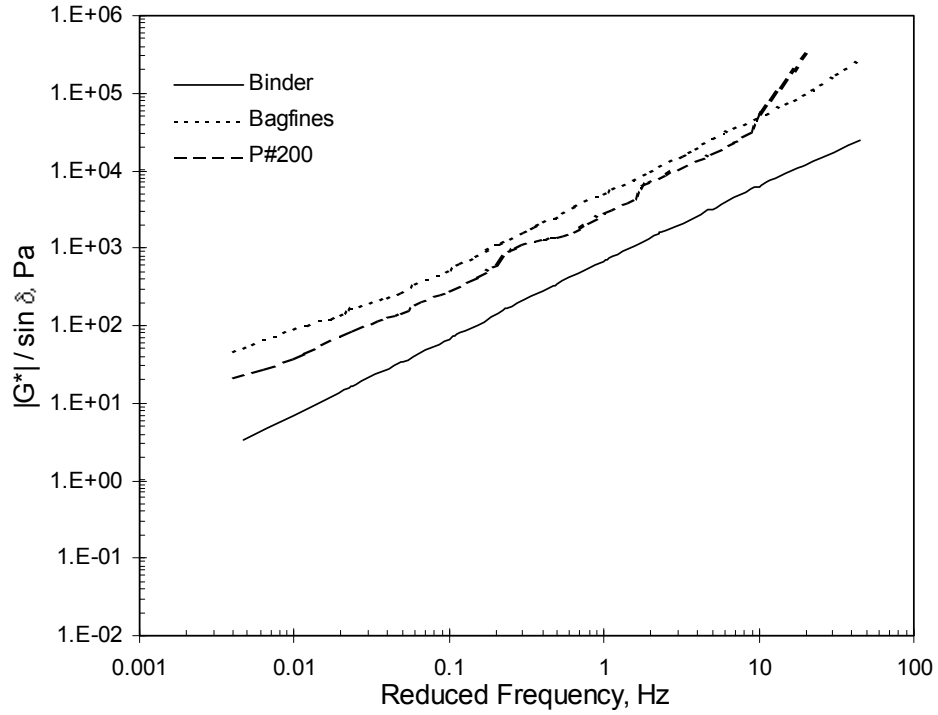


Figure 4-7 Master curves ($|G^*|/\sin \delta$) for Rutherford County, unaged, 64 °C

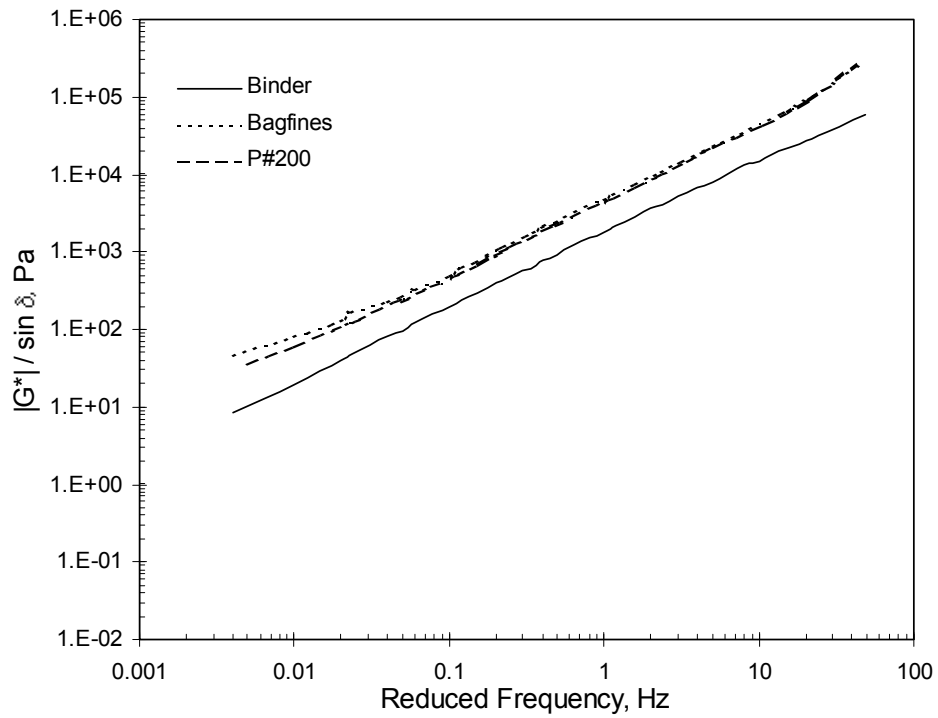


Figure 4-8 Master curves ($|G^*|/\sin \delta$) for Rutherford County, aged, 64 °C

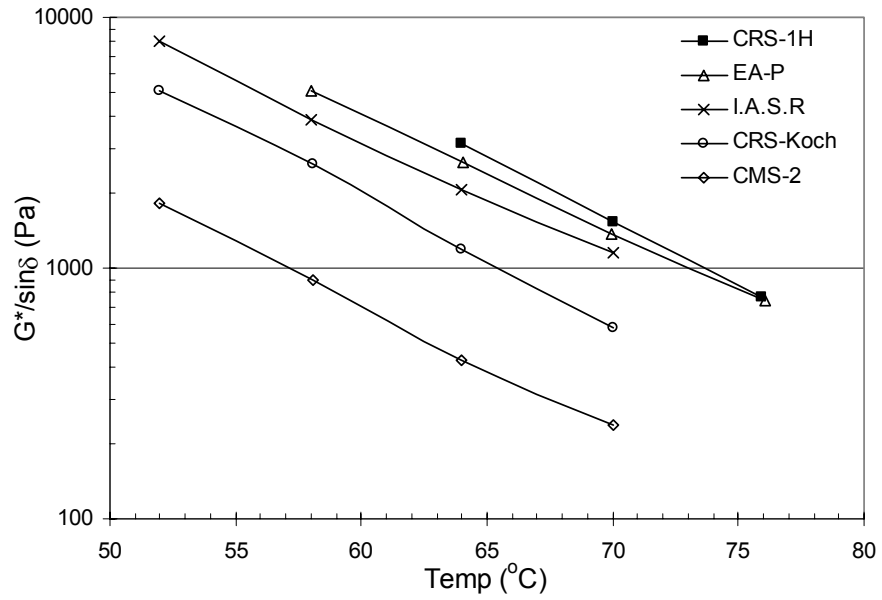


Figure 4-9 Comparison of $|G^*/\sin \delta|$ at various temperatures for residual binders

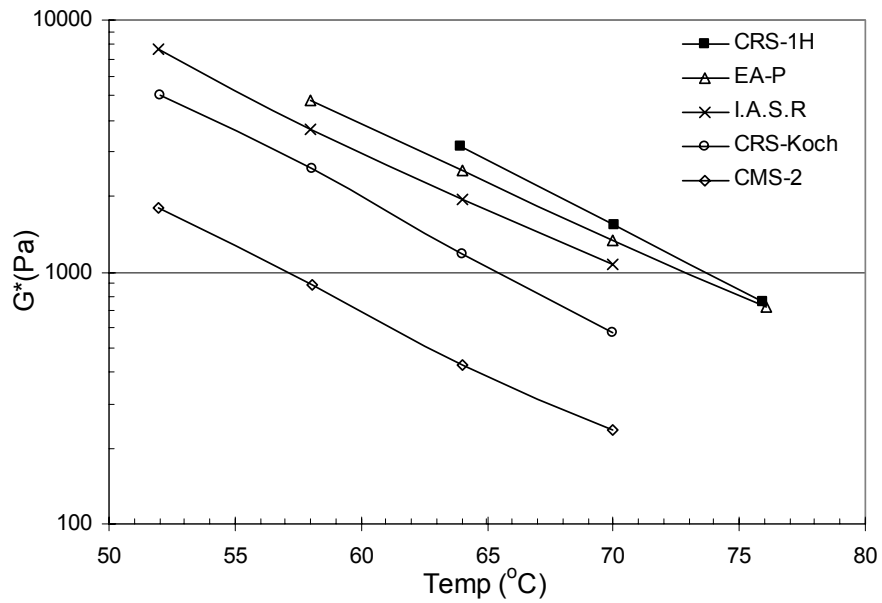


Figure 4-10 Comparison of $|G^*|$ at various temperatures for residual binders

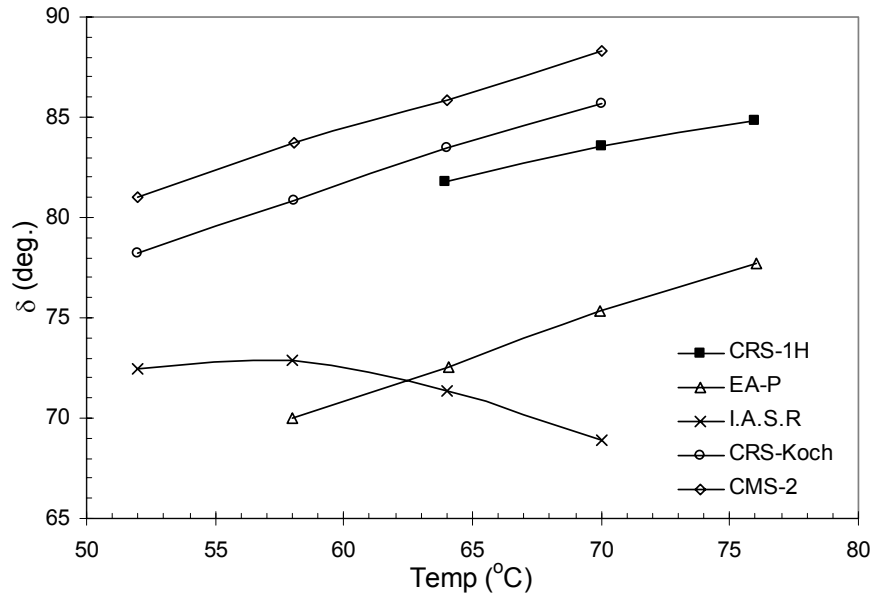


Figure 4-11 Comparison of δ at various temperatures for residual binders

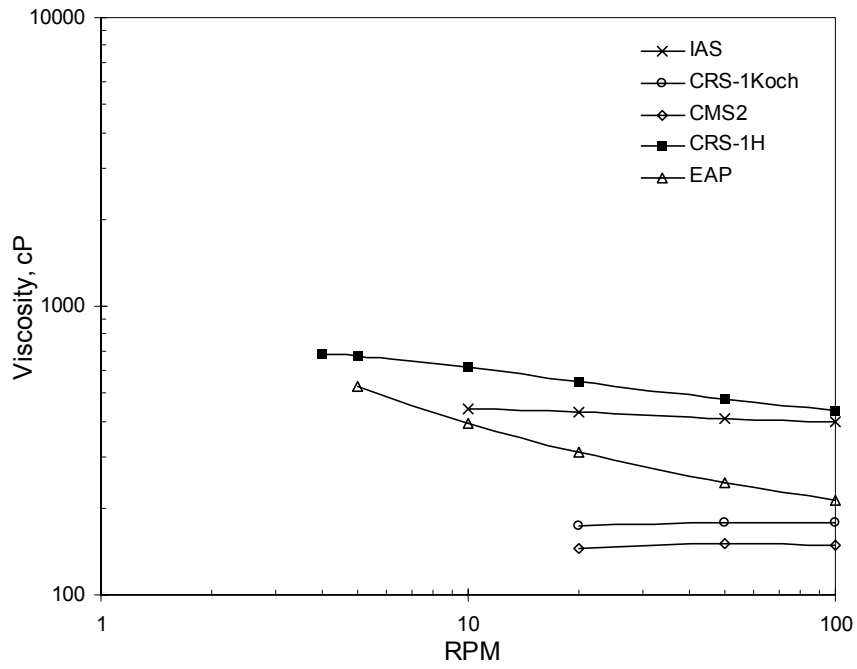


Figure 4-12 Viscosity vs. RPM, 150 °C

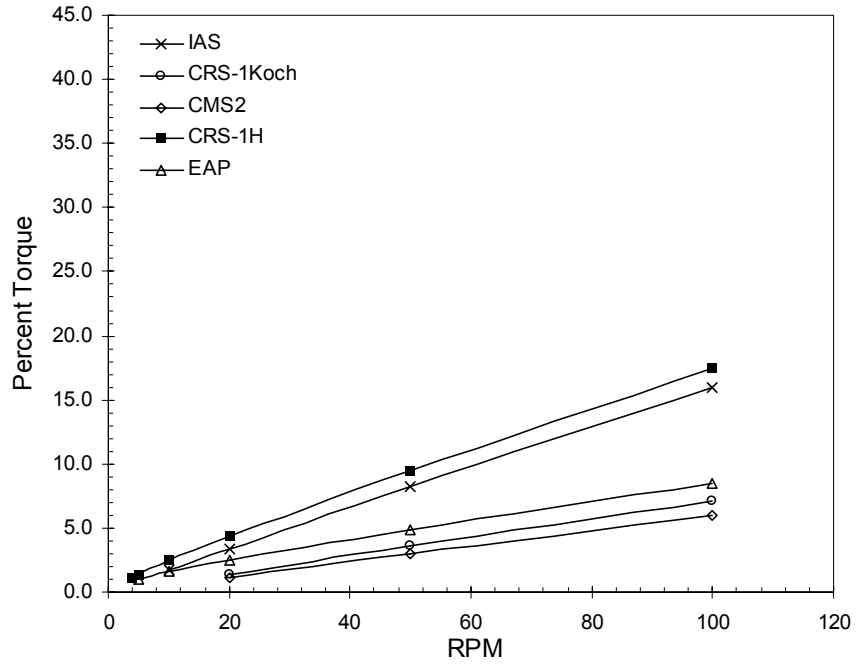


Figure 4-13 Percent torque vs. RPM, 150 °C

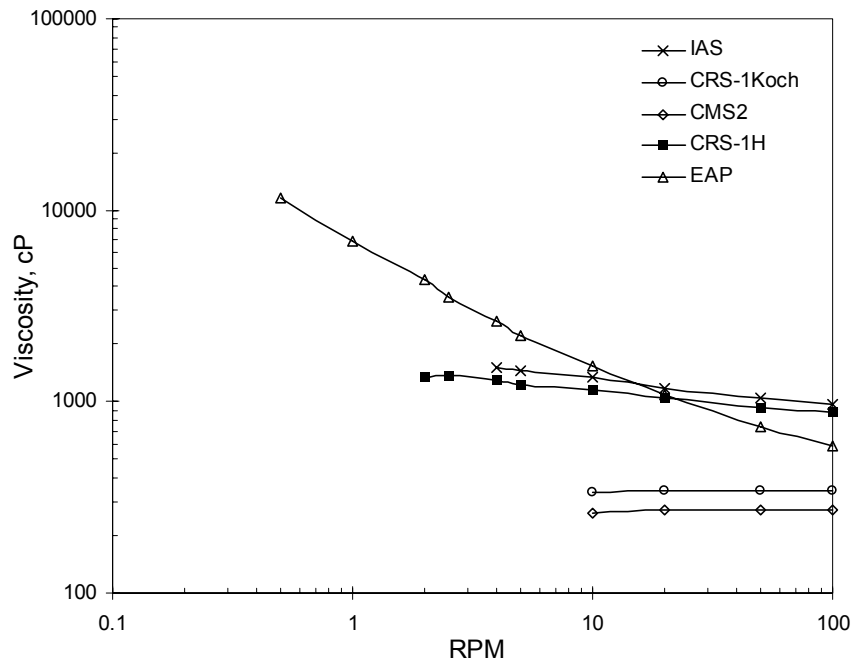


Figure 4-14 Viscosity vs. RPM, 135 °C

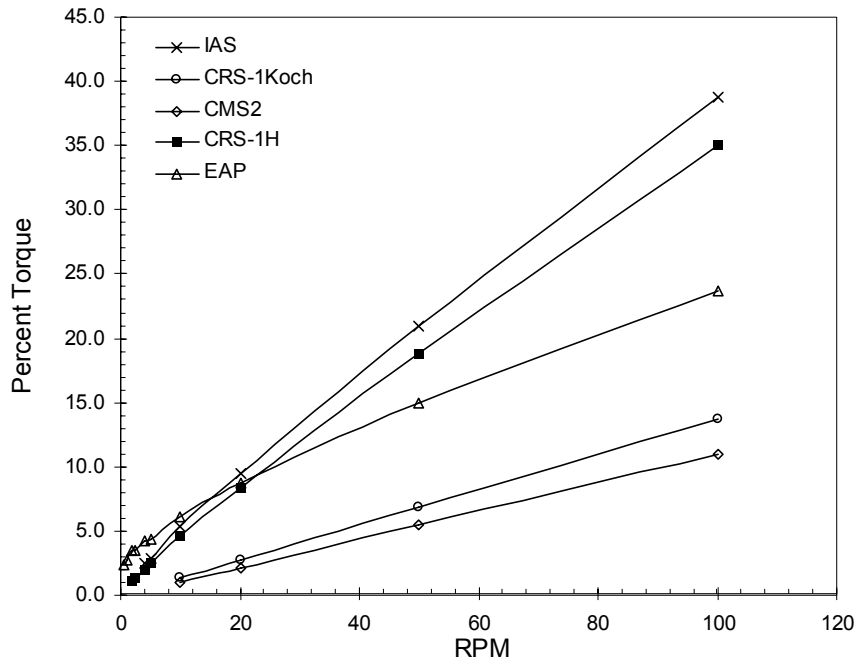


Figure 4-15 Percent torque vs. RPM, 135 °C

5 Performance Testing of SGC Specimens

5.1 Introduction

The main objective of this task was to compare the performance of laboratory samples, prepared with baghouse fines and regular filler. The specimens were compacted using the Superpave Gyrotory Compactor (SGC). These samples were tested for performance characteristics using SST, APA and TSR moisture sensitivity tests.

5.2 Test Parameters

For a given test system, the results of the performance test are governed by several parameters including reliability and repeatability of the test system, and the mix and test parameters. For the mix parameters, the asphalt type and content, and the aggregate type and gradation was fixed based on the job mix formula for the given pavement section. The only mix parameter that varied was the air void content of the laboratory mixes. Table 5-1 shows the air void content of the laboratory prepared specimens with and without the baghouse fines. For these mixes, the air void content of 5 ± 0.5 -percent was targeted based on the JMF requirement of 5-percent voids.

The major test parameters considered in this study were: 1) test temperature, 2) applied stress or strain, 3) test frequency, and 4) test duration. As per the research methodology presented in Chapter 2, the following tests were conducted on laboratory mixes from both Buncombe and Rutherford counties with testing broadly classified in the following two categories:

- Shear testing
 - FSCH (Frequency Sweep at Constant Height Test)
 - RSCH (Repeated Shear at Constant Height Test)
- APA test
- TSR tests

The shear testing consisted of a shear frequency sweep at constant height (FSCH) and repeated shear at constant height (RSCH) tests. Each of these test methods is described in the latter sections. Laboratory specimens 150-mm in diameter were compacted using the SGC and were sawed to the required height of 50 mm.

5.3 Test Temperature

5.3.1 Selection of Testing Temperature

Temperature plays an important role in the design of asphalt mixes. The properties of binder depend significantly on the temperature and, consequently, the mix properties such as resistance to rutting and fatigue vary with temperature. In order to evaluate the load associated performance of the pavement it is imperative that the testing be carried out at a temperature representing the actual field conditions. One of the procedures for determining the pavement temperatures is recommended by AASHTO TP7 - Procedure F (Repeated Shear at Constant Height Test) [5]. This procedure requires conducting the RSCH test at the maximum seven-day pavement temperature at the selected pavement depth. The recommended depth at which the maximum seven-day pavement temperature is calculated is 20-mm from the top surface. The data for this temperature is normally obtained from the weather data at the paving site using the SHRPBIND program [22] developed within the SUPERPAVE™ program.

5.3.2 Temperature Zones

SHRP report (SHRP-A-415) [23] outlines an elaborate procedure for computing the critical and maximum pavement temperatures. It has divided the continental United States into nine climatic regions based on the temperature and humidity of the soils. The nine temperature zones are shown in Figure 5-1. Table 5-2 lists the effective, maximum, and critical temperatures for the nine zones as reported in SHRP-A-415 [23]. The effective temperature is the temperature at which loading damage accumulates at the same average rate in service as in laboratory. Thus, there is a one-to-one correspondence between the laboratory and in-service loading cycles at the effective temperature. The critical temperature

is the temperature at which the maximum amount of damage occurs in service. This temperature can be considered as an ideal temperature for laboratory testing because it minimizes errors due to variations in the mix temperature sensitivity due to its accelerated rate of damage accumulation. North Carolina falls in regions IB and IC with both Buncombe and Rutherford counties being in region IC with critical and maximum temperatures in the range of 35 to 38 °C.

5.3.3 Selection of Depth for Computation of Testing Temperature

The job mix formulae for the mixes from both the counties indicated that there were two 50-mm lifts of HDS asphalt course. Ideally, the testing temperatures for mixes from both the counties should have been 38 °C, but the actual layer thickness' are much lower than 50-mm. The average depths to the uppermost interface measured from the field core surfaces are summarized in Table 5-3 for both counties. Since the parameters under investigation were the tack coat properties, it was necessary that the laboratory test temperature corresponded to that of the tack coats in the field. Consequently, testing temperatures were selected corresponding to the depth of the tack coat (approximately 33-mm for both counties).

5.3.4 Reliability Factors

AASHTO provisional standard TP-7 [5] specifies that the RSCH test be conducted at the maximum seven-day pavement temperature for the selected depth. However, it does not specify the reliability level at which this temperature should be computed. A reliability level of 50-percent was selected for this study.

5.3.5 Temperature Selection Method

The seven-day maximum air temperatures were computed based on the following equations used within the SHRPBIND [22] software:

$$T_{surf} - T_{air} = -0.00618 \times (lat.)^2 + 0.2289 \times (lat.) + 24.4 \quad \text{(Equation 5-1)}$$

Where T_{surf} and T_{air} are the air and surface temperatures respectively in degree Celsius and $lat.$ is the latitude in degrees. From the surface temperature, the pavement temperature is computed using:

$$T_d = T_{surf} \times (1 - 0.063 \times d + 0.007 \times d^2 - 0.0004 \times d^3) \quad \text{(Equation 5-2)}$$

Where T_d and T_{air} are the temperatures at depth d and at surface, respectively, in °F with the depth, d , in inches. In this study, the pavement temperatures were calculated by two different ways. In the first method, the temperature was calculated at the required depth from the air temperature using Equations 5-1 and 5-2. In the second method, the pavement temperature was calculated using the SHRPBIND program. It was found that the temperatures calculated by the two different methods differed by approximately 3 °C. Hence, an average of the two was taken as the critical test temperature. Table 5-3 summarizes the temperatures calculated by the two methods.

Based on an average value, the testing temperatures for Buncombe and Rutherford counties were 50.2 and 54.0 °C, respectively at 33-mm depth and 50-percent reliability. However, in order to compare different tack coats (CRS-2.5 and PG64-22) a single test temperature of 50.2 °C was selected.

5.4 Performance Test Results of Lab Mixes with Baghouse Fines

The objective of this task was to evaluate the effect of baghouse fines on laboratory mixes. Laboratory specimens were fabricated using the SGC. Performance of the specimens containing baghouse fines versus crushed mineral filler (passing #200 sieve) was evaluated using the FSCH and the RSCH tests.

5.4.1 Specimen Fabrication

The specimens were fabricated using the SGC (Superpave Gyrotory Compactor). The aggregates received from NCDOT were separated into various fractions depending on their

sieve sizes and were then blended to the appropriate NCDOT specified JMF (Appendix C) gradations. The exception to this procedure (of separating into various fractions and blending) was that the Rutherford County sand and all the baghouse fines, which were added in bulk as received. Specimens with zero percent baghouse fines were fabricated with mineral filler (fraction passing #200 sieve) whereas, specimens with 100% baghouses had their fraction passing #200 sieve substituted completely by the baghouse fines. For Rutherford County, there were two types of baghouses: the 'fine' baghouse fines and the 'coarse' baghouse fines. For the purpose of laboratory testing, only the 'fine' baghouse fines were used. The asphalt contents for Rutherford and Buncombe Counties were 6.2 and 5.7-percent, respectively, and the non-strip additive requirement was 0.5-percent for both the counties.

The mixing and compaction was carried out at a temperature of 285 °F, and before compaction, the mixes were aged at a temperature of 275 °F for 2 hours. The 6-inch diameter RSCH test specimens were compacted to a height of approximately 3-inches with target air voids of 5±1-percent. Both ends were then sawed to achieve the required height of 2-inches. Table 5-1 shows the air voids content of the specimens used for the RSCH test. It may be noted that the specimen identification for Buncombe and Rutherford counties consists 'W' for the specimens containing baghouse fines, and 'WO' for specimens without the baghouse fines.

5.4.2 FSCH Test

The FSCH test measures the viscoelastic shear properties (dynamic shear modulus, $|G^*|$ and the phase shift, δ) over a range of testing frequencies and at different temperatures. Testing is conducted in a semi-confined condition in which the specimen dilation due to application of shear load is prevented by an axial force – hence, the acronym “constant height” test.

In this study, testing was conducted in accordance with AASHTO TP7 Procedure E [5] in which a sinusoidal shearing strain of amplitude ± 0.005 -percent (0.0001 mm/mm peak-to-peak strain) was applied at frequencies of 10, 5, 2, 1, 0.5, 0.2, 0.1, 0.05, 0.02 and 0.01 Hz. At each frequency, the stress response is measured along with the phase shift between the

stress and strain. The dynamic shear modulus ($|G^*|$) was computed as the ratio of the peak stress over the peak strain. Testing was conducted at 50.2 °C.

Data presented in Table 5-4 through Table 5-9, and Figure 5-2 through Figure 5-7 show the FSCH test results for the mixtures from Buncombe and Rutherford counties. Based on these figures, and, in particular, Table 5-6 and Table 5-9 it may be noted that the baghouse fines have a stiffening effect on the mixtures. That is, on average, specimens containing baghouse fines have higher shear modulus values ($|G^*|$ and $|G^*|/\sin\delta$) compared to those specimens without the baghouse fines. The percentage difference is approximately 30-percent for the Buncombe County mixes and 20-percent for the Rutherford County mixes. These observations are consistent with the results obtained for the mastics using the DSR presented in Chapter 4. Moreover, for both mixes with and without the baghouse fines, the Buncombe County mixes generally show very similar performance to the Rutherford County mixes for the air voids and test temperature used in this study. Based on these results, it is expected that rutting performance will also be in line with the results obtained from FSCH test.

5.4.3 RSCH Test

The RSCH test measures the rutting potential of the mix over a range of temperatures. In this study, the RSCH test was conducted in accordance with AASHTO TP-7, Procedure F [5]. A controlled cyclic sinusoidal shearing stress was applied for a period of 0.1-s followed by a rest period of 0.6-s with a peak shear stress of 68 ± 5 kPa. The test duration was defined to correspond with permanent shear strain accumulation of 5-percent, or 100,000 loading cycles. The measured response was in terms of permanent shear strain accumulation as a function of the number of loading cycles.

The laboratory compacted specimens with and without the baghouse fines were first subjected to the FSCH test described earlier in this chapter. Following the FSCH test, these specimens were then subjected to RSCH test to evaluate the mixture resistance to rutting. Testing was conducted at 50.2 °C.

Table 5-10, Figure 5-8, and Figure 5-9 show the RSCH test results. The accumulated plastic shear strain at 100,000 cycles shown in Table 5-10 confirm the results from FSCH test: 1) for both counties specimens containing baghouse fines show lower accumulated plastic shear strain compared to specimens without the bag house fines with a percentage difference of approximately 15-percent; and 2) respective mixes from Buncombe and Rutherford counties show similar performance. As the accumulated plastic strain for all mixtures are less than 5-percent, it is expected that these mixtures should not show in-situ accumulated rut depth more than 0.5-inch under normal traffic loading.

5.5 Asphalt Pavement Analyzer Tests

The effect of baghouse fines on the rutting resistance of asphalt mixtures was also evaluated using the Asphalt Pavement Analyzer (APA). NCDOT Materials and Test Unit conducted the tests.

“Accelerated pavement testing is defined as the controlled application of a prototype wheel loading, at or above the appropriate legal load limit to a prototype or actual, layered, structural pavement system to determine pavement response and performance under a controlled, accelerated, accumulation of damage in a compressed time period [17].” The APA measures rutting susceptibility by rolling a steel wheel over pressurized rubber hose pressing against a rectangular asphalt concrete slab or a 6-inch diameter circular specimen. The test is normally performed at 40.6 °C and with the rubber hoses pressurized to 0.69 MPa (100 psi). The wheel passes over the hoses and slab at approximately 2.0 km/h (33±1 cycles/min) and the specimen is subjected to 8,000 cycles with each cycle defined as two passes of the wheel back and forth across the specimen. The deformation of the slab or specimen is measured at three points across the specimen and averaged. The Georgia Department of Transportation (GDOT) defines a mixture as susceptible to rutting if the average rut depth for replicate specimens is greater than 7.6-mm. However, the FHWA recommends that the maximum rut depth criteria be set to 5-mm.

Since the APA is a ‘proof’ test or a ‘pass / fail test,’ many variations of the test temperatures and rut depth acceptance criteria exist based on local experience. NCDOT

normally conducts these tests corresponding to the asphalt cements high PG rating with rut depth acceptance criterion of 0.25-inches (6.25-mm). In this study, APA test temperature of 50 °C was selected for consistency with the temperatures used for other performance tests. The 6-inch diameter specimens for APA test were fabricated at NCSU materials laboratory using the SGC (Superpave Gyratory Compactor). The specimens were compacted to a height of 3 inches with a target air void content of 7±1-percent. Table 5-11 shows the air voids content of specimens used for the APA tests. APA testing was carried out at NCDOT. Two cylindrical specimens were used for each test and an average rut depth was determined.

5.5.1 APA Test Results

Test results obtained from NCDOT (Appendix D) indicate that the materials from Buncombe County with and without the baghouse fines had an average rut depth of 6.15-mm and 6.12-mm, respectively. For the Rutherford County, specimens with and without the baghouse fines had an average rut depth of 12.33-mm and 12.78-mm, respectively, two times the depth observed for the Buncombe County.

Based on the test results obtained, it appears that the Buncombe County mixes would be acceptable based on the GDOT criterion but would fail based on the NCDOT criterion. It should be noted that GDOT requires testing to be conducted at 40.6 °C, whereas NCDOT requires a testing temperature of 64 °C as these mixtures contain a PG64-22 asphalt binder. For Rutherford County, both mixtures with and without the baghouse fines would fail.

APA test results indicate that mixtures from both counties are susceptible to excessive rutting. However, it should be noted that pavement sections in these counties have not shown excessive rutting to date. Pavement sections in Buncombe County were observed to have slightly more rutting (which was also evident from the field cores received [28]) compared to the cores from Rutherford County, contrary to the APA test results. Nevertheless, the objective in this study was not to estimate the rutting susceptibility of the mixtures per-se, but to evaluate the effect of baghouse fines on the mixture performance. In this regards, the APA test shows that the baghouse fines used in this study, do not have any adverse effect on the performance of the asphalt mixtures from either counties, a result consistent with all prior performance test results presented in earlier sections.

5.6 Effect of Baghouse Fines on Moisture Sensitivity

NCDOT Materials and Test Unit, in accordance with their procedure, conducted the TSR tests. It may be noted that NCDOT does not require the specimens to be subjected to freeze-thaw cycle as required under AASHTO T283 procedure. Four inch diameter specimens compacted using Marshall procedure were manufactured at NCSU and tested at NCDOT. In all, 8 specimens were made for each asphalt mixture with and without the baghouse fines for both counties. The results of the TSR tests are presented in Table 5-12 through Table 5-16.

Table 5-16 shows the summary of TSR test results for the asphalt mixtures with and without baghouse fines for the Buncombe and Rutherford counties. Test results show that the tensile strength ratios for asphalt mixtures containing baghouse fines for Buncombe and Rutherford counties are 78-percent and 84-percent, respectively, which fail the NCDOT 85-percent tensile strength ratio requirement for surface mixtures. It may be noted that these mixtures do contain anti-strip additive with a dosage suggested in the respective NCDOT JMFs. Mixtures without the baghouse fines meet or exceed the NCDOT requirement with mixtures from Buncombe and Rutherford counties showing an 85-percent and 92-percent tensile strength ratio, respectively. Later, an in-depth study conducted by Tayebali et al [27] based on 6 inch diameter specimens also confirm the finding of this investigation.

5.7 Summary and Conclusion

The main objective of this task was to evaluate the performance of laboratory mixes containing baghouse fines. FSCH and RSCH test results for laboratory mixes containing baghouse fines show the following:

- Baghouse fines have a stiffening effect on mixtures from both counties;
- Mixtures containing baghouse fines are more resistant to rutting as compared to mixtures not containing baghouse fines;

- Respective mixtures from both counties show similar dynamic shear stiffness and rutting characteristics.

The APA test results indicate that mixtures with and without baghouse fines from both counties are susceptible to excessive rutting. However for, both, Buncombe as well as Rutherford counties, it was observed that the baghouse fines did not have an effect in comparison to the mixtures containing regular mineral filler materials. This observation is in agreement with other SST performance test results. However, the TSR test results clearly show that mixtures containing baghouse fines are sensitive to moisture and fail the NCDOT tensile strength ratio requirement. The mixture moisture sensitivity may therefore be one of the contributory factors in the shoving distress observed in the Buncombe County; the other reason being either failure of tack coat itself due to inadequate bond strength or non-uniform application or improper breaking of emulsions. It should be noted that retained moisture due to inadequate curing of tack coat may adversely affect the overlaid asphalt layer in terms of moisture damage especially for those mixes containing excessive baghouse fines.

Table 5-1 Air voids and G_{mm} of 150-mm diameter laboratory mix specimens

Buncombe County				Rutherford County			
Sample ID	Height (mm)	Air voids (%)	Avg. Air Void (%)	Sample ID	Height (mm)	Air void (%)	Avg. Air Void (%)
BW11	50.2	4.9	4.7	RW41	50.5	5.5	5.5
BW12	49.3	4.5		RW42	47.5	5.5	
BWO11	50.4	4.9	4.9	RWO41	47.4	5.6	5.5
BWO12	48.6	4.8		RWO42	48.6	5.3	
G_{mm} – mixes w/baghouse fines			2.511	G_{mm} – mixes w/baghouse fines			2.513
G_{mm} – mixes wo/baghouse fines			2.505	G_{mm} – mixes wo/baghouse fines			2.509

Table 5-2 Nationwide pavement temperatures, [23]

Region	Temperature in °C		
	Effective	Critical	Maximum
I A	27.7	35	37.6
I B	33.0	40	41.8
I C	29.3	35	37.5
II A	28.3	36	38.4
II B	34.2	42	43.7
II C	36.0	43	45.7
III A	30.1	36	38.6
III B	37.2	44	46.6
III C	35.1	42	44.3
Mean	32.3	39.2	41.6

Table 5-3 Average depths and test temperatures

County	Weather Station.	Depth (mm)	Equation Temp.	SHRPBIND Temp.	Average Temp.
Buncombe	Asheville	33	51.4 °C	48.9 °C	50.2 °C
Rutherford	Caroleen	32	55.4 °C	52.5 °C	54.0 °C

Table 5-4 |G*| (Pa) versus frequency (Hz) for lab mixes, 50.2 °C, Buncombe County

Frequency	BW11	BW12	BWO11	BWO12
10	1.44E+08	1.90E+08	9.18E+07	1.62E+08
5	1.10E+08	1.41E+08	6.69E+07	1.17E+08
2	7.94E+07	9.88E+07	4.66E+07	8.02E+07
1	6.38E+07	7.71E+07	3.67E+07	6.17E+07
0.5	5.23E+07	6.15E+07	2.93E+07	5.12E+07
0.2	4.24E+07	4.83E+07	2.30E+07	3.66E+07
0.1	3.78E+07	4.11E+07	2.00E+07	3.08E+07
0.05	3.16E+07	3.49E+07	1.65E+07	2.72E+07
0.02	2.87E+07	3.30E+07	1.48E+07	2.44E+07
0.01	2.71E+07	2.66E+07	1.38E+07	2.10E+07

Table 5-5 δ (degrees) versus frequency (Hz) for lab mixes, 50.2 °C, Buncombe County

Frequency	BW11	BW12	BWO11	BWO12
10	41.11	45.80	49.68	47.84
5	40.46	45.47	48.20	47.79
2	39.37	44.07	46.92	46.45
1	38.41	42.59	43.19	45.93
0.5	36.08	40.72	44.05	43.55
0.2	33.70	37.97	40.55	41.28
0.1	32.40	36.07	37.35	39.46
0.05	29.00	33.47	35.30	35.01
0.02	29.26	34.25	34.74	34.25
0.01	25.68	25.39	29.56	29.78

Table 5-6 Average $|G^*|$, δ , and $|G^*|/\sin \delta$ values, 50.2 °C, lab mixes Buncombe County

Frequency	$ G^* $ (Pa.) (With)	$ G^* $ (Pa.) (W/o)	δ (deg.) (With)	δ (deg.) (W/o)	$ G^* /\sin \delta$ (With)	$ G^* /\sin \delta$ (W/o)
10	1.67E+08	1.27E+08	43.46	48.76	2.42E+08	1.69E+08
5	1.25E+08	9.21E+07	42.97	48.00	1.83E+08	1.24E+08
2	8.91E+07	6.34E+07	41.72	46.69	1.34E+08	8.73E+07
1	7.04E+07	4.92E+07	40.50	44.56	1.08E+08	6.97E+07
0.5	5.69E+07	4.03E+07	38.40	43.80	9.15E+07	5.82E+07
0.2	4.53E+07	2.98E+07	35.83	40.91	7.74E+07	4.54E+07
0.1	3.94E+07	2.54E+07	34.23	38.40	7.02E+07	4.07E+07
0.05	3.32E+07	2.19E+07	31.24	35.16	6.42E+07	3.80E+07
0.02	3.08E+07	1.96E+07	31.75	34.50	5.87E+07	3.47E+07
0.01	2.68E+07	1.74E+07	25.54	29.67	6.23E+07	3.52E+07
Average	6.85E+07	4.86E+07	3.66E+01	4.10E+01	1.09E+08	7.02E+07

Table 5-7 $|G^*|$ (Pa) versus frequency (Hz) for lab mixes, 50.2 °C, Rutherford County

Frequency	RW41	RW42	RWO41	RWO42
10	2.25E+08	2.02E+08	1.74E+08	1.86E+08
5	1.64E+08	1.46E+08	1.23E+08	1.34E+08
2	1.09E+08	9.68E+07	7.83E+07	8.85E+07
1	8.00E+07	7.16E+07	5.68E+07	4.39E+07
0.5	5.98E+07	5.41E+07	4.19E+07	4.47E+07
0.2	4.18E+07	3.83E+07	2.95E+07	3.68E+07
0.1	3.21E+07	3.09E+07	2.36E+07	2.91E+07
0.05	2.56E+07	2.31E+07	1.80E+07	1.15E+07
0.02	2.00E+07	1.98E+07	1.50E+07	1.21E+07
0.01	1.77E+07	1.84E+07	1.33E+07	1.54E+07

Table 5-8 δ (degrees) versus frequency (Hz) for lab mixes, 50.2 °C, Rutherford County

Frequency	RW41	RW42	RWO41	RWO42
10	43.97	45.61	48.26	46.45
5	45.36	46.81	49.51	47.29
2	46.72	47.28	50.07	47.98
1	47.66	45.66	54.41	28.08
0.5	47.79	47.09	50.10	59.49
0.2	45.93	45.22	47.63	57.29
0.1	43.61	42.52	46.53	48.85
0.05	40.86	39.49	43.78	35.35
0.02	39.28	34.86	37.73	32.52
0.01	37.73	32.08	37.85	33.17

Table 5-9 Average |G*|, δ , and |G*|/sin δ values, 50.2 °C, lab mixes Rutherford County

Frequency	G* (Pa.) (With)	G* (Pa.) (W/o)	δ (deg.) (With)	δ (deg.) (W/o)	G* /sin δ (With)	G* /sin δ (W/o)
10	2.14E+08	1.80E+08	44.79	47.36	3.04E+08	2.44E+08
5	1.55E+08	1.28E+08	46.08	48.40	2.15E+08	1.72E+08
2	1.03E+08	8.34E+07	47.00	49.03	1.41E+08	1.11E+08
1	7.58E+07	5.03E+07	46.66	41.24	1.04E+08	8.15E+07
0.5	5.70E+07	4.33E+07	47.44	54.80	7.73E+07	5.32E+07
0.2	4.00E+07	3.31E+07	45.58	52.46	5.60E+07	4.18E+07
0.1	3.15E+07	2.64E+07	43.07	47.69	4.61E+07	3.56E+07
0.05	2.44E+07	1.48E+07	40.18	39.57	3.78E+07	2.30E+07
0.02	1.99E+07	1.36E+07	37.07	35.12	3.31E+07	2.35E+07
0.01	1.81E+07	1.44E+07	34.91	35.51	3.18E+07	2.49E+07
Average	7.38E+07	5.87E+07	4.33E+01	4.51E+01	1.05E+08	8.10E+07

Table 5-10 Strain at the end of RSCH test, 50.2 °C, lab mixes

Specimens 'With' Baghouse Fines			Specimens 'Without' Baghouse Fines		
County	Sample ID	% Strain	County	Sample ID	% Strain
Buncombe	BW11	2.10	Buncombe	BWO11	2.70
Buncombe	BW12	1.59	Buncombe	BWO12	1.57
Average % Strain		1.85	Average % Strain		2.14
Rutherford	RW41	1.70	Rutherford	RWO41	2.18
Rutherford	RW42	1.89	Rutherford	RWO42	2.15
Average % Strain		1.80	Average % Strain		2.17

Table 5-11 Air voids and heights of 6-inch diameter laboratory specimens for APA test

Buncombe County				Rutherford County			
Sample ID	Height (mm)	Air voids (%)	Avg. Air Void (%)	Sample ID	Height (mm)	Air void (%)	Avg. Air Void (%)
BW02	75.6	6.5	6.5	RW05	75.6	7.7	7.6
BW03	75.5	6.5		RW06	75.4	7.4	
BWO1	75.5	6.4	6.5	RWO5	75.4	6.9	6.8
BWO2	75.5	6.6		RWO6	75.5	6.6	

Table 5-12 Buncombe County (With baghouse fines) TSR results (4-inch specimens)

Unconditioned Specimens				Conditioned Specimens			
Sample ID	Height (mm)	Air voids (%)	Max. Load (N)	Sample ID	Height (mm)	Air voids (%)	Max. Load (N)
BW01	63.9	6.9	2200	BW02	64.0	7.0	1600
BW03	63.9	6.8	2060	BW06	63.8	6.6	1750
BW05	63.8	6.7	2040	BW08	63.7	6.9	1550
BW11	63.8	7.0	2270	BW10	63.8	6.9	1700
Average		6.9	2142			6.9	1650

Table 5-13 Buncombe County (W/out baghouse fines) TSR results (4-inch specimens)

Unconditioned Specimens				Conditioned Specimens			
Sample ID	Height (mm)	Air voids (%)	Max. Load (N)	Sample ID	Height (mm)	Air voids (%)	Max. Load (N)
BWO03	64.0	6.6	1980	BWO01	63.6	6.9	1600
BWO06	63.7	6.8	2050	BWO02	63.8	6.5	1750
BWO08	63.9	6.3	2080	BWO05	63.8	6.3	1760
BWO09	63.9	6.8	1900	BWO07	63.8	6.7	1810
Average		6.6	2002			6.6	1730

Table 5-14 Rutherford County (With baghouse fines) TSR results (4-inch specimens)

Unconditioned Specimens				Conditioned Specimens			
Sample ID	Height (mm)	Air voids (%)	Max. Load (N)	Sample ID	Height (mm)	Air voids (%)	Max. Load (N)
RW03	63.7	6.9	2450	RW01	63.8	7.1	2050
RW06	63.7	7.1	2400	RW02	63.8	6.8	2050
RW07	63.8	7.0	2450	RW04	63.7	6.9	2050
RW08	63.8	6.7	2500	RW10	63.8	6.8	2050
Average		6.9	2450			6.9	2050

Table 5-15 Rutherford County (W/out baghouse fines) TSR results (4-inch specimens)

Unconditioned Specimens				Conditioned Specimens			
Sample ID	Height (mm)	Air voids (%)	Max. Load (N)	Sample ID	Height (mm)	Air voids (%)	Max. Load (N)
RWO02	63.9	6.5	2150	RWO01	63.7	6.4	1950
RWO04	63.9	6.4	2100	RWO03	63.9	6.4	2050
RWO07	63.8	6.2	2300	RWO05	64.0	6.3	2025
RWO08	63.8	6.4	2250	RWO06	63.9	6.4	2100
Average		6.4	2200			6.4	2031

Table 5-16 Summary of TSR results

County	Type of Mix	QA/QC Comparative TSR	Average Tensile Strength (kPa)		Tensile Strength Ratio (%)
			Dry	Wet	
Buncombe	With bag-fines	Minor	209.3	162.9	77.8
	Without bag-fines	Minor	203.0	172.8	85.1
Rutherford	With bag-fines	Minor	244.6	204.7	83.7
	Without bag-fines	Minor	219.4	202.5	92.3

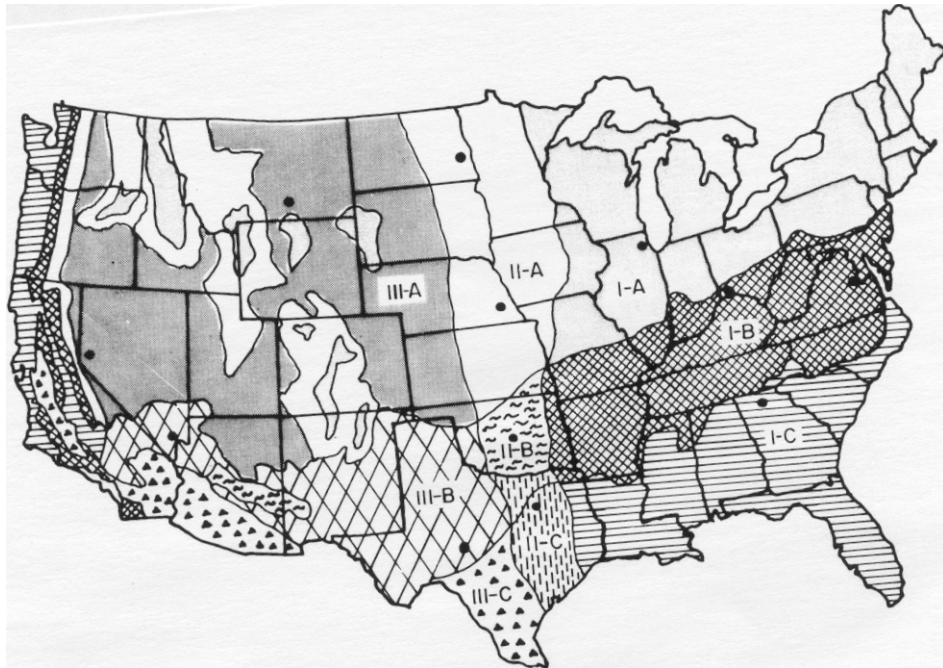


Figure 5-1 Nine climatic regions in US

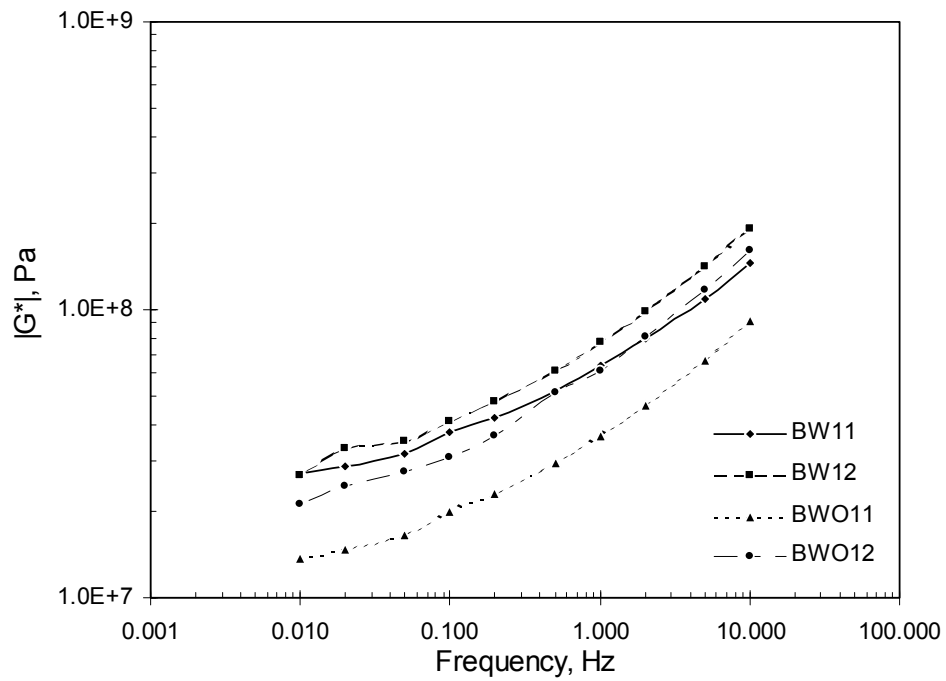


Figure 5-2 Dynamic Shear Modulus ($|G^*|$) vs. freq., 50.2 °C, Buncombe, lab mixes

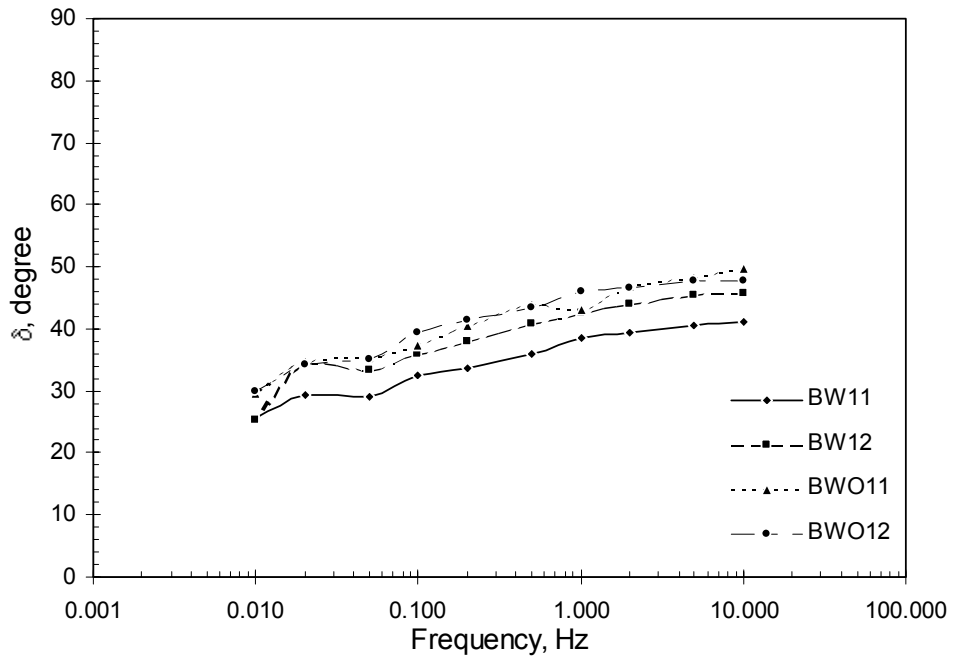


Figure 5-3 Phase angle (δ) versus frequency, 50.2 °C, Buncombe, lab mixes

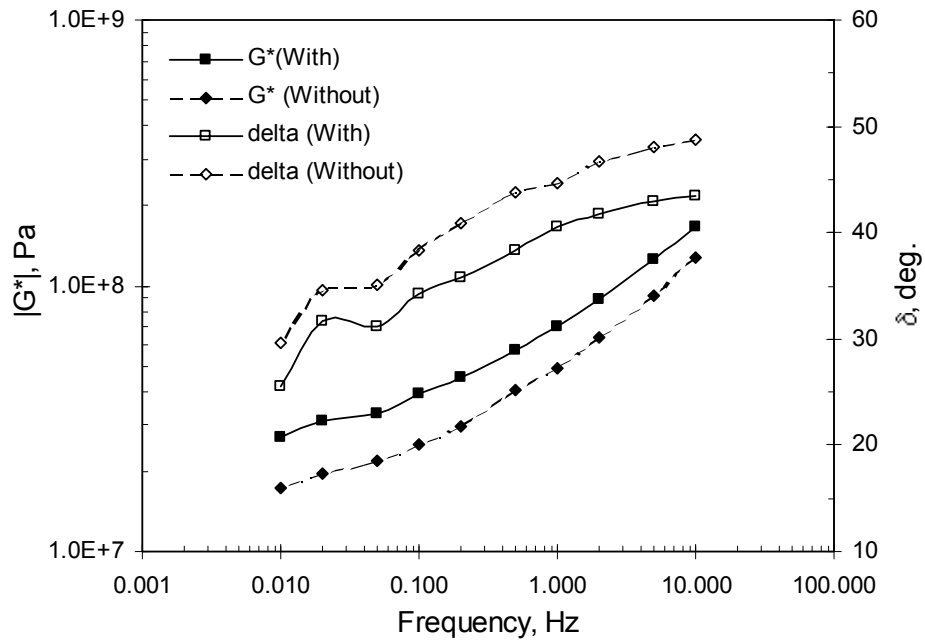


Figure 5-4 Average $|G^*|$ and δ values vs. freq., 50.2 °C, Buncombe, lab mixes

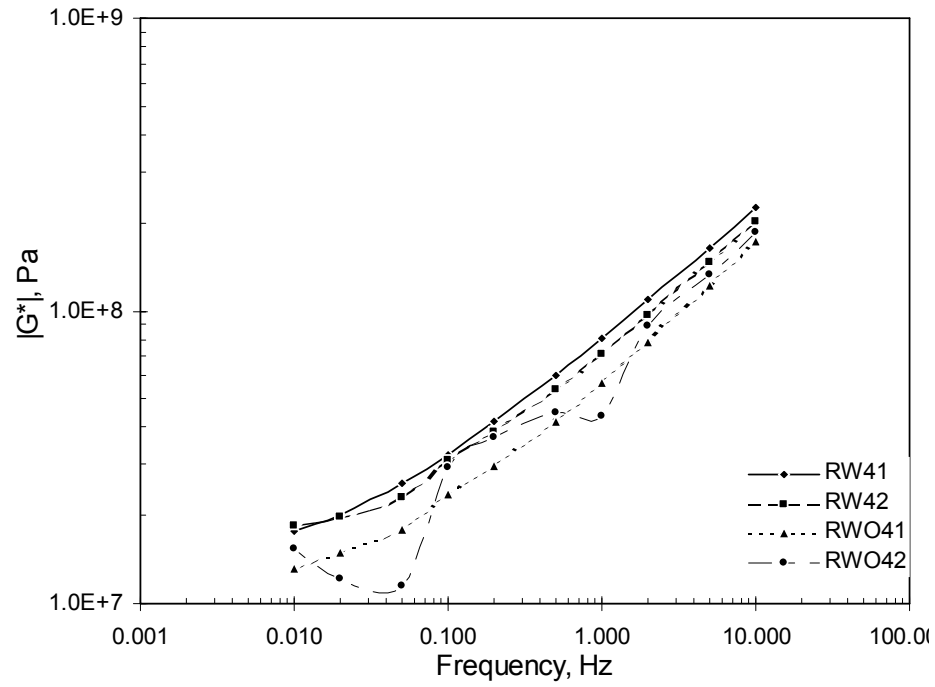


Figure 5-5 Dynamic Shear Modulus ($|G^*|$) vs. freq., 50.2 °C, Rutherford, lab mixes

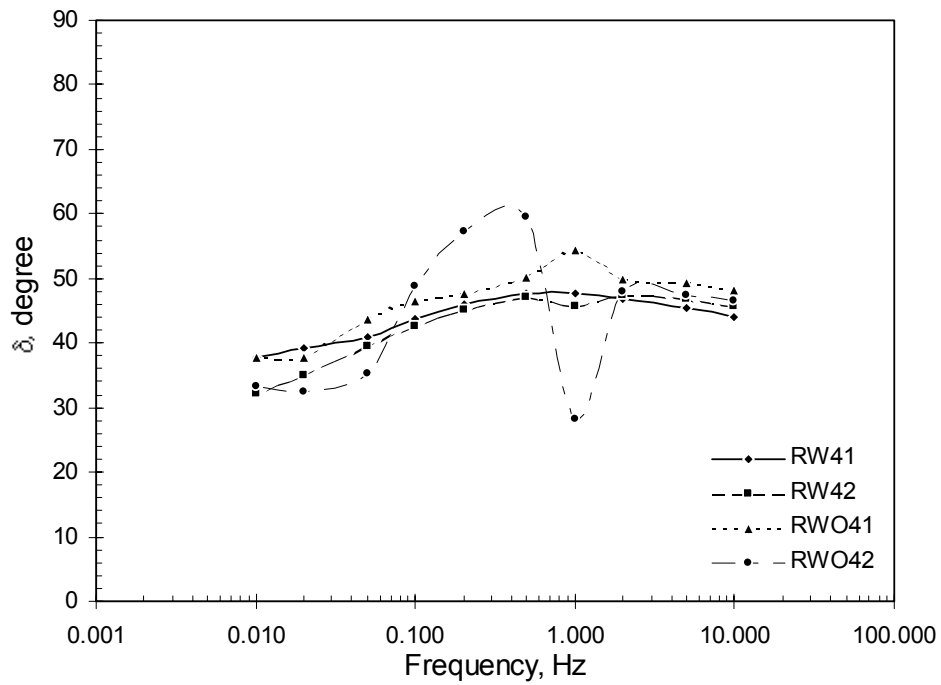


Figure 5-6 Phase angle (δ) vs. frequency, 50.2 °C, Rutherford, lab mixes

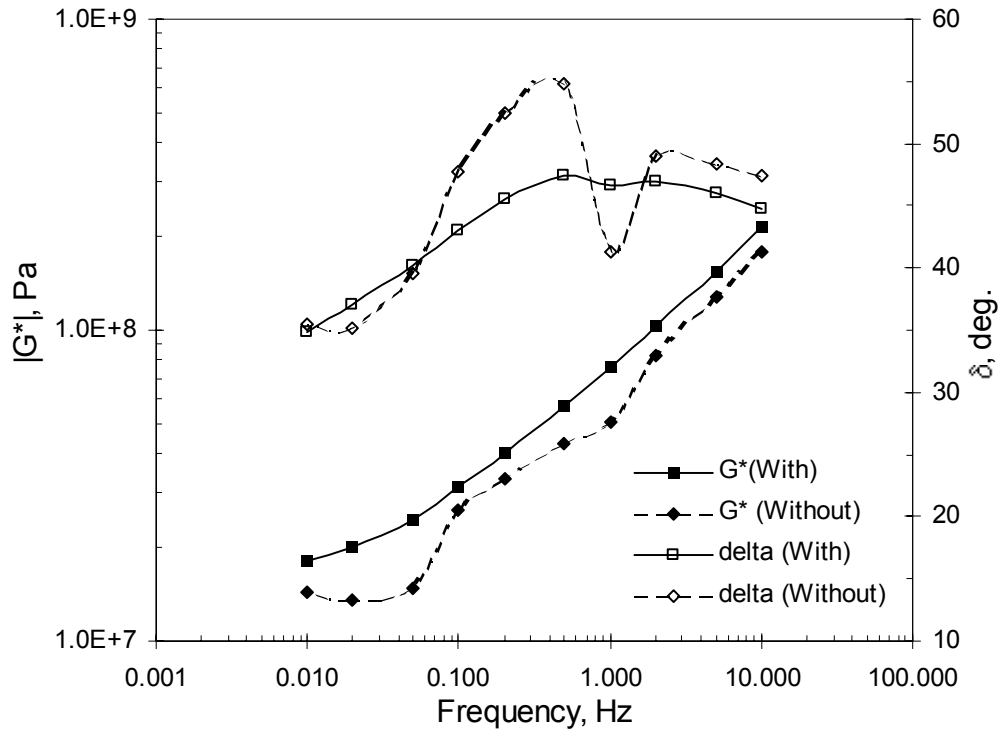


Figure 5-7 Average $|G^*|$ and δ values vs. freq., 50.2 °C, Rutherford, lab mixes

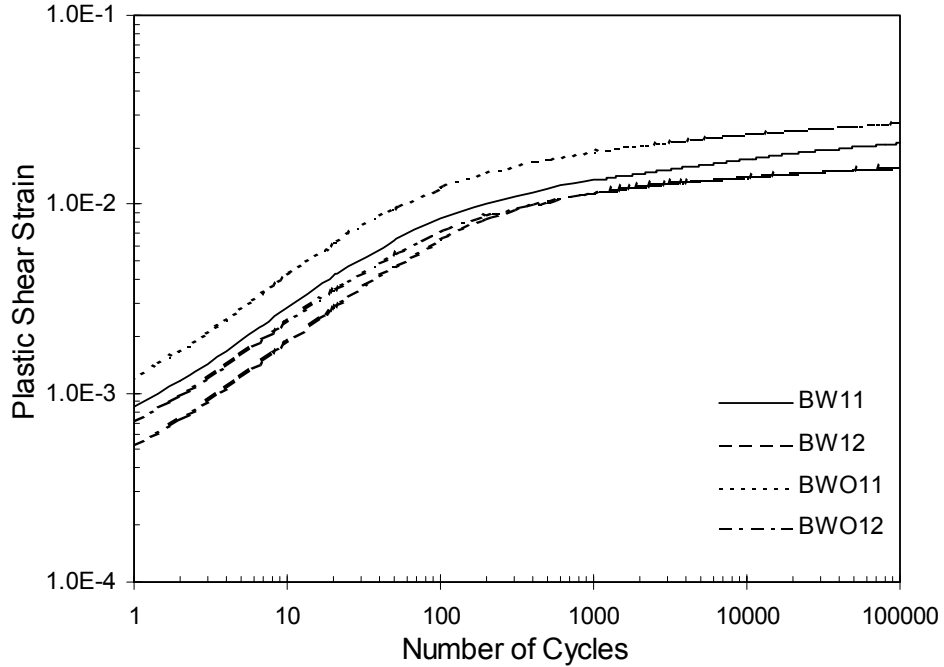


Figure 5-8 Plastic shear strain vs. RSCH cycles, 50.2 °C, Buncombe County, lab mixes

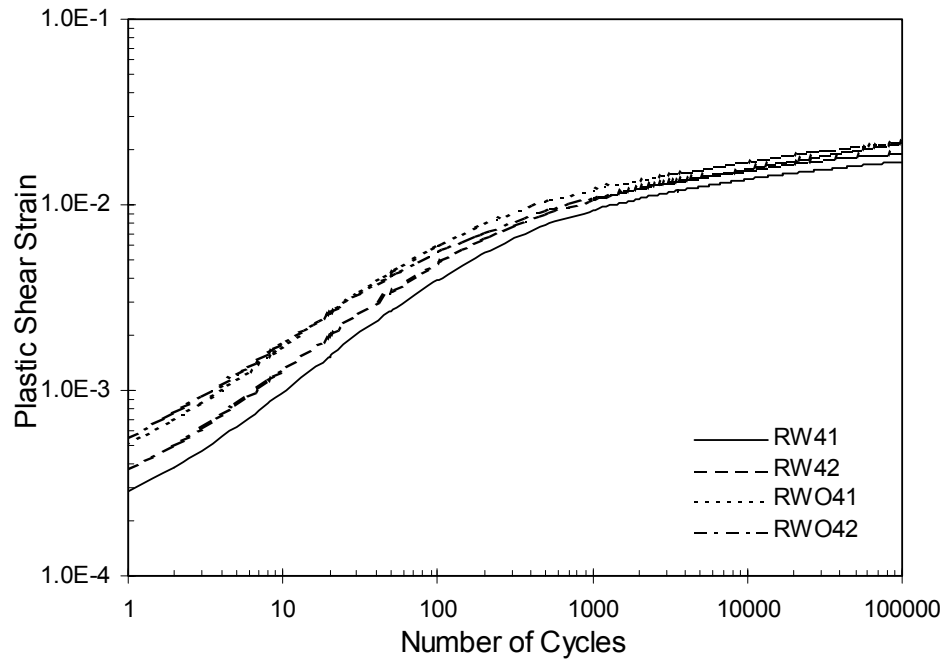


Figure 5-9 Plastic shear strain vs. RSCH cycles, 50.2 °C, Rutherford County, lab mixes

6 Specimen Fabrication Using Rolling Wheel Compactor

6.1 Introduction

This chapter discusses the method used for manufacturing specimens in the laboratory. The testing is to be carried out using SST machine and the specimens would be 6-inch in diameter. The goal was to fabricate specimens closest to the field conditions. Mohammad et al [18] have fabricated specimens in a gyratory compactor in multiple layers. The bottom portion was compacted in a SGC first, followed by application of tack coat and then reinserting the specimen in the mold and compacting loose mix on top of it. This method would have given the best control over the air voids, but would not be close to field conditions where roller based compaction is used.

The alternative was to prepare slabs using a rolling wheel compactor (Figure 6-2 and Figure 6-4) to simulate the field conditions. The equipment used for compaction was gasoline powered rolling wheel compactor that had two drum rollers. The approximate weight was about 2 tons and the roller width was 25 inches. The engine provided the thrust for moving the roller in forward and reverse direction; however the steering had to be done manually. The roller had two tanks of water that can be used to vary the weight and moisten the drums. The wetting of drums was necessary to prevent the sticking of asphalt mix to the drums.

6.2 Fabrication of Steel Molds

Steel molds (Figure 6-7 through Figure 6-10) were fabricated at NCSU to make the slabs. Steel was preferred to wood because it was stronger, less likely to warp or get deformed, and could be heated to the compaction temperature immediately prior to the assembly. The goal was to have molds that would be adjustable so that slabs (specimens) can be made with different heights within a fairly accurate tolerance. To allow uniform compaction inside the mold, the sides along the direction of rolling were sloped inwards. The mold was assembled on a base plate consisting of a plywood laminate topped with an aluminum plate. Figure 6-1 and Figure 6-2 show the picture of assembled molds in along and perpendicular to the direction of compaction. On the surface of the aluminum plate were four

L-sections to which the molds were anchored using steel bolts. If a taller specimen was desired, the mold extensions (shown in Figure 6-7 and Figure 6-9) were placed on the bottom portion, and were anchored using steel bolts. The compaction was achieved by rolling the compactor over the loose mix put in the molds. The effect of compaction was most visible at the edge of the roller. In order to operate the roller in a level position, a wooden platform was constructed all around the mold. In addition, wooden ramps were designed to raise or lower the roller from the wooden platform.

6.3 Specimen Fabrication

6.3.1 Asphalt Concrete Slabs

The material for making the asphalt concrete slabs was received from NCDOT. The material was heated to 160 °C in a convection oven for 4-5 hours. The molds were also heated at the same temperature. Depending on the situation, the heated molds were assembled either on the base plate or were placed as extensions over the existing mold. After securing the molds with steel bolts and nuts, the wooden platforms were placed on all sides of the mold to make the level of compactor flush with top surface of the mold.

A predetermined amount of the heated mix was, subsequently, poured into the mold and spread uniformly. The weight of the mix added to the mold was obtained iteratively to get a target air void of 4%. The mix was rodded with a spatula for initial compaction to remove air pockets and obtain a uniform spread throughout. The compaction process started immediately with the roller drums being moistened with water. The passes were made only in one (longitudinal) direction as is done in the field. At the end of every pass, the roller was turned slightly so as to cause the edge of the roller to move progressively from one end of the mold to the other. After every few passes, the flatness of the top surface was checked using a water level. This process continued till a fairly flat profile was obtained. After compaction, the slab was cooled for 24 hours before placing a tack coat, or performing any cutting and coring operation.

6.3.2 Portland Cement Concrete Slabs

Garner granite aggregate, natural sand, and Portland cement (Type I/II) were used to cast slabs. The mold was assembled and bolted to the base plate. It was coated with a thin layer of oil to prevent the sticking of hardened cement to the mold. After thorough mixing in the cement mixer, the mix was poured into the molds. The mix was then rodded to remove air cavities from the mold and leveled using a wooden float. It was allowed to stand for 30-45 minutes so that the bleed water rose to the surface. The excess bleed water on the surface was removed and, the surface was made smooth with a magnesium trowel (Figure 6-3).

The slab was then allowed to sit for 24 hours before the mold was disassembled. After removal from the mold, the slab was covered with wet cotton towels and was sealed in a polythene plastic sheet (Figure 6-3 near top edge). Water was added daily to keep the towels moist and aid the hydration of the slab. After continuous hydration for 7 days, the slab was kept in sun (summer time) for about 48 hours to dry and shrink before applying the tack coat.

6.3.3 Cement Treated Base Slab

The procedure used to make cement treated base slabs was similar to the PCC slabs mentioned earlier. The material was mixed in a mixer and poured into the mold. Using a metal rod, the mix was rodded and leveled using a float. It was then covered with a slightly damp cloth to retain the moisture. After 24 hours the mold was disassembled; however, as the cement content in the CTB slabs was about 5%, the strength of the slabs was very low. The slabs could not withstand the normal handling stresses and crumbled as soon as they were removed from the mold.

After two unsuccessful attempts to fabricate the CTB slabs, it was decided to fabricate the CTB specimens in smaller 6-inch diameter mold and follow the procedure similar to that outlined by Mohammad et al [18]. The CTB material was poured in a 6-inch diameter modified proctor metal mold in 5 equal lifts to a height of about 4.584 inches. After every lift, the layer was compacted using 56 blows of the Modified Proctor Test hammer. Immediately after compaction, the specimen was covered with a damp towel to retain moisture. After about 8-10 hours, the specimens were extruded from the molds and wrapped

in cotton towels and plastic. The towels were kept wet to cure CTB for 7 days. After 7 days, the specimens were cut to a height of 1-inch (Figure 6-5). These 1-inch CTB ‘discs’ were coated with prime coat on one side (Figure 6-6). After breaking of the prime coat, the ‘discs’ were inserted in the gyratory compactor molds with the coated side facing up. The problem with this approach was that the ‘discs’ expanded after extrusion from the molds and could not be reinserted. So, using a metal file, the sides of the ‘discs’ were filed to slightly reduce the diameter of the discs. Then hot loose asphalt mix was poured in the mold and compacted to a height of 1-inch. The target air void for this overlying layer was 4%. The samples were extruded and allowed to cool before testing. Figure 8-23, on page 132, shows a picture of composite CTB-AC specimen.

6.4 Tack / Prime Coat Application

NCDOT specifications (§605 of Standard Specifications for Roads and Structures, 2002) require the placement of tack coat beneath every layer of asphalt plant mix. The required rate of application is 0.04 to 0.08 gallons per square yard. The tack coat rate chosen for preparing the laboratory samples was 0.06 gallons per square yard, which is in the middle of the range. In consultation with the NCDOT, PG64-22 binder and CMS-2 emulsion were chosen as tack coat materials.

The tack coat was applied 24 hours after rolling the asphalt slab. This would allow adequate time for cooling of the mix. For PCC, the slabs were left in sun for 48 hours to ensure that the shrinkage cracks do not occur after applying tack coat. The surface of the asphalt (or PCC) slab was cleaned with a wire brush and blasted with pressurized air to remove the loose dust particles. The CMS-2 emulsion was stirred and applied using a regular paint brush. The weight of the CMS-2 container was monitored to ensure the correct rate of application. After application, the slab was kept in a draft of fan air for 24 hours to ensure the breaking of the emulsion. In most cases, the surface was adequately ‘tacky’ to touch.

A similar procedure was followed for applying PG64-22 binder as tack coat, except that the binder was heated to about 185 °C on a hot plate. The application surface was heated with heat lamps to ensure easier application of tack coat. The weight of the binder was

monitored frequently to get to the correct rate of application. Although no ‘breakage’ of tack coat was required for PG64-22 asphalt, the next layer was paved about 24 hours after applying tack coat to maintain consistency in relation to the CMS-2 emulsion.

Section 600 of NCDOT Standard Specifications for Roads and Structures specifies the rate of application of prime coat as 0.2 to 0.5 gallons per square yard. The maximum amount of emulsion applied to the CTB specimens without overflow constrained the application rate to 0.24 gallons per square yard, which is within the permissible range. CSS-1, EPR-1 and EA-P were used as prime coat materials. The procedure for application of prime coat was similar to that of tack coat. The individual CTB ‘discs’ were weighed on a balance and were ‘painted’ with emulsions to get to the required application rate. The prime coat was allowed to break for 24 hours before another layer was compacted on top of the discs.

In case where no tack coat or prime coat was desired, the next layer was paved without prime or tack coat.

6.5 Coring and Cutting Samples

For material characterization, a three inch slab was used. The dimension of the slab used for acquiring specimens was 2 ft × 2 ft. In all, nine cores (each of 6 inch diameter) were drilled from the slab with a spacing of 1½ inches between two adjacent cores. Subsequently, the 3 inch thick cores were reduced to a height of 2 inches by shaving off the top and bottom ½ inch portions.

Composite slabs (AC over AC and AC over PCC) were 4 inch in thickness. Nine cores were drilled from these slabs, each core spaced 1½ inches apart from adjacent cores. The interface was kept at midway by removing the top and bottom portions of the core. The final height of the specimen was 2 inches, as required for SST testing.

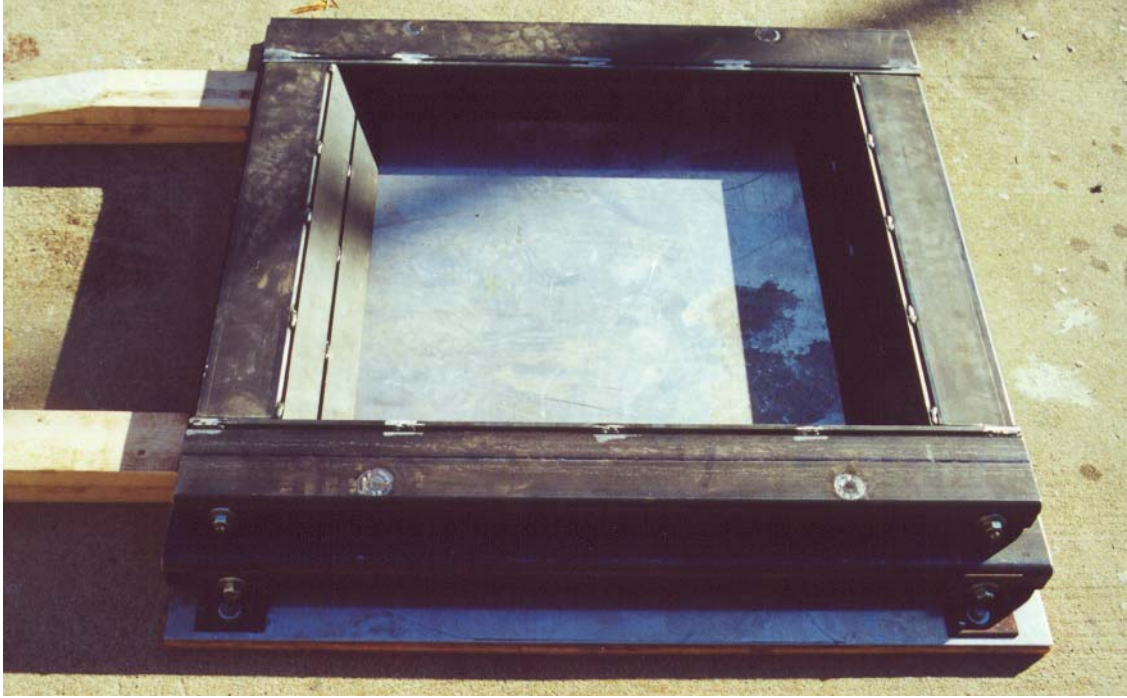


Figure 6-1 View of mold with adjustable ramps (on left)



Figure 6-2 Mold with roller

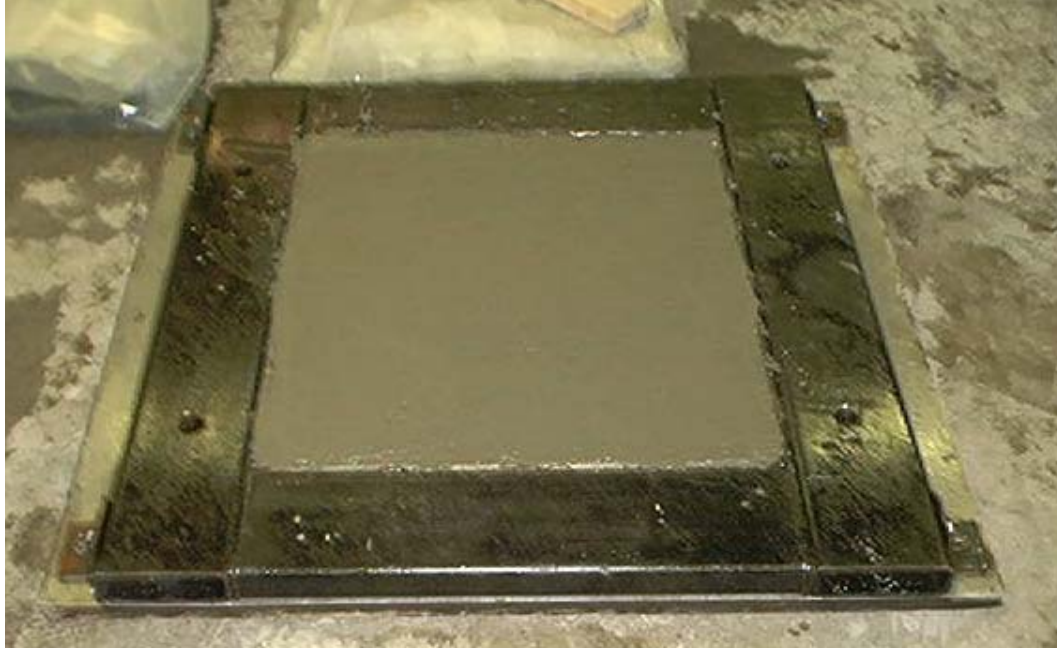


Figure 6-3 Freshly cast PCC slab



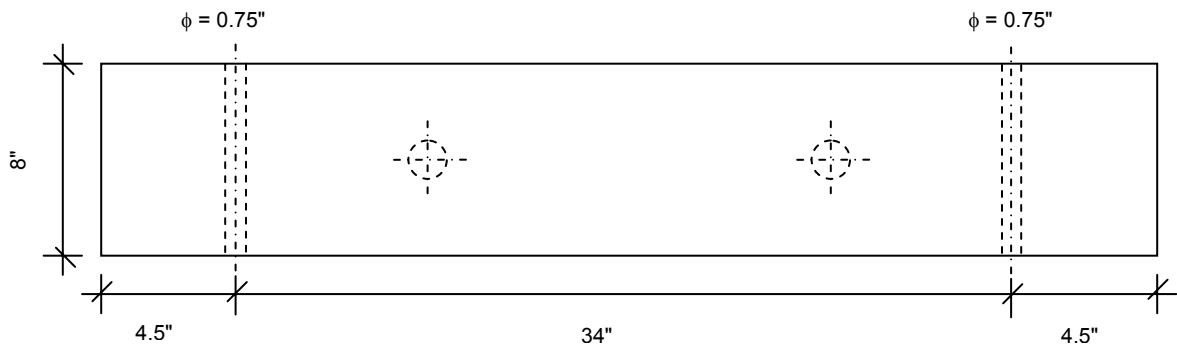
Figure 6-4 Side view with roller on the mold



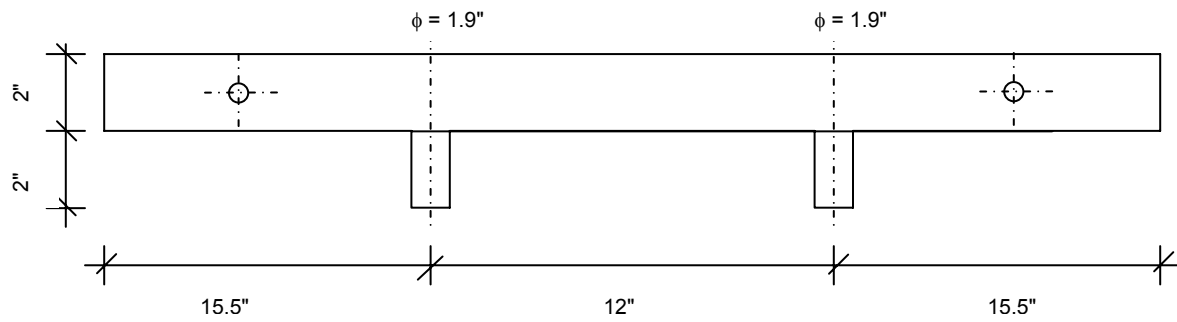
Figure 6-5 Photo of a 1-inch thick CTB 'disk'



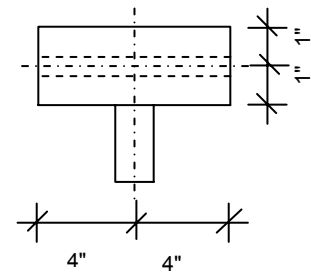
Figure 6-6 CTB 'disks' coated with emulsion



PLAN

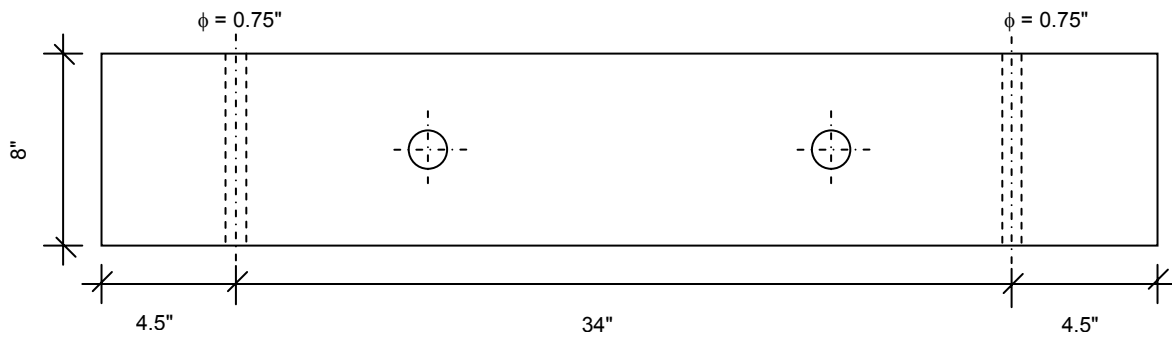


FRONT VIEW

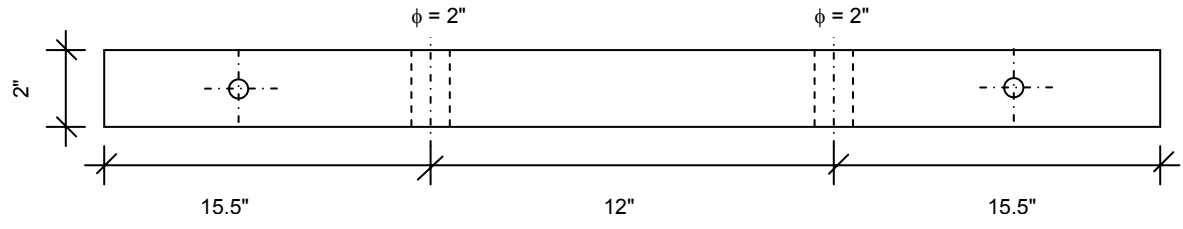


SIDE VIEW

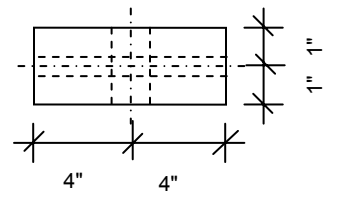
Figure 6-7 Mold Top – Part I



PLAN

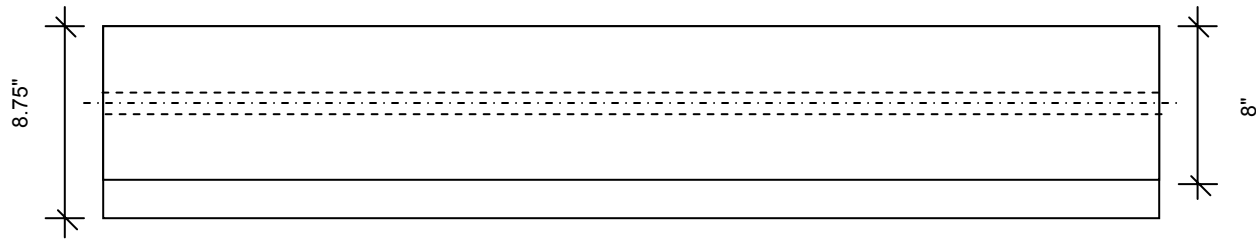


FRONT VIEW

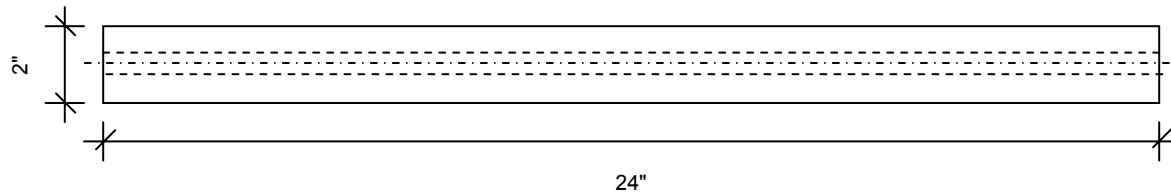


SIDE VIEW

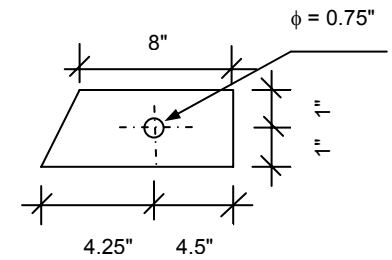
Figure 6-8 Mold Bottom – Part I



PLAN

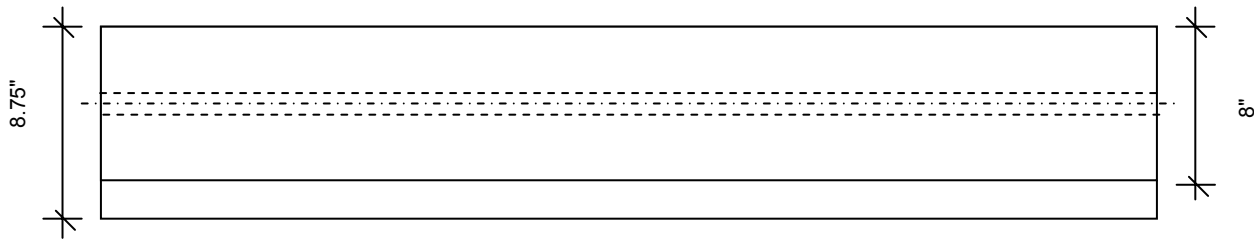


FRONT VIEW

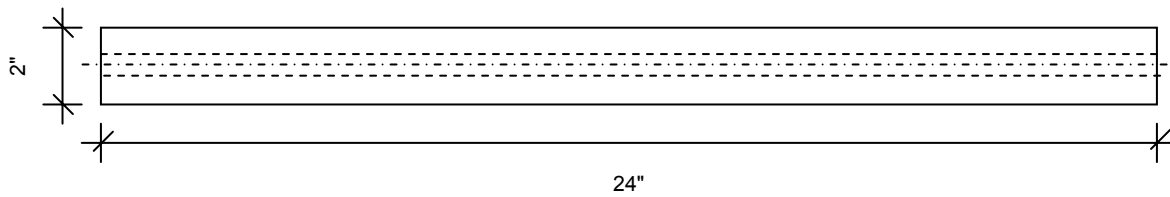


SIDE VIEW

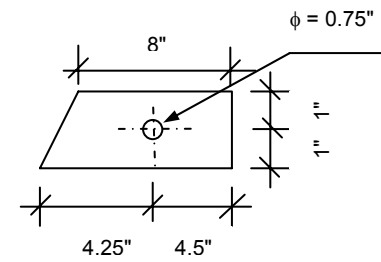
Figure 6-9 Mold Top – Part II



PLAN



FRONT VIEW



SIDE VIEW

Figure 6-10 Mold Bottom – Part II

7 Material Characterization

7.1 Introduction

The objective of this task was to obtain material characteristics needed for the mechanistic analysis of the pavement sections. In this section, the properties of asphalt mix and PCC were evaluated using the SST (Simple Shear Tester) tests and UTM (Universal Testing Machine) respectively. Test methods utilized for measuring the properties were Shear Frequency Sweep Test at Constant Height (FSCH), Axial Frequency Sweep Test (AFST), and unconfined compressive tests for PCC specimens.

7.2 Asphalt Mix Characterization

The asphalt mix (JMF enclosed in Appendix C, page 173), received from NCDOT, was characterized by the following performance tests:

- Shear tests
 - Frequency Sweep Test at Constant Height (FSCH),
 - Repeated Shear Test at Constant Height (RSCH),
- Axial tests
 - Frequency Sweep Test (AFST), and
 - Repeated Axial Test.

Specimens for the shear tests were fabricated using rolling wheel compaction (Section 6.3.1), and cored and cut (Section 6.5) to a height of 50-mm. After coring and cutting, the specimens were fan dried to remove the residual water and bulk specific gravity (ASTM D 2726) was determined. The target air void content of the specimens was 4.0 ± 0.5 %. The G_{mm} (maximum theoretical specific gravity) determined according to ASTM D 2041 was **2.442** for the loose mix. Table 7-1 lists the air void contents of the samples obtained.

Specimens for the axial tests were fabricated in the laboratory using the Servopac™ gyratory compactor. The mix was preheated to a temperature of 160 °C in the ovens for 3

hours. A known quantity of the mix was then poured into the compactor molds and compacted to a target air void content of 5.5%. The targeted air void content was slightly higher so that after coring and cutting the final air void content would be 4%, which is the desired air void content. The average height of the specimens was 17.8 cm. The specimens were extruded and, after the sample cooled, each specimen was cored to a 4-in diameter and the top and bottom portions shaved to give a final height of 6-in (15.2 cm). The specimens used for axial testing were 4×6 inch in size with an air void of 4±0.5%.

7.2.1 Frequency Sweep Test at Constant Height (FSCH)

The FSCH test measures the viscoelastic shear properties over a range of testing frequencies and temperatures. The testing was carried out at 20, 30, 40 and 60 °C. Table 7-2 through Table 7-9 show the FSCH test results for AC mixes. The results are graphically presented in Figure 7-1 through Figure 7-10. The mix shear stiffness ($|G^*|$) reduces with increasing temperature or lowering of frequency. The results for shear phase angle (δ) are a slightly different. It is expected that with increasing frequency, the phase angle would reduce but this is not the case at 60 °C (Figure 7-8). The phase angle increases with increasing frequency at this relatively high temperature. Further, at 40 °C, the phase angle curve (Figure 7-6) is shaped ‘concave downwards.’ The phase angle, at 40 °C, increases with frequency (at lower frequencies) and then reduces with increasing frequency (higher frequencies). This behavior is summarized in the phase angle master curves shown in Figure 7-12 and Figure 7-14. At higher frequencies the mix is more elastic than viscous; hence the phase angle reduces with increasing frequency. At lower frequencies, however, the binder (in the mix) is mostly viscous and the aggregate, being elastic, contributes primarily to the mix strength. The relative contribution of aggregate to strength increases causing phase angle to reduce (alternatively, more elastic mix) with reducing frequency. The master curves at 30 and 40 °C (Figure 7-11 through Figure 7-16) characterize the behavior of asphalt mix over a range of frequencies.

7.2.2 Repeated Shear Test at Constant Height (RSCH)

The rutting potential of a mix is characterized by the RSCH test (details in §5.4.3). As rutting is more likely to occur at higher temperatures, the tests were carried out at temperatures of 40 and 60 °C. The purpose of this test was to ensure that the mix did not fail prematurely during the shear ramp test. The test results are given in Table 7-10 and Figure 7-17. The tests were conducted to a maximum of 100,000 cycles or 5.0% strain whichever happened earlier. It was observed that specimens tested at 60 °C failed at an average of 20,000 cycles compared to specimens tested at 40 °C. The 60 °C test results (Figure 7-17) indicate an accumulation of tertiary strain in the samples. The specimens at 40 °C accumulated an average total strain of 1.05% at the end of test. This indicates the mix has a significant ability to resist rutting at 40 °C. Based on the information at 40 °C the testing at 20 °C would have yielded lower plastic strain at 100,000 cycles. The plastic shear strain at 5,000 RSCH cycles can also be used as an indicator of the mix behavior. It can be observed that at 60 °C, the accumulated plastic strain at 5000 cycles is 2.95% compared to 0.67% at 40 °C. Given the low accumulation of plastic strain at 40 °C, the mix is expected to perform well at this temperature.

7.2.3 Axial Frequency Sweep Test (AFST)

In the earlier two sections (Sections 7.2.1 and 7.2.2), the performance of the AC mix was evaluated using FSCH and RSCH tests. In those tests, the shear properties were evaluated. This section describes the evaluation of dynamic axial modulus and the phase angle of the mix.

The AFST test is similar to the FSCH test except that a dynamic uniaxial loading is applied as opposed to shear. The test was conducted in a controlled strain mode of loading with a sinusoidal axial strain of amplitude of $\pm 0.005\%$ (0.0001 mm/mm peak to peak strain) applied at 10, 5, 2, 1, 0.5 and 0.2 Hz. At each frequency, the stress response was measured along with the axial phase shift (δ) between the stress and strain, and the dynamic axial modulus ($|E^*|$) was computed as the ratio of peak stress over peak strain. This test was attempted in two ways: unglued specimens, and glued specimens. In case of unglued

specimens, the specimens were sandwiched between two platens without gluing. A variable seating load (from 30 psi at 20 °C to 10 psi at 60 °C) was applied to keep the platens from losing contact with the specimen during testing. The results obtained had high variability and were unpredictable. To reduce the variability, it was decided to glue the specimens to the platens. The specimens were tested with zero seating load. The air void contents of the axial test specimens are given in Table 7-11.

Figure 7-18 through Figure 7-20, and Table 7-12 through Table 7-15 list the results of the axial frequency sweep test. It can be seen that with increasing test temperature, the axial stiffness decreases and the phase angle increases. The trend is similar to the shear behavior. The results are not reported at low frequencies at 60 °C as they are highly variable.

7.2.4 Repeated Axial Test

The repeated axial test, similar to the RSCH test, (details in section 5.4.3) was used to characterize the axial deformation of the mix. The loading pattern was similar to the RSCH tests, except that the load was applied axially instead of shear. A controlled cyclic sinusoidal axial stress was applied for a period of 0.1 s followed by a rest period of 0.6 s with a peak axial stress of 68 ± 5 kPa. The test duration was defined to correspond with permanent axial strain accumulation of 1-percent, or 100,000 loading cycles. The measured response was in terms of permanent axial strain accumulation as function of the number of loading cycles.

Figure 7-21 and Table 7-16 show the results of the test. It can be seen that at 60 °C, the mix is prone to axial deformation than at 40 °C. The average number of cycles at 60 °C was 11400 for 1.4% axial strain, whereas at 40 °C the cycles average to more than 100,000 for 0.18% strain. Figure 7-21 shows the plot of accumulated plastic strain versus the number of cycles. The shape of the curve is concave upward and the rate of accumulation increases with number of cycles at 60 °C. However at 40 °C it can be said that the rate of accumulation starts decreasing after initial 1000 cycles. Figure 7-22 shows the overall relationship between $|G^*|$ and $|E^*|$ values across test temperatures and frequencies. It can be seen that the relationship is linear; however the value of Poisson's ratio based on the equation of the best fit line is 0.69 – a theoretical impossibility. This aberration could be due to different sized

samples used for shear and axial tests. Similarly, Figure 7-23 shows the relation between shear and axial phase angle for AC mixes. In this case, it can be said that the shear phase angle is almost the same axial phase angle. The relationships between shear and axial properties can be used to determine one if the other is known regardless of the frequency and test temperature.

7.3 Portland Cement Concrete (PCC) Characterization

Using locally available aggregate, natural sand and Type I cement PCC mix was made. The composition was a typical 3:2:1 (rock:sand:cement) proportioning with a target water-cement ratio of 0.40. The aggregates used were classified as #67 according to AASHTO M43 specifications and were obtained from Garner quarry of Martin Marietta. The goal was to design a typical concrete for testing the bond strength of PCC overlaid with asphalt mix.

The natural sand and aggregate properties were determined according to procedures outlined in standards AASHTO T84 (Standard Method of Test for Specific Gravity and Absorption of Fine Aggregate) and AASHTO T85 (Standard Method of Test for Specific Gravity and Absorption of Coarse Aggregate) respectively. Table 7-17 lists the moisture contents and bulk specific gravities obtained for the materials used. The specific gravity of cement was *assumed* to be 3.15, a commonly used value, in most concrete calculations. To allow for air entrainment and adequate time to cast the mix into samples (or slabs) air entraining agent (AEA) and set-retarder were used. The target yield to prepare required number of test samples or slabs was 1.5 ft³. The actual finalized batch weights, including the amounts required to make a cubic yard of concrete, are listed in Table 7-18.

7.3.1 Mixing, Casting and Curing of Specimens

The mixing process started with wetting the inside of the mixer with water and draining it completely. All the materials, including the AEA and set-retarder, were weighed out before starting the process. Then about half of the rock, sand and water were added to the concrete mixer and mixed for 2 minutes. The AEA was added followed by about a quarter of rock and the sand. The mixing process was continued till small bubbles could be seen in the

aggregate-sand slurry. The bubble formation was due to the addition of the AEA to the slurry. This process took an additional minute of mixing. The set-retarder was added at this point to the mixer. After 1 minute of mixing, the mixer was stopped, and cement was added. The cement was covered with remaining sand and aggregate to prevent the loss of cement due to mixing process. The mixing was started and the remaining water was added slowly through the side walls of the mixer. The mixing continued for about 3-4 minutes before the mix was dumped out of the mixer.

Immediately after mixing ended, a cone slump test (AASHTO T119 – Standard Method of Test for Slump of Portland Cement Concrete) was performed on the plastic mix. The slump cone was moistened and placed on a moist rigid surface. The cone was held down by standing on the two foot pieces and plastic concrete, about 1/3 of the cone volume, was poured into the cone. It was tamped 25 times by a tamping rod and a second layer, about the same volume, was poured into the mold. After tamping 25 times, a third layer was added and the mix was tamped 25 times. Afterwards, the top surface was leveled and the cone lifted vertically. The vertical difference between the top of the mold and the original center of the concrete specimen is the slump of the concrete. The average of three slump tests was 4.75 in.

The unit weight of fresh concrete was determined according to procedure outlined in standard ASTM C138 (Standard Test Method for Density, Yield and Air Content of Concrete). In this procedure, an aluminum alloy bucket was used to consolidate the concrete. The volume of the bucket was 0.25 ft³. The concrete was placed in this bucket in three layers of equal volume. After placing every layer, it was rodded using a metal rod 25 times. After rodding, the sides of the container were tamped 10 times by a mallet to remove the air bubbles that might have been trapped due to rodding. After rodding and tamping the final layer, the excess concrete was struck off the surface of the bucket with a straight edge, and floated to get a flat and smooth surface. The outside walls of the bucket were washed with clean water and wiped dry. The entire bucket was weighed. The mass of the concrete was divided by the volume of the bucket to give the unit weight. The average unit weight of the concrete was 138 pcf.

The fresh concrete was cast into 4×8 and 6×12 inch cylinders and 4×4×16 inch beams according to procedure in AASHTO T23 (Standard Method of Test for Making and Curing

Concrete Test Specimens in the Field). Before casting the mix, the insides of the molds were coated with a thin layer of industrial grease. For casting the cylinders, plastic molds were used and the material was compacted in three equal layers, each layer being rodded 25 times before addition of the second layer. For beams specimens, cast into metal molds, the compaction was done in two layers. Each layer was rodded uniformly 32 times before adding the next layer. After rodding the topmost layer, the excess concrete was struck off the top of the mold and the surface floated. Thin polythene sheets were used to cover the exposed surface of fresh concrete to prevent loss of moisture during the initial curing phase. Twenty four hours after casting, the cylinders were extruded from the plastic molds using compressed air. The metal molds were disassembled and the beams removed. Immediately after removal from molds, the specimens were immersed in a water bath and allowed to cure. Immediately prior to testing, the specimens were removed from the water bath. This was done to reduce the chances of having lower strength due to drying cracks. This was important, especially for flexural specimens, where surface cracks could cause tensile stresses in extreme fibers causing lower strength. Testing was carried out at 7, 14 and 28 days.

7.3.2 Compressive Strength of Cylindrical Concrete Specimens

The basic test to characterize concrete is the compressive strength of concrete. The test was conducted in accordance with standard ASTM C39 (Standard Test Method for Compressive Strength of Cylindrical Concrete Specimens) procedure. The standard states that this test is applicable for concrete mixes having a density of at least 50 pcf. For this test, 4×8 inch specimens were used. Neoprene caps were placed at the top and bottom to enclose the specimen. This was necessary to ensure that the load was applied axially and any non-uniformity on the surface would be leveled out. The moist specimens were placed in a UTM and were subjected to an axially compressive load at a rate of 20-50 psi/s till failure. The peak load was recorded and the failure stress computed by dividing with the cross-sectional area of the cylinder. The results, an average of three tests, are listed in Table 7-19. The average 7, 14 and 28 day strengths were 4810, 5250, and 5750 psi respectively. Most of the specimens tested had a biaxial failure near the edge, a characteristic of testing performed using neoprene caps.

7.3.3 Modulus of Rupture for Concrete Specimens

The flexural strength of PCC was determined using the third point loading test on concrete beams. In this test, a beam of dimensions 4×4×16 inches, was loaded according to specifications in ASTM C78 (Standard Test Method for Flexural Strength of Concrete – Using Simple Beam with Third-Point Loading). The span of the beam between two supports was three times the depth, i.e. 12 inches, with 2 inch overhang on either support. Two point loads were applied at 1/3 and 2/3 length of the span. A three point loading test would cause the middle third of the beam span to be in pure uniform bending with no shear. Thus it would measure the resistance of concrete to pure flexure. The rate of loading was such that the stresses in the extreme fiber increased at a rate of 125 to 175 psi/min. For all the three replicates, the samples failed in the middle third span. The test was conducted at 7 days and the average value for modulus of rupture was 635 psi.

7.3.4 Splitting Tension Test for Concrete Specimens

The tensile strength of PCC was determined using the splitting tensile test. The test was conducted in accordance with AASHTO T198 (Standard Method of Test for Splitting Tensile Strength of Cylindrical Concrete Specimens) at 7 days on 6×12 inch cylinders. The cylinders were tested on their sides and were split diametrically by compressive load. The rate of loading was 100 to 200 psi/min. The peak load at which the failure occurred was used to calculate the splitting tensile strength of the specimen. Based on an average of three tests, the 7 day splitting tensile strength was 410 psi.

7.3.5 Elastic Modulus Test for Concrete Specimens

The elastic modulus of concrete was determined at 7 days in accordance with ASTM C 469 (Standard Test Method for Static Modulus of Elasticity and Poisson's Ratio of Concrete in Compression). A deflection measuring jig was mounted on a 6×12 inch cylinder to measure the deformation of the cylinder under compressive load. Figure 7-24 shows the sketch of the assembly. The jig consisted of two rings attached to the cylinder by means of

screws. The spacing between the two rings was 8 inch. Thus the effective height of the cylinder was 8 inches. The jig was such that one end of the rings was fixed, whereas the diametric end had a dial gauge mounted on it. By geometry, a unit deformation of the cylinder would be recorded as two units on the dial gauge. The strain would, therefore, be half the dial gauge reading divided by the 8, which is the effective height of the cylinder. Based on the result of the compressive strength of the concrete, the maximum stress to which the specimen was loaded was 40%. In this region, the stress versus strain curve is almost a straight line and its slope is the elastic modulus of concrete. Figure 7-25 and Table 7-20 show the results of the elastic modulus test performed. The E-value of concrete as obtained from the plot is 3×10^6 psi.

7.4 Cement Treated Base (CTB) Characterization

Base course is a layer below the surface course in a pavement section and is constructed above the subbase or directly on the subgrade. This section deals with preparing CTB samples and determining their properties. Stabilized bases have higher strength and provide better support to the overlying HMA layer than unbound granular materials. Stabilization can be done either by adding cement, lime or asphalt to crushed aggregate to increase the strength. Type I cement was used for stabilization of the bases tested.

7.4.1 CTB Composition

Aggregates from Garner quarry of Martin Marietta and Type I Portland cement were used to prepare CTB samples. Blending was achieved by combining #67 aggregate, washed screenings and material passing #200 sieves in 70:25:5 proportions. Sieve analysis was performed on individual aggregate stockpiles to obtain gradation of each fraction. Table 7-21, Table 7-22, and Figure 7-26 show the results of the individual stockpiles and the final blend. After batching aggregate, 5% cement by weight of aggregate was added.

7.4.2 Atterberg Limits for CTB Aggregates

Section 1010, subsection 4 (§1010-4) of NCDOT Standard Specifications for Roads and Structures specifies the gradation and Atterberg limits for aggregates used to make (Portland) cement treated base (CTB). In accordance with requirements of AASHTO T 89 or ASTM D 4318 (Standard Test Methods for Liquid Limit, Plastic Limit, and Plasticity Index of Soils), the aggregate blend was sieved on a #40 (0.425 mm) sieve. The fraction passing #40 was used to conduct this test. About 200 g of material was sampled and the test was performed using the standard liquid limit device (Casagrande cup). In this case, the maximum number of blows on the Casagrande cup was about 10 over a range of moisture contents. Thus, it was concluded that the material was non-plastic.

The outcome from Casagrande cup test required the use of the modified method for liquid limit for non-plastic materials as per NCDOT specifications. The modified test required mixing the soil with water to form a uniform mass of stiff consistency. The mass was then spread in a dish, similar to the Casagrande cup procedure, but without grooving. A clean dry spatula was pressed firmly on the soil mass and lifted without dragging. The surface of the spatula in contact with soil was observed for water. This process was repeated with increasing water content till water just started to adhere to the spatula in the form of beads. The water content, at this consistency, is called as the liquid limit. Table 7-24 shows the liquid limit value obtained; the average is 29. This falls within the DOT specified range of 0-30. The plastic limit could not be determined as the material could not be rolled into threads on a glass plate. The plasticity index for the CTB was, therefore, NP (non-plastic).

7.4.3 Modified Proctor Density Test

This section describes the modified proctor density test conducted in accordance with ASTM D1557 (Standard Test Methods for Laboratory Compaction Characteristics of Soil using Modified Effort). The aggregates and cement were blended proportion before adding water. The compaction was done in a standard modified proctor mold having dimensions of 6×4.58 inches (volume 0.075 ft³). The compaction was done in five layers with each layer having about the same volume. After putting in a layer in the mold, it was compacted by applying 56 blows with a modified proctor hammer. The excess material was scraped out

from the top of the mold and the sides. The weight of the empty mold and the mold with specimen were determined. The wet density of the specimen could be obtained by dividing the weight of the specimen by the volume of the mold. Table 7-23 shows the results obtained for the test. The water content was continuously increased from 3.5 to 7%. A small representative part from the larger sample was dried and the moisture content determined. The dry density was calculated and the results are presented graphically in Figure 7-27. The peak dry density as seen from the plot is 146 pcf and the optimum moisture content is 5.6%. The CTB specimens used to make the composite samples were compacted with 6.0% moisture content, slightly higher than the optimum moisture content. (NCDOT specifications - §540 of Standard Specifications for Roads and Structures - state that the compaction of CTB should occur between optimum and optimum + 1.5% moisture content.)

An estimate of 7-day unconfined compressive strength of 600 psi for CTB was obtained in consultation with NCDOT. Based on the nomograph presented in Figure 7-28, the modulus corresponding to 600 psi unconfined strength was estimated to be 6.9×10^5 psi. This value was used for layered analysis in Chapter 9.

Table 7-1 Air voids of AC mix samples

Sample ID	Height (mm)	Air voids (%)
M1	50.36	4.3
M2	48.93	4.4
M3	49.20	4.3
M4	47.68	4.3

Table 7-2 $|G^*|$ vs. frequency for AC mix, 20 °C, in Pa

Frequency (Hz)	M1	M2	M3	M4	Average
10	1.87E+09	1.65E+09	1.70E+09	1.79E+09	1.75E+09
5	1.63E+09	1.46E+09	1.52E+09	1.59E+09	1.55E+09
2	1.29E+09	1.16E+09	1.20E+09	1.27E+09	1.23E+09
1	1.14E+09	1.07E+09	1.22E+09	1.15E+09	1.15E+09
0.5	8.60E+08	8.73E+08	8.29E+08	9.01E+08	8.66E+08
0.2	6.45E+08	6.51E+08	6.90E+08	6.76E+08	6.66E+08
0.1	4.98E+08	5.25E+08	6.02E+08	5.27E+08	5.38E+08
0.05	3.13E+08	3.33E+08	2.03E+08	3.95E+08	3.11E+08
0.02	2.28E+08	2.50E+08	1.91E+08	2.77E+08	2.37E+08
0.01	1.76E+08	2.49E+08	2.78E+08	2.18E+08	2.30E+08

Table 7-3 Shear phase angle (degrees) vs. frequency for AC mix, 20 °C

Frequency (Hz)	M1	M2	M3	M4	Average
10	17.14	15.71	16.12	14.46	15.86
5	19.14	17.45	17.27	16.21	17.52
2	22.49	19.19	25.63	19.71	21.76
1	22.79	20.98	23.79	19.91	21.87
0.5	27.15	26.12	26.36	22.89	25.63
0.2	32.00	30.97	32.18	28.40	30.89
0.1	35.61	36.69	37.60	31.29	35.30
0.05	28.85	31.52	18.33	30.84	27.39
0.02	35.99	38.49	29.88	34.90	34.82
0.01	38.49	47.24	49.96	37.78	43.37

Table 7-4 $|G^*|$ vs. frequency for AC mix, 30 °C, in Pa

Frequency (Hz)	M1	M2	M3	M4	Average
10	9.62E+08	9.49E+08	1.00E+09	9.05E+08	9.55E+08
5	7.70E+08	7.65E+08	8.01E+08	7.23E+08	7.65E+08
2	5.57E+08	5.66E+08	5.78E+08	5.20E+08	5.55E+08
1	4.18E+08	4.12E+08	4.42E+08	3.91E+08	4.16E+08
0.5	3.14E+08	3.23E+08	3.25E+08	2.91E+08	3.13E+08
0.2	2.08E+08	2.17E+08	2.18E+08	1.94E+08	2.09E+08
0.1	1.54E+08	1.59E+08	1.61E+08	1.46E+08	1.55E+08
0.05	1.01E+08	1.09E+08	1.10E+08	9.60E+07	1.04E+08
0.02	6.89E+07	7.74E+07	6.92E+07	6.61E+07	7.04E+07
0.01	5.08E+07	5.74E+07	5.31E+07	5.03E+07	5.29E+07

Table 7-5 Shear phase angle (degrees) vs. frequency for AC mix, 30 °C

Frequency (Hz)	M1	M2	M3	M4	Average
10	27.80	26.33	27.45	28.87	27.61
5	30.58	29.17	30.25	31.64	30.41
2	33.88	33.03	34.01	35.15	34.02
1	37.70	33.21	40.61	38.23	37.44
0.5	39.73	38.67	39.44	41.25	39.77
0.2	43.92	42.65	43.75	44.51	43.71
0.1	46.39	44.68	45.50	46.41	45.75
0.05	45.39	43.61	46.71	43.77	44.87
0.02	46.98	50.20	46.32	47.60	47.78
0.01	47.87	49.21	52.98	45.99	49.01

Table 7-6 $|G^*|$ vs. frequency for AC mix, 40 °C, in Pa

Frequency (Hz)	M1	M2	M3	M4	Average
10	4.55E+08	4.46E+08	4.45E+08	4.54E+08	4.50E+08
5	3.40E+08	3.37E+08	3.29E+08	3.37E+08	3.36E+08
2	2.29E+08	2.34E+08	2.26E+08	2.26E+08	2.29E+08
1	1.66E+08	1.72E+08	1.67E+08	1.66E+08	1.68E+08
0.5	1.22E+08	1.21E+08	1.20E+08	1.21E+08	1.21E+08
0.2	8.21E+07	8.15E+07	7.95E+07	8.06E+07	8.09E+07
0.1	6.30E+07	5.82E+07	5.91E+07	6.02E+07	6.01E+07
0.05	4.68E+07	3.81E+07	4.25E+07	4.57E+07	4.32E+07
0.02	3.61E+07	2.92E+07	3.19E+07	3.46E+07	3.29E+07
0.01	2.93E+07	2.56E+07	2.72E+07	2.81E+07	2.75E+07

Table 7-7 Shear phase angle (degrees) vs. frequency for AC mix, 40 °C

Frequency (Hz)	M1	M2	M3	M4	Average
10	37.57	37.21	38.35	37.66	37.70
5	40.26	39.59	40.84	40.50	40.30
2	42.85	40.19	44.88	43.25	42.79
1	45.02	47.16	44.91	44.42	45.38
0.5	45.79	45.83	46.66	46.50	46.19
0.2	45.92	47.46	47.32	46.16	46.72
0.1	43.78	45.27	45.47	44.02	44.63
0.05	42.58	43.38	41.62	43.55	42.78
0.02	40.49	40.29	39.96	40.64	40.34
0.01	37.62	40.91	40.00	40.61	39.79

Table 7-8 $|G^*|$ vs. frequency for AC mix, 60 °C, in Pa

Frequency (Hz)	M1	M2	M3	M4	Average
10	1.03E+08	8.75E+07	1.04E+08	1.03E+08	9.95E+07
5	7.84E+07	6.84E+07	7.79E+07	7.89E+07	7.59E+07
2	5.99E+07	5.22E+07	6.95E+07	5.73E+07	5.97E+07
1	4.85E+07	4.38E+07	4.91E+07	4.79E+07	4.73E+07
0.5	4.04E+07	3.78E+07	3.96E+07	4.04E+07	3.96E+07
0.2	3.34E+07	3.23E+07	3.09E+07	3.35E+07	3.25E+07
0.1	3.02E+07	2.90E+07	2.62E+07	2.96E+07	2.88E+07
0.05	2.59E+07	2.66E+07	2.33E+07	2.70E+07	2.57E+07
0.02	2.35E+07	2.43E+07	2.12E+07	2.39E+07	2.32E+07
0.01	2.19E+07	2.30E+07	1.85E+07	2.19E+07	2.13E+07

Table 7-9 Shear phase angle (degrees) vs. frequency for AC mix, 60 °C

Frequency (Hz)	M1	M2	M3	M4	Average
10	42.21	40.56	41.88	42.37	39.81
5	40.01	38.06	40.37	40.81	39.07
2	39.96	34.87	45.14	36.30	33.94
1	35.08	31.86	33.83	34.99	31.64
0.5	31.54	30.19	32.32	32.50	28.85
0.2	28.85	27.54	29.72	29.29	26.74
0.1	26.13	24.79	29.06	26.97	24.63
0.05	23.87	23.06	27.41	24.17	22.37
0.02	22.90	20.43	22.36	23.78	20.57
0.01	18.24	17.45	26.66	19.93	39.81

Table 7-10 RSCH cycles, at 40 and 60 °C

Sample ID	Test Temperature (°C)	Max RSCH cycles	Max Plastic Strain	Plastic Strain @5000 cycles
M1	60	13000	4.60%	3.05%
M2	60	27000	4.80%	2.84%
M3	40	100000	0.76%	0.52%
M4	40	100000	1.34%	0.82%

Table 7-11 Air voids of axial test samples

Sample ID	Test temperature	Tests	Air voids
SA01	60 °C	Repeated Axial Test	3.8%
SA03			3.9%
SA04	40 °C	Repeated Axial Test	3.8%
SA05			4.0%
SA07	20, 30, 40, 60 °C	Axial Frequency Sweep Test	4.0%
SA12			3.8%

Table 7-12 |E*| vs. frequency for AC mix, 20 and 30 °C, in Pa

Frequency (Hz)	20 C			30 C		
	SA07	SA12	Average	SA07	SA12	Average
10	6.14E+09	5.57E+09	5.86E+09	3.47E+09	3.40E+09	3.43E+09
5	5.40E+09	4.81E+09	5.11E+09	2.83E+09	2.74E+09	2.79E+09
2	4.45E+09	3.87E+09	4.16E+09	2.10E+09	1.99E+09	2.04E+09
1	3.77E+09	3.20E+09	3.49E+09	1.61E+09	1.49E+09	1.55E+09
0.5	3.13E+09	2.58E+09	2.86E+09	1.23E+09	1.11E+09	1.17E+09
0.2	2.37E+09	1.88E+09	2.12E+09	8.18E+08	7.08E+08	7.63E+08

Table 7-13 Axial phase angle (degrees) vs. frequency for AC mix, 20 and 30 °C

Frequency (Hz)	20 C			30 C		
	SA07	SA12	Average	SA07	SA12	Average
10	16.84	18.74	17.79	25.17	26.84	26.00
5	18.49	20.74	19.61	27.66	29.79	28.72
2	21.01	23.76	22.38	31.24	33.95	32.60
1	23.10	26.30	24.70	33.87	37.62	35.75
0.5	25.79	29.12	27.45	36.76	40.62	38.69
0.2	29.44	33.11	31.27	40.12	44.91	42.51

Table 7-14 |E*| vs. frequency for AC mix, 40 and 60 °C, in Pa

Frequency (Hz)	40 C			60 C		
	SA07	SA12	Average	SA07	SA12	Average
10	1.87E+09	1.69E+09	1.78E+09	5.46E+08	3.36E+08	4.41E+08
5	1.42E+09	1.28E+09	1.35E+09	3.94E+08	2.28E+08	3.11E+08
2	9.57E+08	8.53E+08	9.05E+08	2.83E+08	1.57E+08	2.20E+08
1	6.90E+08	6.11E+08	6.51E+08	2.07E+08	1.02E+08	1.55E+08
0.5	4.85E+08	4.40E+08	4.63E+08	–	–	–
0.2	2.97E+08	2.76E+08	2.87E+08	–	–	–

Table 7-15 Axial phase angle (degrees) vs. frequency for AC mix, 40 and 60 °C

Frequency (Hz)	40 C			60 C		
	SA07	SA12	Average	SA07	SA12	Average
10	33.19	34.42	33.81	41.14	44.23	42.69
5	35.79	36.29	36.04	40.81	44.73	42.77
2	39.24	38.87	39.05	38.06	43.64	40.85
1	41.34	39.87	40.60	37.17	42.72	39.95
0.5	43.04	40.90	41.97	–	–	–
0.2	44.72	41.20	42.96	–	–	–

Table 7-16 Repeated axial test cycles, at 40 and 60 °C

Sample ID	Test Temperature (°C)	Max axial cycles	Max Plastic Strain
SA01	60	8800	1.37%
SA03	60	14000	1.44%
SA04	40	100000	0.19%
SA05	40	100000	0.17%

Table 7-17 Aggregate moisture contents and specific gravities

Property	Sand	Rock	Cement
SG (SSD)	2.630	2.632	3.15 ²
Total moisture	0.40%	0.40%	0%
Absorption	0.60%	0.66%	0%

Table 7-18 Batch weights for PCC

Material	Trial Weight (lb)	Batch Weight (pcy)	SSD Weight (pcy)
Cement	35.5	622	622
Sand	66.6	1166	1168
Rock	95.5	1672	1676
Water	15.2	266	259
AEA	6 ml	0.56 oz/cwt	0.56 oz/cwt
Retarder	20 ml	1.88 oz/cwt	1.88 oz/cwt

Table 7-19 Properties of concrete

Property	Value
w/c ratio	0.42
Slump	4.75 in
Unit wt	138 pcf
7d strength	4810 psi
14d strength	5250 psi
28d strength	5750 psi
7d Elastic modulus	3.0E+06 psi
7d Splitting tension	410 psi
7d Modulus of rupture	635 psi

Table 7-20 Elastic modulus for PCC

Load (lb)	Stress (psi)	Dial (in)	Strain
4800	169.8	8.00E-04	5.00E-05
5775	204.2	8.00E-04	5.00E-05
24000	848.8	4.00E-03	2.50E-04
24000	848.8	4.30E-03	2.69E-04
27000	954.9	4.70E-03	2.94E-04
31000	1096.4	5.60E-03	3.50E-04
31000	1096.4	5.60E-03	3.50E-04

² The cement specific gravity has been assumed to be 3.15. The absorption and total moisture content of cement is assumed to be 0%.

Table 7-21 Gradation (% passing) for aggregate piles used for CTB

Sieve size	#67	Screenings	P #200	Blended	DOT Specs
1.5"	100.0	100.0	100.0	100.0	
1.0"	100.0	100.0	100.0	100.0	76-100
0.5"	77.0	100.0	100.0	83.9	54-86
#4	15.2	99.0	100.0	40.4	35-64
#10	6.9	75.0	100.0	28.6	24-54
#40	3.9	29.1	100.0	15.0	12-36
#200	1.1	2.0	100.0	6.3	5-14
Proportion	70	25	5		

Table 7-22 Gradation criteria for material passing #10 sieve (soil mortar)

Sieve Size	Blend	DOT Specs
#40	53%	38-87%
#200	22%	11-36%

Table 7-23 Moisture density determination for CTB

Test No.	Mold Weight (lb) = 13.11			Mold Volume (ft ³) = 0.075			
	Wt of Mold+CTB (lb)	Wt of Soil (lb)	Wet Unit wt (pcf)	Wt of wet sample (lb)	Wt of dry sample (lb)	Water content (%)	Dry unit weight (pcf)
1	23.73	10.63	141.72	0.810	0.782	3.59	136.81
2	23.94	10.84	144.52	1.045	1.002	4.24	138.65
3	24.40	11.29	150.52	1.149	1.094	5.07	143.25
4	24.66	11.55	153.98	1.041	0.986	5.60	145.82
5	24.60	11.49	153.18	1.186	1.114	6.45	143.90
6	24.53	11.42	152.25	1.118	1.045	6.99	142.30

Table 7-24 Liquid limit property for CTB using DOT modified method

Sample	Wt of can (g)	Wt of can + wet soil (g)	Wt of can + dry soil (g)	Liquid Limit
1	15.60	32.73	28.98	28.0%
2	16.11	37.11	32.32	29.5%
3	15.99	42.99	36.83	29.6%

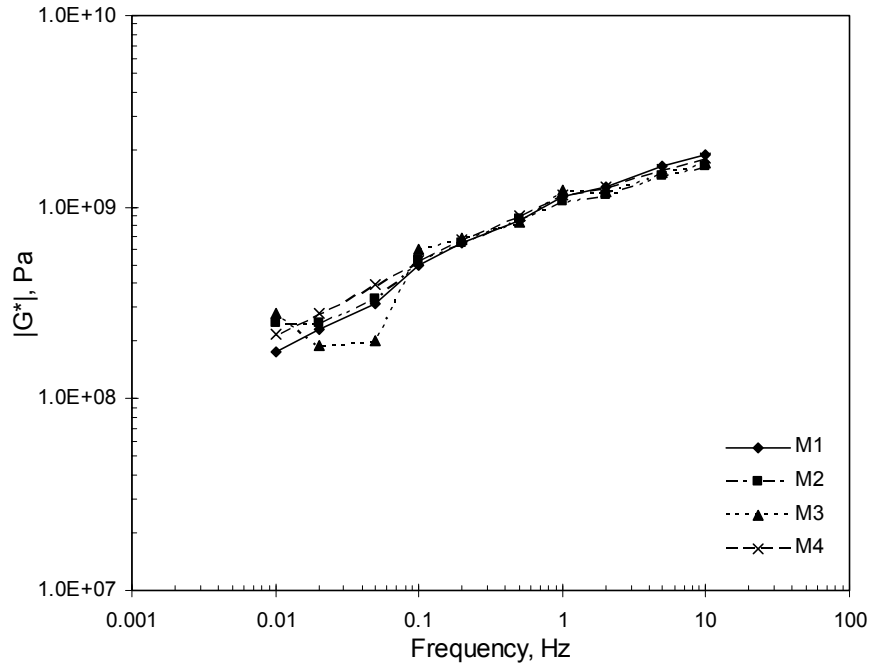


Figure 7-1 Dynamic shear modulus ($|G^*|$) vs. frequency for AC mix, 20 °C

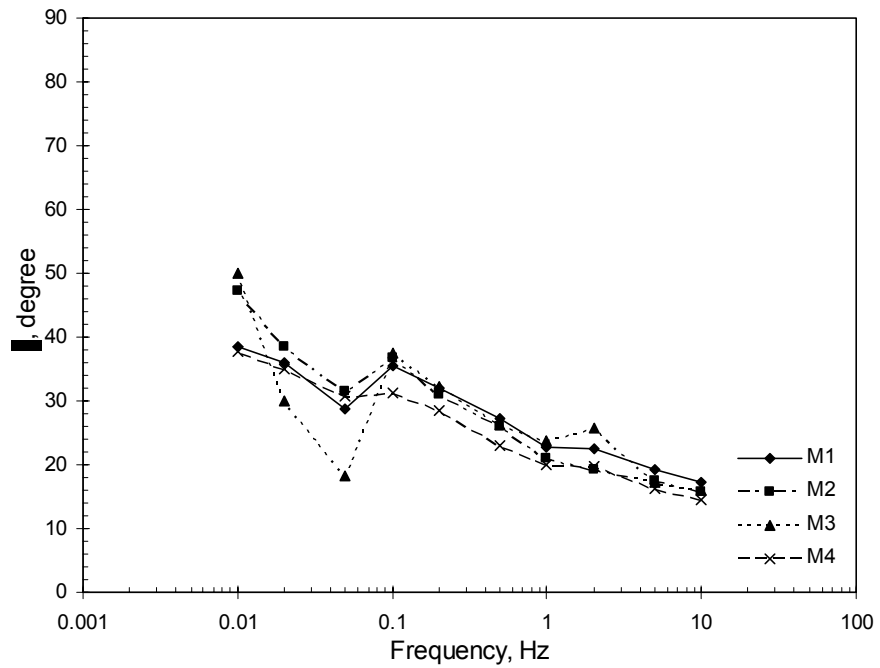


Figure 7-2 Shear phase angle (δ) vs. frequency for AC mix, 20 °C

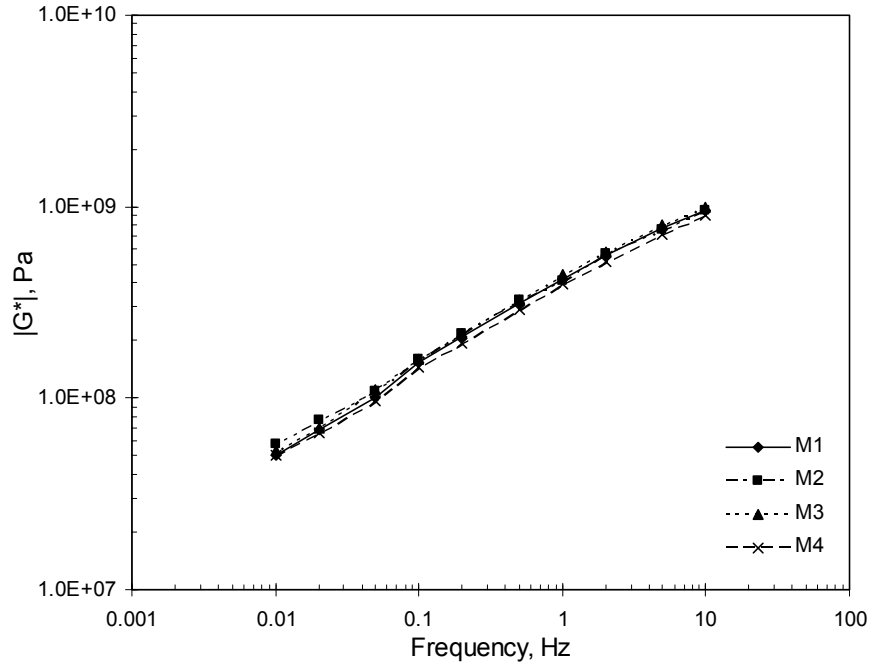


Figure 7-3 Dynamic shear modulus ($|G^*|$) vs. frequency for AC mix, 30 °C

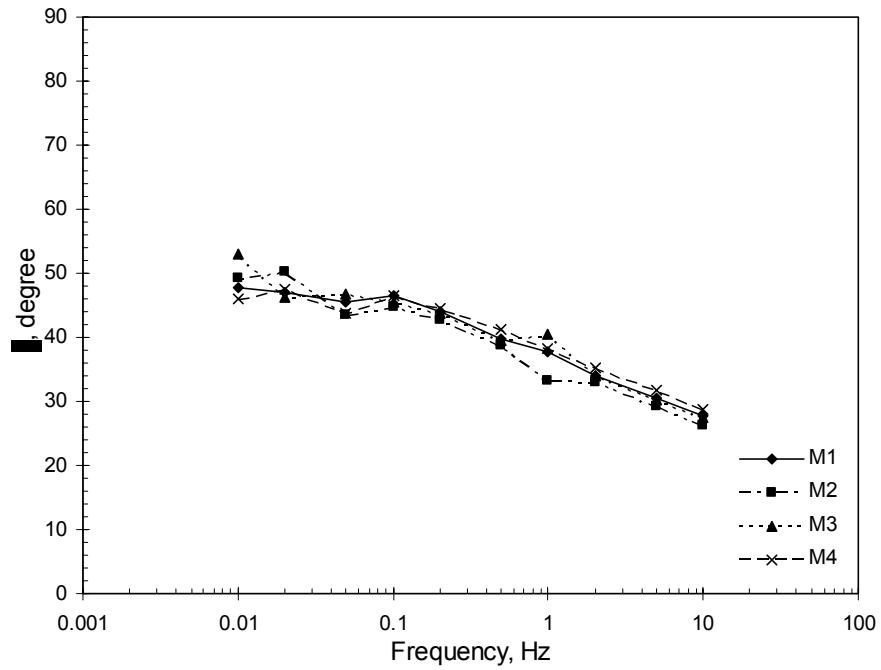


Figure 7-4 Shear phase angle (δ) vs. frequency for AC mix, 30 °C

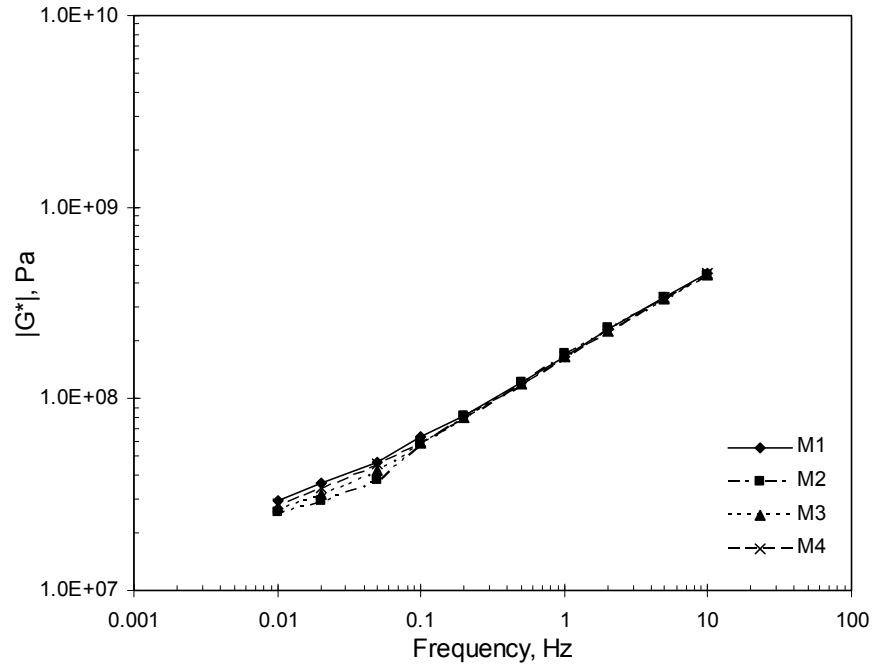


Figure 7-5 Dynamic shear modulus ($|G^*|$) vs. frequency for AC mix, 40 °C

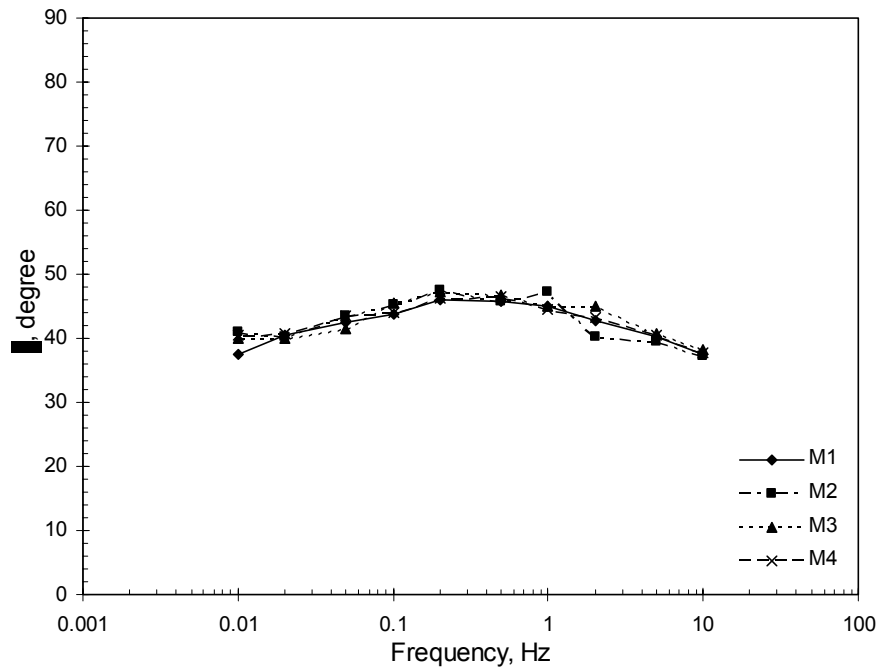


Figure 7-6 Shear phase angle (δ) vs. frequency for AC mix, 40 °C

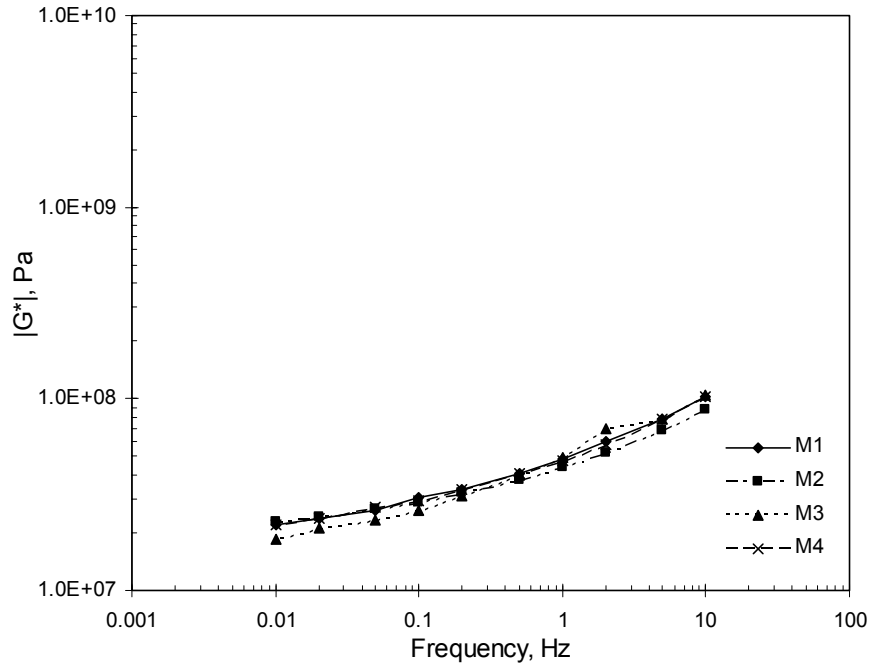


Figure 7-7 Dynamic shear modulus ($|G^*|$) vs. frequency for AC mix, 60 °C

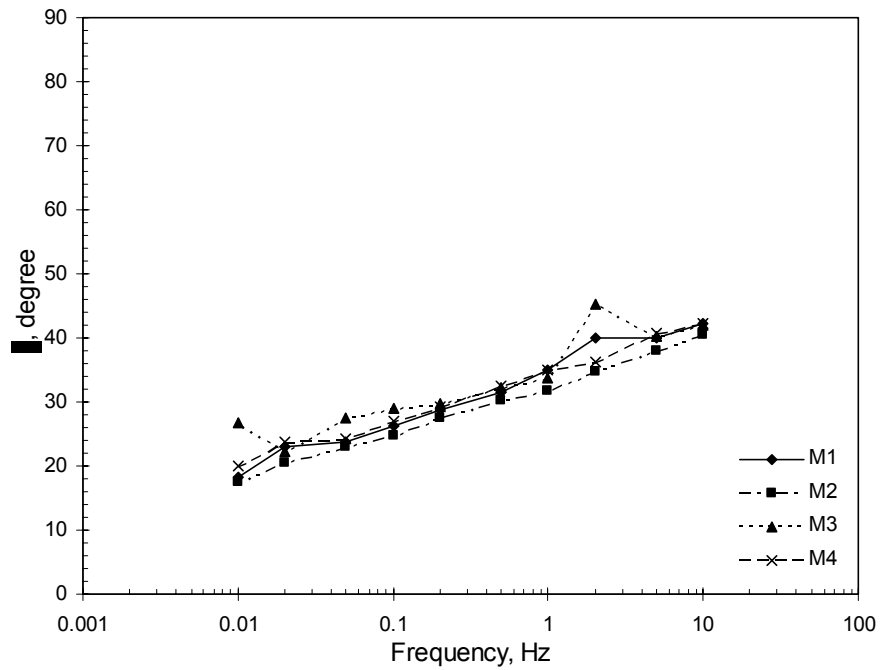


Figure 7-8 Shear phase angle (δ) vs. frequency for AC mix, 60 °C

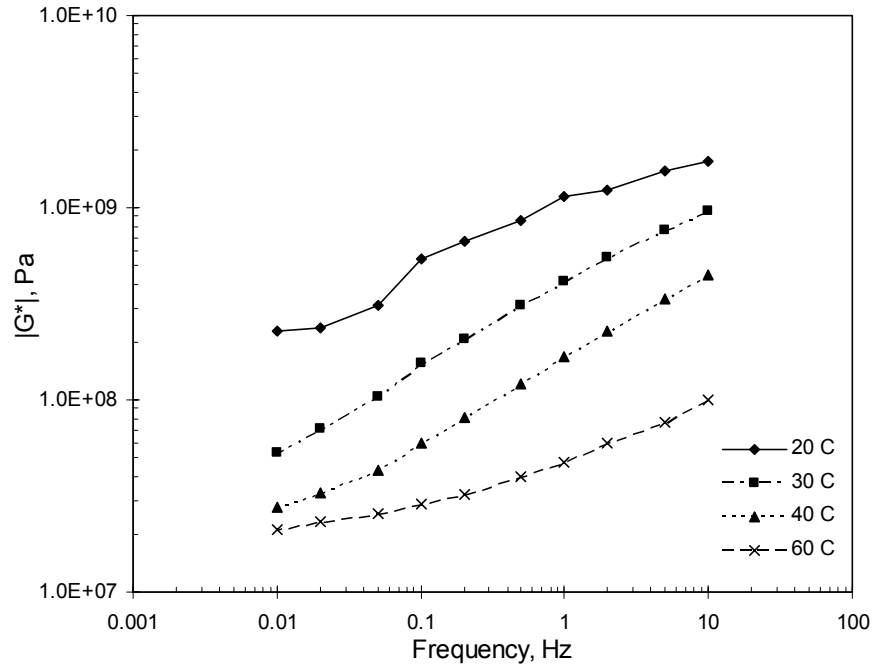


Figure 7-9 Average dynamic shear modulus ($|G^*|$) vs. frequency for AC mix

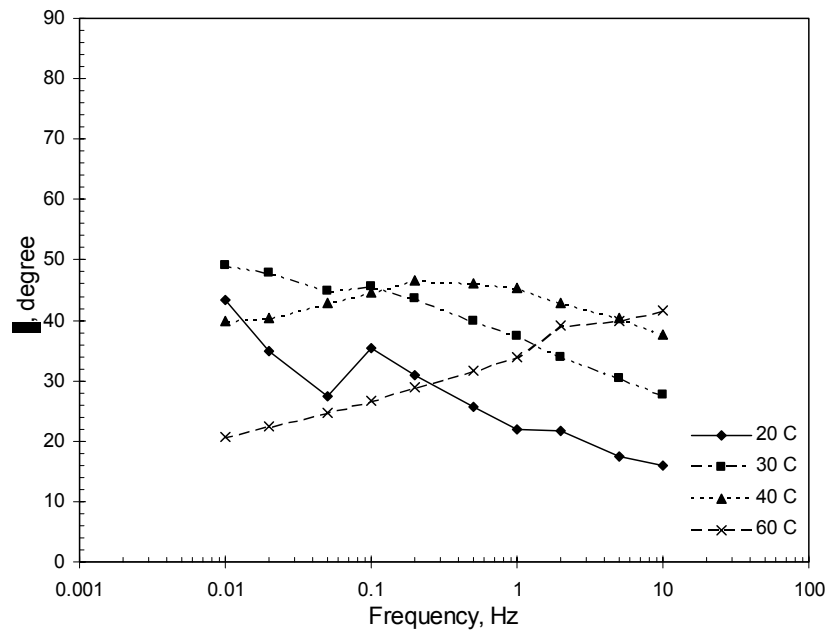


Figure 7-10 Average shear phase angle (δ) vs. frequency for AC mix

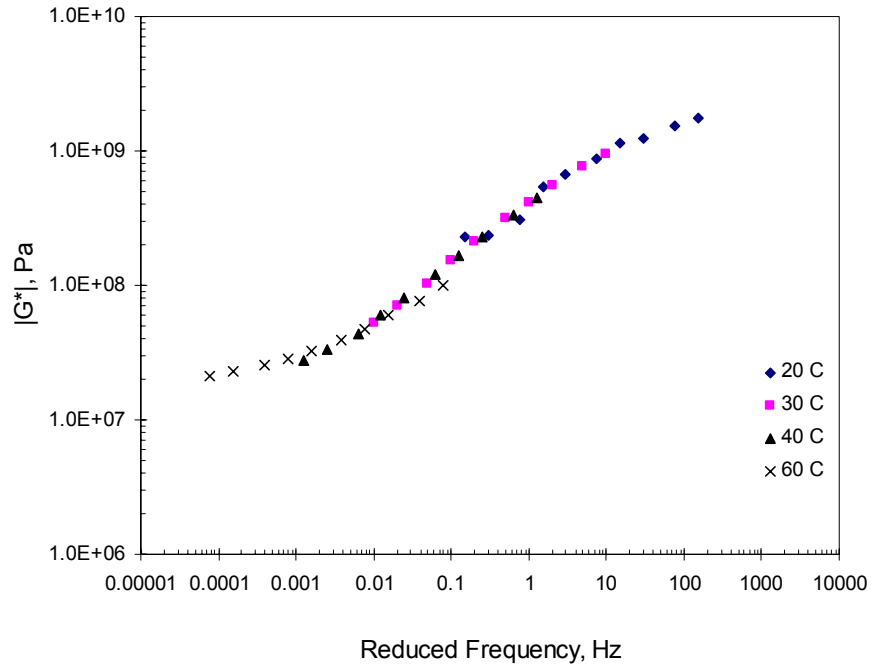


Figure 7-11 $|G^*|$ master curve for AC mix, 30 °C

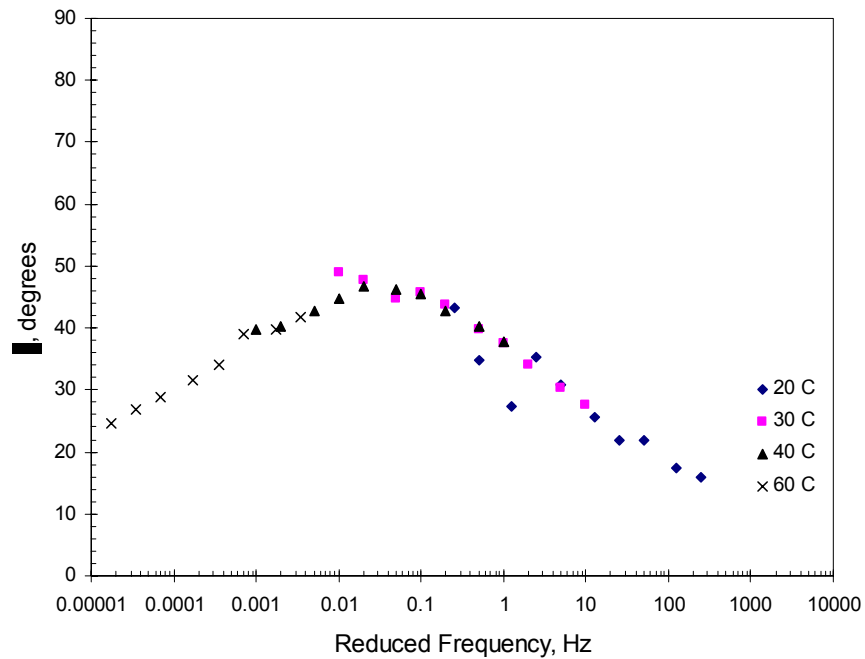


Figure 7-12 Shear phase angle (δ) master curve for AC mix, 30 °C

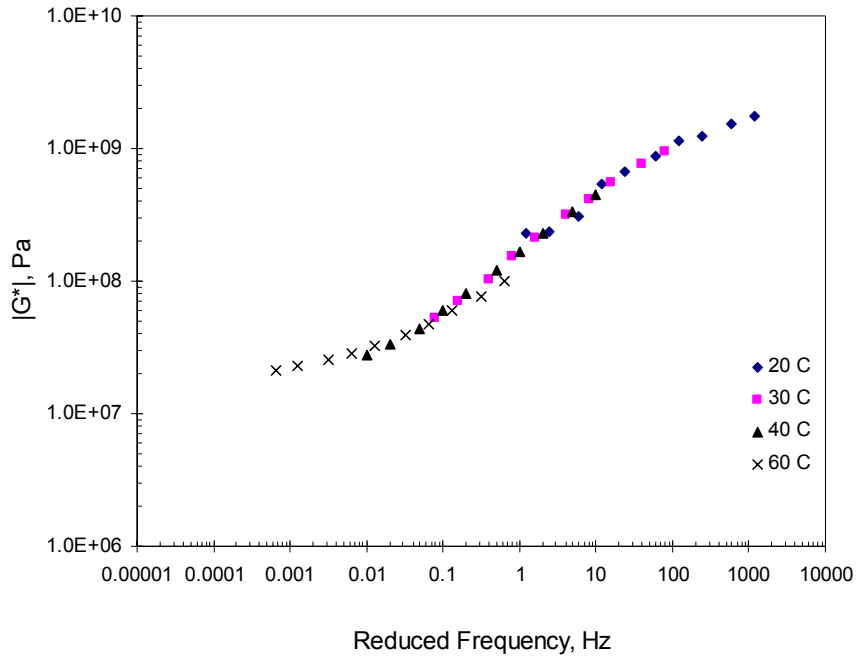


Figure 7-13 $|G^*|$ master curve for AC mix, 40 °C

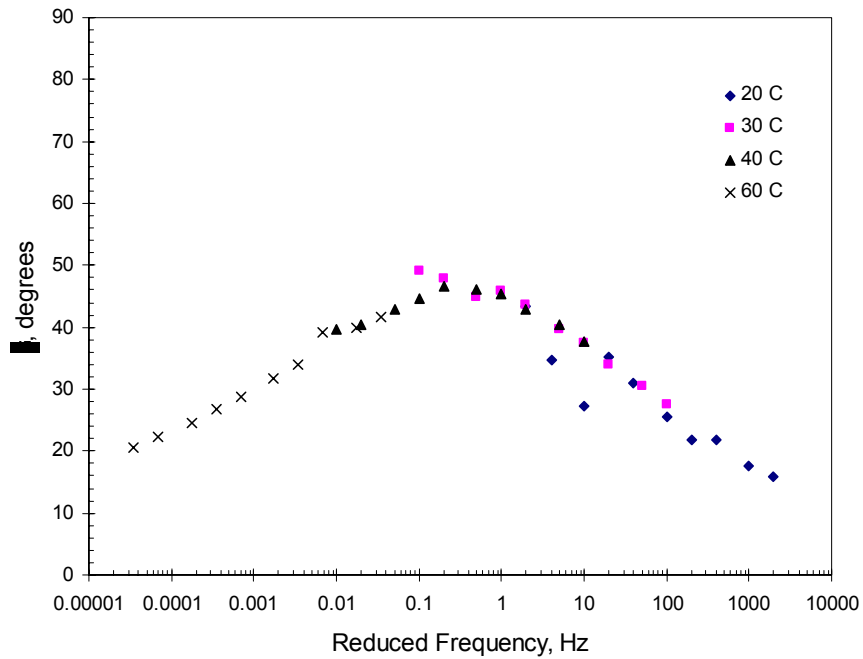


Figure 7-14 Shear phase angle (δ) master curve for AC mix, 40 °C

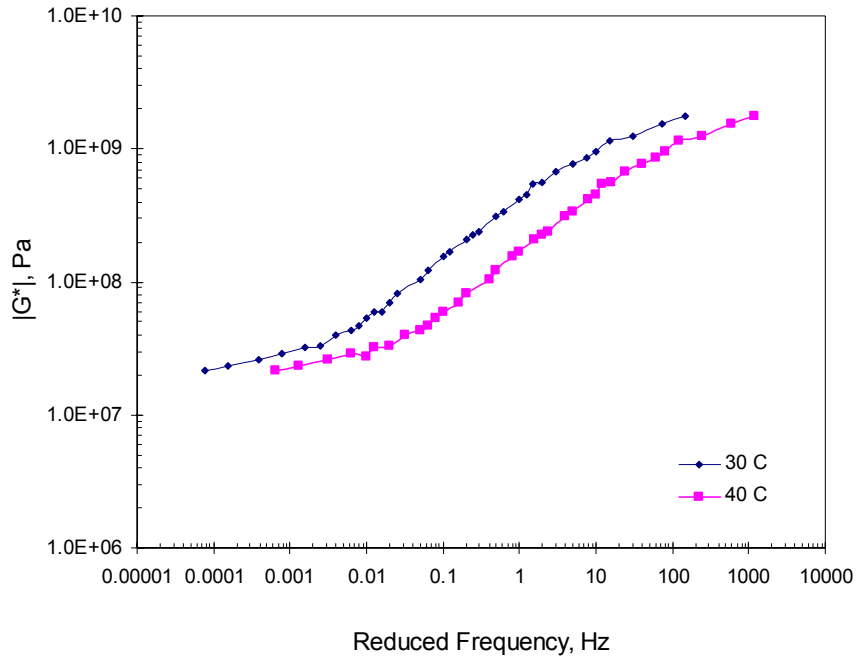


Figure 7-15 $|G^*|$ master curve for AC mix, 30 and 40 °C

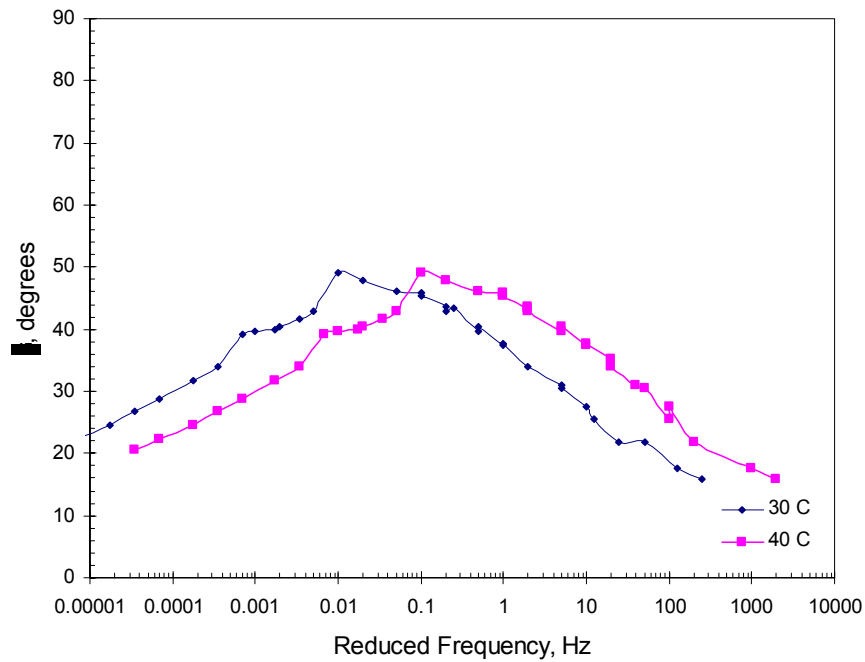


Figure 7-16 Shear phase angle (δ) master curve for AC mix, 30 and 40 °C

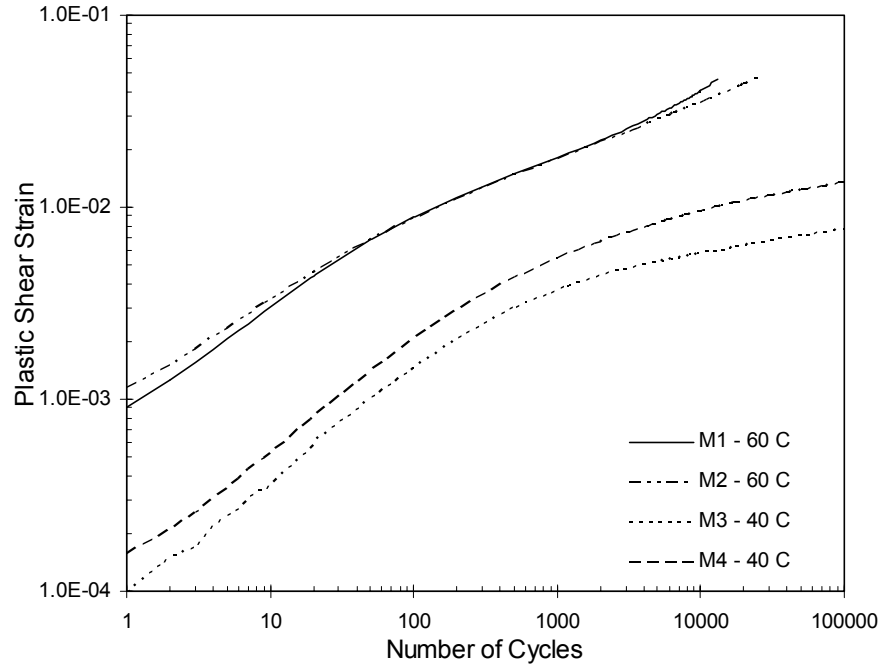


Figure 7-17 Plastic shear strain vs. RSCH cycles, 40 and 60 °C for AC mixes

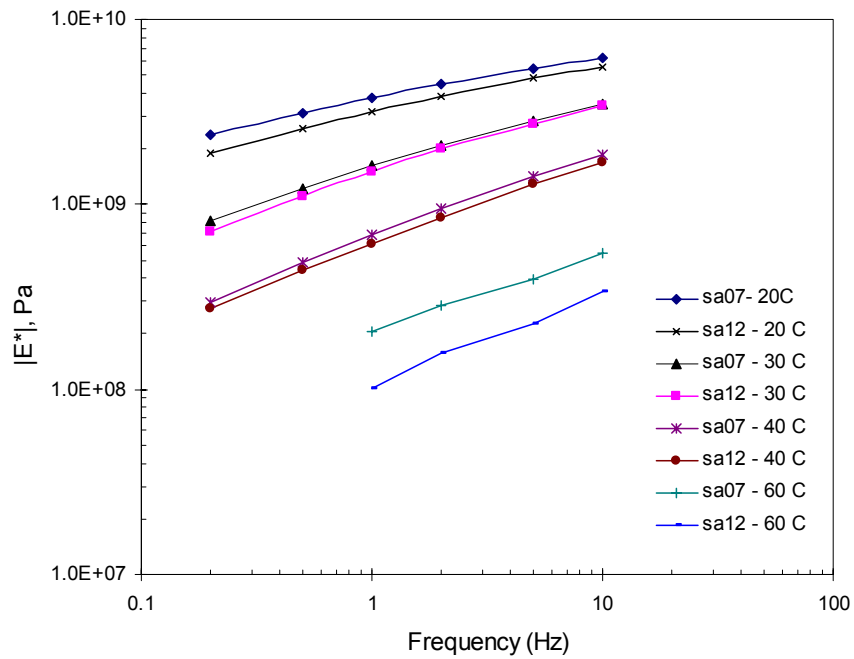


Figure 7-18 Dynamic axial modulus ($|E^*|$) vs. frequency for AC mix

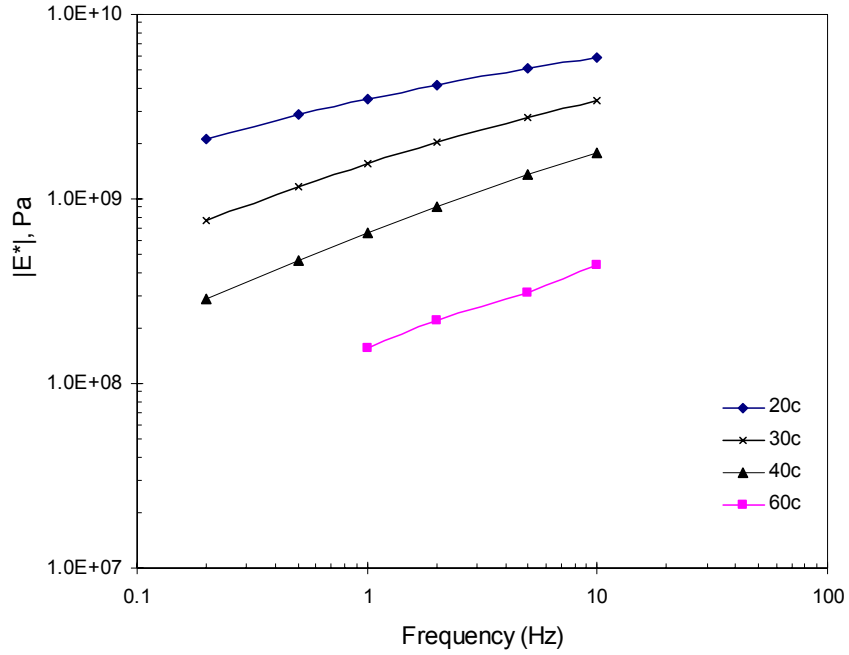


Figure 7-19 Average dynamic axial modulus ($|E^*|$) vs. frequency for AC mix

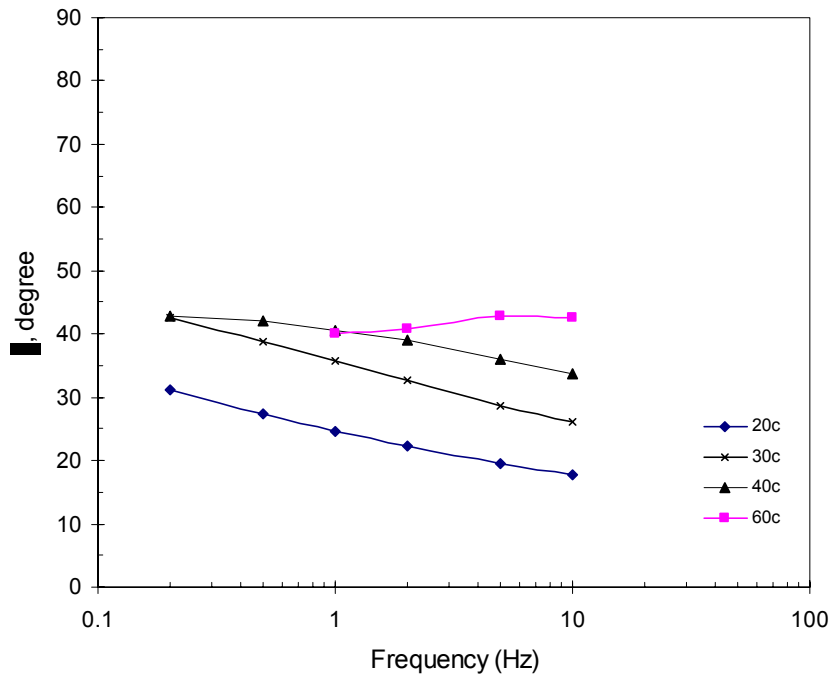


Figure 7-20 Average axial phase angle (δ) vs. frequency for AC mix

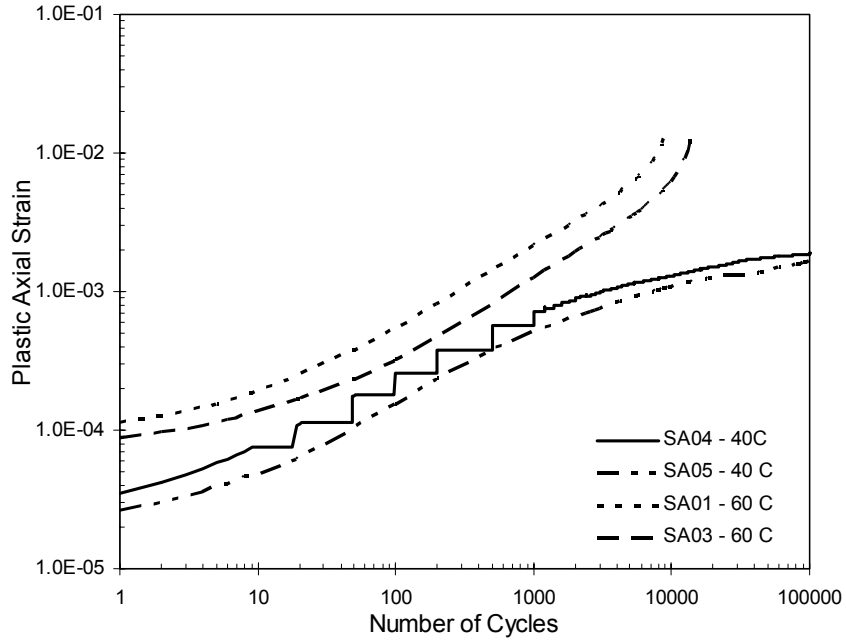


Figure 7-21 Plastic axial strain vs. cycles, 40 and 60 °C for AC mixes

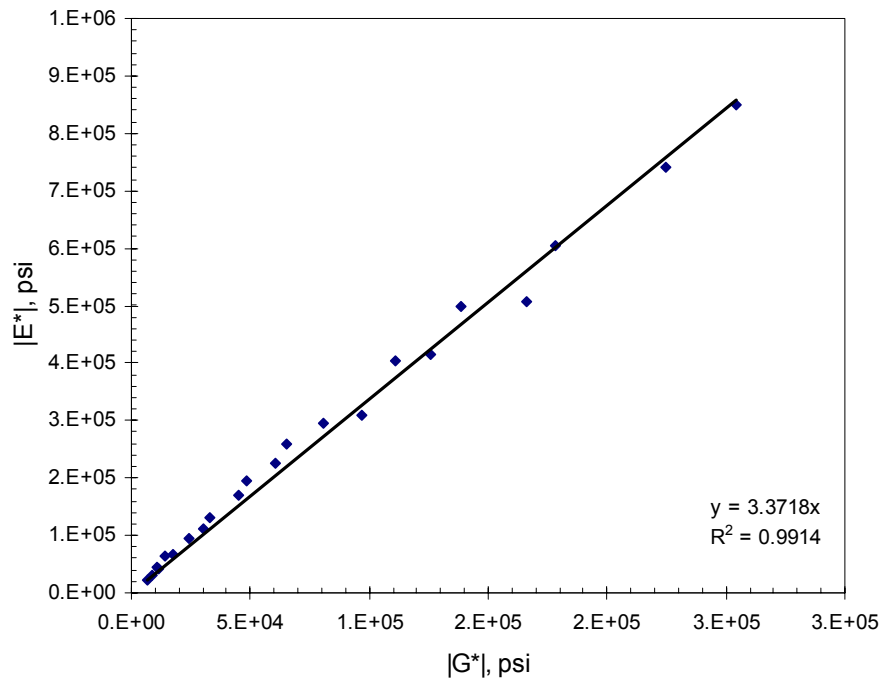


Figure 7-22 Relationship between $|G^*|$ and $|E^*|$ for AC mixes

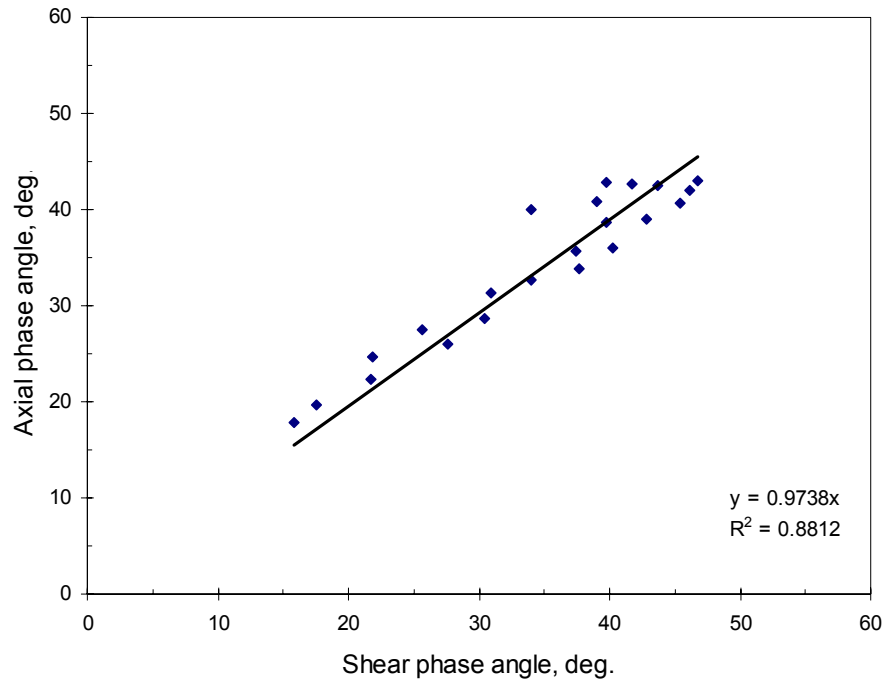


Figure 7-23 Relationship between shear and axial phase angle for AC mixes

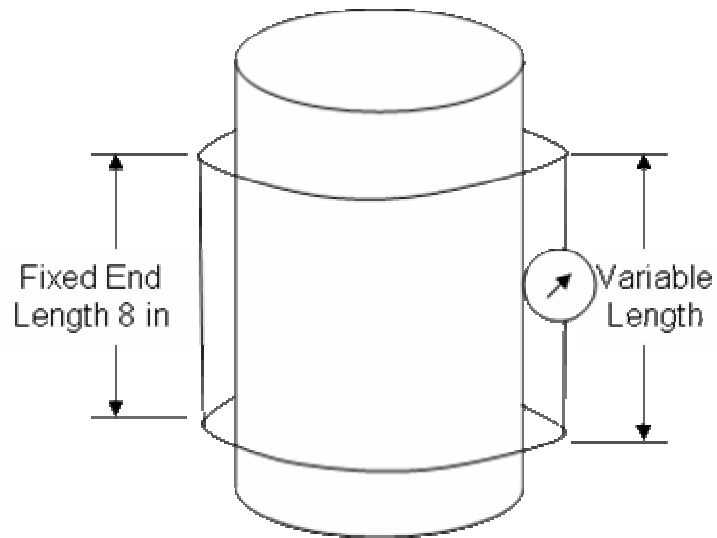


Figure 7-24 Set up for elastic modulus of concrete using a 6x12 cylinder

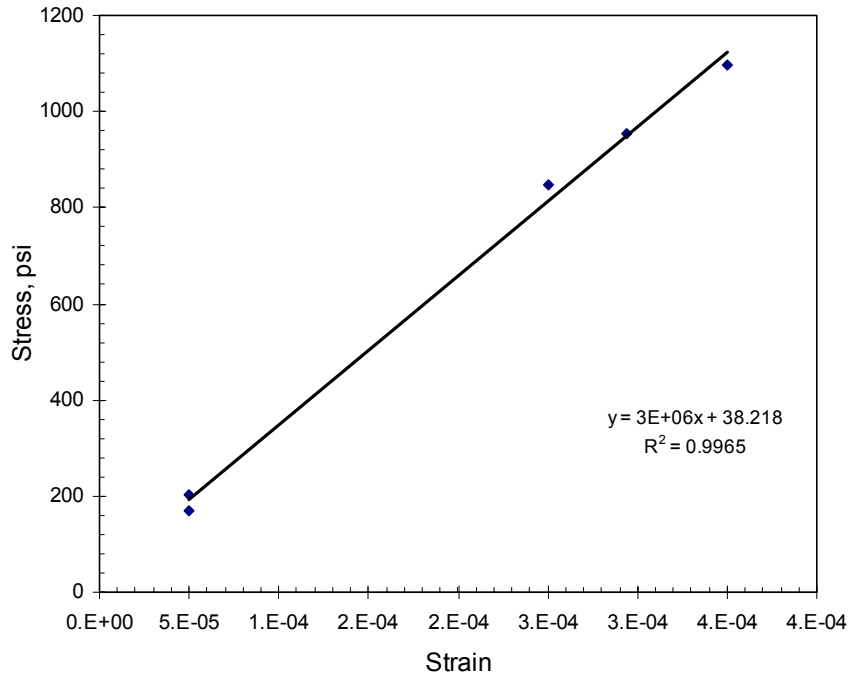


Figure 7-25 Axial stress vs. strain at 7 days for PCC

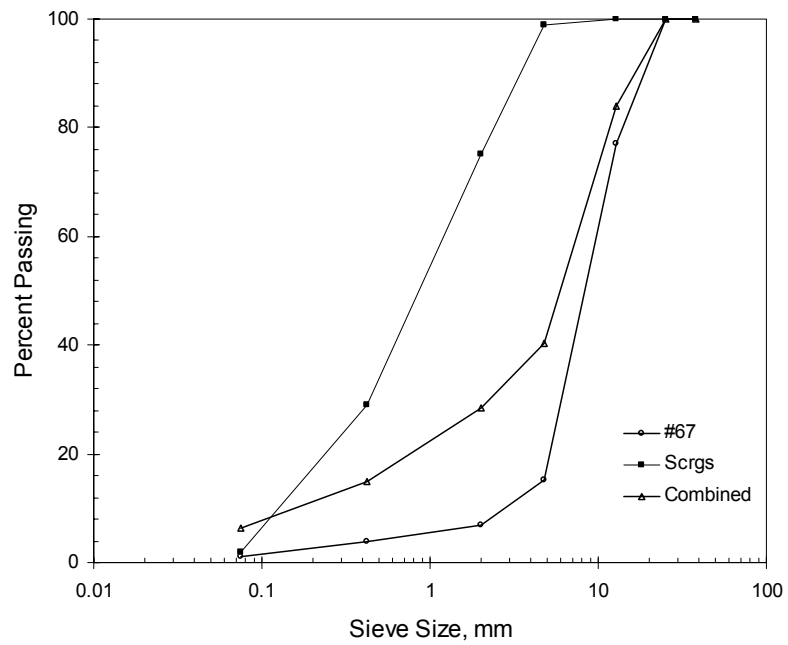


Figure 7-26 Gradation of materials used for CTB

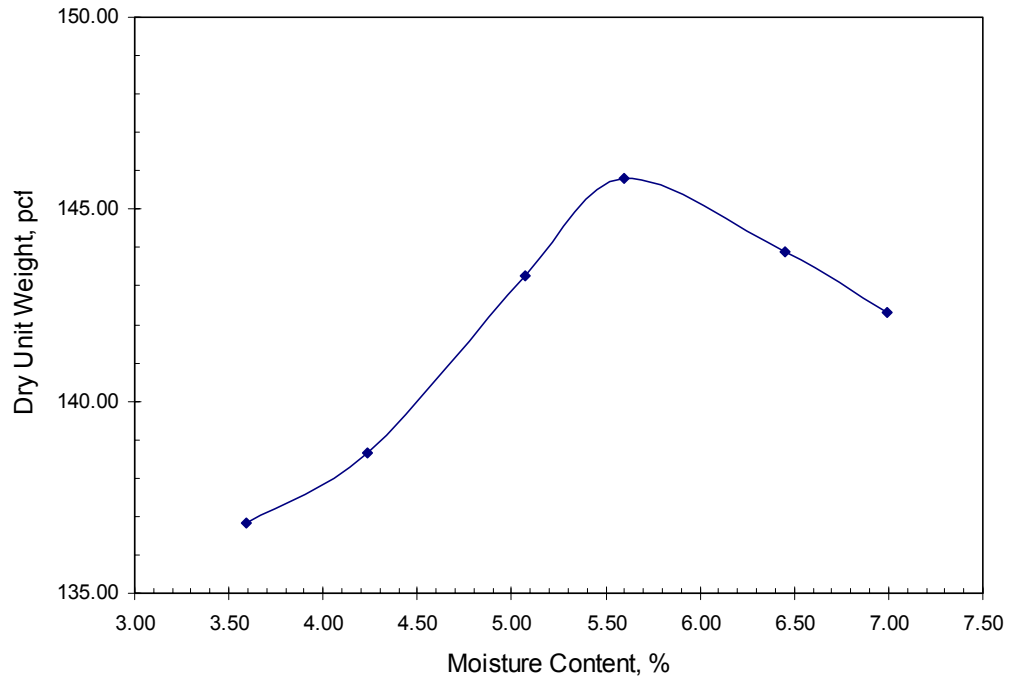


Figure 7-27 Moisture density curve for CTB

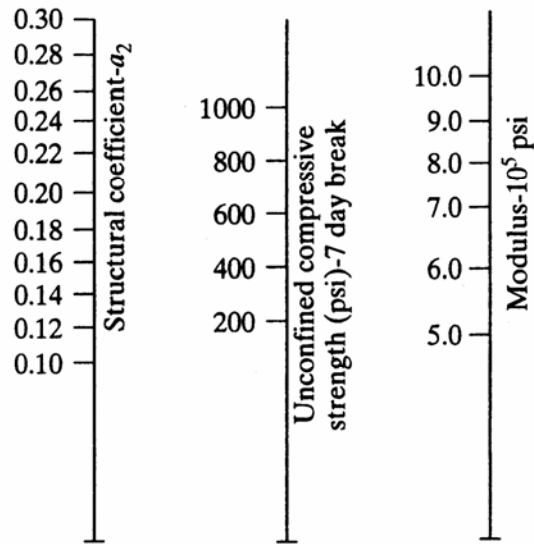


Figure 7-28 Resilient modulus of cement treated bases (CTB), [1, 14]

8 Bond Strength Determination

8.1 Introduction

The response of a layered composite asphalt pavement depends on the interlayer bond. Shahin, et al [21] have shown that even minor loss of bond between layers can cause stresses in the overlays to increase dramatically. The results are amplified at intersections where vehicles accelerate and brake resulting in application of large horizontal forces. The loss of bond will cause higher tensile strains at the bottom of the overlay and increased vertical compressive strains on the subgrade. Both of these deformations will cause a reduction in life of the pavement. The horizontal surface shear forces will cause crescent shaped cracks (Figure 1-4) in the top layer. The development of such cracks will reduce the strength further as well as cause penetration of surface water resulting in an accelerated decline of pavement performance. To eliminate such distresses, either the interfacial shear stresses can be reduced by using a thicker overlay or using a tack coat with higher bond strength. This chapter examines bond strengths of various materials. The following tests were conducted:

- Shear ramp tests
 - AC bonded to AC (AC-AC) – 20, 40, and 60 °C
 - AC bonded to PCC (PCC-AC) – 20, 40 and 60 °C
 - AC bonded to CTB (CTB-AC) – 40 and 60 °C
- Axial ramp tests
 - AC bonded to AC (AC-AC) – 40 and 60 °C

8.1.1 Shear Test Description

A simple shear test at constant height was conducted to determine the bond strength between various types of materials. The test was conducted in a controlled strain mode in which the composite sample was sheared at a constant displacement rate (1.0 and 2.5 mm/min). The rates were based on a study conducted by Uzan et al [31] in which rectangular AC samples were sheared using a direct shear test. The test was conducted at temperatures of

40 and 60 °C, and in some cases at 20 °C. The composite samples were glued to metal platens and were sheared at constant height in the SST. The peak shear load per unit area was the failure shear strength. Axial load and displacement were monitored during the test. The specimens were sheared to a displacement of 5-mm.

8.2 Bond Strength using Metal Platens

Metal platens (anodized aluminum) were used to determine the bond strength of tack and prime coat emulsions. Tack coat was applied to the one of the platens at the standard rate of 0.06 gallons per square yard. Using the gluing jig for SST specimens, the two platens were aligned and a minimal axial pressure of 10 psi was applied to keep them in contact. After 8 hours, the platens were removed from the jig and left in a draft oven at 40 °C to break the emulsions. Twenty four hours after gluing; the platens were sheared using the SST machine at shear displacement rates of 1.0 and 2.5 mm per minute. The test results were highly variable and the entire procedure was error prone due to following reasons:

- At the time of coating, the emulsions were in an unbroken state and, therefore, very fluid. When the two platens were pressed against each other, the liquid emulsion tended to ooze out from the sides. This changed the effective rate of application of tack coat and ultimately the interlayer asphalt film thickness available for bonding.
- When the platens were pressed against each other, the water from the emulsion was trapped in between the two impervious platens. The trapped water could, potentially, adversely affect the bond strength. This is not the case with bonded AC, PCC or CTB specimens as the emulsions are allowed to break.
- When the platens were inserted into the SST and clamped, they tended to separate before testing. This was due to presence of inadequately cured tack coats or due to high forces applied by the SST or extremely low strength of the tack coat.
- An alternative approach attempted was to allow the emulsion to break on one of the platens and, after 24 hours, bond it with another platen. But this approach had similar problems. At the pavement interface, the asphalt penetration into adjacent layers

provides a stronger bond compared to the bond developed between two impervious platens.

- The relative strength of any tack (or prime) coat, by itself, is small when compared to the interfacial strength of a composite pavement specimen it helps bond together. The use of heavy metal platens and SST to test the strength of tack (or prime) coats yielded erroneous results due to noise and low sensitivity of the equipment. A better alternative would be to use platens comparable to the size of a DSR spindle and a sensitive machine. An alternative is to use ATACKER™³ device that uses a light weight aluminum spindle (sizes – 1, 2, and 4 inch in diameter) and a dial gauge that can measure the load to ½ lb accuracy. The set up is similar to DSR. The specimens are sheared or pulled apart in a strain-controlled mode and the load at which the two plates separate is noted as the bond strength.

Overall, the results from these tests did not contribute much to this study due to practical problems encountered in the testing protocol.

8.3 Bond Strength of AC-AC specimens

8.3.1 Axial and Shear Ramp Test

Axial ramp test is similar to the simple shear test, except that the load is applied axially in controlled strain mode. Similarly, for shear ramp test, the samples were sheared at a constant strain rate. The rate of displacement used for axial and shear tests was 1 and 2.5 mm/minute. The axial test is used to measure the adhesion of the interfaces glued by a tack coat whereas the shear test measures the interfacial shear resistance. The specimens used were 2-inch thick and 6-inch in diameter with interface between the two layers roughly at mid-height. This test was performed on composite asphalt concrete specimens (AC bonded to AC) to determine the effectiveness of PG64-22 versus CMS-2 as a tack coat. Control specimens were also prepared without using a tack coat. However, during the coring and cutting process, control samples (Figure 8-1) made without any tack coat separated at the interface and, therefore, could not be tested.

³ ATACKER™ is equipment developed by Instron Inc, of Raleigh, NC.

8.3.2 Axial Test Results

The axial test results are presented in Table 8-1 and Table 8-2. It can be seen that low strain rate produces lower peak load values. For CMS-2 at 40 °C, when the displacement rate reduces from 2.5 mm/minute to 1.0 mm/minute, the shear strength changes from 221 to 95 psi – a reduction of 57%. Similarly, for CMS-2, the reduction in peak axial strength when tested at a lower rate of 1 mm/minute is 48 percent at 60 °C. Comparing the axial test data for 40 and 60 °C, for CMS-2, (Table 8-1 and Table 8-2) the peak axial stress falls with rise in temperature. When the temperature increases from 40 to 60 °C, the peak axial strength reduces by 85% and 75% for 1.0 and 2.5 mm/min displacement rates respectively.

For the same axial displacement rates, the corresponding peak load values and axial strains are much higher for PG64-22 binder than the CMS-2 emulsion. This suggests that PG64-22 binder has a higher axial strength than CMS-2 emulsion at both temperatures. This is expected because:

- Amount (wt/sq. yd) of residual asphalt available at the interface is higher for PG64-22 binder than for CMS-2 emulsion (which as about 33%) water.
- In addition, the PG rating of the residual asphalt in CMS-2 is PG52 (Table 4-2).

The failure of CMS-2 tacked specimens in axial testing mode was observed to be at the interface as shown in Figure 8-2 and Figure 8-3; however for PG64-22 tacked specimens the failure was not well defined as CMS-2 tacked specimens, as shown in Figure 8-4 and Figure 8-5. This observation confirms that PG64-22 provides better adhesion than CMS-2 emulsion.

8.3.3 Shear Test Results

The results for shear tests are presented in Table 8-3 through Table 8-5. The test was conducted in a constant height mode to simulate the confinement observed in situ. Negative axial stresses shown in the tables indicate compressive load and are due to prevention of dilation of specimens during the shearing process. The pattern for shear failure varies depending on the testing temperature and rate of shear. The test results are graphically

presented in Figure 8-6 through Figure 8-8. The failure pattern (Figure 8-9 through Figure 8-12) observed for the shear test at 40 °C is similar to that of a monolithic sample – there was a development of a crack along the principal diagonal, typical of a shear failure for, both, CMS-2 and PG64-22 tacked specimens. This indicated that the bond was as strong as the mix at 40 °C. From Table 8-3 to Table 8-5, it can be seen that there is very little difference in the bond strength of specimens tacked with CMS-2 and PG64-22, especially at a higher displacement rate of 2.5 mm/minute. There is a small difference in bond strength at lower strain rate of 1 mm/minute with the average (across all temperatures) difference in general being about 14% with PG64-22 tacked specimens showing higher bond strength.

For CMS-2 tacked specimens the interfacial failure was observed regardless of the rate of shear displacement at 20 °C. For PG64-22, at 20 °C, failure at lower displacement rate was monolithic (Figure 8-13) but at higher displacement rate the failure was interfacial (Figure 8-14). At 20 °C and 1-mm/minute displacement rate, the peak bond strength of CMS-2 is lower than PG64-22 by 8%.

The shear strength values drop drastically at 60 °C, with PG64-22 specimens performing marginally better than CMS-2 specimens. A higher displacement rate produces a higher strength as is clear from data in Table 8-5. The difference between the shear strengths of PG64-22 and CMS-2 emulsion is 9% and 45% at displacement rates of 1.0 and 2.5 mm/min. Referring to Figure 8-6 and Figure 8-7, it can be seen that failures occur rapidly under higher displacement rates than compared to lower strain rates. Further, the occurrence of peak load shifts to the right with increase in temperature and reduction of displacement rate – a phenomenon occurring due to mix getting softer. The failure of composite specimens at 60 °C was observed to be at the interface suggesting that the bond was the weakest link at that temperature.

Figure 8-8 shows the summary of bond strength as function of temperature. It can be seen from this figure that, in general, the CMS-2 bond strength is not very much different compared to PG64-22. From Figure 8-8, the bond strength values at 25 °C, for CMS-2 and PG64-22 tacked specimens is 960 and 1020 kPa respectively (at displacement rate of 1.0 mm/minute). Studies by Sholar et al [24] measured the bond strengths of various AC-AC interfaces in shear at 25 °C at different time intervals. The AC-AC samples were sheared at a

constant displacement rate of 19.1 mm/minute. Table 8-6 shows the bond strengths (in shear) for various sections, from Sholar et al [24], in the last round of testing. The values are then interpolated to obtain the strength at an application rate of 0.06 gal./yd² (0.272 L/m²). The interpolated bond strengths (in shear) range from 921 to 1011 kPa which is fairly close to the values obtained from Figure 8-8 (960 and 1020 kPa).

8.4 Bond Strength of PCC-AC specimens

The composite specimens of PCC and AC were tested in shear using the ramp tests described earlier. The testing was conducted at 20, 40 and 60 °C. In all, three cases were considered: no tack coat, PG64-22 binder as tack coat and CMS-2 emulsion as tack coat. For specimens prepared without tack coat, immediately after curing and drying the slab, the surface of PCC slab was cleaned and an asphalt layer was paved on the PCC slab. While dismantling the mold and coring the slab, the two layers of AC and PCC tended to separate (Figure 8-15 and Figure 8-16). The black slab is the asphalt concrete slab paved on top of the white PCC slab. This occurred on two attempts and it was evident that bond formation did not occur between these two layers.

For composite specimens tacked with PG64-22 binder and CMS-2 emulsion, the shear results are listed in Table 8-7 through Table 8-9, and Figure 8-17 through Figure 8-19. The behavior of PCC-AC interface bond is the property of tack coat as well as the asphalt mix; PCC only serves as a rigid layer to which the AC is tacked as the PCC stiffness is much higher than the AC mix. As a consequence, the aggregates from AC layer do not get to penetrate into the voids of the PCC layer increasing the likelihood of lower bond strength. The properties of PCC do not change significantly with temperature or rate of shear. It can be seen that with increasing temperature, the bond strength continues to reduce.

For PCC-AC specimens, PG64-22 composite specimens have slightly lower shear strengths at a displacement rate of 1.0 mm/min compared to CMS-2. However, the trend at higher strain rates reflects PG64-22 as a stronger tack coat. It can be argued that the bond strength of PG64-22 is very close to the actual mix strength at lower strain rates and, therefore, CMS-2, PG64-22 rate equally well in shear strength. The CMS-2 bond strength,

however, is lower than PG64-22 by 2.5%, 17.9%, and 31.8% (displacement rate of 2.5mm/min) at 20, 40, and 60 °C respectively. The difference in the shear strengths progressively widens with increasing temperature, between PG64-22 and CMS-2 at higher temperatures. With increasing temperatures, the development of peak shear stress (Figure 8-17 and Figure 8-18) gets less clearly defined. At 20 °C the peaks for CMS-2 and PG64-22 are clearly defined; at 40 °C the peaks are not as clearly defined and at 60 °C they cannot be identified at all. This is due to progressive weakening of the bond strength between PCC and AC. Further, the failure (signified by occurrence of peak) is instantaneous and well-defined at lower temperatures whereas at higher temperatures it is gradual. Most of the specimens, regardless of the tack coat, show a clear-cut slipping at the interface. While the PCC layer has been minimally affected, cracks developed in the AC layer for interfaces tacked with PG64-22 as is evident in Figure 8-20. It suggests that the strength of PG64-22 bond is at least as strong as the mix. In case of CMS-2 specimens, the failure was at the interface for all the specimens. Figure 8-21 shows a failed PCC-AC composite tacked with CMS-2. The deformation in AC was negligible with all slippage occurring at the interface suggesting bond strength as the weakest link.

Studies conducted by Mukhtar and Dempsey [19] tested composite PCC-AC specimens (Figure 1-11) at a constant displacement rate of 1.0, 3.0 and 300 inch per minute. Table 8-10 and Figure 8-22 summarize the strengths obtained at various temperatures at an axial confining pressure of 79 psi. Comparing the values at 20 °C, from Figure 8-22, it can be seen that the interfacial shear strengths are about 750, 1125 and 1750 kPa at displacement rates of 1, 30, and 300 inch per minute. The shear strength (~750 kPa) at 1.0 inch per minute displacement rate at 20 °C is about twice the value obtained under this study (Table 8-7). It can be observed (Table 8-7) that the maximum axial stress mobilized during the PCC-AC testing was 20 psi compressive. Thus the effect of axial confinement could have contributed to higher shear strengths in case of Mukhtar and Dempsey [19].

The bond strengths of PCC-AC composite specimens are lower than the corresponding strengths of AC-AC except at 60 °C. Thus, keeping everything else equal, dissimilar surfaces (like PCC and AC) produce a weaker bond compared to bond between similar surfaces (AC-AC). The difference between the dynamic moduli of PCC and AC could be a contributory

factor to the lower strength of the interface. Further, the PCC layer being relatively impervious, the tack coat does not penetrate into it potentially affecting the bond strength. In case of AC-AC interfaces, the elevated temperature of the overlay mix during the paving process could cause the underlying layer to soften up causing them to fuse and thereby enhancing the bond strength. Overall, based on the data it can be concluded that PG64-22 performs marginally better than CMS-2 emulsion when used to bond PCC and AC. Figure 8-19 summarizes the bond strength as a function of temperature.

8.5 Bond Strength of CTB-AC specimens

This section deals with the shear strength of composite specimens (Figure 8-23) made of CTB and AC. The testing was carried out at 40 and 60 °C at shear displacement rates of 1.0 and 2.5 mm per minute at constant height. Three types of emulsions – CSS-1h, EA-P and EPR-1 – were used as prime coats. In addition, composite CTB-AC samples without any prime coat were manufactured to be used as a control case. The performance of unprimed CTB-AC samples was similar to non-tacked composite (AC-AC and PCC-AC) specimens. The bond formation between CTB and AC was not strong enough to withstand the handling stresses. After extruding the samples from gyratory molds, AC and CTB layers could be easily pulled apart by hand. The results from the tests for primed samples are summarized in Table 8-12 and Table 8-12, and Figure 8-24 through Figure 8-27.

It should be noted that unlike AC-AC and PCC-AC, the CTB-AC specimens show decreasing shear bond strength with increasing applied shear strain rate. The CTB has very low strength and brittle behavior. During the shearing process it is possible that aggregates near the interface from the CTB must be loosened and reoriented causing dilation of the specimen. As the test was carried out at constant height, the loosening of aggregates and subsequent dilation could cause a jump in axial stresses. These increased axial stresses lead to an increase in the shear resistance of the interface. The behavior (Figure 8-24 through Figure 8-26) of CTB-AC interface when subjected to a shear strain (at constant height) shows substantially higher shear strengths compared to AC-AC and PCC-AC composite specimens.

At 40 °C, CSS-1h performs better than the other two prime coats, EA-P and EPR-1. The strengths of EA-P and EPR-1, at 40 °C, are 30.9% and 17.2% lower than CSS-1h at a displacement rate of 1.0 mm per minute. At a higher displacement rate (2.5 mm per minute) and at 40 °C, the shear strengths of EA-P and EPR-1 are 41.6% and 2.8% lower than CSS-1h. Based on shear strengths at 40 °C, the prime coats with decreasing order of shear strengths can be rated as CSS-1h, EPR-1, and EA-P. Another observation is that, at 40 °C, the reduction in strength with increasing rate of shear displacement (from 1.0 to 2.5 mm per minute) is 25.6%, 37.1% and 12.7% for CSS-1h, EA-P, and EPR-1 respectively. The reason, perhaps, would be due to inadequate time for development of aggregate interlock owing to faster interlayer movement. Observation of tested CSS-1h (at 40 °C) samples indicated a failure pattern consistent with a monolithic specimen. No debonding or layer separation was observed and diagonal cracks were seen in AC and CTB (Figure 8-28). For EA-P specimens (at 40 °C), diagonal cracking in AC as well as a shear failure at interface was observed but for EPR-1 only interfacial shear with minor cracking in the AC layer was observed.

At 60 °C, the EA-P primed specimens show a high degree of variability. Indeed the strength was so low that the specimens could be de-bonded by hand (Figure 8-30). Therefore, these results were discarded. At 60 °C, CSS-1h bond strength is higher than EPR-1 at 2.5 mm per minute rate of shear. The failure pattern observed for CSS-1h specimens at 60 °C was similar to the pattern observed at 40 °C. For EA-P and EPR-1 specimens the failure was due to interlayer debonding (Figure 8-29, Figure 8-30). The shear strengths at 60 °C are comparable to shear strengths at 40 °C for CSS-1h and EA-P. That means it is possible that the rough CTB surface plays a greater role compared to the bonding agent, especially under axial confinement.

Based on the test results, it can be concluded that priming does increase the bond between the CTB and the AC layer; however temperature plays only a minor role. The mobilization of bond strength appears to be primarily due to a combination of prime coat adhesion and more importantly aggregate interlock. Figure 8-27 summarizes the results for bond strength versus temperature.

8.6 Summary and Conclusions

The objective of this task was to evaluate the performance of composite samples made by bonding AC-AC, PCC-AC and CTB-AC. Of particular interest was the effect of type of tack coat and test temperatures. The observations and conclusions from the bond strength determination tests are summarized below:

1. The shear and axial ramp tests clearly differentiate between the bond strengths of various tack and prime coats. The numbers from these tests are consistent with the visually observed failure pattern of the test specimens.
2. The problems encountered in testing the bond strength of the tack (or prime) coat using SST metal platens were due to size effects, loss of asphalt from sides, and problems in curing the emulsions. The heavy weight of platens and low sensitivity of SST vis-à-vis low strength of asphalt posed hurdles to get meaningful results. A better alternative would be to use a device like Atacker™ to measure the adhesion properties where the size of equipment is small and the accuracy higher.
3. The absence of tack or prime coat would severely hinder development of bond between two layers causing undue slippage. This is evident from the debonding that occurred between non-tacked AC-AC, PCC-AC and CTB-AC interfaces.
4. For AC-AC composites the strength of PG64-22 binder, when used as a tack coat, provides comparable adhesion to CMS-2 emulsion. This is supported by similar axial and shear strengths of PG64-22 tacked specimens compared to CMS-2 tacked specimens.
5. For PCC-AC composites, the results confirm the earlier observation that CMS-2 provides comparable adhesion to PG64-22.
6. The bond between two similar surfaces (AC-AC vis-à-vis PCC-AC) is stronger than the bond between two dissimilar surfaces. Further the absorption of emulsion into underlying AC layer and the increased chance for aggregate interlock could potentially contribute to the higher strength of AC-AC interface compared to that of PCC-AC interface.
7. CSS-1h performs better than EA-P and EPR-1 as prime coats. The apparent strength of CTB-AC bond is higher due to the dilation of composite specimens. The strength of CTB-AC composites appears to be influenced significantly by the aggregate interlock.

Overall, the relative performance of various tack and prime coats could be determined based on SST tests. Emulsions, though easy to use, could pose problems if improperly applied or cured prior to paving AC layer. The use of PG64-22 binder as a tack coat could not only eliminate these problems but provide better bonding as well.

Table 8-1 Results for AC-AC axial ramp tests (tensile), 40 °C

Specimen ID	Height (mm)	Air voids (%)	Displ. Rate (mm/min)	Tack Coat	Peak Axial Stress (kPa)	Average Peak Axial Stress (kPa)
10c4 6-16-2	49.96	3.7	1.0	CMS-2	113.74	95.19
10x 6-16-2	50.48	3.6	1.0	CMS-2	76.64	
25c4 6-3-2	51.36	3.9	2.5	CMS-2	307.80	221.28
25m2 6-16-2	50.93	3.8	2.5	CMS-2	134.78	
10c4 4-15-2	52.65	3.6	1.0	PG64-22	145.17	149.40
10x 5-16-2	51.55	3.8	1.0	PG64-22	153.62	
25m1 5-16-2	50.17	4.3	2.5	PG64-22	240.07	285.53
25m2 5-16-2	51.20	4.3	2.5	PG64-22	330.99	

Table 8-2 Results for AC-AC axial ramp tests (tensile), 60 °C

Specimen ID	Height (mm)	Air voids (%)	Displ. Rate (mm/min)	Tack Coat	Peak Axial Stress (kPa)	Average Peak Axial Stress (kPa)
10m1 7-20-2	50.39	4.4	1.0	CMS-2	9.10	14.75
10m3 6-16-2	49.20	4.5	1.0	CMS-2	20.40	
25c3 7-20-2	49.88	4.3	2.5	CMS-2	62.35	57.19
25x 7-20-2	50.95	4.5	2.5	CMS-2	52.03	
10c2 4-15-2	48.47	4.5	1.0	PG64-22	19.16	20.87
10m4 5-16-2	50.83	4.5	1.0	PG64-22	22.58	
25c2 5-16-2	49.56	4.2	2.5	PG64-22	59.06	70.29
25m3 9-3-2	49.05	4.3	2.5	PG64-22	81.52	

Table 8-3 Results for AC-AC shear ramp tests, 20 °C

Specimen ID	Height (mm)	Air voids (%)	Displ. Rate (mm/min)	Tack Coat	Axial Stress (kPa)	Peak Shear Stress (kPa)	Average Peak Shear Stress (kPa)
1mmc2	49.91	4.3	1.0	CMS-2	-923.32	1098.39	1077.94
1mmc3	50.73	4.4	1.0	CMS-2	-986.23	1057.48	
25mmm1	50.87	4.2	2.5	CMS-2	-967.73	1232.25	1096.87
25mmm2	50.17	4.1	2.5	CMS-2	-729.49	961.49	
1mmc2	53.09	3.8	1.0	PG64-22	-894.55	1076.37	1177.01
1mmc21	50.41	4.2	1.0	PG64-22	-1010.72	1277.65	
25mmm3	48.70	4.1	2.5	PG64-22	-53.67	617.61	625.94
25mmx	49.69	4.3	2.5	PG64-22	-58.47	634.26	

Table 8-4 Results for AC-AC shear ramp tests, 40 °C

Specimen ID	Height (mm)	Air voids (%)	Displ. Rate (mm/min)	Tack Coat	Axial Stress (kPa)	Peak Shear Stress (kPa)	Average Peak Shear Stress (kPa)
10m1 6-16-2	49.58	4.2	1.0	CMS-2	-485.37	384.94	448.57
10m3 6-3-2	47.81	4.1	1.0	CMS-2	-652.51	512.20	
25c1 6-3-2	51.58	4.1	2.5	CMS-2	-641.14	521.53	479.16
25c1 1 6-16-2	52.27	4.3	2.5	CMS-2	-560.57	436.78	
10c3 4-15-2	51.05	3.9	1.0	PG64-22	-653.78	492.93	451.02
10m1 4-15-2	52.38	3.8	1.0	PG64-22	-504.93	409.11	
25m1 5-7-2	51.91	3.7	2.5	PG64-22	-686.60	568.26	554.03
25m2 5-7-2	51.14	3.7	2.5	PG64-22	-662.86	539.79	

Table 8-5 Results for AC-AC shear ramp tests, 60 °C

Specimen ID	Height (mm)	Air voids (%)	Displ. Rate (mm/min)	Tack Coat	Peak Shear Stress (kPa)	Average Peak Shear Stress (kPa)
10m1 6-3-2	51.74	3.6	1.0	CMS-2	0.84	2.96
10m4 6-16-2	50.29	3.5	1.0	CMS-2	5.08	
25m2 7-20-2	51.07	3.7	2.5	CMS-2	4.62	7.02
25c2 7-20-2	49.83	4.2	2.5	CMS-2	9.42	
10c3 5-7-2	50.04	3.5	1.0	PG64-22	5.78	5.34
10x 9-3-2	49.22	4.3	1.0	PG64-22	4.90	
25m1 9-3-2	48.48	3.6	2.5	PG64-22	7.93	7.71
25c1 5-16-2	50.55	4.2	2.5	PG64-22	7.49	

Table 8-6 Summary of shear strengths from Sholar et al, [24]

Section	Measured Bond Strength (kPa)		Interpolated Bond Strength (kPa) @0.272 L/sq. m (0.06 gal/sq. yd)
	@0.226 L/sq. m	@0.362 L/sq. m	
US-90	1022	989	1011
I-95 non-milled	943	876	921
I-95 milled	1059	911	1009

Table 8-7 Results for PCC-AC shear ramp tests, 20 °C

Specimen ID	Height (mm)	Displ. Rate (mm/min)	Tack Coat	Axial Stress (kPa)	Peak Shear Stress (kPa)	Average Peak Shear Stress (kPa)
1mm7	51.21	1.0	CMS-2	58.13	235.05	332.16
1mm8	49.54	1.0	CMS-2	-22.84	429.26	
25mm6	50.87	2.5	CMS-2	-40.62	109.51	360.18
25mm9	53.58	2.5	CMS-2	-110.03	611.86	
1mm6	50.91	1.0	PG64-22	-53.12	446.89	224.11
1mm16	48.01	1.0	PG64-22	-85.46	102.03	
1mm18	47.40	1.0	PG64-22	-140.10	123.42	
25mm14	50.07	2.5	PG64-22	-132.47	226.04	363.96
25mm8	50.18	2.5	PG64-22	-70.23	501.88	

Table 8-8 Results for PCC-AC shear ramp tests, 40 °C

Specimen ID	Height (mm)	Displ. Rate (mm/min)	Tack Coat	Axial Stress (kPa)	Peak Shear Stress (kPa)	Average Peak Shear Stress (kPa)
1mm12	48.95	1.0	CMS-2	-108.48	78.11	63.47
1mm13	50.35	1.0	CMS-2	-27.92	48.82	
25mm11	46.87	2.5	CMS-2	-38.19	121.31	106.35
25mm14	49.90	2.5	CMS-2	-115.57	91.38	
1mm04	52.54	1.0	PG64-22	-73.38	78.32	62.05
1mm13	49.72	1.0	PG64-22	-49.39	45.78	
25mm02	52.46	2.5	PG64-22	-9.13	99.03	129.57
25mm10	49.74	2.5	PG64-22	-114.73	160.11	

Table 8-9 Results for PCC-AC shear ramp tests, 60 °C

Specimen ID	Height (mm)	Displ. Rate (mm/min)	Tack Coat	Axial Stress (kPa)	Peak Shear Stress (kPa)	Average Peak Shear Stress (kPa)
1mm04	50.07	1.0	CMS-2	-17.18	21.64	25.13
1mm10	51.80	1.0	CMS-2	-29.01	28.61	
25mm01	50.74	2.5	CMS-2	-17.853	19.15	20.38
25mm02	49.84	2.5	CMS-2	-14.92	21.60	
1mm07	49.80	1.0	PG64-22	-8.58	13.74	20.93
1mm15	44.69	1.0	PG64-22	-25.02	28.11	
25mm01	49.91	2.5	PG64-22	-9.63	18.13	29.86
25mm12	50.63	2.5	PG64-22	-54.42	41.59	

Table 8-10 Summary of PCC-AC bond strengths, [19]

Temperature (°F)	Temperature (°C)	Shear Displacement Rate		
		1 in./min	30 in./min.	300 in./min
0	-17.78	882.5	806.7	703.3
20	-6.67	1234.2	1275.5	1268.6
40	4.44	1213.5	1316.9	1599.6
60	15.56	848.1	1206.6	1840.9
80	26.67	606.7	992.8	1482.4
100	37.78	461.9	675.7	903.2

Table 8-11 Results for CTB-AC shear ramp tests, 40 °C

Specimen ID	Height (mm)	Displ. Rate (mm/min)	Tack Coat	Axial Stress (kPa)	Peak Shear Stress (kPa)	Average Peak Shear Stress (kPa)
1mm06	50.34	1.0	CSS-1h	-433.95	353.52	367.49
1mm10	50.42	1.0	CSS-1h	-454.80	381.46	
25mm07	51.01	2.5	CSS-1h	-384.17	328.16	273.23
25mm09	50.27	2.5	CSS-1h	-252.53	218.31	
1mm12	52.87	1.0	EA-P	-262.10	201.83	253.82
1mm02	52.01	1.0	EA-P	-421.71	305.80	
25mm03	54.56	2.5	EA-P	-237.98	155.92	159.62
25mm13	51.15	2.5	EA-P	-244.48	163.32	
1mm02	51.12	1.0	EPR-1	-305.84	225.03	304.38
1mm04	50.22	1.0	EPR-1	-465.11	351.91	
1mm05	51.37	1.0	EPR-1	-429.51	336.19	
25mm03	52.51	2.5	EPR-1	-397.30	280.99	265.65
25mm99	52.54	2.5	EPR-1	-336.37	250.31	

Table 8-12 Results for CTB-AC shear ramp tests, 60 °C

Specimen ID	Height (mm)	Displ. Rate (mm/min)	Tack Coat	Axial Stress (kPa)	Peak Shear Stress (kPa)	Average Peak Shear Stress (kPa)
1mm01	50.27	1.0	CSS-1h	-464.15	343.00	327.60
1mm05	51.51	1.0	CSS-1h	-414.71	312.19	
25mm02	50.54	2.5	CSS-1h	-439.87	308.00	288.58
25mm08	53.78	2.5	CSS-1h	-368.20	269.16	
1mm10	50.75	1.0	EA-P	-548.90	390.34	408.94
1mm11	54.85	1.0	EA-P	-653.41	427.53	
25mm08	50.84	2.5	EA-P	-73.04	66.93	153.95
25mm11	54.85	2.5	EA-P	-338.59	240.37	
1mmOA	50.39	1.0	EPR-1	-256.48	177.18	218.27
1mmOI	51.39	1.0	EPR-1	-389.84	259.35	
25mmOQ	52.65	2.5	EPR-1	-209.00	134.49	176.12
25mm01	53.12	2.5	EPR-1	-312.59	258.29	
25XOC	51.46	2.5	EPR-1	-197.55	135.59	



Figure 8-1 Debonded composite AC-AC slab without tack coat



Figure 8-2 Axial failure of CMS-2 specimen (C4 6-3-2) at 2.5 mm/min, 40 °C



Figure 8-3 Axial failure of CMS-2 specimen (C4 6-3-2) at 2.5 mm/min, 40 °C



Figure 8-4 Axial failure of PG64-22 specimen (M1 5-16-2) at 2.5 mm/min, 40 °C



Figure 8-5 Axial failure of PG64-22 specimen (M1 5-16-2) at 2.5 mm/min, 40 °C

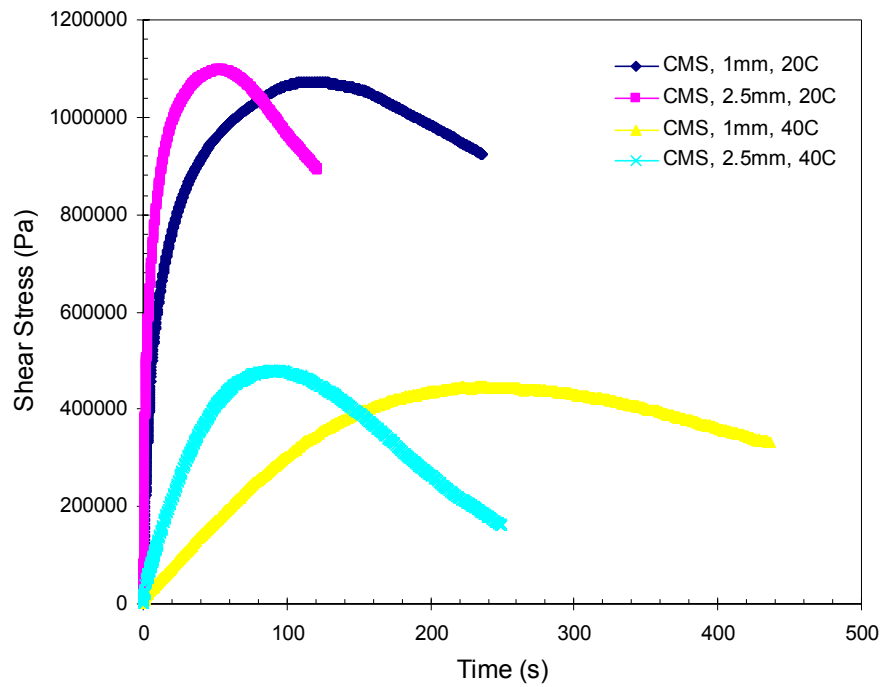


Figure 8-6 Average shear stress vs. time for AC-AC interface tacked with CMS-2

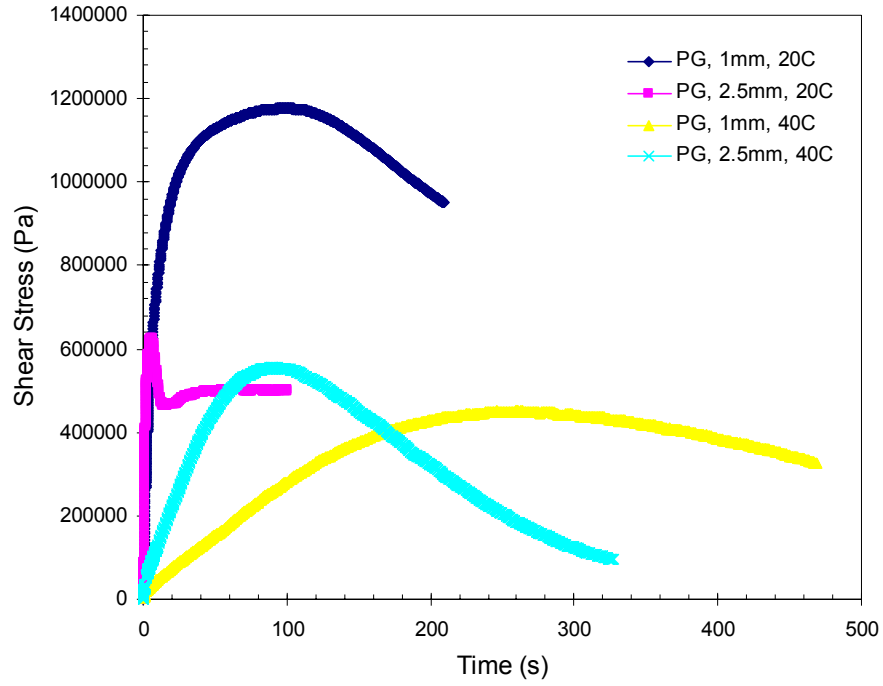


Figure 8-7 Average shear stress vs. time for AC-AC interface tacked with PG64-22

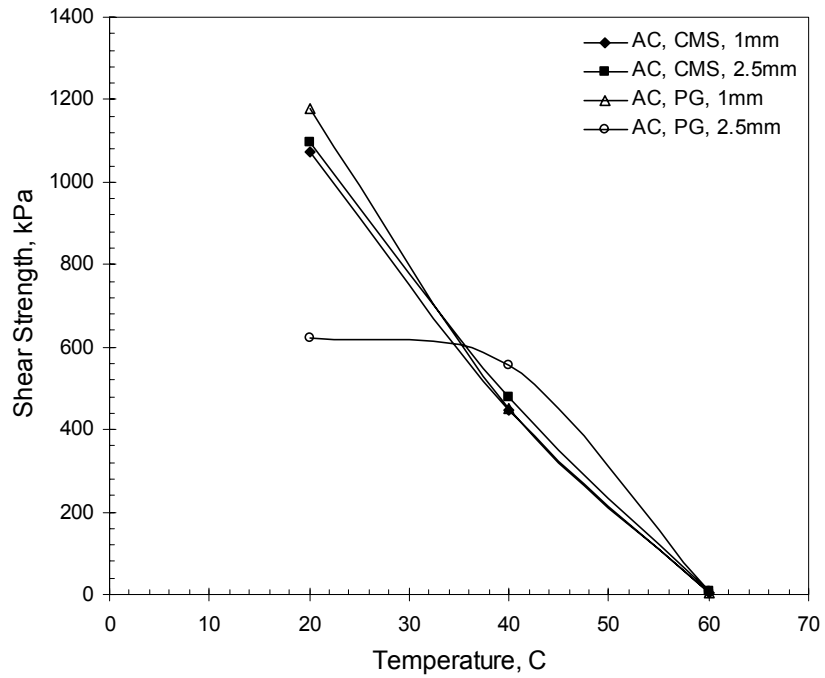


Figure 8-8 Summary of bond strengths for AC-AC interface



Figure 8-9 Shear failure of CMS-2 specimen (m1 6-16-2) at 1.0mm/min, 40 °C



Figure 8-10 Shear failure of CMS-2 specimen (m3 6-3-2) at 1.0mm/min, 40 °C



Figure 8-11 Shear failure of CMS-2 specimen (c1 6-3-2) at 2.5mm/min, 40 °C



Figure 8-12 Shear failure of PG64-22 specimen (m1 5-7-2) at 2.5 mm/min, 40 °C



Figure 8-13 Shear failure of PG64-22 specimen (1mmc2_1) at 1.0 mm/min, 20 °C



Figure 8-14 Shear failure of PG64-22 specimen (25mm3) at 2.5 mm/min, 20 °C



Figure 8-15 Debonding of composite PCC-AC specimen without tack coat



Figure 8-16 Debonded composite PCC-AC slabs without tack coat

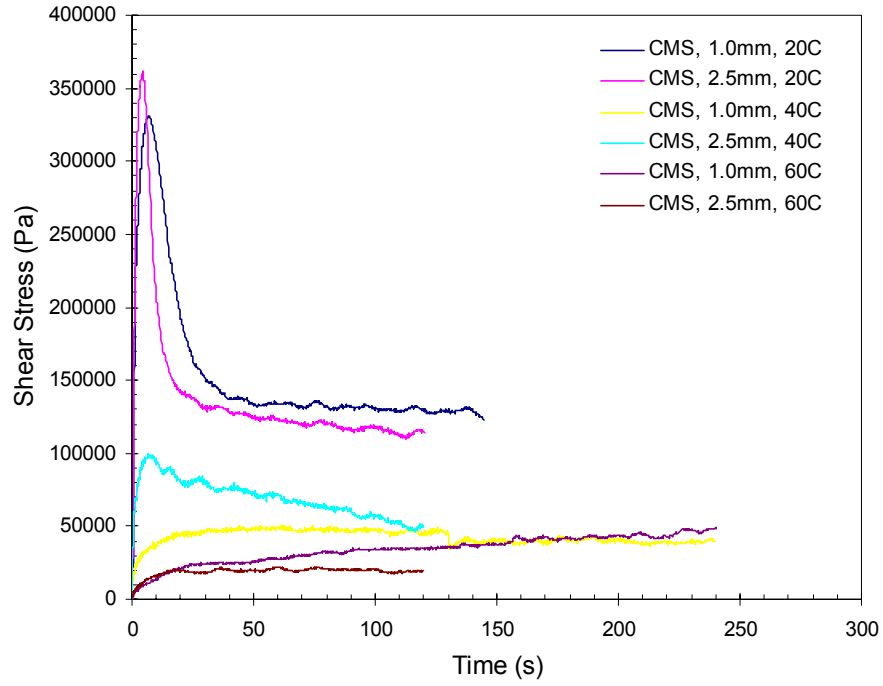


Figure 8-17 Average shear stress vs. time for PCC-AC interface tacked with CMS-2

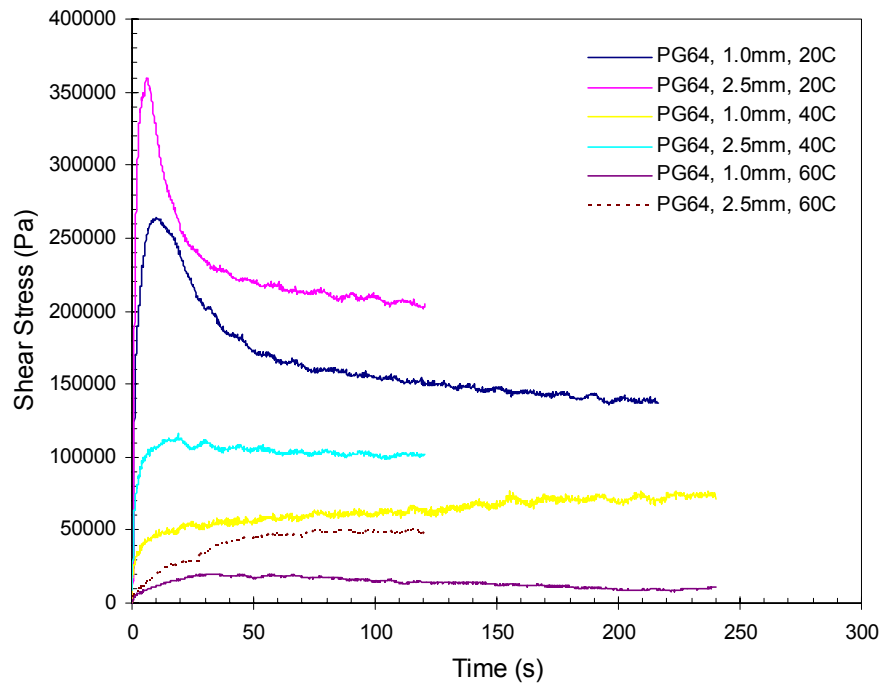


Figure 8-18 Average shear stress vs. time for PCC-AC interface tacked with PG64-22

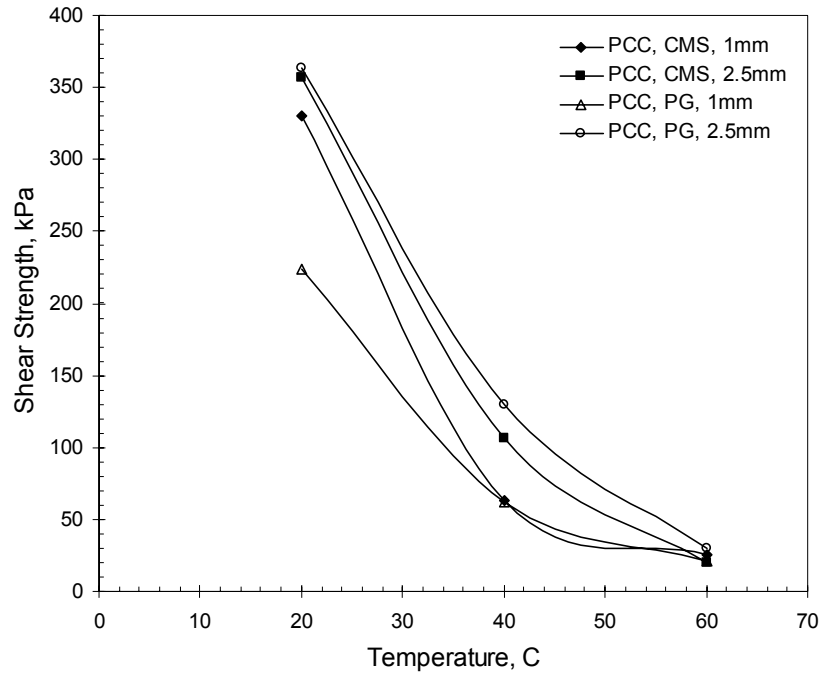


Figure 8-19 Summary of bond strengths for PCC-AC interface



Figure 8-20 PCC-AC specimen tacked with PG64-22 (cracks highlighted in white)



Figure 8-21 PCC-AC specimen tacked with CMS-2

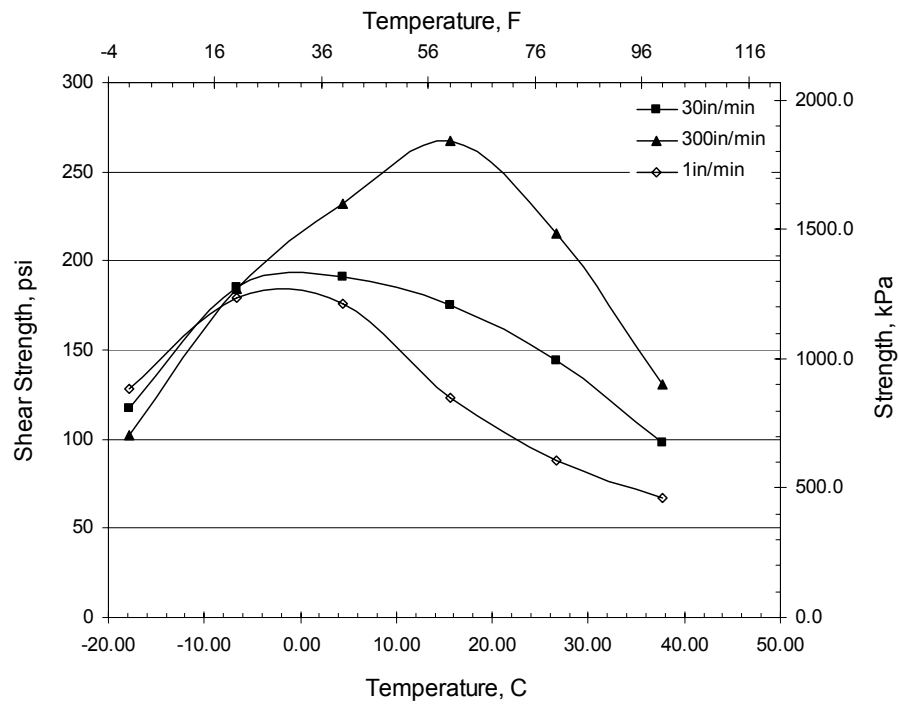


Figure 8-22 Summary of PCC-AC shear bond strengths, [19]



Figure 8-23 Composite CTB-AC specimen

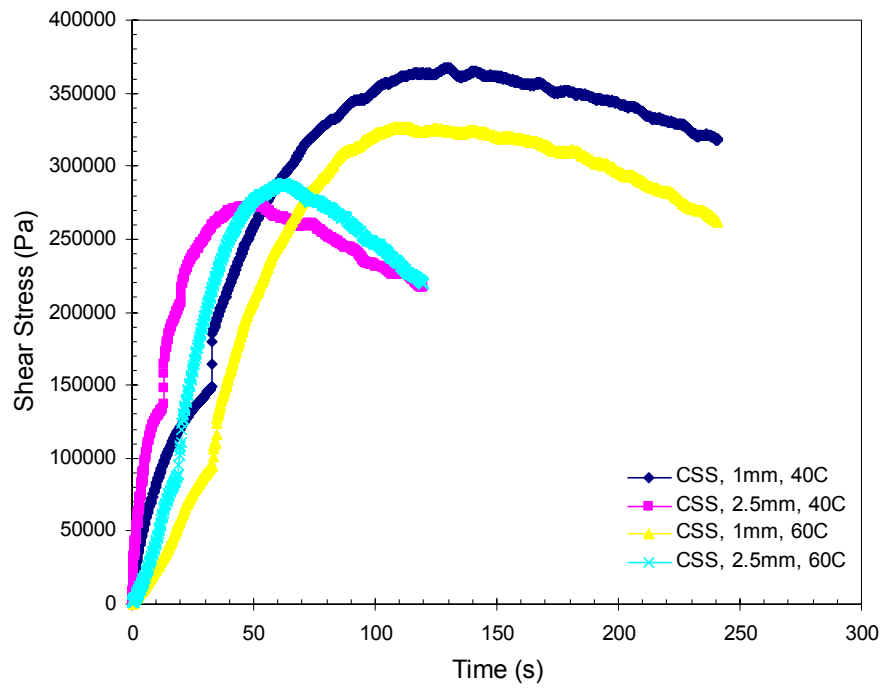


Figure 8-24 Average shear stress vs. time for CTB-AC interface primed with CSS-1h

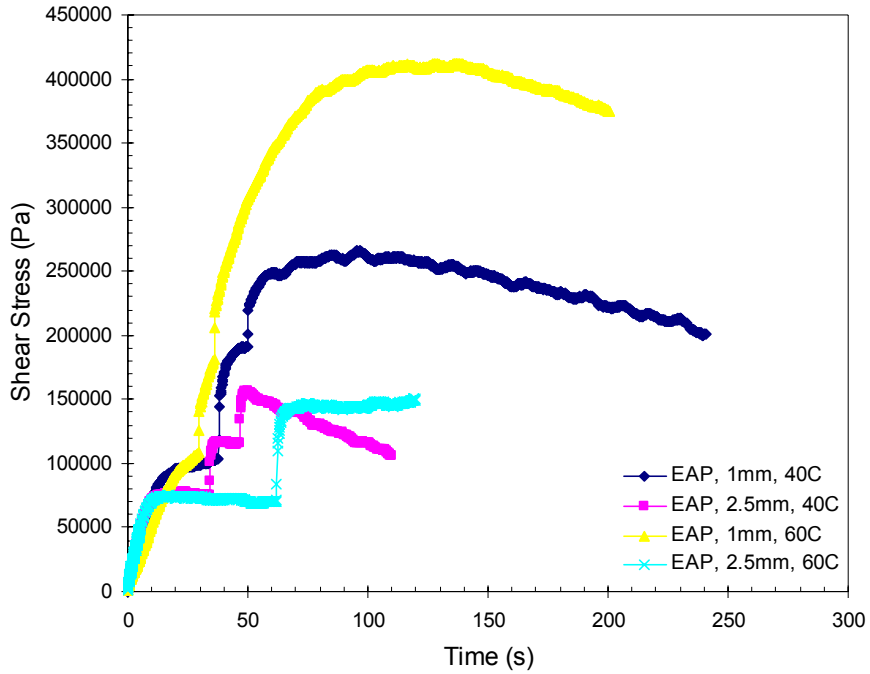


Figure 8-25 Average shear stress vs. time for CTB-AC interface primed with EAP

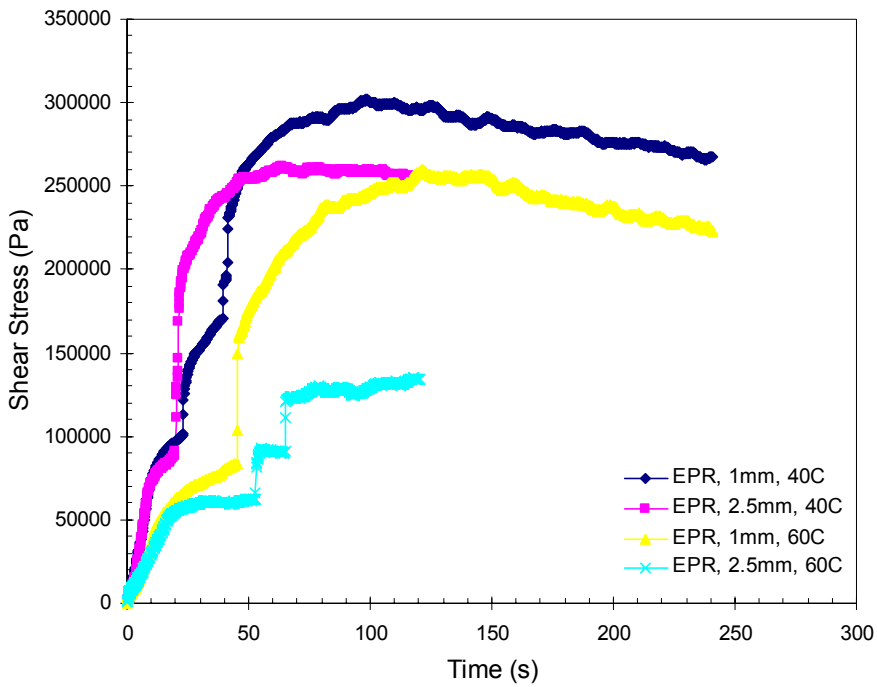


Figure 8-26 Average shear stress vs. time for CTB-AC interface primed with EPR-1

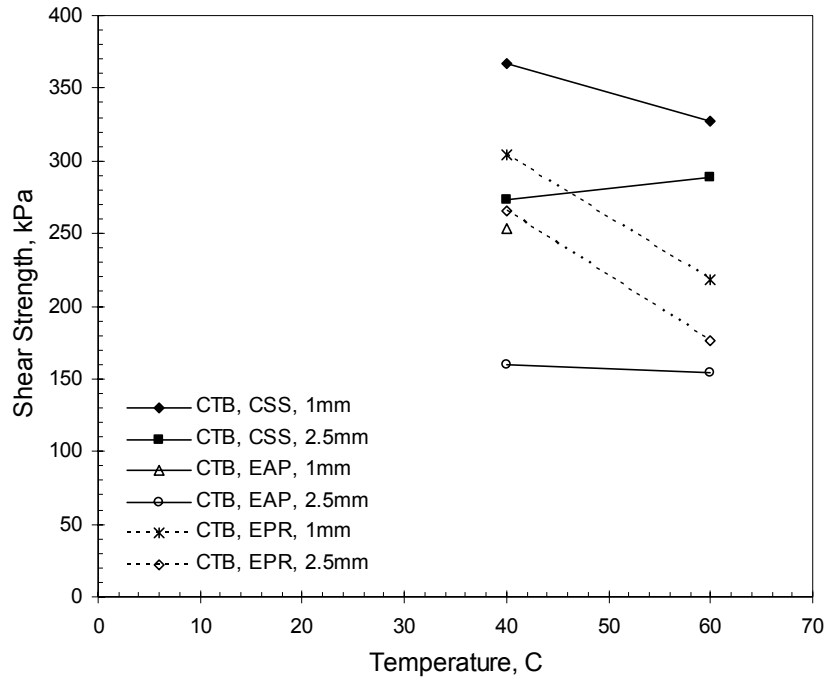


Figure 8-27 Summary of bond strengths for CTB-AC interface



Figure 8-28 CTB-AC specimen primed with CSS-1h, sheared at 1mm/min (40 °C)



Figure 8-29 CTB-AC specimen primed with EPR-1, sheared at 1mm/min (60 °C)



Figure 8-30 Debonded CTB-AC specimen primed with EA-P, 60 °C

9 Development of Design Guidelines for Use of Tack and Prime Coats

9.1 3-D Layered Elastic Program Description

The final objective of the determination of interfacial bond strength is to develop guidelines that can be used to minimize interlayer slippage. A detailed parametric study was conducted to investigate the effect of system parameters including layer thickness and stiffness on the stress-strain-displacement fields induced in the pavement.

Although BISAR (Bitumen Structures Analysis in Roads) developed by Shell Research is a program that considers vertical and horizontal loadings in a multilayered system, its shortcoming is that it can be used only for three layered system. Another program, ELSYM5, developed at University of California, Berkeley uses a similar approach to analyze a multilayered system but cannot analyze the effect of horizontal loads.

In this investigation, a computer program was developed by Xu, et al [32] as part of this research to study stresses, strains and displacements modeling in various types of pavement sections using a 3-D approach. The following simplifying assumptions, similar to Burmister's theory [10], are made in modeling the pavement:

- The pavement is made up of layered elastic materials that are homogenous, isotropic and follow Hooke's law.
- Each layer is weightless, of uniform thickness, and extends infinitely in horizontal directions.
- The bottommost layer is of infinite depth, and the stresses and displacements at infinite depth are zero.
- The layer surfaces are fully bonded and it is reflected by stress and displacement continuity across interfaces.
- The surface shear and normal stresses on the top of the uppermost layer are zero outside loading areas.

- The contact pressure is same as the tire pressure, and the tire contact areas are circular with uniform distribution of shear and normal stresses occurring over area of contact.

The method of calculating the stresses, strains and displacements in the pavement sections is semi-analytic. The model formulation in this method is analytic but the solution is obtained numerically. Using Hankel transforms (Small and Booker, [25, 26]) the three dimensional analytic problem is reduced to two or one dimensions, simplifying the solution process.

9.2 Load Conditions

The loading for analysis is assumed to be a standard, static, 18-kip dual tire assembly. This assembly consists of two tires at each end of the axle. The axle length is 6-ft, and the dual tire separation at each end is 1-ft (center-to-center). Only tires at one end of the axle are considered for analysis as the assembly at the other end of axle is considered too far away to have any significant impact on loading under consideration. Figure 9-1 shows the layout of dual tires at end of the axle and the orientation of the axes. The vehicle axle is oriented along Y-axis and the direction of motion is along positive X-axis. For convenience, the origin is assumed to lie midway on the line joining the center of two tire assembly. The vertical load on each tire is 4500-lb, a quarter of the load on the whole assembly. The tires are inflated to a pressure of 100 psi and, therefore, the contact pressure between the tire and the pavement is 100 psi as well. For each tire, the vertical load divided by the contact pressure (100 psi) gives the contact area which is 45-in² in this case. Assuming a circular contact area, the radius of contact area is 3.785-in.

The effect of horizontal load (shear) is modeled by considering three cases: (a) pure vertical load with no horizontal load, (b) vertical load with 40% of vertical load as shear load and, (c) vertical load with 70% of vertical load as shear load. The case with pure vertical load represents the situation when the vehicle is stationary or moving at a high speed. Kummer and Meyer [16] have recommended a skid number of at least 37, measured at 40 mph, for main rural highways. Skid number is coefficient of friction multiplied by 100. The case with 40% shear load is equivalent to having 40% horizontal shear at moderate speeds. Barber [8]

has shown that the coefficient of friction between the tires and the pavement can be as high as 0.8 when the effect of wind is considered. This type of loading is obtained while traveling on a 75-ft radius curve with no banking at 30-mph. Studies by Kummer and Meyer [16] have recommended a skid number value of 60 at or near 0 mph. Based on these two findings, a maximum value of 0.7 was chosen for coefficient of friction for worst case scenario. For the purpose of this study, the shear loads are considered only in the direction of motion of traffic that simulates the forces while braking. Typical skid number values are shown in Table 9-1.

9.3 Temperature Effects

The properties of asphalt mix depend on the binder properties which, in turn, are significantly influenced by temperature. In addition, the bond strength of any interface tacked with asphalt is also dependent on temperature. Thus, the resistance of a pavement to horizontal loads depends on temperature as well. This section deals with incorporation of temperature effects into design of pavements to minimize interfacial shear failure.

Most of delamination and eventual shoving occurs either at high temperature or very high loads or a combination of the two. The pavement temperature considered for analysis in this study is the maximum 7-day high temperature at the selected depth. Using either LTPPBind™ (<http://www.tfhr.gov/>) or SHRPBind™ [22] programs, the ambient 7-day maximum air temperature is obtained. For details, please refer to Section 5.3, which deals with the computation of pavement temperatures using the program for a given location. Using the technique outlined in Section 5.3, pavement temperatures were calculated for Enka, NC. Enka, NC was chosen as the mix used in this study was from a plant in this area. Figure 9-2 shows the variation of high pavement temperature as a function of depth for Enka, NC. The temperature at mid-height for any asphalt layer was assumed to be the representative temperature for the whole layer. The asphalt mix stiffness was calculated based on the temperature at its mid-height using the data obtained and presented in Chapter 7. Using the dynamic moduli of the AC mix (Table 7-12 and Table 7-14), Figure 9-3 was developed showing the dynamic axial moduli for AC mix at various temperatures. PCC and CTB moduli are assumed to not change with temperature and hence are assumed to be constant. The interfacial temperatures were calculated using Figure 9-2 and the bond

strengths measured at various temperatures (presented in Chapter 8) were interpolated at the interface temperature. Table 9-2 and Table 9-3 summarize the bond strengths obtained for various interfaces.

9.4 Analysis of AC-AC Bonding

Using representative pavement section, shown in Figure 9-4, the analysis was conducted using the computer program developed in the study. The properties of aggregate base course (ABC), cement-treated subbase (CT Subbase), and subgrade were typically available values [14] and are shown in the figures. The properties of the overlay (AC) as well as the underlying layer (AC) are assumed to be solely dependent on temperature; although in practice the underlying AC layer might have lower stiffness due to weathering action of traffic and climate. The analysis was conducted at numerous points along Y-axis (vehicle axle) and on a line parallel to X-axis passing through center of one of the tires. Figure F-1 and Figure F-2 in Appendix F summarize the mobilized interfacial shear stresses for AC-AC combination case. The maximum shear stress at the interface was determined at each point using the following equation:

$$\tau_{\max} = \sqrt{\tau_{zx}^2 + \tau_{zy}^2} \quad \text{(Equation 9-1)}$$

Figure 9-5 and Figure 9-6 show the mobilized shear stresses at 20 °C and 7-day maximum average high temperature, respectively. It can be seen from Figure 9-5 that the interfacial shear stress increases with increasing magnitude of horizontal shear load. Further, an increase in layer thickness reduces the interfacial shear stress as would be expected. The higher shear stress produced due to presence of horizontal loading also reduces with increasing thickness. Thus, unaccounted horizontal loads are more likely to have an adverse effect on pavements with thin overlays than thicker ones. At 20 °C, the bond strength of AC-AC is much higher (regardless of the tack coat used) than the mobilized shear stresses. This indicates that, at 20 °C, delamination will not occur. The thickness of the overlay at 20 °C should be the minimum required by practical and construction guidelines as debonding is not likely to take place irrespective of the tack coat used.

Figure 9-6 shows the mobilized shear strengths combined with interfacial bond strengths at 7-day maximum average high temperature. The shear stresses decrease with increase in layer thickness whereas the bond strength increases with layer thickness. (Increasing layer thickness causes the interfacial temperatures to be lower and lower temperature results in higher bond strength.) The intersection of these two sets of curves gives the minimum required thickness for pavement design to prevent delamination. It can be observed that the minimum required thickness for PG64-22 and CMS-2 tack coats based on a shear displacement rate of 1.0 mm/min is 2.5 to 3.5 inches depending on magnitude of shear (horizontal) load. For pure vertical loads, the thickness is 2.5-inch, whereas if 70% horizontal shear is taken into account the thickness is 3.5-inch for, both, PG64-22 and CMS-2 based on 1-mm/minute strain rate. The difference in performance of PG64-22 and CMS-2 as tack coat at low strain rates is marginal.

At a strain rate of 2.5 mm/min, the PG64-22 binder performs better as a tack coat than CMS-2. The minimum required thickness for 70% horizontal load for PG64-22 is 2.25-inch whereas for CMS-2 it is 3.25-inch. Based on this data it can be concluded that PG64-22 performs better or equal to CMS-2 emulsion. Considering that the residual asphalt has a grading of PG52 for CMS-2, the result of this analysis seems to be reasonable.

9.5 Analysis of PCC-AC Bonding

Figure 9-7 shows the pavement structure used for analysis of a concrete pavement. The pavement consists of an 8-inch thick concrete slab overlaid by a variable thickness of AC overlay. The stiffness of the overlay as well as the interface shear strength was calculated at various temperatures, and the design curves generated. Figure F-3 and Figure F-4 in Appendix F summarize the mobilized interfacial shear stresses in PCC-AC combination case. Figure 9-8 and Figure 9-9 show the developed shear stresses versus thickness of overlay for various types of loading conditions. It can be observed that the mobilized interfacial shear stresses reduce with increasing temperature. This indicates that with increasing temperature, the shear deformation of the asphalt layer increases. From Figure 9-8 it can be seen that at a strain rate of 2.5 mm/minute, the performance of PG64-22 and CMS-2 as tack coats is almost

similar. The minimum required thickness for overlay is 2-inch considering the worst case scenario, and a little more than 1-inch considering a moderate horizontal shear loading.

It can be observed from Figure 9-9 that at 7-day maximum temperature, CMS-2 and PG64-22 generate equal bond strengths. The interpolated bond strength at higher temperatures turns out to be significantly lower for PCC-AC interface compared to AC-AC combination. This implies that debonding would occur for all overlay thicknesses; however this does not happen in practice. The surface roughness of PCC provides sufficient friction to reduce the chances of delamination. The likelihood of debonding occurring for PCC-AC interfaces at higher temperatures is minimized if minimum design thickness requirements can be met.

9.6 Analysis of CTB-AC Bonding

Figure 9-10 shows the pavement structure used for CTB-AC bonding analysis. Figure F-5 and Figure F-6 in Appendix F summarize the mobilized interfacial shear stresses in CTB-AC combination case. The bond strength determination for CTB-AC interface was conducted at 40 and 60 °C, and Figure 9-11 and Figure 9-12 show the development of shear stresses at 40 °C and 7-day maximum average temperature. Analysis conducted at 40 °C at 1.0 mm/minute strain rate, shows a minimum required design thickness of 2.25, 3.0 and 3.75 inches for CSS-1h, EPR-1, and EA-P emulsion as prime coats at 70% horizontal shear. However, at 40 °C and 2.5 mm/minute displacement rate, the minimum design thickness increases to 3.75 inches for CSS-1h and EPR-1, and to 6 inches for EA-P. Figure 9-12 shows design curves for 7-day maximum average temperatures. CSS-1h emulsion performs better than EA-P and EPR-1 emulsion as prime coats. The required design thickness for CSS-1h at 70% horizontal shear loads is 2.5 and 4.0 inches at 2.5 and 1.0 mm/minute displacement rate. For EA-P, the design thickness is 4.5 inches regardless of the rate of shear at 70% horizontal load. For EPR-1, the required thickness is 4.0 and 4.5 inches at 1.0 and 2.5 mm/min shear displacement rate. Based on the performance, the emulsions can be rated as CSS-1h, EPR-1 and EA-P. Nevertheless, this analysis clearly confirms the practice recommendation by some DOT's and AI that prime coat should be used for AC overlay thickness smaller than 4-5 inches thick, regardless of its type (cutback versus emulsion).

9.7 Outline of Guideline Development for Use of Tack or Prime Coat

Using the steps outlined below, the procedure described in this chapter can be applied to any pavement section for bond strength analysis. The procedure is following:

1. Select a design pavement structure, e.g. similar to shown in Figure 9-4 or Figure 9-10.
2. For the pavement geographical location, develop a temperature curve, e.g. similar to Figure 9-2.
3. Determine the dynamic moduli values for the materials used therein. For AC mixes, determine the values at various temperatures (Figure 9-3). The appropriate moduli for AC layers can be computed based on the temperature at its mid height.
4. Determine the interfacial temperatures based on layer thicknesses and interpolate the peak bond strength values available in Table 9-2 and Table 9-3. This procedure can be extended to develop quantitative guidelines to determine the optimum rate of tack coat application.
5. Using the FLA program compute the interlayer stress ($\sqrt{\tau_{zx}^2 + \tau_{zy}^2}$) at various points.

Generally, the peak stresses will occur at the edge of the wheel. Skid numbers presented in Table 9-1 can be used to compute the minimum horizontal loads at various speed levels. Various loading conditions can be considered, including horizontal loads, and the mobilized interfacial stress curves for different thicknesses can be plotted (similar to Figure 9-6 and Figure 9-12).

6. Superimpose the interpolated bond strength values (Figure 9-12) on these curves to obtain the minimum required thickness. The minimum required thickness would be the intersection of the 'bond strength curve' and the 'mobilized shear stress' curve.

9.8 Summary and Conclusions

This chapter covers the development of design guidelines to reduce interfacial bond failures. Using SHRPBind and LTPPBind programs, the pavement temperature was determined for various depths for Enka, Buncombe County, NC. The dynamic axial moduli for asphalt mixes and the interfacial bond strengths were computed at various depths. The loading conditions considered for analyses were the standard 18-kip axle combined with zero, 40% and 70% horizontal shear loads. For each scenario, complete analysis was performed. Using a layered elastic program stresses, strains and displacements were computed in the pavement at various locations. The program used a 3-D semi-analytic method to compute the stresses and strains but the method of solution was numeric.

Appendix F shows the distribution of mobilized interfacial shear stresses for various combinations. The peak stress occurs, for horizontal load cases, at the front edge of the wheel. At low overlay thicknesses, the stresses are higher and localized, and they dissipate very fast with increasing distance from the center of the wheel. With increasing thickness, the stress distribution becomes more uniform with stresses dissipating less rapidly with distance from the center of the wheel. The application of horizontal load increases the shear stress at the interfaces in all combinations, AC-AC, PCC-AC and CTB-AC.

For AC-AC interface, CMS-2 performs as good as PG64-22 binder as tack coat. The difference in their bond strengths at high temperatures is marginal. At 20 °C, the chance of debonding at AC-AC interface is negligible. At 7-day maximum average high temperatures expected in-situ, the overlay thickness has to be designed appropriately based on the procedure developed herein to assure that chances of delamination are minimized. For PCC-AC interface, the chances of debonding are significantly lower if minimal thickness design requirements are met. For CTB-AC interface, clearly CSS-1h performs better than EA-P and EPR-1 as prime coats. Furthermore, an overlay thickness of minimum 4-5 inches will ensure that the prime coat bond will not fail or debonding will not occur.

Table 9-1 Recommended minimum skid numbers for rural highways [16]

Mean Traffic Speed, V , (mph)	Skid Number	
	SN ⁴	SN ₄₀ ⁵
0	60	–
10	50	–
20	40	–
30	36	31
40	33	33
50	32	37
60	31	41
70	31	46
80	31	51

Table 9-2 Interfacial shear bond strength summary for PG64-22 and CMS-2

Interface	Temperature (°C)	Strain rate (mm/min)	CMS-2	PG64-22
			Shear Strength (psi)	Shear Strength (psi)
AC-AC	20	1.0	156.3	170.7
		2.5	159.1	90.8 ⁶
	40	1.0	65.1	65.4
		2.5	69.5	80.4
	60	1.0	0.43	0.77
		2.5	1.02	1.12
PCC-AC	20	1.0	48.25	32.5
		2.5	52.3	52.8
	40	1.0	9.2	9.0
		2.5	15.4	18.8
	60	1.0	3.6	3.0
		2.5	3.0	4.3

Table 9-3 AC-CTB shear bond strength summary for CSS-1h, EA-P, and EPR-1

Temp. (°C)	Strain rate (mm/min)	CSS-1h	EA-P	EPR-1
		Shear Strength (psi)	Shear Strength (psi)	Shear Strength (psi)
40	1.0	53.3	36.8	44.1
	2.5	39.6	23.2	38.5
60	1.0	47.5	59.3 ⁷	31.7
	2.5	41.9	22.3	25.5

⁴ SN = skid number, measured at mean traffic speeds

⁵ SN₄₀ = skid number, measured at 40 mph

⁶ This value is too low when compared with others.

⁷ Value is high compared to other trends.

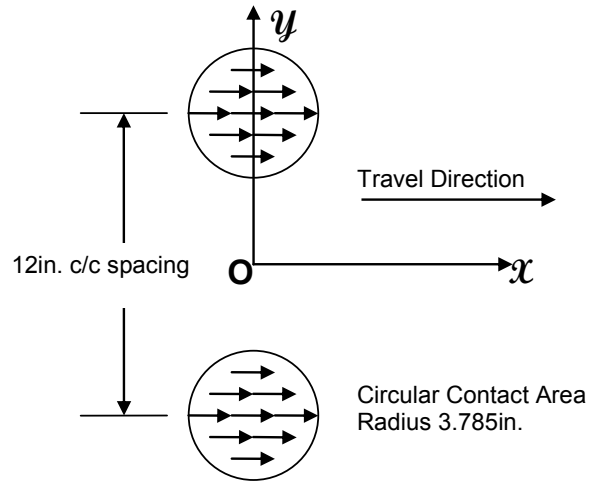


Figure 9-1 Tire layout, travel direction, and axes orientation

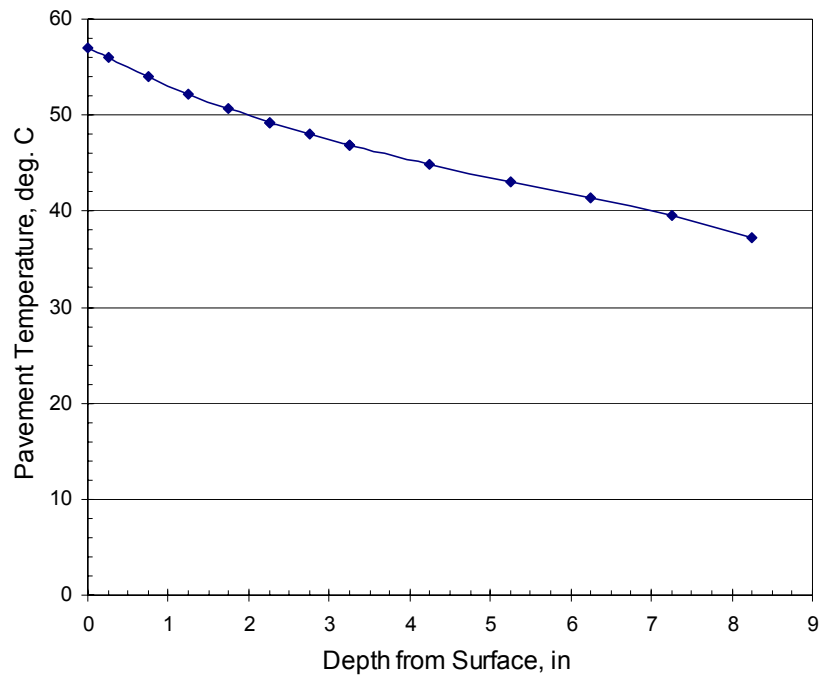


Figure 9-2 AC average 7-day maximum high pavement temp. vs. depth

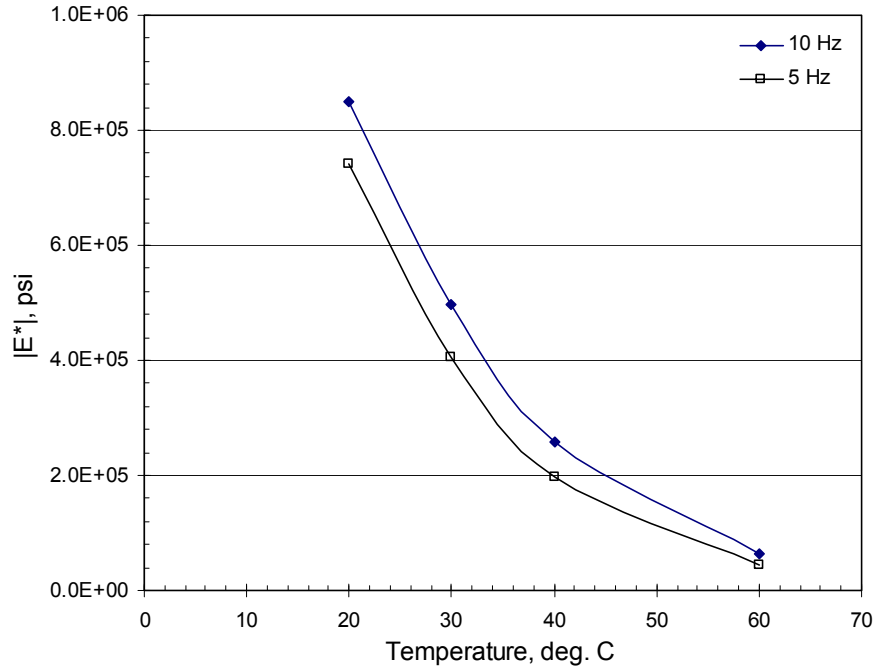


Figure 9-3 Dynamic axial modulus for asphalt mixes vs. temperature

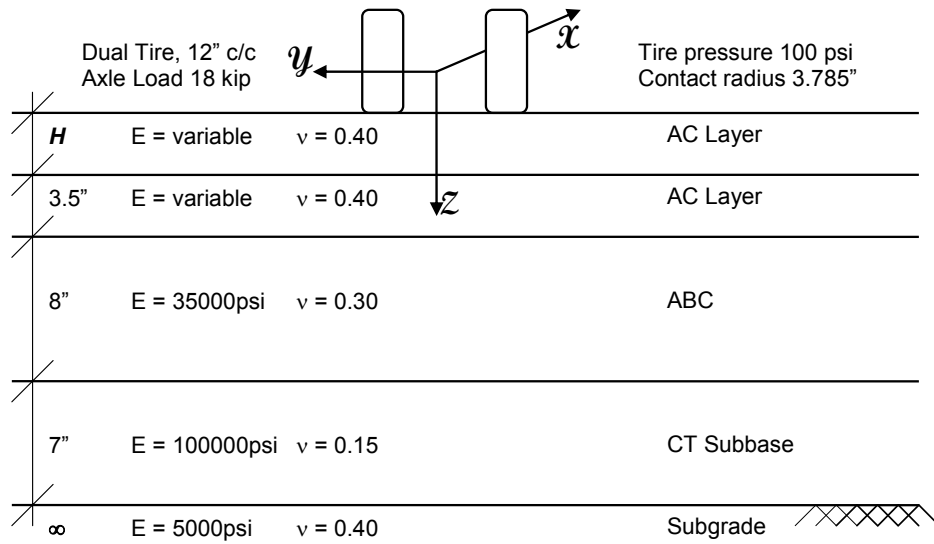


Figure 9-4 Pavement structure and layer properties, AC over AC

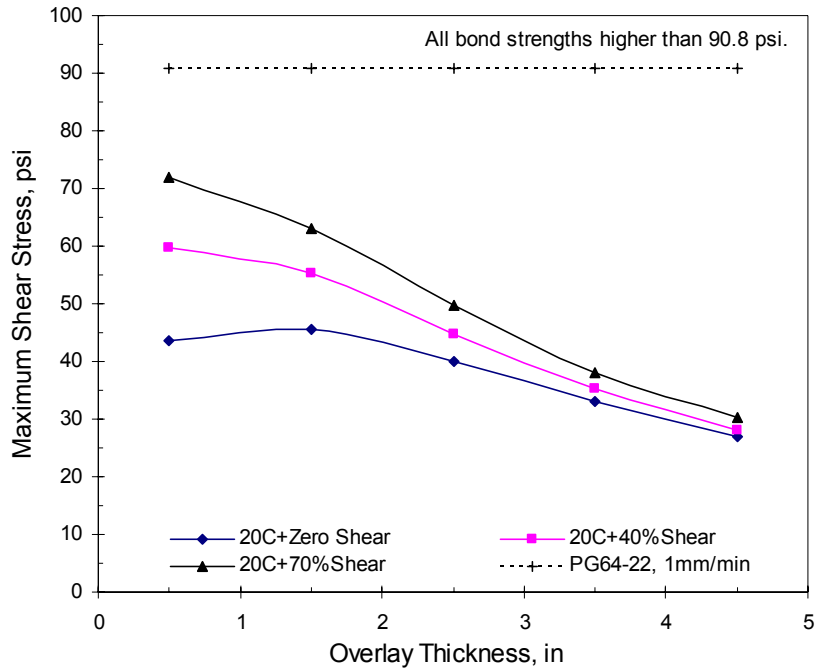


Figure 9-5 Mobilized interfacial shear vs. overlay thickness, AC-AC, 20 °C

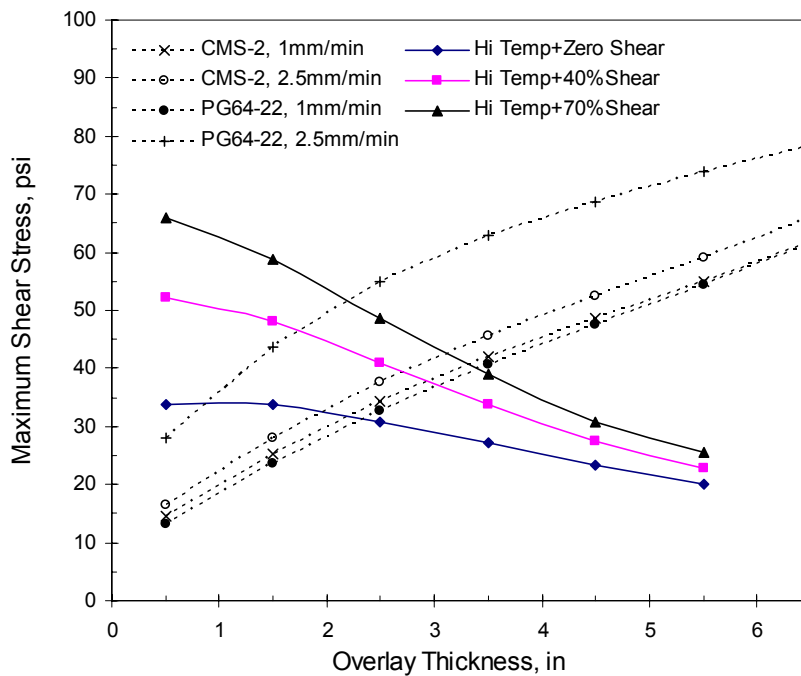


Figure 9-6 Mobilized interfacial shear vs. overlay thickness, AC-AC, 7-d max temp.

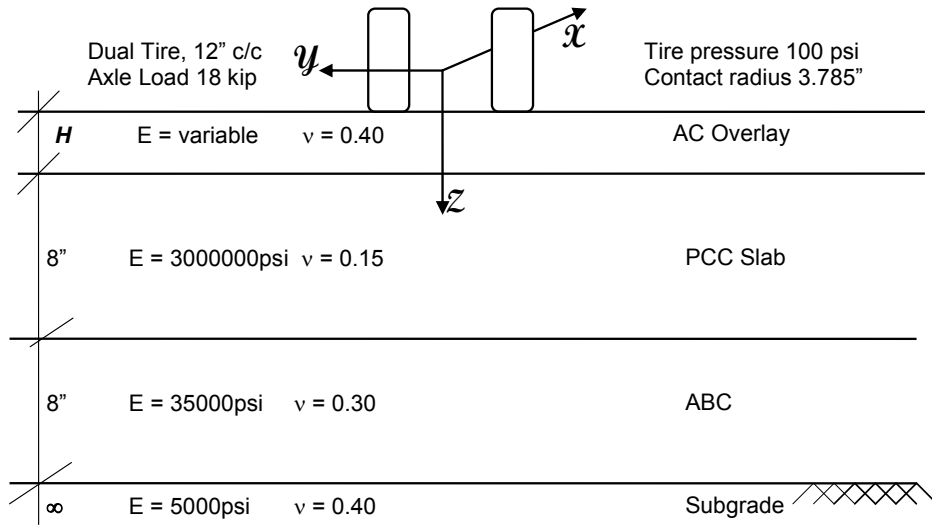


Figure 9-7 Pavement structure and layer properties, AC over PCC

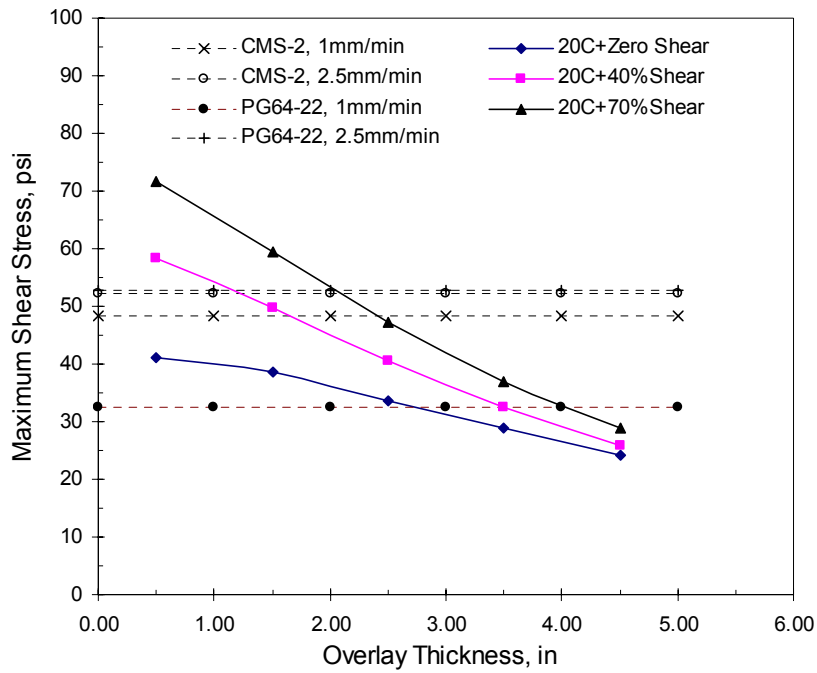


Figure 9-8 Mobilized interfacial shear vs. overlay thickness, PCC-AC, 20 °C

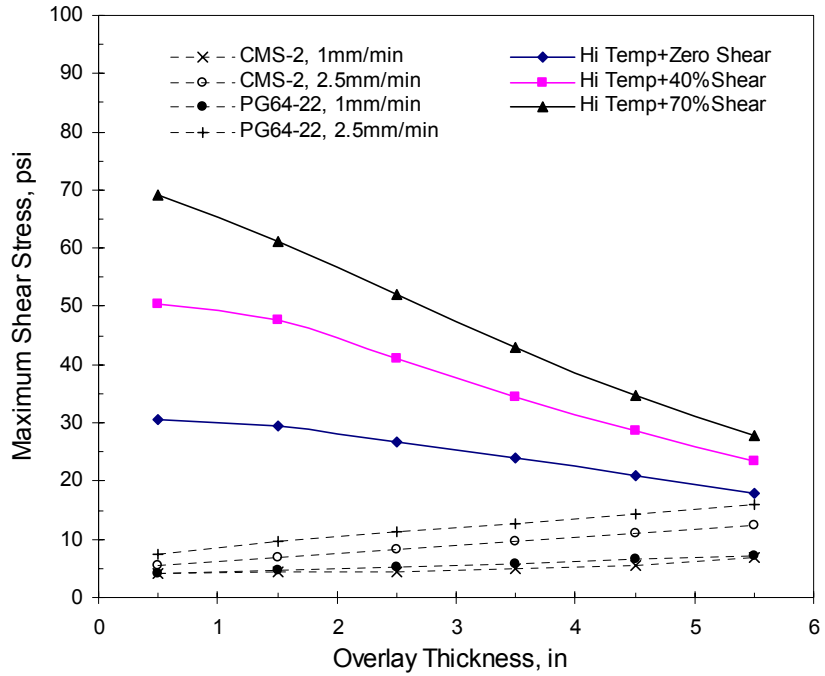


Figure 9-9 Mobilized interfacial shear vs. overlay thickness, PCC-AC, 7-d max temp.

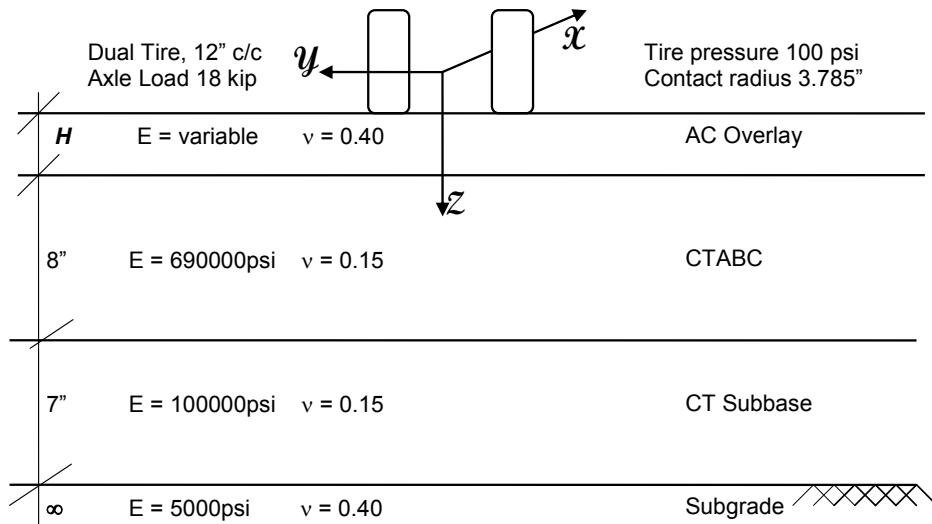


Figure 9-10 Pavement structure and layer properties, AC over CTB

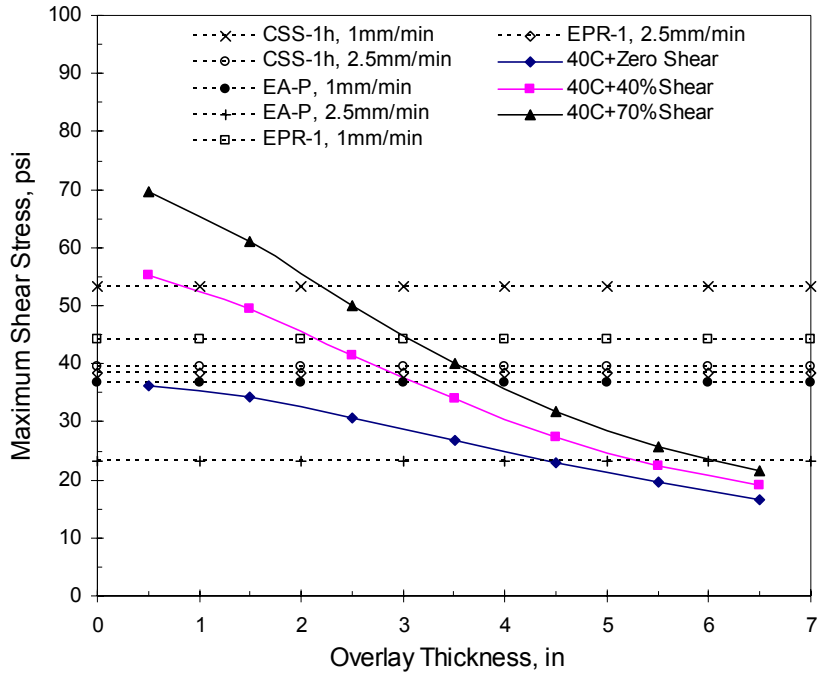


Figure 9-11 Mobilized interfacial shear vs. overlay thickness, CTB-AC, 40 °C

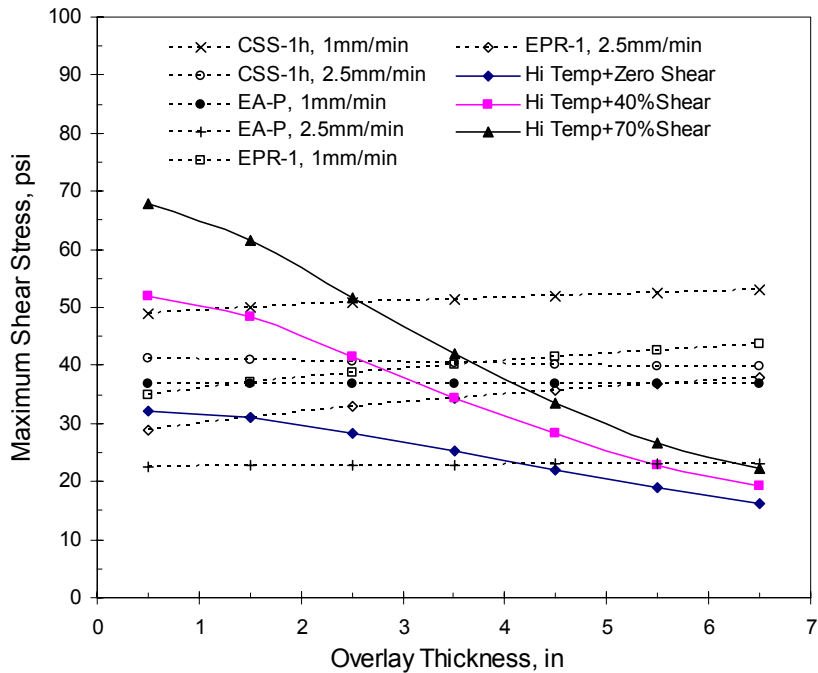


Figure 9-12 Mobilized interfacial shear vs. overlay thickness, CTB-AC, 7-d max temp.

10 Summary, Conclusions and Recommendations

10.1 Summary and Conclusions

This study investigated the causes(s) of excessive delamination and shoving distress observed in NCDOT Division 13. Two potential causes of these distresses were identified to be: (a.) Unstable mixtures caused due to intermittent purging of baghouse fines, and, (b.) Improper choice and/or application of tack coat.

Work conducted by Tayebali et al [28] evaluated the field cores and their compliance with NCDOT specifications. The field cores were obtained based on a survey conducted in Division 13 of NCDOT. Field cores from two counties, Buncombe and Rutherford, were selected for evaluation. The results of gradation, volumetric, and stability analysis indicated that the in-situ asphalt mixes used in Buncombe and Rutherford counties were generally within the NCDOT design specifications, and should have performed well under normal traffic conditions. Buncombe County sections, however, had excessive delamination and shoving distresses whereas Rutherford County sections did not show an occurrence of any of such distresses. It was originally hypothesized that one of the contributory factors to the delamination and shoving was the intermittent purging of baghouse fines in the field asphalt mixtures and, therefore, additional laboratory tests were conducted to verify the claim.

Gradation analysis using particle analyzer, however, showed comparable gradations for baghouses and regular mineral fillers for both counties. The dynamic mechanical analysis of mastics using DSR suggested that baghouse fines might lead to stiffening of the binders, and consequently increased rut resistance of AC mixes. Further, there was no significant difference in $|G^*|$ values of mastics prepared with baghouses versus regular filler. Laboratory FSCH and RSCH tests conducted on mixes with baghouse fines showed that:

- Baghouse fines have a stiffening on mixes from both counties;
- Mixes containing baghouse fines are more resistant to rutting compared to mixtures without baghouse fines; and
- Mixes from both counties show similar dynamic shear stiffness and rutting characteristics.

Mixtures containing regular mineral filler and baghouse fines were subjected to APA testing at NCDOT Materials and Test Unit. Test results showed that the accumulated rut depths for mixtures from Buncombe and Rutherford counties were approximately 6.15-mm (1/4-inch) and 12.5-mm (1/2-inch), respectively, for both mixtures with and without baghouse fines. Although, these rut depths suggest excessive rutting susceptibility for mixes based on the NCDOT specification, it confirms findings based on other tests that indicated that the performance of mixtures with and without baghouse fines are very similar. However, the modified AASHTO T283 test clearly indicated that the mixtures containing baghouse fines were moisture sensitive as compared to the mixtures containing regular mineral filler even though, an anti-strip additive was used for both mixtures. The TSR ratios for the Buncombe County mixtures were 78 and 85-percent for mixtures with and without baghouse fines, respectively. The TSR ratios for Rutherford County mixtures were 83 and 92-percent for mixtures with and without baghouse fines, respectively.

Based on the results of this investigation, it is concluded that the intermittent purging of baghouse fines could be the contributory factor in the delamination and shoving distress observed in NCDOT Division 13. It appears that the mechanism by which this distress is manifested is the following:

- Some in-situ mixtures may contain very high proportion of baghouse fines in relation to regular fines due to intermittent purging of the baghouse fines. Although the NCDOT JMF requires use of an anti-strip additive, the dosage does not appear to be sufficient to counter act moisture damage leading to in-situ mixture deterioration and, consequently, loss of strength and stability. Once the moisture damaged mixture is susceptible to shoving under traffic loading, the CRS-2 emulsion is not able to provide the tacking strength necessary for the surface layer to remain bonded to the lower layer, hence, leading to delamination.
- In Rutherford County where some pavement sections may contain relatively higher amount of baghouse fines due to intermittent purging, the PG64-22 binder used as tack coat appeared to provide sufficient bonding that may prevent asphalt layer from delaminating even though mixtures may undergo slight moisture damage.

Apart from intermittently purging baghouse fines into mixes, the pavement sections in Rutherford and Buncombe counties use CRS-2 emulsion and PG64-22 binder as tack coat. The improper use of tack coat could be a contributory factor to delamination distresses observed in those counties. It was, therefore, decided to investigate the contribution of prime and tack coat bond strength contribution to the integrity of pavements in relation to overlay AC thickness. The goal was to develop a mechanistic design procedure to minimize the occurrence of delamination distresses.

A survey was conducted across all the state highway departments and agencies to acquire information about the use of prime and tack coats in the field. Of the 26 responding agencies, ten reported that there was no requirement on use of prime coat for new construction. A majority of the remaining sixteen used a combination of cutbacks and emulsions for prime coats. Only two states, Georgia and New Jersey, require use of prime coat if the AC thickness is less than 5 inches, and Missouri requires it if the AC thickness is less than 4 inches. For prime and tack coats, there was no objective test to ensure proper curing. This could, potentially, lead to a lot of problems during the service life.

DSR test results on residual binders from emulsions were used to determine their PG grade. Generally, with higher the PG rating greater would be the expected shear strength. Using rolling wheel compaction, composite AC-AC, and PCC-AC specimens were fabricated in the lab. The target air void content for all AC specimens was 4%. Problems encountered in fabricating CTB slabs, required CTB-AC composite fabrication in gyratory molds. Before paving the overlay, the lower layer was tacked or primed, and the emulsions were allowed to cure for 24 hours. The rate of application was 0.06 and 0.24 gallons per square yard for tack coat and prime coat, respectively. The samples were then cored and cut to 6-inch diameter and 2-inch height before being tested in simple shear at various temperatures.

A displacement rate of 1.0 and 2.5 mm per minute was used to determine the bond strength of the specimens. The test results concluded that:

- Non-bonded surfaces have extremely low strengths compared to bonded surfaces.
Therefore, use of a bonding agent (tack or prime coat) is always recommended during constructions.

- For AC-AC composites, the performance of PG64-22 binder as a tack coat is better than CMS-2 emulsion. This is supported by higher axial and shear strengths of PG64-22 tacked specimens compared to CMS-2 specimens.
- For PCC-AC specimens, the behavior of PG64-22 as tack coat is comparable to CMS-2. One reason for this could be due to the fact that the rate of application of residual asphalt could be higher for PG64-22 than for CMS-2. In particular, it was found that PG64-22 performance at higher temperature and lower strain rate was relatively poor. The bond strengths recorded for PCC-AC combination were substantially lower compared to AC-AC. Secondly; the relative imperviousness of PCC (vis-à-vis AC) could lead to less absorption of asphalt from tack coat and, consequently, a poorer bond at high temperature and low strain rate. The relative differences in PCC and AC moduli could also be a contributory factor as well as the absence of corrugations on the PCC slab. In the field, the underlying concrete pavement has grooves or milled surface that increases the friction between the overlay and the PCC slab.
- The bond development in CTB-AC case was due to a contribution of the prime coat as well as aggregate interlock. CSS-1h emulsion performed better than EA-P and EPR-1 emulsions as prime coat.

Using shear and axial frequency sweep tests, the dynamic moduli of asphalt mix were determined at various temperatures and, properties for PCC were determined at 28 days. Based on the pavement temperature at various depths, the dynamic moduli and interfacial bond strengths were interpolated to yield temperature-corrected values. These values (dynamic moduli) coupled with the standard 18-kip loading data were, then, input into the FLA program developed in this investigation. The program computed the stresses, strains and displacements at various points in the pavement structure as function of vertical as well as horizontal shear loading. The maximum shear stresses were computed at the interface for different loading conditions. The variation of maximum mobilized shear stresses was then plotted against the interpolated bond strengths to obtain the required minimum design thicknesses.

For AC-AC, at 7-day maximum average temperatures, the overlay design thickness using CMS-2 and PG64-22 tack coat and shear displacement rate of 1.0 mm/minute was

comparable (3.5 inch); however at 2.5 mm/minute displacement rate PG64-22 (2.5 inch) gave a lower design thickness than CMS-2 (3.25 inch) indicating a superior performance. Mechanistic analysis indicates that delamination will not be a problem for AC-AC combination at 20 °C as the bond strengths are much higher than the mobilized interfacial shear stresses. For PCC-AC combination, at 20 °C and 2.5 mm/minute displacement rate, the design thickness for AC overlay is slightly higher than 2-inch; at the same temperature and 1.0 mm/minute the design thickness for CMS-2 and PG64-22 is 2.5 and 4 inch, respectively. Therefore, it can be concluded that CMS-2 yields lower thickness for PCC-AC combination than PG64-22 binder. As indicated earlier, this could be due to excess PG64-22 (compared to the residual asphalt in CMS-2), smooth PCC surface, and low rate of tack coat absorption by the PCC surface. At 7-day maximum temperature, for PCC-AC combination, the interpolated bond strengths are much lower than the mobilized shear stresses. Therefore, the choice of tack coats is dependent not only on the types of interfaces under consideration but also on the rate of application. Higher rate of tack coat is undesirable when using impervious and smooth surfaces as PCC. At higher temperature, instead of providing a good bond, it will actually act as a slippage surface. In severe cases it may even lead to bleeding on the thin AC overlay layer.

For CTB-AC interface, CSS-1h emulsion seems to be better than EA-P and EPR-1. Overall, based on the results of this study, the following conclusions can be drawn:

- Addition of baghouse fines could cause stiffening of AC mixes. However, appropriate amounts of anti-strip additive needs to be added to counteract the added moisture susceptibility due to the presence of baghouse fines.
- The contribution of tack coat to the bond strength is dependent on the grade of the residual asphalt as well as the interfaces under consideration. PG64-22 performs slightly better for the AC-AC case whereas CMS-2 performs marginally better for PCC-AC case.
- For thin pavement sections, the use of prime coats is recommended to increase the bond between the AC layer and the underlying layers. Similarly, use of a suitable tack coat is recommended for all overlay construction with minimum AC layer thickness of 2.5-3.5 inches when PG64-22 or CMS-2 emulsion is used as tack coat. If a different tack coat

is used, the minimum thickness can be obtained for the given site using the design guidelines developed in this study.

- CSS-1h performs better as a prime coat than EA-P and EPR-1 emulsions.
- For emulsions used as prime and tack coats, it is necessary to ensure complete curing before paving new layer. Any inappropriate curing could reduce the bond as well as trap moisture causing problems later in service.
- The choice of proper tack coat (CMS-2 versus PG64-22) should be based on operational considerations. Use of PG64-22 as tack coat enables the tacked section to be open to traffic immediately after application. Further the convenience of night time paving as well as minor effect on exposure moisture outweighs the trouble of dealing with hot asphalt. Curing problems with emulsions prevail over the uniformity and ease of their application.

Finally, this research study provides a methodology and design guide based on mechanistic analysis to select appropriate tack or prime coat for the given field conditions. Based on selection of the tack or prime coat, the AC layer thickness can be adjusted to minimize the delamination distresses.

10.2 Future Scope

The study conducted herein compared the bond strengths of various materials at 1.0 and 2.5 mm/minute shear displacement rate. Following aspects need to be examined further:

- The current results should be validated by testing laboratory fabricated composite slabs under wheel-tracking device, and field testing.
- The current study is based on laboratory tests, testing of the field cores from various pavement sections (good performing vs. poor performing) should be explored to get a correlation between the laboratory test results and field observations.
- Laboratory testing could be conducted under multi-axial loading states to simulate in-situ condition closely.

- The various loading conditions used for analysis use a static load. A relationship needs to be developed between the following:
 - Vehicular speed and the rate of shear strain as function of depth, and
 - Vehicular speed and loading frequency.
- The analyses conducted using the FLA program assume isotropy, elastic behavior, and homogeneity. Approaches that consider anisotropy and viscoelastic behavior could offer significant insight into the complex behavior of asphalt materials.

11 References

1. American Association of State Highway and Transportation Officials, "AASHTO Guide for Design of Pavement Structures," pp. II-23, 1993.
2. American Association of State Highway and Transportation Officials, "Standard Specification for Performance Graded Asphalt Binder," *AASHTO Designation MP1*, 1996.
3. American Association of State Highway and Transportation Officials, "Standard Method for Preparing and Determining the Density of Hot Mix Asphalt (HMA) Specimens by Means of the SHRP Gyrotory Compactor," *AASHTO Designation TP4*, 1996.
4. American Association of State Highway and Transportation Officials, "Standard Test Method for Determining the Rheological Properties of Asphalt Binder Using a Dynamic Shear Rheometer (DSR)," *AASHTO Designation TP5*, 1996.
5. American Association of State Highway and Transportation Officials, "Standard Test Method for Determining the Permanent Deformation and Fatigue Cracking Characteristics of Hot Mix Asphalt using a Simple Shear Test Device," *AASHTO Designation TP7*, 1996.
6. Ameri-Gaznon, M., and Little, D., "Octahedral Shear Stress Analyses on an ACP Overlay on a Rigid Base," *Proceedings of the Association of Asphalt Paving Technologists*, vol. 59, pp. 443-479, 1990.
7. Asphalt Institute, "Asphalt in Pavement Maintenance," *Manual Series No. 16 (MS-16)*, Third Edition, 1996.
8. Barber, E. S., "Shear Loads on Pavements," *Public Roads*, vol. 32, no. 6, pp. 141-144, 1963.
9. Bonnaure, F., Gavois, A., and Udron, J., "A New Method for Predicting the Fatigue Life of Bituminous Mixes," *Proceedings of the Association of Asphalt Paving Technologists*, vol. 49, pp. 499-529, 1980.

10. Burmister, D. M., "The General Theory of Stresses and Displacements in Layered Systems," *Journal of Applied Physics*, vol. 16, pp. 89-94, 126-127, 296-302, February 1945.
11. Epps, J. A., and Button, J. W., "The Slippage Question on Airport Pavements," Texas Transportation Institute, *Interim Report*, RF3424-2.
12. Hachiya, Y., and Sato, K., "Effect of Tack Coat on Bonding Characteristics at Interface between Asphalt Concrete Layers," *Proceedings of 8th International Conference on Asphalt Pavements*, vol. 1, pp. 349-362, 1997.
13. Harris, B. M., and Stuart, K. D., "Analysis of Mineral Fillers and Mastics used in Stone Matrix," *Proceedings of the Association of Asphalt Paving Technologists*, vol. 64, pp. 54-95, 1995.
14. Huang, Y. H., "Pavement Analysis and Design," Pearson Prentice Hall, second edition, 2004.
15. Ishai, I., and Livneh, M., "Functional and Structural Role of Prime Coat in Asphalt Pavement Structures," *Proceedings of the Association of Asphalt Paving Technologists*, vol. 53, pp. 98-118, 1984.
16. Kummer, H. W., and Meyer, W. E., "Tentative Skid-Resistance Requirements for Main Rural Highways," *NCHRP Report 37*, Highway Research Board, 1967.
17. Metcalf, J. B., "Accelerated Pavement Testing, a Brief Review Directed Towards Asphalt Interests," *Proceedings of the Association of Asphalt Paving Technologists*, vol. 67, pp. 553-572, 1998.
18. Mohammad, L. N., Raqib, M. A., and Huang, B., "Influence of Asphalt Tack Coat Materials on Interface Shear Strength," *Transportation Research Record*, no 1789, pp. 56-65, 2002.
19. Mukhtar, M. T., and Dempsey, B. J., "Interlayer Stress Absorbing Composite (ISAC) for Mitigating Reflection Cracking in Asphalt Concrete Overlays," *Final Report Project IHR-533*, Illinois Cooperative Highway Research Program, June, 1996.

20. Paul, H. R., and Scherocman, J. A., "Friction Testing of Tack Coat Surfaces," *Transportation Research Record*, no. 1616, pp. 6-12, 1998.
21. Shahin, M. Y., Kirchner, K., Blackmon, E.W., and Tomita, H., "Effect of Layer Slippage on Performance of Asphalt-Concrete Pavements," *Transportation Research Record*, no. 1095, pp. 79-85, 1986.
22. "SHRP Superpave Binder Selection Program – SHRPBIND," version 2.1, *Federal Highway Administration*, Pavement Performance Division, McLean, Virginia, 1985.
23. "SHRP-A-415 Permanent Deformation of Asphalt Aggregate Mixes," *Strategic Highway Research Program*, National Research Council, Washington DC, 1994.
24. Sholar, G. A., Page, G. C., Musselman, J. A., Upshaw, P. B., Moseley, H. L., "Preliminary Investigation of a Test Method to Evaluate Bond Strength of Bituminous Tack Coats," *Proceedings of the Association of Asphalt Paving Technologists*, Preprints, pp. 107-137, 2004.
25. Small, J. C., and Booker, J. R., "Finite Layer Analysis of Layered Elastic Materials Using a Flexibility Approach. Part 1 – Strip Loadings," *International Journal for Numerical Methods in Engineering*, vol. 20, pp. 1025-1037, 1984.
26. Small, J. C., and Booker, J. R., "Finite Layer Analysis of Layered Elastic Materials Using a Flexibility Approach. Part 2 – Circular and Rectangular Loadings," *International Journal for Numerical Methods in Engineering*, vol. 23, pp. 959-978, 1986.
27. Tayebali, A. A., Fischer, W. K., Huang, Y. X., and Kulkarni, M. B., "Effect of Percentage Baghouse Fines on the Amount and Type of Anti-Stripping Agent Required to Control Moisture Sensitivity," *Final Report*, North Carolina Department of Transportation, June 2003.
28. Tayebali, A. A., Kulkarni, M. B., and Waller, H. F., "Delamination and Shoving of Asphalt Concrete Layers Containing Baghouse Fines," *North Carolina Department of Transportation Project 1999-03*, FHWA/NC/2002-011, May 2000.

29. Tschegg, E., Kroer, G., Tan, D., Stanzl-Tschegg, S., and Litzka, J., "Investigation of Bonding between Asphalt Layers on Road Construction," *Journal of Transportation Engineering*, vol. 121, no. 4, pp. 309-316, 1995.
30. Uzan, J., "Influence of the Interface Condition on Stress Distribution in a Layered System," *Transportation Research Record*, no. 616, pp. 71-73, 1976.
31. Uzan, J., Livneh, M., and Eshed, Y., "Investigation of Adhesion Properties between Asphaltic-Concrete Layers," *Proceedings of the Association of Asphalt Paving Technologists*, vol. 47, pp. 495-521, 1978.
32. Xu, Q., Rahman, M. S., and Tayebali, A. A., "FLA: A Computer Program for Finite Layer Analysis of Stresses in Pavements," Department of Civil Engineering, North Carolina State University, June 2002.

Appendix A

Questionnaire – ON PRIME AND TACK COATS

A Mechanistic Approach to Evaluate Contribution of Prime and Tack Coat
In Composite Asphalt Pavements

North Carolina Department of Transportation, Project HWY-2001-04

Scope of the Survey: An evaluation of the effectiveness of emulsified asphalt prime coats as compared to cutback asphalt prime coats, and to make a survey of the state practices with respect to types and rates of application of both prime coats and tack coats.

Responding Agency: _____

Name and Title of Individual Completing Questionnaire: _____

Does your agency require the use of a prime coat on new construction?

Yes ___ NO ___

If the answer to question 1 is yes, what are the required type of material and the normal rate of application?

Is the use of prime coat related to asphalt pavement thickness? If so, explain

Is a specific cure time specified? Yes ___ No ___

If yes, how much cure time? _____

What types of laboratory tests are required for prime coat material(s) ?

Are any types of field performance test(s) required? Yes ___ NO ___. If yes, please explain _____

Have you been able to detect any difference in pavement performance by using or not using a prime coat? Yes ___ No ___. If yes, please explain _____

Do you have opinion as to the merits of an emulsified asphalt prime as compared to a cutback asphalt prime? Yes ___ NO ___. If yes, please explain _____

What types of asphalt materials are used for tack coats – types and application rates?

If you use emulsified asphalt tack coats for nighttime paving, what provisions are made for the emulsion breaking prior to placement of the hot-mix asphalt?

Please return completed questionnaire to:

Prof. Akhtar A. Tayebali, P.E.

North Carolina State University

Department of Civil Engineering

Campus Box 7908

Raleigh, NC 27695-7908

Ph: (919) 515-7611

Completed questionnaires can be faxed at (919) 515-7908. If you prefer to fill this questionnaire in electronic format, please send an e-mail to tayebali@eos.ncsu.edu.

Appendix B

State	Prime Coat	Prime Coat Materials	PC Rate (gal/yd ²)	PC relation to AC thickness	Cure Time	How much?	Lab Tests for Prime Coats	Field PT?	Field Performance Test Description	Diff. in perf.?	Explanation	Explanation: why emulsion is better than cutback or vice versa.	Tack Coat Types	Tack Coat Rates (gal/yd ²)	Night time provisions
AK	Y/ N	MC-30 or CSS-1	250-750 ml/sq. m	N, The application of tack coat is dependent on individual designers and on the paving location.	N		MC-30 must meet M82. CSS-1 must meet M140.	N		N	-	Y, Cutbacks penetrate better than the emulsified asphalts.	Special Tack Emulsion -1	200-400 ml/sq.m	Tack coat may not be placed on a wet surface or when the roadway surface temp is below 5 deg. C.
AL	Y	AE-P, MC-30, MC-70 for tight bases. MC-250, MC 70, RC-250 for open bases, EPR	0.22 - 0.25 20% redn. for CTB	No	N		M81, M82, spot test is not required.	N		Y	Protects base from wind/water erosion and promotes the maintenance of optimum m/c by creating an impermeable membrane.	Better penetration and better coverage from cutback asphalt.	CRS-2, CRS-2h, CSS-1, CSS-1h, CSQ-1hp, PG 67-22	As directed by engr but < 0.07	Eliminating the use of emulsified asphalt tack coats because it is not possible to determine whether emulsion has broken or not.
AR	N	MC cutbacks	0.4	N, Except for a minimum thickness of hot mix on minor roadways.	Y	3 days	Distillation, softening point, penetration, viscosity, spot test.	N		N	-	-	RC cutbacks, emulsions	0.03 - 0.10	Observation of the inspector.
AZ	N	-	-	-	-	-	Kinematic Viscosity	N		N	-	N, MC-250 is the only thing used in AZ.	AC, SS-1	AC @ 0.06, SS-1 & ERA-25 - 1:1 dilute w/ water @ 0.08	Nothing specified. Emulsion must break before paving of AC.
CT	Y	Emulsions.	0.14-0.45 liter/sq. m	No, but prime coats are required only on airports.	Y	Tacky to touch.	Percent residue, viscosity..	N		N	-	-	SS-1, SS-1H	0.14-0.45 liter/sq. m	None.

State	Prime Coat	Prime Coat Materials	PC Rate (gal/yd ²)	PC relation to AC thickness	Cure Time	How much?	Lab Tests for Prime Coats	Field PT?	Field Performance Test Description	Diff. in perf.?	Explanation	Explanation: why emulsion is better than cutback or vice versa.	Tack Coat Types	Tack Coat Rates (gal/yd ²)	Night time provisions
FL	Y	RC-70, RC-250. SS-1, CSS-1, SS-1H diluted. AE-60, AE-90, AE-150, AE-200, Sp. MS-Emulsion diluted at a ratio of six parts of emulsion to four parts of water. AEP, EP (RS type), EPR-1 Prime.	> 0.1	N	N		Sec. 916-3 and 916-4 of FDOT.	N	-	Y	Prime is thought to act as a barrier to moisture to frequent rains in Florida. Better bond between AC and base course. Also acts as barrier for moisture when penetration happens through cracks.	-	-	-	-
GA	Y	RC-30, RC-70, MC-30, MC-70, EAP-1	0.7 - 1.4 liters/sq. m	PC required on all soil-cement and lime stabilized bases and on all other bases unless AC > 125 mm	N		T55, T79, T48, T201, T78, T51, T44, T49, T50, T72, T111	N	-	-	-	-	PG 58-22, PG64-22, PG67-22	0.18 - 0.27 liters / sq. m	N/A
ID	N	MC-70, MC-250, CSS-1	0.3	No, related more to the amount of traffic on the base. Helps when thin lifts of asphalt are present	N		M82 - cutbacks T59 - emulsions	N	PC matl. Accepted by certification. Verification samples taken; may or may not be tested.	Y	Thinner pavements (0,2') shove and tear on grades and in curves where prime is not used.	Cutbacks penetrate better but environmental problems.	Diluted CSS-1	0.05	None at this time.
IL	Y	RC-70	0.02	Only on full depth pavements is prime coat required. N	Y	Min. 1 hour.	Sp. Gr, Kin. Visc., Distillation, Test on residue, penetration, ductility, % soluble in TCE	N	-	N	Considered paving without in late 1997. Cost savings considered minimal and not worth the risk.	We allow emulsions for resurfacing projects - with success.	resurfacing: SS-1, SS-1H, CSS-1, CSS-1H, HFE60, HFE90, RC-70	0.05-0.1	Just emulsion breaking.
KS	N	-	-	Not used.	-	-	-	-	-	-	-	Emulsions do not penetrate.	CSS-1H, SS-1H diluted 50%	0.03-0.05	Must break down before overlay.

State	Prime Coat	Prime Coat Materials	PC Rate (gal/yd ²)	PC relation to AC thickness	Cure Time	How much?	Lab Tests for Prime Coats	Field PT?	Field Performance Test Description	Diff. in perf.?	Explanation	Explanation: why emulsion is better than cutback or vice versa.	Tack Coat Types	Tack Coat Rates (gal/yd ²)	Night time provisions
KY	Y	Primer-L: cutback asphalt emulsion.	1.6-2.0 lb/sq. yd	No	Y	"must cure!"	Saybolt Furol, Water Content, Asphalt Content, Coating, Residue Test Float, Solubility in Trichloro-ethylene	Y	Sampling of Primer_L @ 1 per 15000 tons of AC and the same tests.	N	-	Cutbacks perform better as sealants but concern about health and environment.	SS-1, SS-1H, CSS-1, CSS-1H, AE-60, RS-1, CRS-1	0.4 lb/sq. yd	It is necessary to have all water to be evaporated before any paving process.
ME	N	-	0.02 for overlays, 0.04 for milled and 0.01 for new mixes tacked at Contractors option	N, Tack coat is not needed for new construction only on overlaid pavement's or lower layers that have been exposed to winter or have got dirty.	N	-	M140 Ductility, Penetration, Sieve test for lumps, Oil content, Float test, Viscosity at 25 deg. C.	N	-	Y	Contractors find easy to densify SUPERPAVE mixes. QA bonus makes up for the cost of the tack. Less delamination and when applied properly it is impossible to separate tacked layers in cores without a saw.	N	Emulsions and are required only when overlaying an old pavement that is dirty or has wintered over.	-	Little night time paving but breaking can be decided in artificial lights.
MN	N	Although the specifications exist in the "handbook" Prime Coat is not used in practice. MC-30, MC-70.	0.45-1.35 liter/sq. m	-	-	-	-	-	-	-	-	N	MC-250, MC-800, C-70, C-250, C-800, SS-1, SS-1H, MS-2, RS-1, RS-2, CSS-1, CSS-1H, CRS-1, CRS-2	0.23 lit/sq.m for cutbacks and undiluted emulsions. 0.91 lit/sq.m for diluted emulsions. Water may be added upto 0% for SS-1, SS-1H, CSS-1 and CSS-1H.	Currently requiring the emulsion to break completely.

State	Prime Coat	Prime Coat Materials	PC Rate (gal/yd ²)	PC relation to AC thickness	Cure Time	How much?	Lab Tests for Prime Coats	Field PT?	Field Performance Test Description	Diff. in perf.?	Explanation	Explanation: why emulsion is better than cutback or vice versa.	Tack Coat Types	Tack Coat Rates (gal/yd ²)	Night time provisions
MO	Y	RC-70, MC-30 or SS-1	0.2-0.5	Primer not used for plant mix bituminous base with a thickness of 4" or more.	N	-	M81, M82 or M140	N	-	N	We have always required the use of prime coat.	Y, Emulsions have more pickup versus cutback.	SS-1, SS-1H, CSS-1, CSS-1H	0.02-0.1	No provisions for emulsion tack coats during night time paving.
MS	Y	CTB - MC-70, EA-1. Lime treated: EA-1, SS-1, CSS-1, CMS-2h, MS-2h	CTB-0.1-0.25. Lime: 0.25	N	N	-	T59, M82, M140, M208	N	-	Y	Indirectly, we know that unprimed chemically stabilized courses do suffer moisture damage, but it could be related as much to the stabilization effort as it is to the prime coat.	Y, emulsions are easier for contractors to use and work well when applied properly.	SS-1, CSS-1 and some AC-30	-	-
NE	N	-	-	-	-	-	-	-	-	N	-	Y, Environmental Issue.	CSS-1H when diluted with water to reduce AC content to 30% of total vol.	0.1-0.2 on existing or milled surfaces. OR 0.05-0.1 on freshly laid AC.	Required to be broken before placement. But it is not always the case. We have not discovered any problems when unbroken tack was covered with hot mix.
NH	N	-	-	PC not required since 1974.	-	-	-	N	-	-	-	N	RS-1, CRS-1	0.025	Emulsion breaking should be very quick.
NJ	Y	MC-30, MC-70	0.68-1.58 liter/sq. m	The engineer may waive the application of prime coat if a minimum of 125 mm of plant AC mix is placed on unbound aggregate course prior to opening to traffic.	N	-	M82	Y	No volatile organic substances under normal use conditions.	N	Currently attempting to eliminate the prime coat requirement. More often eliminated than not on projects.	-	RC-70, RC-T, RS-1, SS-1, SS-1h, CSS-1, CSS-1h. Emulsion used determined by Calendar.	See sec. 404.13	Tacky to touch.

State	Prime Coat	Prime Coat Materials	PC Rate (gal/yd ²)	PC relation to AC thickness	Cure Time	How much?	Lab Tests for Prime Coats	Field PT?	Field Performance Test Description	Diff. in perf.?	Explanation	Explanation: why emulsion is better than cutback or vice versa.	Tack Coat Types	Tack Coat Rates (gal/yd ²)	Night time provisions
NY	N	-	-	-	-	-	-	-	-	-	-	-	HFMS-2h, SS-1h, CSS-1h	diluted application rate: 0.14-0.32 lit./sq. m	Currently under discussion.
OK	Y/N	MC-30, MC-70 or emulsions in Oklahoma, Tulsa and Commanche Counties	0.1-0.4	N	N	Sufficient to allow proper penetration and hardening of prime coat.	Kinematic Viscosity @140 C, Flash Point, % Water, Distillation, Abs Viscosity, Ductility, Solubility in Trichloroethylene, Spot Test.	Y/N	No performance tests but lab tests, viscosity (140), Distillation.	Y	We had one project this year that had significant plane slippage problems due to use of tack coats in lieu of prime coat.	Y, Emulsions to be used where environment is a concern and also if conditions warrant and wherever there is sufficient time for curing.	RS-1, RS-2, MS-1, MS-2, MS-2h, HFMS-1, HFMS-2, HFMS-2h, HFMS-2s, SS-1, SS-1h, CRS-1, CRS-2, CMS-1, CMS-2, CSS-1, CSS-1h	0.1	Emulsions disallowed after sunset.
RI	N	-	-	-	-	-	-	-	-	-	-	-	SS-1	0.05	Emulsions used for night time paving but no provisions exist for breaking prior to placement.
SC	Y	-	0.25-0.3	N	N	-	Saybolt Furol, Residue by Distillation.	N	-	N	-	N	CRS-2, HFMS-1	0.05-0.15 based on residual asphalt.	None, contractors electing to use RS emulsion if needed.
TN	Y	AE-P, CAE-P	0.2-0.5	N	N	-	M140, Saybolt Furol, Settlement, Residue, Distillate, Float, Penetration, Solubility.	N	-	N	-	N	SS-1, CSS-1, PG64-22	0.05 for smooth (max.) and 0.2 (max) for milled.	None

State	Prime Coat	Prime Coat Materials	PC Rate (gal/yd ²)	PC relation to AC thickness	Cure Time	How much?	Lab Tests for Prime Coats	Field PT?	Field Performance Test Description	Diff. in perf.?	Explanation	Explanation: why emulsion is better than cutback or vice versa.	Tack Coat Types	Tack Coat Rates (gal/yd ²)	Night time provisions
TX	Y	MC-30, AEP, PCE, EAP&T, CSS-1 and SS-1	0.1	Emulsions can be used but have to be worked into the top inch and recompact.	N	-	Item 300 of "Asphalts, Oils and Emulsions."	N	For new materials, testing is required.	N	Compulsory, therefore nothing to compare with.	Y, MC-30 penetrates best. For open bases, emulsion may be good.	diluted SS-1, CSS-1	0.05	Not aware of any special considerations.
WV	Y	SS-1, SS-1h, CSS-1, CSS-1h diluted with water. Inverted emulsions permitted but rarely used.	0.3 - 0.6	N	N	-	M140, M208	N	-	N	-	Cutbacks penetrate better but environmental problems and costly.	Mostly SS emulsions (cationic, anionic, inverted)	0.2 - 0.3; SS-1h diluted with 50% water is commonly used.	No special requirements.
WY	Y	MC-70	3.2 lb/sq yd	No	N	-	M82, Kinematic viscosity, distillation. Have an acceptance schedule based on properties.	N	-	Y	We feel the prime facilitates placing the first lift of pavement and also provides some water proofing.	N	SS-1 or CSS-1	0.25 lb/sq yd	Do very little night time paving.

Appendix C

Job Mix Formula

99410 NORTH CAROLINA DEPARTMENT OF TRANSPORTATION
 RALEIGH, NORTH CAROLINA 27611

HOT MIX ASPHALT JOB MIX FORMULA

APAC-CAROLINA, INC

TYPE MIX: BCSC, TYPE HDS

ENKA, NC

JOB MIX FORM NO: 93-447-052

EFFECTIVE DATE: 07-27-93

PLANT CERTIFICATION NO: DM-310

PROJECT NO:

COUNTY: BUNCOMBE

AGGREGATE SOURCES AND BLEND PERCENTAGES

<u>SUPPLIER</u>	<u>LOCATION/SOURCE</u>	<u>MATERIAL</u>	<u>BLEND(%)</u>
VULCAN MATERIALS	ENKA QUARRY	#78M	42
VULCAN MATERIALS	ENKA QUARRY	W.SCRGS.	30
VULCAN MATERIALS	ENKA QUARRY	D.SCRGS.	28

TOTAL: 100.0%

JMF COMBINED GRADATION

<u>SIEVE SIZE</u>	<u>% PASSING</u>
2''	
1 1/2''	
1''	
3/4''	100
1/2''	98
3/8''	95
NO. 4	72
8	50
16	39
40	24
80	12
200	5.0

ASPHALT CEMENT %(TOT) 5.7

GRADE	PG64-22
EST ASH	11-3-93 0.3
MAX. SP. GV.	2.486
LABORATORY SP. GV.	2.364
VOIDS IN TOTAL MIX %	4.9
MIN. % COMPACTION	95.0
MIX TEMPERATURE F.	285
FLOW (0.01 IN.)	11
STABILITY (LBS.)	3000
NON STRIP ADDITIVE %	0.50
MODIFIER %	0.00

ASPHALT CEMENT SUPPLIER : SPECS.
 TACK COAT SUPPLIER : SPECS.
 NON-STRIP ADD. SUPPLIER : PAVE BOND LP – CINCINNATI, OHIO
 MODIFIER SUPPLIER :

COMMENTS:

% AC DECREASED TO INCREASE VOIDS. BLEND CHANGES TO CONTROL GRADATION & VOIDS IN MIX. #8 SIEVE CHANGE BASED ON FIELD TEST RESULTS.

DATE JMF VOID:

APPROVED BY:
 J.E. GRADY, JR.
 PAVEMENT CONSTRUCTION ENGR.

99410 NORTH CAROLINA DEPARTMENT OF TRANSPORTATION
 RALEIGH, NORTH CAROLINA 27611

HOT MIX ASPHALT JOB MIX FORMULA

THOMPSON CONTRACTORS, INC

TYPE MIX: BCSC, TYPE HDS

RUTHERFORDTON, NC

JOB MIX FORM NO: 93-903-051

EFFECTIVE DATE: 02-07-94

PLANT CERTIFICATION NO: DM-286

PROJECT NO:

COUNTY: RUTHERFORD

AGGREGATE SOURCES AND BLEND PERCENTAGES

<u>SUPPLIER</u>	<u>LOCATION/SOURCE</u>	<u>MATERIAL</u>	<u>BLEND(%)</u>
THOMPSON CONTRACTORS	MILLER CREEK QUARRY	#78M	47
THOMPSON CONTRACTORS	MILLER CREEK QUARRY	SCRGS.	33
THOMPSON CONTRACTORS	BROAD RIVER	SAND	20

TOTAL: 100.0%

JMF COMBINED GRADATION

<u>SIEVE SIZE</u>	<u>% PASSING</u>
2''	
1 1/2''	
1''	
3/4''	100
1/2''	98
3/8''	95
NO. 4	69
8	53
16	43
40	24
80	11
200	5.9

ASPHALT CEMENT %(TOT) 6.2

GRADE	PG64-22
EST ASH	11-3-93 0.4
MAX. SP. GV.	2.502
LABORATORY SP. GV.	2.378
VOIDS IN TOTAL MIX %	5.0
MIN. % COMPACTION	95.0
MIX TEMPERATURE F.	285
FLOW (0.01 IN.)	9
STABILITY (LBS.)	1900
NON STRIP ADDITIVE %	0.50
MODIFIER %	0.00

ASPHALT CEMENT SUPPLIER : SPECS.
 TACK COAT SUPPLIER : SPECS.
 NON-STRIP ADD. SUPPLIER : PERMA-TAC — SCAN ROAD
 MODIFIER SUPPLIER :

COMMENTS:

DATE JMF VOID:

APPROVED BY:
 J.E. GRADY, JR.
 PAVEMENT CONSTRUCTION ENGR.

NORTH CAROLINA DEPARTMENT OF TRANSPORTATION
 RALEIGH, NORTH CAROLINA 27611

HOT MIX ASPHALT JOB MIX FORMULA

APAC-CAROLINA, INC.

TYPE MIX: BCSC, TYPE I-2

ENKA, NC

JOB MIX FORM NO: 01-229-161

EFFECTIVE DATE: 05-11-01

PLANT CERTIFICATION NO: DM-310

PROJECT NO:

COUNTY:

AGGREGATE SOURCES AND BLEND PERCENTAGES

SUPPLIER	LOCATION/SOURCE	MATERIAL	BLEND (%)
VULCAN MATERIALS	ENKA QUARRY	78M	26.0
VULCAN MATERIALS	ENKA QUARRY	W.SCRGS.	63.0
VULCAN MATERIALS	ENKA QUARRY	D.SCRGS.	11.0

 TOTAL 100.0%

JMF COMBINED SIEVE SIZE	GRADATION % PASSING
2 "	100
1 1/2"	100
1 "	100
3/4"	100
1/2"	100
3/8"	97
NO. 4	77
8	62
16	44
40	50
80	13
NO. 200	5.9

ASPHALT CEMENT %(TOT) 7.0

GRADE	PG64-22
EST ASH	
MAX. SP. GV.	2.469
LABORATORY SP. GV.	2.333
VOIDS IN TOTAL MIX %	5.5
MIN. % COMPACTION	95.0
MIX TEMPERATURE F.	300
FLOW (0.01 IN.)	11
STABILITY (LBS.)	2020
NON STRIP ADDITIVE %	0.60
MODIFIER %	0.00

ASPHALT CEMENT SUPPLIER: SOUTH STATES KNOXVILLE
 TACK COAT SUPPLIER : SPECS.
 NON-STRIP ADD. SUPPLIER: ARR-MAZ LOF 6500
 MODIFIER SUPPLIER :

COMMENTS:

DATE JMF VOID:

APPROVED BY:
 J.E. GRADY, JR.
 PAVEMENT CONSTRUCTION ENGR.

Appendix D

APA Test Results

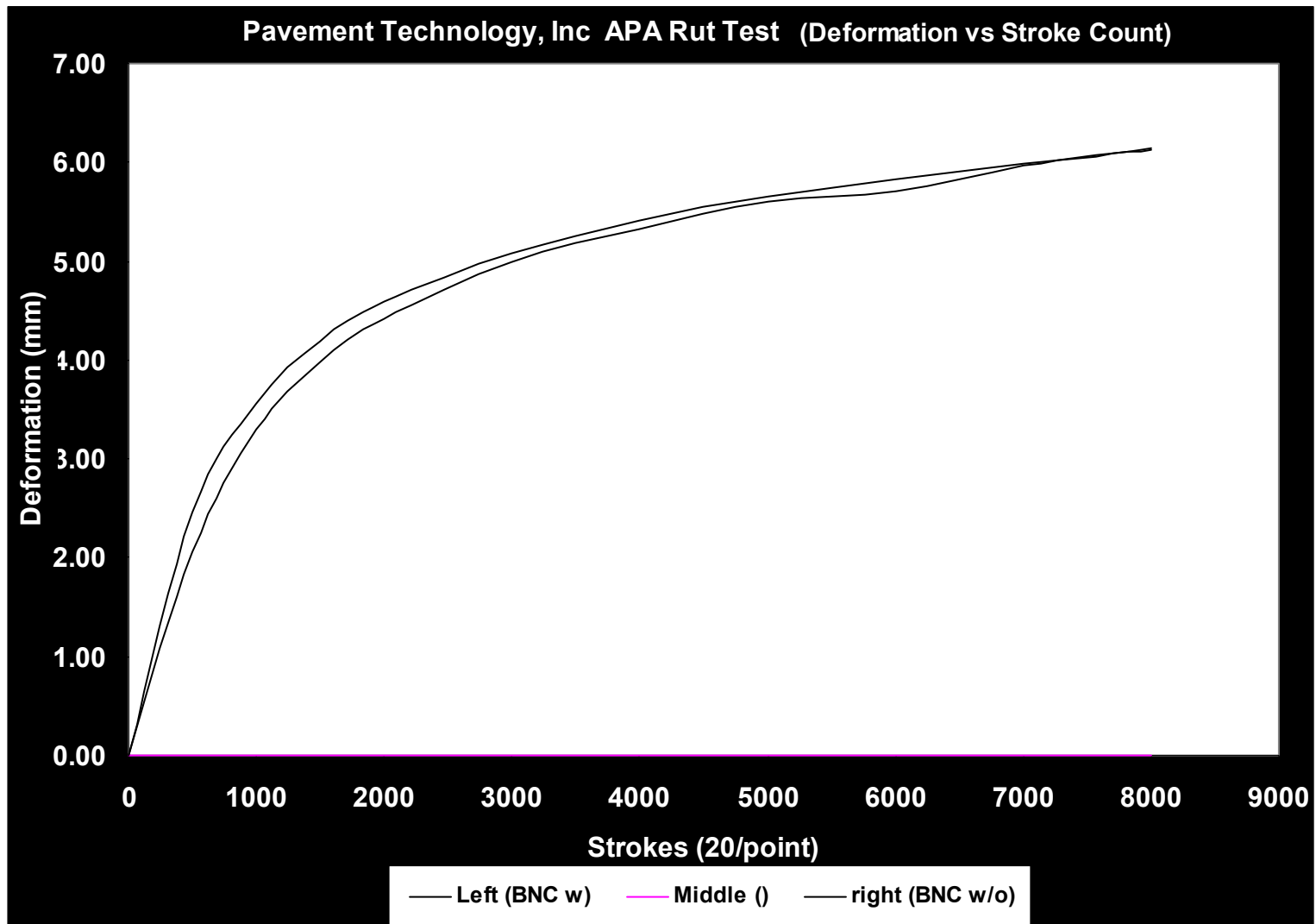
Rutting Test Data Sheet

Project No. : NC State Test No. : R1210-1 Temperature : -50 (deg. C)
 Mix ID No. : Buncombe Co. Test Date : 12/10/99 Wheel Load : 100 (lbs)
 Mix Type : Data File : R1210_1.ptd Hose Pressure : 100 (psi)
 Operator : Run Status: Complete Run Time 2:14:43 (hh:mm:ss)

Left Sample ID			Bulk S Gravity					% Air Void			
Stroke Count	Temperature		Depth Gauge Reading(mm)					Manual Average	Net Man Deflection	APA-DAS Average	Percent Change
	F	C	1	2	3	4	5				
0									0	0	
500										2.467	
1000										3.554	44.1
1500										4.181	17.6
2000										4.592	9.8
3000										5.081	10.7
4000										5.403	6.3
5000										5.653	4.6
6000										5.831	3.2
7000										5.981	2.6
8000										6.152	2.9
8001										6.152	0

Middle Sample ID			Bulk S Gravity					% Air Void			
Stroke Count	Temperature		Depth Gauge Reading(mm)					Manual Average	Net Man Deflection	APA-DAS Average	Percent Change
	F	C	1	2	3	4	5				
0									0	0	
500										0	
1000										0	
1500										0	
2000										0	
3000										0	
4000										0	
5000										0	
6000										0	
7000										0	
8000										0	
8001										0	

Right Sample ID BNC w/o			Bulk S Gravity					% Air Void			
Stroke Count	Temperature		Depth Gauge Reading(mm)					Manual Average	Net Man Deflection	APA-DAS Average	Percent Change
	F	C	1	2	3	4	5				
0									0	0	
500										2.065	
1000										3.294	59.5
1500										3.98	20.8
2000										4.418	11
3000										4.993	13
4000										5.317	6.5
5000										5.595	5.2
6000										5.715	2.1
7000										5.967	4.4
8000										6.128	2.7
8001										6.124	-0.1



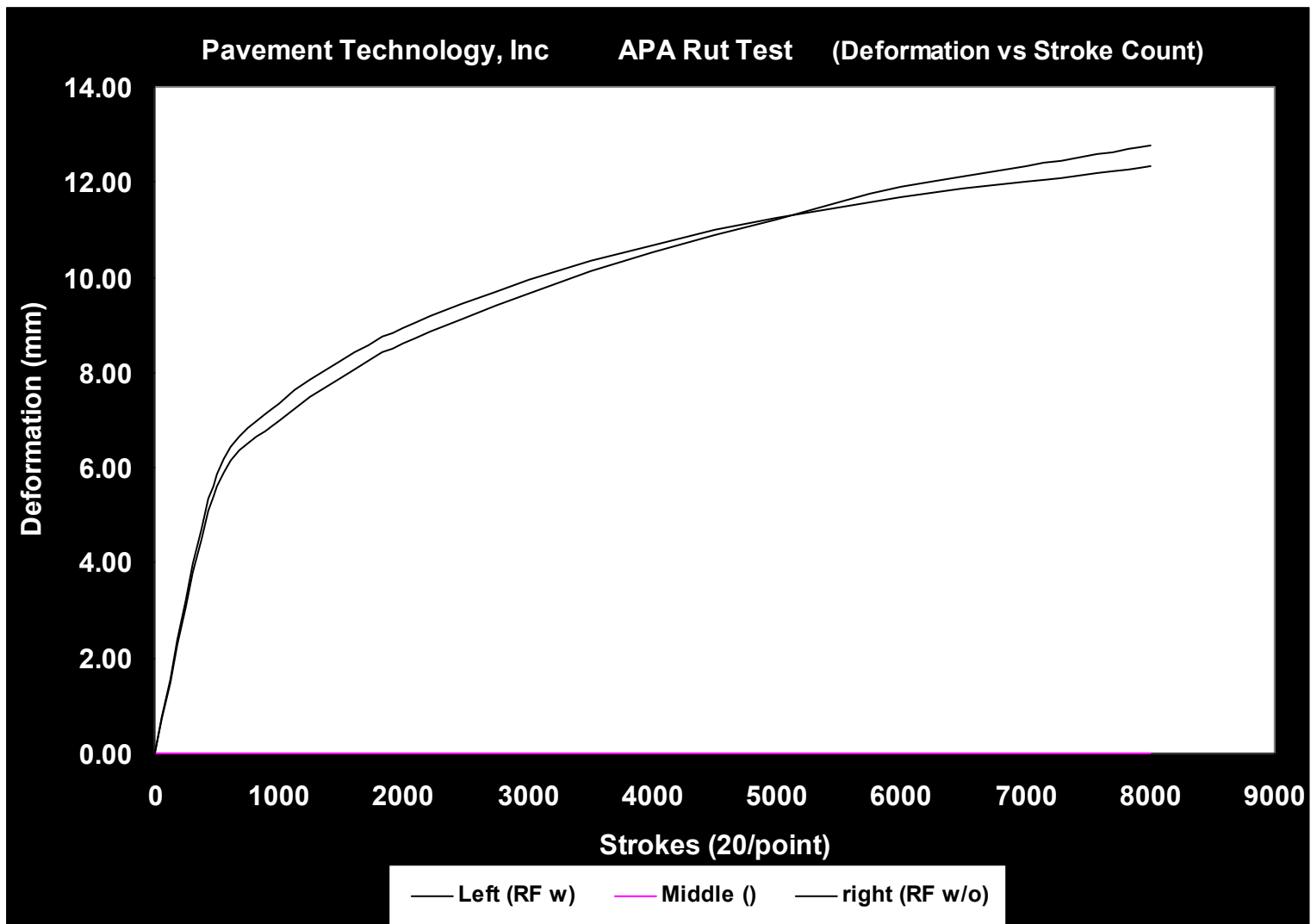
Rutting Test Data Sheet

Project No. : **NC State** Test No. : R1209-1 Temperature : **50** (deg. C)
 Mix ID No. : **Rutherford Co.** Test Date : 12/09/99 Wheel Load : **100** (lbs)
 Mix Type : Data File : R1209_1.ptd Hose Pressure : **400** (psi)
 Operator : Run Status: Complete Run Time **2:14:38** (hh:mm:ss)

Left Sample ID			Bulk S Gravity					% Air Void			
Stroke Count	Temperature		Depth Gauge Reading(mm)					Manual Average	Net Man Deflection	APA-DAS Average	Percent Change
	F	C	1	2	3	4	5				
0									0	0	
500										5.858	
1000										7.328	25.1
1500										8.237	12.4
2000										8.929	8.4
3000										9.953	11.5
4000										10.657	7.1
5000										11.246	5.5
6000										11.691	4
7000										12.01	2.7
8000										12.335	2.7
8001										12.335	0

Middle Sample ID			Bulk S Gravity					% Air Void			
Stroke Count	Temperature		Depth Gauge Reading(mm)					Manual Average	Net Man Deflection	APA-DAS Average	Percent Change
	F	C	1	2	3	4	5				
0									0	0	
500										0	
1000										0	
1500										0	
2000										0	
3000										0	
4000										0	
5000										0	
6000										0	
7000										0	
8000										0	
8001										0	

Right Sample ID BNC w/o			Bulk S Gravity					% Air Void			
Stroke Count	Temperature		Depth Gauge Reading(mm)					Manual Average	Net Man Deflection	APA-DAS Average	Percent Change
	F	C	1	2	3	4	5				
0									0	0	
500										5.616	
1000										6.982	24.3
1500										7.901	13.2
2000										8.602	8.9
3000										9.655	12.2
4000										10.513	8.9
5000										11.197	6.5
6000										11.891	6.2
7000										12.331	3.7
8000										12.782	3.7
8001										12.782	0



Appendix E

DSR Test Results

Table E- 1 |G*| and δ values for binders at 58 °C

Frequency (Hz)	Buncombe County				Rutherford County			
	Virgin		Aged		Virgin		Aged	
	G* (Pa)	δ (deg)	G* (Pa)	δ (deg)	G* (Pa)	δ (deg)	G* (Pa)	δ (deg)
1.00E-02	2.13E+01	8.94E+01	5.55E+01	8.93E+01	1.58E+01	8.91E+01	4.79E+01	8.93E+01
5.00E-02	1.06E+02	8.93E+01	2.74E+02	8.82E+01	7.84E+01	8.95E+01	2.35E+02	8.81E+01
1.00E-01	2.12E+02	8.90E+01	5.41E+02	8.72E+01	1.57E+02	8.91E+01	4.63E+02	8.71E+01
1.50E-01	3.16E+02	8.89E+01	8.03E+02	8.65E+01	2.34E+02	8.89E+01	6.86E+02	8.65E+01
5.00E-01	1.03E+03	8.76E+01	2.52E+03	8.42E+01	7.68E+02	8.77E+01	2.15E+03	8.41E+01
1.00E+00	2.00E+03	8.65E+01	4.80E+03	8.28E+01	1.50E+03	8.68E+01	4.10E+03	8.26E+01
1.59E+00	3.11E+03	8.58E+01	7.46E+03	8.16E+01	2.36E+03	8.61E+01	6.35E+03	8.16E+01
5.00E+00	9.22E+03	8.38E+01	2.04E+04	7.87E+01	6.96E+03	8.41E+01	1.73E+04	7.88E+01
1.00E+01	1.75E+04	8.23E+01	3.72E+04	7.69E+01	1.33E+04	8.26E+01	3.17E+04	7.71E+01
2.00E+01	3.30E+04	8.03E+01	6.70E+04	7.49E+01	2.49E+04	8.06E+01	5.64E+04	7.51E+01

Table E- 2 |G*| and δ values for binders at 64 °C

Frequency (Hz)	Buncombe County				Rutherford County			
	Virgin		Aged		Virgin		Aged	
	G* (Pa)	δ (deg)	G* (Pa)	δ (deg)	G* (Pa)	δ (deg)	G* (Pa)	δ (deg)
1.00E-02	9.10E+00	8.78E+01	2.28E+01	8.97E+01	6.96E+00	8.92E+01	1.94E+01	8.94E+01
5.00E-02	4.49E+01	8.93E+01	1.14E+02	8.92E+01	3.39E+01	8.94E+01	9.63E+01	8.91E+01
1.00E-01	9.00E+01	8.94E+01	2.26E+02	8.86E+01	6.78E+01	8.95E+01	1.93E+02	8.85E+01
1.50E-01	1.35E+02	8.92E+01	3.38E+02	8.82E+01	1.02E+02	8.93E+01	2.88E+02	8.80E+01
5.00E-01	4.46E+02	8.85E+01	1.09E+03	8.62E+01	3.35E+02	8.86E+01	9.27E+02	8.61E+01
1.00E+00	8.81E+02	8.78E+01	2.10E+03	8.50E+01	6.64E+02	8.80E+01	1.79E+03	8.49E+01
1.59E+00	1.35E+03	8.71E+01	3.29E+03	8.40E+01	1.05E+03	8.73E+01	2.77E+03	8.38E+01
5.00E+00	4.18E+03	8.53E+01	9.31E+03	8.14E+01	3.15E+03	8.53E+01	7.92E+03	8.13E+01
1.00E+01	8.02E+03	8.37E+01	1.74E+04	7.96E+01	6.08E+03	8.36E+01	1.48E+04	7.96E+01
2.00E+01	1.53E+04	8.15E+01	3.15E+04	7.74E+01	1.16E+04	8.08E+01	2.70E+04	7.77E+01

Table E- 3 |G*| and δ values for binders at 70 °C

Frequency (Hz)	Buncombe County				Rutherford County			
	Virgin		Aged		Virgin		Aged	
	G* (Pa)	δ (deg)	G* (Pa)	δ (deg)	G* (Pa)	δ (deg)	G* (Pa)	δ (deg)
1.00E-02	4.24E+00	8.85E+01	9.56E+00	8.93E+01	3.29E+00	8.89E+01	8.25E+00	8.94E+01
5.00E-02	2.05E+01	8.90E+01	4.72E+01	8.95E+01	1.65E+01	8.93E+01	4.02E+01	8.96E+01
1.00E-01	4.10E+01	8.92E+01	9.46E+01	8.93E+01	3.29E+01	8.95E+01	8.12E+01	8.93E+01
1.50E-01	6.17E+01	8.93E+01	1.41E+02	8.90E+01	4.95E+01	8.94E+01	1.21E+02	8.90E+01
5.00E-01	2.05E+02	8.90E+01	4.65E+02	8.77E+01	1.64E+02	8.91E+01	3.99E+02	8.77E+01
1.00E+00	4.09E+02	8.86E+01	9.13E+02	8.67E+01	3.28E+02	8.87E+01	7.82E+02	8.66E+01
1.59E+00	6.33E+02	8.80E+01	1.44E+03	8.57E+01	5.15E+02	8.82E+01	1.22E+03	8.57E+01
5.00E+00	1.98E+03	8.61E+01	4.20E+03	8.33E+01	1.58E+03	8.62E+01	3.59E+03	8.31E+01
1.00E+01	3.86E+03	8.43E+01	7.94E+03	8.14E+01	3.09E+03	8.45E+01	6.80E+03	8.11E+01
2.00E+01	7.49E+03	8.14E+01	1.48E+04	7.87E+01	5.94E+03	8.11E+01	1.27E+04	7.83E+01

Table E- 4 |G*| and δ values for baghouse mastics at 58 °C

Frequency (Hz)	Buncombe County				Rutherford County			
	Virgin		Aged		Virgin		Aged	
	G* (Pa)	δ (deg)	G* (Pa)	δ (deg)	G* (Pa)	δ (deg)	G* (Pa)	δ (deg)
1.00E-02	2.59E+02	7.95E+01	3.74E+02	8.26E+01	1.63E+02	8.13E+01	1.62E+02	8.20E+01
5.00E-02	1.05E+03	8.37E+01	1.57E+03	8.57E+01	6.14E+02	8.77E+01	5.95E+02	8.78E+01
1.00E-01	1.99E+03	8.51E+01	2.92E+03	8.64E+01	1.20E+03	8.77E+01	1.17E+03	8.78E+01
1.50E-01	2.87E+03	8.56E+01	4.29E+03	8.64E+01	1.80E+03	8.75E+01	1.75E+03	8.76E+01
5.00E-01	8.88E+03	8.64E+01	1.33E+04	8.58E+01	5.77E+03	8.61E+01	5.51E+03	8.56E+01
1.00E+00	1.70E+04	8.66E+01	2.52E+04	8.53E+01	1.13E+04	8.44E+01	1.07E+04	8.38E+01
1.59E+00	2.75E+04	8.66E+01	4.07E+04	8.47E+01	1.71E+04	8.29E+01	1.68E+04	8.26E+01
5.00E+00	7.47E+04	8.93E+01	1.08E+05	8.65E+01	5.11E+04	7.58E+01	4.89E+04	7.47E+01
1.00E+01	1.38E+05	8.28E+01	1.97E+05	8.84E+01	9.99E+04	6.68E+01	9.61E+04	6.48E+01
2.00E+01	**	**	3.71E+05	7.82E+01	2.09E+05	5.33E+01	2.03E+05	5.24E+01

Table E- 5 |G*| and δ values for baghouse mastics at 64 °C

Frequency (Hz)	Buncombe County				Rutherford County			
	Virgin		Aged		Virgin		Aged	
	G* (Pa)	δ (deg)	G* (Pa)	δ (deg)	G* (Pa)	δ (deg)	G* (Pa)	δ (deg)
1.00E-02	1.19E+02	7.69E+01	1.35E+02	8.30E+01	8.68E+01	7.80E+01	8.08E+01	7.81E+01
5.00E-02	4.41E+02	8.03E+01	5.95E+02	8.62E+01	2.72E+02	8.65E+01	2.64E+02	8.69E+01
1.00E-01	8.19E+02	8.22E+01	1.18E+03	8.67E+01	5.16E+02	8.78E+01	4.99E+02	8.78E+01
1.50E-01	1.21E+03	8.38E+01	1.75E+03	8.72E+01	7.65E+02	8.77E+01	7.43E+02	8.76E+01
5.00E-01	3.67E+03	8.68E+01	5.53E+03	8.79E+01	2.48E+03	8.61E+01	2.42E+03	8.59E+01
1.00E+00	6.67E+03	8.92E+01	1.05E+04	8.84E+01	4.86E+03	8.35E+01	4.74E+03	8.37E+01
1.59E+00	1.05E+04	8.73E+01	1.68E+04	8.91E+01	7.59E+03	8.16E+01	7.45E+03	8.13E+01
5.00E+00	3.16E+04	7.43E+01	4.78E+04	8.34E+01	2.40E+04	7.10E+01	2.31E+04	7.08E+01
1.00E+01	6.65E+04	5.77E+01	9.27E+04	7.22E+01	5.20E+04	5.43E+01	4.94E+04	5.48E+01
2.00E+01	1.79E+05	3.56E+01	2.00E+05	5.34E+01	1.29E+05	3.89E+01	1.27E+05	3.67E+01

Table E- 6 |G*| and δ values for baghouse mastics at 70 °C

Frequency (Hz)	Buncombe County				Rutherford County			
	Virgin		Aged		Virgin		Aged	
	G* (Pa)	δ (deg)	G* (Pa)	δ (deg)	G* (Pa)	δ (deg)	G* (Pa)	δ (deg)
1.00E-02	5.58E+01	7.27E+01	1.02E+02	7.22E+01	4.33E+01	7.30E+01	4.42E+01	7.23E+01
5.00E-02	1.75E+02	7.91E+01	3.62E+02	7.75E+01	1.36E+02	8.28E+01	1.30E+02	8.43E+01
1.00E-01	3.15E+02	8.11E+01	6.55E+02	7.93E+01	2.31E+02	8.66E+01	2.25E+02	8.68E+01
1.50E-01	4.67E+02	8.28E+01	1.00E+03	8.13E+01	3.38E+02	8.71E+01	3.28E+02	8.70E+01
5.00E-01	1.47E+03	8.82E+01	2.75E+03	8.52E+01	1.10E+03	8.49E+01	1.07E+03	8.45E+01
1.00E+00	2.78E+03	8.57E+01	4.74E+03	8.83E+01	2.20E+03	8.08E+01	2.12E+03	8.08E+01
1.59E+00	5.23E+03	8.23E+01	8.13E+03	8.72E+01	3.31E+03	7.66E+01	3.22E+03	7.73E+01
5.00E+00	1.57E+04	5.25E+01	2.29E+04	6.84E+01	1.25E+04	5.37E+01	1.17E+04	6.05E+01
1.00E+01	4.72E+04	3.06E+01	5.37E+04	4.91E+01	3.38E+04	3.39E+01	2.98E+04	4.23E+01
2.00E+01	1.39E+05	1.80E+01	1.76E+05	2.54E+01	1.13E+05	1.84E+01	1.06E+05	1.93E+01

** Values discarded

Table E- 7 |G*| and δ values for P#200 mastics at 58 °C

Frequency (Hz)	Buncombe County				Rutherford County			
	Virgin		Aged		Virgin		Aged	
	G* (Pa)	δ (deg)	G* (Pa)	δ (deg)	G* (Pa)	δ (deg)	G* (Pa)	δ (deg)
1.00E-02	1.79E+02	7.95E+01	2.81E+02	8.04E+01	4.26E+03	8.43E+01	1.14E+02	8.63E+01
5.00E-02	6.28E+02	8.68E+01	9.57E+02	8.69E+01	5.96E+04	8.82E+01	5.03E+02	8.85E+01
1.00E-01	1.23E+03	8.74E+01	1.86E+03	8.68E+01	1.72E+04	8.82E+01	9.88E+02	8.78E+01
1.50E-01	1.83E+03	8.73E+01	2.75E+03	8.66E+01	1.00E+03	8.76E+01	1.46E+03	8.74E+01
5.00E-01	5.88E+03	8.62E+01	8.70E+03	8.52E+01	3.23E+03	8.58E+01	4.67E+03	8.54E+01
1.00E+00	1.15E+04	8.47E+01	1.69E+04	8.38E+01	6.36E+03	8.41E+01	9.03E+03	8.34E+01
1.59E+00	1.76E+04	8.35E+01	2.64E+04	8.25E+01	1.01E+06	7.85E+01	1.43E+04	8.23E+01
5.00E+00	5.32E+04	7.72E+01	7.47E+04	7.66E+01	3.02E+04	7.34E+01	4.15E+04	7.27E+01
1.00E+01	1.03E+05	6.82E+01	1.41E+05	7.00E+01	2.06E+07	5.11E+01	8.23E+04	6.65E+01
2.00E+01	2.13E+05	5.58E+01	2.81E+05	5.88E+01	8.87E+07	3.47E+01	1.87E+05	4.67E+01

Table E- 8 |G*| and δ values for P#200 mastics at 64 °C

Frequency (Hz)	Buncombe County				Rutherford County			
	Virgin		Aged		Virgin		Aged	
	G* (Pa)	δ (deg)	G* (Pa)	δ (deg)	G* (Pa)	δ (deg)	G* (Pa)	δ (deg)
1.00E-02	9.04E+01	7.59E+01	1.35E+02	7.83E+01	3.73E+01	8.14E+01	5.87E+01	8.35E+01
5.00E-02	2.82E+02	8.60E+01	4.26E+02	8.65E+01	1.46E+02	8.66E+01	2.31E+02	8.81E+01
1.00E-01	5.29E+02	8.74E+01	8.18E+02	8.72E+01	2.81E+02	8.79E+01	4.44E+02	8.82E+01
1.50E-01	7.82E+02	8.73E+01	1.21E+03	8.71E+01	4.20E+02	8.77E+01	6.60E+02	8.80E+01
5.00E-01	2.53E+03	8.61E+01	3.92E+03	8.59E+01	1.37E+03	8.54E+01	2.15E+03	8.56E+01
1.00E+00	5.01E+03	8.42E+01	7.66E+03	8.44E+01	2.76E+03	8.25E+01	4.16E+03	8.25E+01
1.59E+00	7.78E+03	8.19E+01	1.20E+04	8.30E+01	4.17E+03	7.96E+01	6.75E+03	8.19E+01
5.00E+00	2.45E+04	6.96E+01	3.55E+04	7.47E+01	1.44E+04	6.17E+01	2.07E+04	7.13E+01
1.00E+01	5.32E+04	5.47E+01	7.02E+04	6.31E+01	3.59E+04	4.19E+01	4.61E+04	5.15E+01
2.00E+01	1.41E+05	3.64E+01	1.47E+05	5.45E+01	1.15E+05	2.22E+01	1.21E+05	3.37E+01

Table E- 9 |G*| and δ values for P#200 mastics at 70 °C

Frequency (Hz)	Buncombe County				Rutherford County			
	Virgin		Aged		Virgin		Aged	
	G* (Pa)	δ (deg)	G* (Pa)	δ (deg)	G* (Pa)	δ (deg)	G* (Pa)	δ (deg)
1.00E-02	4.82E+01	7.01E+01	6.44E+01	7.39E+01	2.09E+01	8.23E+01	3.56E+01	8.23E+01
5.00E-02	1.46E+02	8.24E+01	2.08E+02	8.44E+01	7.33E+01	8.54E+01	1.29E+02	8.77E+01
1.00E-01	2.49E+02	8.63E+01	3.76E+02	8.68E+01	1.27E+02	8.72E+01	2.47E+02	8.82E+01
1.50E-01	3.62E+02	8.66E+01	5.57E+02	8.70E+01	1.85E+02	8.70E+01	3.61E+02	8.80E+01
5.00E-01	1.18E+03	8.49E+01	1.79E+03	8.54E+01	6.13E+02	8.27E+01	1.18E+03	8.50E+01
1.00E+00	2.36E+03	8.24E+01	3.57E+03	8.31E+01	1.25E+03	7.64E+01	2.36E+03	8.12E+01
1.59E+00	3.72E+03	8.19E+01	5.60E+03	7.98E+01	1.51E+03	6.78E+01	3.59E+03	7.61E+01
5.00E+00	1.25E+04	6.29E+01	1.79E+04	6.37E+01	8.29E+03	4.53E+01	1.31E+04	5.58E+01
1.00E+01	3.53E+04	3.50E+01	4.16E+04	4.71E+01	2.92E+04	2.18E+01	3.11E+04	4.17E+01
2.00E+01	1.13E+05	2.00E+01	1.29E+05	2.30E+01	1.00E+05	1.14E+01	1.02E+05	2.18E+01

Table E- 10 $|G^*|\sin \delta$ values for Buncombe County materials, 58 °C

Frequency (Hz)	Binder		Baghouse Mastic		P#200 Mastic	
	Virgin	Aged	Virgin	Aged	Virgin	Aged
1.00E-02	2.13E+01	5.55E+01	2.54E+02	3.71E+02	1.76E+02	2.77E+02
5.00E-02	1.06E+02	2.74E+02	1.05E+03	1.56E+03	6.27E+02	9.56E+02
1.00E-01	2.12E+02	5.41E+02	1.98E+03	2.92E+03	1.22E+03	1.86E+03
1.50E-01	3.16E+02	8.01E+02	2.86E+03	4.28E+03	1.83E+03	2.74E+03
5.00E-01	1.03E+03	2.51E+03	8.86E+03	1.33E+04	5.86E+03	8.67E+03
1.00E+00	2.00E+03	4.76E+03	1.69E+04	2.51E+04	1.14E+04	1.68E+04
1.59E+00	3.10E+03	7.38E+03	2.75E+04	4.05E+04	1.75E+04	2.62E+04
5.00E+00	9.17E+03	2.00E+04	7.47E+04	1.08E+05	5.19E+04	7.26E+04
1.00E+01	1.74E+04	3.62E+04	1.37E+05	1.97E+05	9.60E+04	1.33E+05
2.00E+01	3.25E+04	6.47E+04	**	3.63E+05	1.76E+05	2.40E+05
Average	6.58E+03	1.37E+04	3.01E+04	7.56E+04	3.63E+04	5.03E+04

Table E- 11 $|G^*|\sin \delta$ values for Buncombe County materials, 64 °C

Frequency (Hz)	Binder		Baghouse Mastic		P#200 Mastic	
	Virgin	Aged	Virgin	Aged	Virgin	Aged
1.00E-02	9.10E+00	2.28E+01	1.16E+02	1.34E+02	8.77E+01	1.33E+02
5.00E-02	4.49E+01	1.14E+02	4.34E+02	5.94E+02	2.81E+02	4.25E+02
1.00E-01	9.00E+01	2.26E+02	8.12E+02	1.18E+03	5.29E+02	8.17E+02
1.50E-01	1.35E+02	3.37E+02	1.20E+03	1.75E+03	7.82E+02	1.21E+03
5.00E-01	4.46E+02	1.08E+03	3.66E+03	5.53E+03	2.53E+03	3.91E+03
1.00E+00	8.80E+02	2.09E+03	6.67E+03	1.05E+04	4.98E+03	7.63E+03
1.59E+00	1.35E+03	3.27E+03	1.05E+04	1.68E+04	7.71E+03	1.19E+04
5.00E+00	4.16E+03	9.20E+03	3.04E+04	4.75E+04	2.30E+04	3.42E+04
1.00E+01	7.97E+03	1.71E+04	5.62E+04	8.83E+04	4.34E+04	6.26E+04
2.00E+01	1.51E+04	3.08E+04	1.04E+05	1.61E+05	8.39E+04	1.20E+05
Average	3.02E+03	6.42E+03	2.14E+04	3.33E+04	1.67E+04	2.43E+04

Table E- 12 $|G^*|\sin \delta$ values for Buncombe County materials, 70 °C

Frequency (Hz)	Binder		Baghouse Mastic		P#200 Mastic	
	Virgin	Aged	Virgin	Aged	Virgin	Aged
1.00E-02	4.24E+00	9.56E+00	5.33E+01	9.68E+01	4.53E+01	6.19E+01
5.00E-02	2.05E+01	4.72E+01	1.72E+02	3.53E+02	1.45E+02	2.07E+02
1.00E-01	4.10E+01	9.46E+01	3.11E+02	6.43E+02	2.49E+02	3.76E+02
1.50E-01	6.17E+01	1.41E+02	4.63E+02	9.92E+02	3.61E+02	5.56E+02
5.00E-01	2.05E+02	4.64E+02	1.47E+03	2.74E+03	1.18E+03	1.78E+03
1.00E+00	4.09E+02	9.11E+02	2.77E+03	4.74E+03	2.34E+03	3.54E+03
1.59E+00	6.33E+02	1.43E+03	5.18E+03	8.12E+03	3.69E+03	5.51E+03
5.00E+00	1.98E+03	4.17E+03	1.25E+04	2.13E+04	1.12E+04	1.61E+04
1.00E+01	3.84E+03	7.85E+03	2.40E+04	4.06E+04	2.03E+04	3.05E+04
2.00E+01	7.40E+03	1.45E+04	4.29E+04	7.55E+04	3.87E+04	5.06E+04
Average	1.46E+03	2.96E+03	8.97E+03	1.55E+04	7.81E+03	1.09E+04

Table E- 13 |G*|/sin δ values for Buncombe County materials, 58 °C

Frequency (Hz)	Binder		Baghouse Mastic		P#200 Mastic	
	Virgin	Aged	Virgin	Aged	Virgin	Aged
1.00E-02	2.13E+01	5.55E+01	2.63E+02	3.77E+02	1.82E+02	2.85E+02
5.00E-02	1.06E+02	2.74E+02	1.06E+03	1.57E+03	6.29E+02	9.59E+02
1.00E-01	2.12E+02	5.42E+02	1.99E+03	2.93E+03	1.23E+03	1.86E+03
1.50E-01	3.16E+02	8.04E+02	2.88E+03	4.30E+03	1.83E+03	2.75E+03
5.00E-01	1.03E+03	2.53E+03	8.90E+03	1.33E+04	5.89E+03	8.73E+03
1.00E+00	2.01E+03	4.84E+03	1.70E+04	2.53E+04	1.15E+04	1.70E+04
1.59E+00	3.12E+03	7.54E+03	2.76E+04	4.08E+04	1.78E+04	2.67E+04
5.00E+00	9.28E+03	2.08E+04	7.47E+04	1.08E+05	5.46E+04	7.68E+04
1.00E+01	1.77E+04	3.82E+04	1.39E+05	1.97E+05	1.11E+05	1.50E+05
2.00E+01	3.34E+04	6.94E+04	**	3.79E+05	2.58E+05	3.28E+05
Average	6.72E+03	1.45E+04	3.04E+04	7.73E+04	4.63E+04	6.14E+04

Table E- 14 |G*|/sin δ values for Buncombe County materials, 64 °C

Frequency (Hz)	Binder		Baghouse Mastic		P#200 Mastic	
	Virgin	Aged	Virgin	Aged	Virgin	Aged
1.00E-02	9.11E+00	2.28E+01	1.23E+02	1.36E+02	9.32E+01	1.38E+02
5.00E-02	4.49E+01	1.14E+02	4.47E+02	5.97E+02	2.83E+02	4.27E+02
1.00E-01	9.00E+01	2.26E+02	8.27E+02	1.18E+03	5.30E+02	8.19E+02
1.50E-01	1.35E+02	3.37E+02	1.22E+03	1.75E+03	7.83E+02	1.21E+03
5.00E-01	4.46E+02	1.08E+03	3.67E+03	5.54E+03	2.54E+03	3.93E+03
1.00E+00	8.82E+02	2.09E+03	6.67E+03	1.05E+04	5.03E+03	7.70E+03
1.59E+00	1.35E+03	3.27E+03	1.06E+04	1.68E+04	7.86E+03	1.21E+04
5.00E+00	4.19E+03	9.20E+03	3.28E+04	4.81E+04	2.62E+04	3.68E+04
1.00E+01	8.06E+03	1.71E+04	7.87E+04	9.74E+04	6.51E+04	7.87E+04
2.00E+01	1.54E+04	3.08E+04	3.07E+05	2.50E+05	2.38E+05	1.81E+05
Average	3.06E+03	6.42E+03	4.42E+04	4.32E+04	3.46E+04	3.23E+04

Table E- 15 |G*|/sin δ values for Buncombe County materials, 70 °C

Frequency (Hz)	Binder		Baghouse Mastic		P#200 Mastic	
	Virgin	Aged	Virgin	Aged	Virgin	Aged
1.00E-02	4.24E+00	9.56E+00	5.84E+01	1.07E+02	5.13E+01	6.71E+01
5.00E-02	2.05E+01	4.72E+01	1.78E+02	3.71E+02	1.48E+02	2.09E+02
1.00E-01	4.10E+01	9.46E+01	3.19E+02	6.67E+02	2.50E+02	3.77E+02
1.50E-01	6.17E+01	1.42E+02	4.70E+02	1.01E+03	3.62E+02	5.57E+02
5.00E-01	2.05E+02	4.65E+02	1.47E+03	2.76E+03	1.19E+03	1.79E+03
1.00E+00	4.09E+02	9.14E+02	2.79E+03	4.74E+03	2.38E+03	3.59E+03
1.59E+00	6.34E+02	1.44E+03	5.28E+03	8.14E+03	3.76E+03	5.69E+03
5.00E+00	1.99E+03	4.23E+03	1.98E+04	2.47E+04	1.41E+04	2.00E+04
1.00E+01	3.88E+03	8.03E+03	9.27E+04	7.10E+04	6.16E+04	5.68E+04
2.00E+01	7.57E+03	1.51E+04	4.50E+05	4.11E+05	3.31E+05	3.31E+05
Average	1.48E+03	3.05E+03	5.73E+04	5.25E+04	4.14E+04	4.20E+04

Table E- 16 $|G^*|\cos \delta$ values for Buncombe County materials, 58 °C

Frequency (Hz)	Binder		Baghouse Mastic		P#200 Mastic	
	Virgin	Aged	Virgin	Aged	Virgin	Aged
1.00E-02	2.26E-01	6.48E-01	4.72E+01	4.81E+01	3.24E+01	4.66E+01
5.00E-02	1.31E+00	8.63E+00	1.15E+02	1.17E+02	3.47E+01	5.23E+01
1.00E-01	3.56E+00	2.63E+01	1.69E+02	1.85E+02	5.64E+01	1.02E+02
1.50E-01	6.31E+00	4.84E+01	2.18E+02	2.71E+02	8.54E+01	1.61E+02
5.00E-01	4.36E+01	2.54E+02	5.57E+02	9.76E+02	3.90E+02	7.23E+02
1.00E+00	1.21E+02	6.05E+02	1.01E+03	2.08E+03	1.06E+03	1.81E+03
1.59E+00	2.27E+02	1.09E+03	1.65E+03	3.75E+03	2.00E+03	3.46E+03
5.00E+00	9.92E+02	3.99E+03	8.53E+02	6.62E+03	1.18E+04	1.73E+04
1.00E+01	2.35E+03	8.43E+03	1.74E+04	5.50E+03	3.83E+04	4.83E+04
2.00E+01	5.56E+03	1.75E+04	**	7.60E+04	1.20E+05	1.46E+05
Average	9.31E+02	3.19E+03	2.44E+03	9.55E+03	1.74E+04	2.17E+04

Table E- 17 $|G^*|\cos \delta$ values for Buncombe County materials, 64 °C

Frequency (Hz)	Binder		Baghouse Mastic		P#200 Mastic	
	Virgin	Aged	Virgin	Aged	Virgin	Aged
1.00E-02	3.48E-01	1.33E-01	2.71E+01	1.64E+01	2.21E+01	2.74E+01
5.00E-02	5.27E-01	1.57E+00	7.40E+01	3.93E+01	1.97E+01	2.57E+01
1.00E-01	9.81E-01	5.37E+00	1.12E+02	6.83E+01	2.38E+01	3.93E+01
1.50E-01	1.80E+00	1.05E+01	1.31E+02	8.45E+01	3.67E+01	6.15E+01
5.00E-01	1.18E+01	7.16E+01	2.06E+02	2.06E+02	1.71E+02	2.79E+02
1.00E+00	3.31E+01	1.82E+02	9.28E+01	2.89E+02	5.07E+02	7.48E+02
1.59E+00	6.72E+01	3.45E+02	4.90E+02	2.74E+02	1.10E+03	1.46E+03
5.00E+00	3.46E+02	1.40E+03	8.54E+03	5.50E+03	8.56E+03	9.35E+03
1.00E+01	8.76E+02	3.14E+03	3.56E+04	2.84E+04	3.07E+04	3.18E+04
2.00E+01	2.25E+03	6.89E+03	1.45E+05	1.20E+05	1.14E+05	8.56E+04
Average	3.59E+02	1.20E+03	1.90E+04	1.54E+04	1.55E+04	1.29E+04

Table E- 18 $|G^*|\cos \delta$ values for Buncombe County materials, 70 °C

Frequency (Hz)	Binder		Baghouse Mastic		P#200 Mastic	
	Virgin	Aged	Virgin	Aged	Virgin	Aged
1.00E-02	1.08E-01	1.18E-01	1.66E+01	3.12E+01	1.64E+01	1.79E+01
5.00E-02	3.40E-01	4.02E-01	3.30E+01	7.81E+01	1.94E+01	2.02E+01
1.00E-01	5.40E-01	1.19E+00	4.88E+01	1.22E+02	1.63E+01	2.08E+01
1.50E-01	7.81E-01	2.45E+00	5.85E+01	1.51E+02	2.12E+01	2.93E+01
5.00E-01	3.46E+00	1.83E+01	4.62E+01	2.32E+02	1.04E+02	1.43E+02
1.00E+00	9.91E+00	5.31E+01	2.06E+02	1.41E+02	3.11E+02	4.31E+02
1.59E+00	2.22E+01	1.06E+02	7.02E+02	3.98E+02	5.23E+02	9.95E+02
5.00E+00	1.35E+02	4.93E+02	9.56E+03	8.45E+03	5.71E+03	7.94E+03
1.00E+01	3.85E+02	1.19E+03	4.06E+04	3.51E+04	2.89E+04	2.83E+04
2.00E+01	1.12E+03	2.90E+03	1.32E+05	1.59E+05	1.06E+05	1.19E+05
Average	1.68E+02	4.77E+02	1.83E+04	2.04E+04	1.42E+04	1.57E+04

Table E- 19 |G*|sin δ values for Rutherford County materials, 58 °C

Frequency (Hz)	Binder		Baghouse Mastic		P#200 Mastic	
	Virgin	Aged	Virgin	Aged	Virgin	Aged
1.00E-02	1.58E+01	4.79E+01	1.61E+02	1.61E+02	***	1.14E+02
5.00E-02	7.84E+01	2.35E+02	6.13E+02	5.94E+02	***	5.03E+02
1.00E-01	1.57E+02	4.62E+02	1.20E+03	1.17E+03	***	9.87E+02
1.50E-01	2.34E+02	6.85E+02	1.79E+03	1.75E+03	***	1.46E+03
5.00E-01	7.67E+02	2.14E+03	5.76E+03	5.50E+03	***	4.65E+03
1.00E+00	1.50E+03	4.07E+03	1.12E+04	1.07E+04	***	8.97E+03
1.59E+00	2.36E+03	6.28E+03	1.70E+04	1.66E+04	***	1.41E+04
5.00E+00	6.92E+03	1.70E+04	4.96E+04	4.72E+04	***	3.96E+04
1.00E+01	1.32E+04	3.09E+04	9.18E+04	8.69E+04	***	7.54E+04
2.00E+01	2.45E+04	5.44E+04	1.67E+05	1.61E+05	***	1.36E+05
Average	4.97E+03	1.16E+04	3.46E+04	3.31E+04	***	2.82E+04

Table E- 20 |G*|sin δ values for Rutherford County materials, 64 °C

Frequency (Hz)	Binder		Baghouse Mastic		P#200 Mastic	
	Virgin	Aged	Virgin	Aged	Virgin	Aged
1.00E-02	6.96E+00	1.94E+01	8.49E+01	7.91E+01	3.69E+01	5.83E+01
5.00E-02	3.38E+01	9.63E+01	2.71E+02	2.63E+02	1.46E+02	2.31E+02
1.00E-01	6.78E+01	1.93E+02	5.15E+02	4.99E+02	2.81E+02	4.44E+02
1.50E-01	1.02E+02	2.88E+02	7.65E+02	7.43E+02	4.20E+02	6.60E+02
5.00E-01	3.35E+02	9.25E+02	2.47E+03	2.41E+03	1.36E+03	2.15E+03
1.00E+00	6.63E+02	1.78E+03	4.83E+03	4.71E+03	2.73E+03	4.12E+03
1.59E+00	1.05E+03	2.76E+03	7.51E+03	7.36E+03	4.10E+03	6.68E+03
5.00E+00	3.14E+03	7.83E+03	2.27E+04	2.18E+04	1.27E+04	1.96E+04
1.00E+01	6.04E+03	1.45E+04	4.22E+04	4.04E+04	2.40E+04	3.61E+04
2.00E+01	1.15E+04	2.64E+04	8.08E+04	7.59E+04	4.34E+04	6.70E+04
Average	2.29E+03	5.48E+03	1.62E+04	1.54E+04	8.91E+03	1.37E+04

Table E- 21 |G*|sin δ values for Rutherford County materials, 70 °C

Frequency (Hz)	Binder		Baghouse Mastic		P#200 Mastic	
	Virgin	Aged	Virgin	Aged	Virgin	Aged
1.00E-02	3.29E+00	8.24E+00	4.14E+01	4.21E+01	2.07E+01	3.52E+01
5.00E-02	1.65E+01	4.02E+01	1.35E+02	1.29E+02	7.30E+01	1.29E+02
1.00E-01	3.29E+01	8.11E+01	2.30E+02	2.24E+02	1.27E+02	2.47E+02
1.50E-01	4.95E+01	1.21E+02	3.37E+02	3.27E+02	1.85E+02	3.60E+02
5.00E-01	1.64E+02	3.98E+02	1.10E+03	1.07E+03	6.08E+02	1.17E+03
1.00E+00	3.27E+02	7.81E+02	2.17E+03	2.09E+03	1.21E+03	2.33E+03
1.59E+00	5.15E+02	1.22E+03	3.22E+03	3.14E+03	1.39E+03	3.48E+03
5.00E+00	1.58E+03	3.56E+03	1.01E+04	1.01E+04	5.89E+03	1.09E+04
1.00E+01	3.07E+03	6.72E+03	1.89E+04	2.00E+04	1.09E+04	2.07E+04
2.00E+01	5.87E+03	1.24E+04	3.57E+04	3.50E+04	1.98E+04	3.78E+04
Average	1.16E+03	2.54E+03	7.19E+03	7.23E+03	4.02E+03	7.71E+03

Table E- 22 $|G^*|/\sin \delta$ values for Rutherford County materials, 58 °C

Frequency (Hz)	Binder		Baghouse Mastic		P#200 Mastic	
	Virgin	Aged	Virgin	Aged	Virgin	Aged
1.00E-02	1.58E+01	4.79E+01	1.65E+02	1.64E+02	***	1.14E+02
5.00E-02	7.84E+01	2.35E+02	6.14E+02	5.95E+02	***	5.03E+02
1.00E-01	1.57E+02	4.64E+02	1.21E+03	1.17E+03	***	9.88E+02
1.50E-01	2.34E+02	6.88E+02	1.80E+03	1.75E+03	***	1.47E+03
5.00E-01	7.68E+02	2.17E+03	5.79E+03	5.53E+03	***	4.68E+03
1.00E+00	1.51E+03	4.13E+03	1.13E+04	1.08E+04	***	9.09E+03
1.59E+00	2.37E+03	6.42E+03	1.73E+04	1.69E+04	***	1.44E+04
5.00E+00	6.99E+03	1.77E+04	5.27E+04	5.07E+04	***	4.35E+04
1.00E+01	1.34E+04	3.25E+04	1.09E+05	1.06E+05	***	8.97E+04
2.00E+01	2.52E+04	5.83E+04	2.60E+05	2.56E+05	***	2.57E+05
Average	5.07E+03	1.23E+04	4.60E+04	4.50E+04	***	4.21E+04

Table E- 23 $|G^*|/\sin \delta$ values for Rutherford County materials, 64 °C

Frequency (Hz)	Binder		Baghouse Mastic		P#200 Mastic	
	Virgin	Aged	Virgin	Aged	Virgin	Aged
1.00E-02	6.96E+00	1.94E+01	8.87E+01	8.26E+01	3.77E+01	5.91E+01
5.00E-02	3.39E+01	9.63E+01	2.72E+02	2.64E+02	1.47E+02	2.32E+02
1.00E-01	6.78E+01	1.93E+02	5.16E+02	4.99E+02	2.81E+02	4.44E+02
1.50E-01	1.02E+02	2.88E+02	7.66E+02	7.44E+02	4.21E+02	6.60E+02
5.00E-01	3.35E+02	9.29E+02	2.48E+03	2.42E+03	1.37E+03	2.16E+03
1.00E+00	6.64E+02	1.80E+03	4.89E+03	4.77E+03	2.78E+03	4.19E+03
1.59E+00	1.05E+03	2.79E+03	7.67E+03	7.53E+03	4.24E+03	6.81E+03
5.00E+00	3.16E+03	8.02E+03	2.54E+04	2.44E+04	1.63E+04	2.19E+04
1.00E+01	6.11E+03	1.50E+04	6.40E+04	6.04E+04	5.38E+04	5.90E+04
2.00E+01	1.18E+04	2.77E+04	2.05E+05	2.12E+05	3.03E+05	2.18E+05
Average	2.33E+03	5.68E+03	3.11E+04	3.13E+04	3.83E+04	3.14E+04

Table E- 24 $|G^*|/\sin \delta$ values for Rutherford County materials, 70 °C

Frequency (Hz)	Binder		Baghouse Mastic		P#200 Mastic	
	Virgin	Aged	Virgin	Aged	Virgin	Aged
1.00E-02	3.29E+00	8.25E+00	4.53E+01	4.64E+01	2.11E+01	3.59E+01
5.00E-02	1.65E+01	4.02E+01	1.37E+02	1.30E+02	7.35E+01	1.29E+02
1.00E-01	3.29E+01	8.12E+01	2.31E+02	2.25E+02	1.27E+02	2.47E+02
1.50E-01	4.95E+01	1.21E+02	3.38E+02	3.28E+02	1.86E+02	3.61E+02
5.00E-01	1.64E+02	3.99E+02	1.11E+03	1.08E+03	6.18E+02	1.18E+03
1.00E+00	3.28E+02	7.84E+02	2.23E+03	2.15E+03	1.28E+03	2.38E+03
1.59E+00	5.15E+02	1.22E+03	3.41E+03	3.30E+03	1.63E+03	3.70E+03
5.00E+00	1.59E+03	3.62E+03	1.56E+04	1.34E+04	1.16E+04	1.59E+04
1.00E+01	3.10E+03	6.88E+03	6.07E+04	4.43E+04	7.85E+04	4.68E+04
2.00E+01	6.02E+03	1.30E+04	3.59E+05	3.22E+05	5.09E+05	2.73E+05
Average	1.18E+03	2.61E+03	4.42E+04	3.87E+04	6.03E+04	3.44E+04

Table E- 25 |G*|cos δ values for Rutherford County materials, 58 °C

Frequency (Hz)	Binder		Baghouse Mastic		P#200 Mastic	
	Virgin	Aged	Virgin	Aged	Virgin	Aged
1.00E-02	2.62E-01	6.17E-01	2.47E+01	2.26E+01	***	7.31E+00
5.00E-02	6.74E-01	7.60E+00	2.50E+01	2.30E+01	***	1.33E+01
1.00E-01	2.43E+00	2.33E+01	4.73E+01	4.55E+01	***	3.78E+01
1.50E-01	4.62E+00	4.23E+01	7.72E+01	7.22E+01	***	6.73E+01
5.00E-01	3.04E+01	2.20E+02	3.97E+02	4.21E+02	***	3.75E+02
1.00E+00	8.49E+01	5.27E+02	1.10E+03	1.15E+03	***	1.04E+03
1.59E+00	1.61E+02	9.31E+02	2.10E+03	2.16E+03	***	1.92E+03
5.00E+00	7.18E+02	3.36E+03	1.25E+04	1.29E+04	***	1.23E+04
1.00E+01	1.70E+03	7.07E+03	3.93E+04	4.10E+04	***	3.29E+04
2.00E+01	4.06E+03	1.45E+04	1.25E+05	1.24E+05	***	1.28E+05
Average	6.76E+02	2.67E+03	1.80E+04	1.82E+04	***	1.77E+04

Table E- 26 |G*|cos δ values for Rutherford County materials, 64 °C

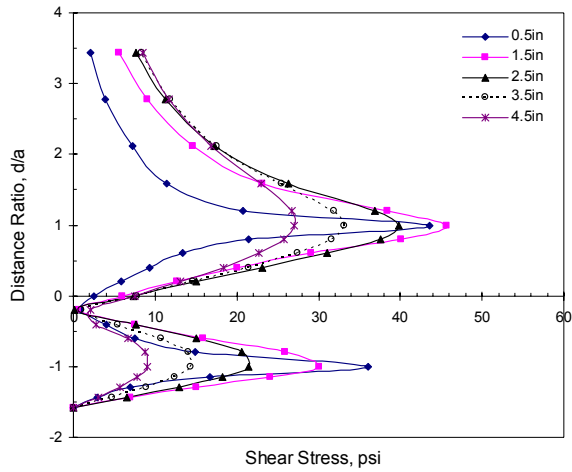
Frequency (Hz)	Binder		Baghouse Mastic		P#200 Mastic	
	Virgin	Aged	Virgin	Aged	Virgin	Aged
1.00E-02	9.46E-02	1.92E-01	1.81E+01	1.67E+01	5.59E+00	6.64E+00
5.00E-02	3.31E-01	1.53E+00	1.66E+01	1.42E+01	8.65E+00	7.70E+00
1.00E-01	5.89E-01	5.08E+00	2.00E+01	1.88E+01	1.02E+01	1.40E+01
1.50E-01	1.29E+00	1.02E+01	3.13E+01	3.08E+01	1.69E+01	2.32E+01
5.00E-01	8.32E+00	6.24E+01	1.69E+02	1.73E+02	1.10E+02	1.65E+02
1.00E+00	2.32E+01	1.60E+02	5.48E+02	5.24E+02	3.59E+02	5.46E+02
1.59E+00	4.96E+01	2.99E+02	1.10E+03	1.12E+03	7.56E+02	9.47E+02
5.00E+00	2.60E+02	1.20E+03	7.84E+03	7.58E+03	6.81E+03	6.65E+03
1.00E+01	6.78E+02	2.66E+03	3.03E+04	2.85E+04	2.67E+04	2.87E+04
2.00E+01	1.85E+03	5.78E+03	1.00E+05	1.02E+05	1.06E+05	1.01E+05
Average	2.87E+02	1.02E+03	1.40E+04	1.40E+04	1.41E+04	1.38E+04

Table E- 27 |G*|cos δ values for Rutherford County materials, 70 °C

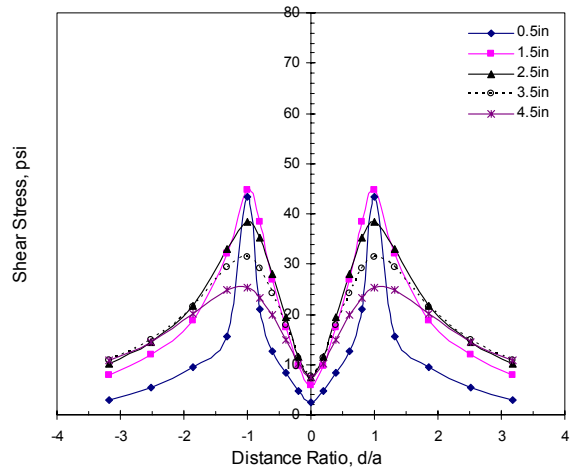
Frequency (Hz)	Binder		Baghouse Mastic		P#200 Mastic	
	Virgin	Aged	Virgin	Aged	Virgin	Aged
1.00E-02	6.13E-02	8.51E-02	1.26E+01	1.34E+01	2.78E+00	4.73E+00
5.00E-02	2.08E-01	3.10E-01	1.70E+01	1.29E+01	5.89E+00	5.07E+00
1.00E-01	2.73E-01	1.01E+00	1.39E+01	1.24E+01	6.17E+00	7.62E+00
1.50E-01	5.18E-01	2.12E+00	1.73E+01	1.73E+01	9.72E+00	1.23E+01
5.00E-01	2.46E+00	1.60E+01	9.88E+01	1.03E+02	7.80E+01	1.03E+02
1.00E+00	7.19E+00	4.69E+01	3.52E+02	3.40E+02	2.94E+02	3.59E+02
1.59E+00	1.65E+01	9.14E+01	7.69E+02	7.07E+02	5.69E+02	8.63E+02
5.00E+00	1.04E+02	4.32E+02	7.42E+03	5.74E+03	5.82E+03	7.39E+03
1.00E+01	2.93E+02	1.05E+03	2.81E+04	2.20E+04	2.71E+04	2.32E+04
2.00E+01	9.25E+02	2.58E+03	1.07E+05	1.00E+05	9.83E+04	9.43E+04
Average	1.35E+02	4.22E+02	1.44E+04	1.29E+04	1.32E+04	1.26E+04

Appendix F

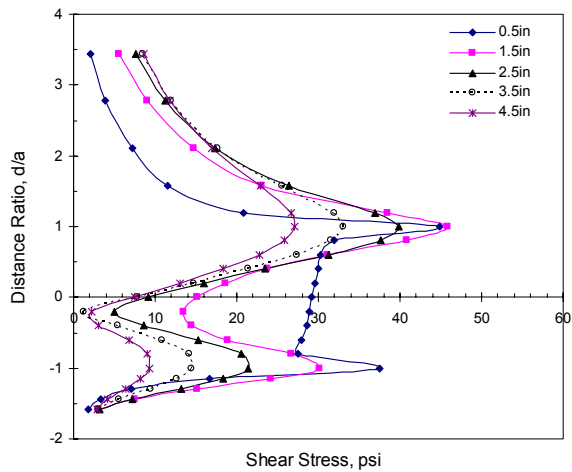
Mobilized Interfacial Shear Stresses



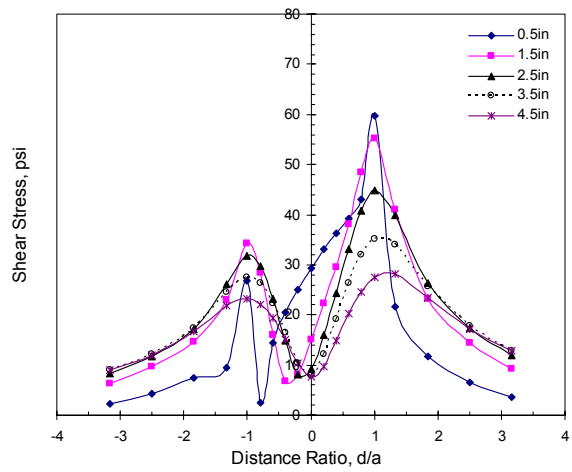
(a) Shear distribution along axle for vertical load with zero horizontal shear



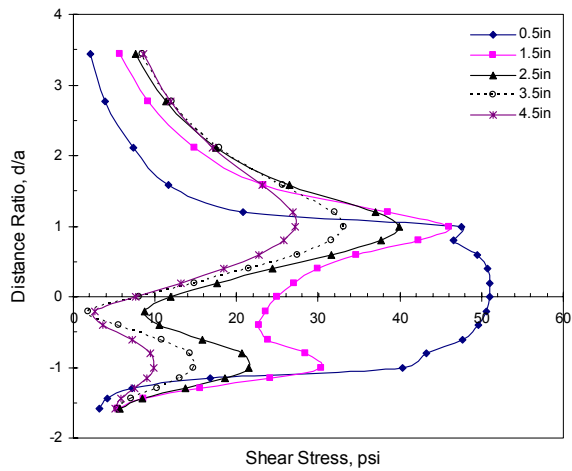
(b) Shear distribution perpendicular to axle for vertical load with zero horizontal shear



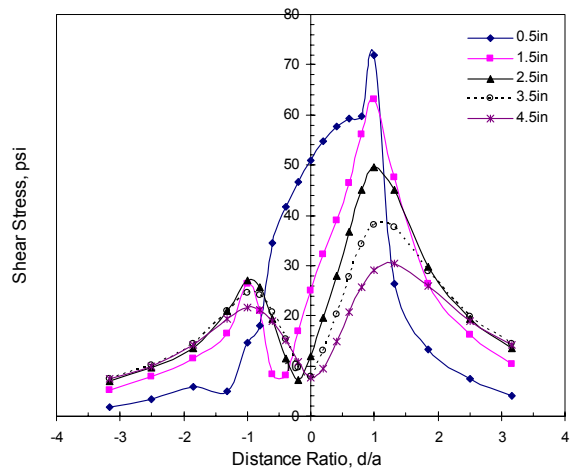
(c) Shear distribution along axle for vertical load with 40% horizontal shear



(d) Shear distribution perpendicular to axle for vertical load with 40% horizontal shear

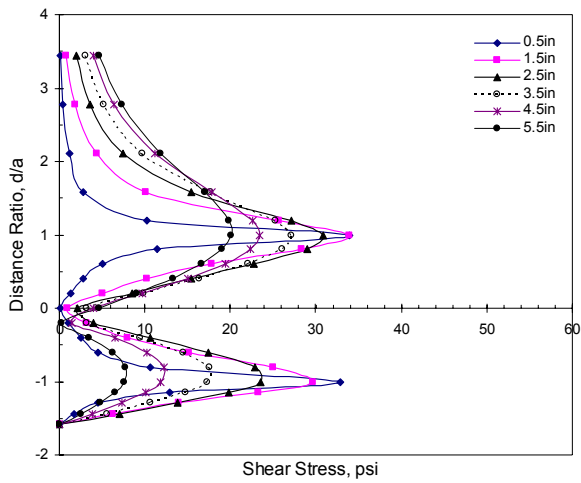


(e) Shear distribution along axle for vertical load with 70% horizontal shear

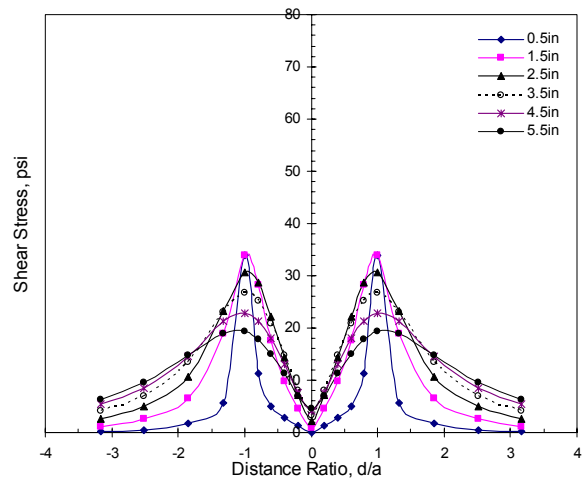


(f) Shear distribution perpendicular to axle for vertical load with 70% horizontal shear

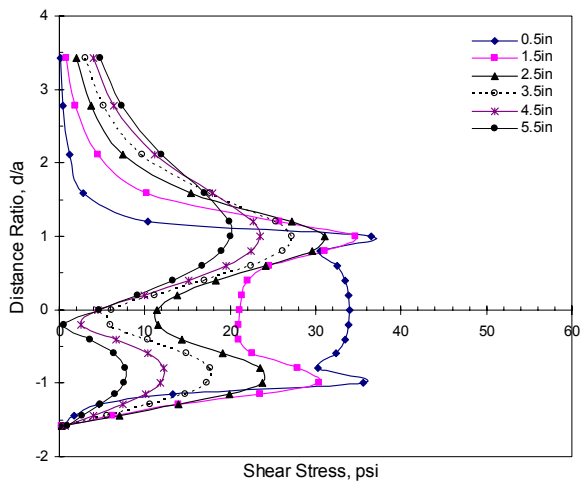
Figure F-1(a-f) Mobilized interfacial shear stresses for AC-AC combination at 20 °C



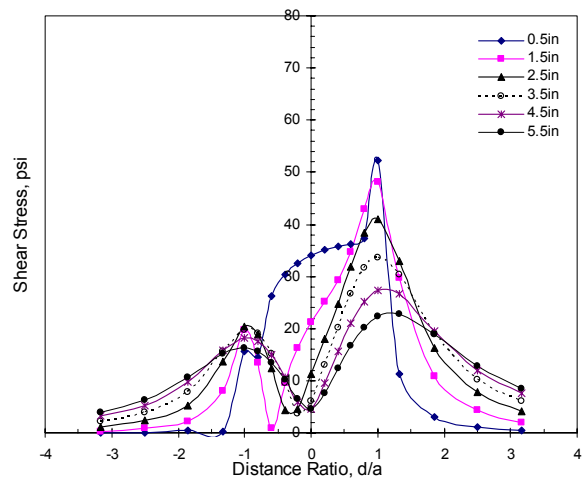
(a) Shear distribution along axle for vertical load with zero horizontal shear



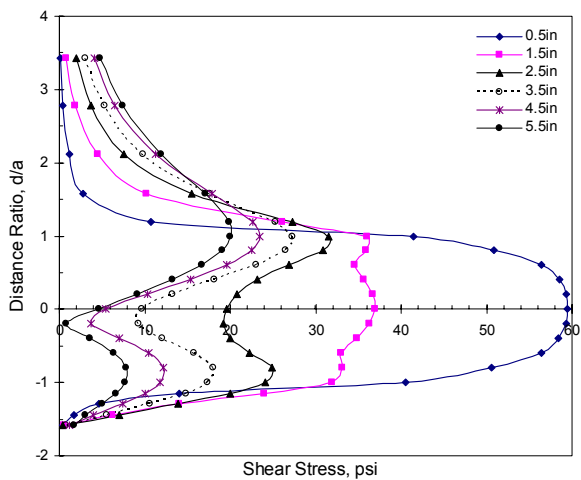
(b) Shear distribution perpendicular to axle for vertical load with zero horizontal shear



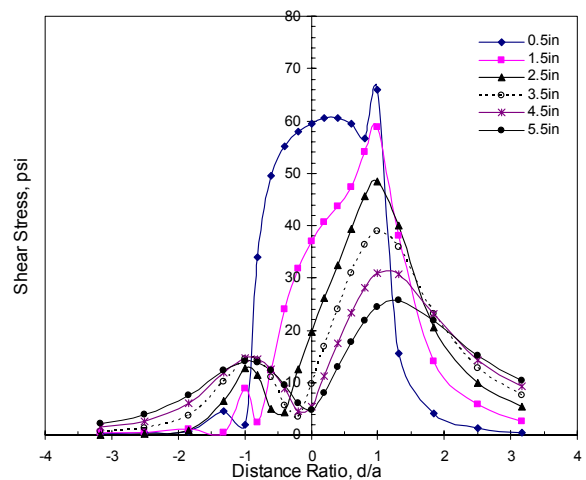
(c) Shear distribution along axle for vertical load with 40% horizontal shear



(d) Shear distribution perpendicular to axle for vertical load with 40% horizontal shear

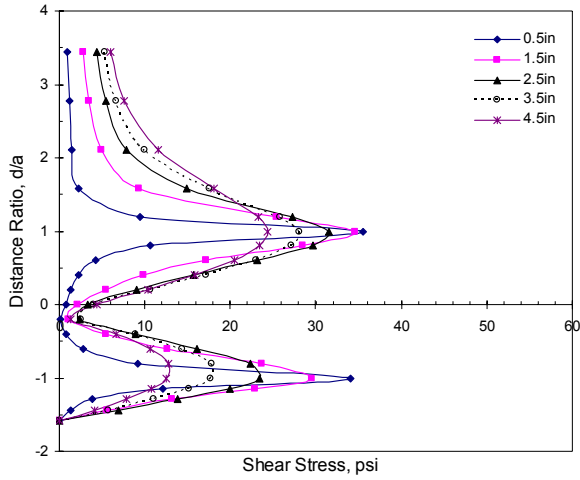


(e) Shear distribution along axle for vertical load with 70% horizontal shear

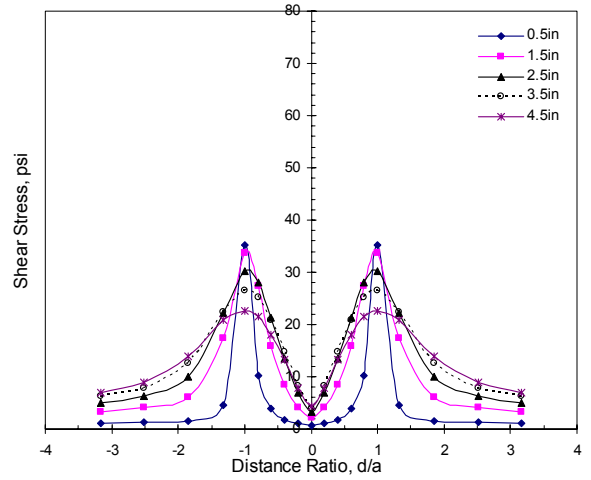


(f) Shear distribution perpendicular to axle for vertical load with 70% horizontal shear

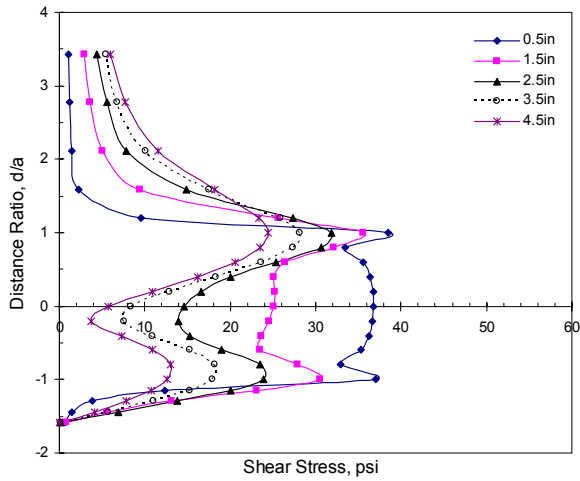
Figure F-2(a-f) Mobilized interfacial shear stresses for AC-AC, high temp.



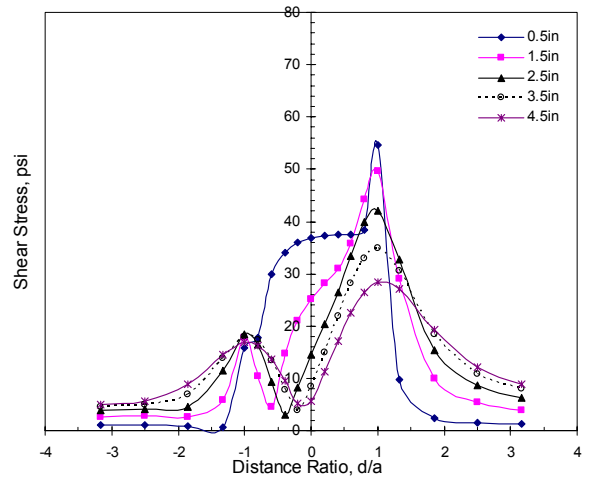
(a) Shear distribution along axle for vertical load with zero horizontal shear



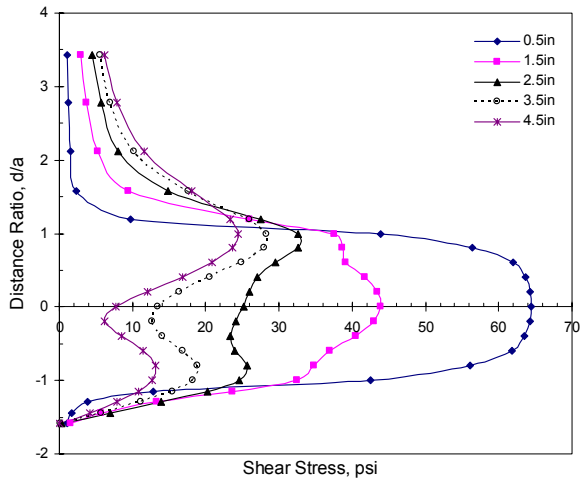
(b) Shear distribution perpendicular to axle for vertical load with zero horizontal shear



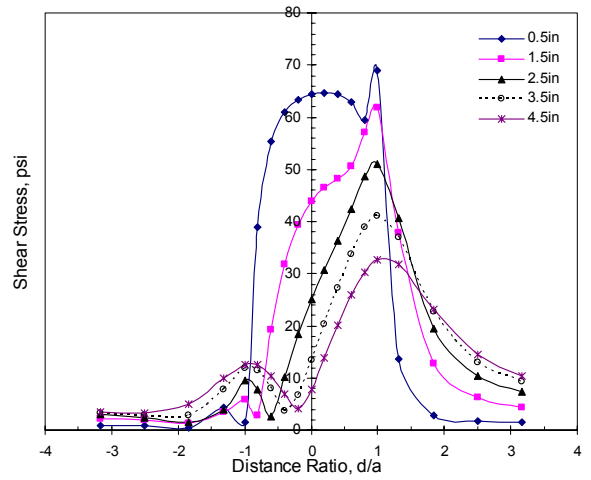
(c) Shear distribution along axle for vertical load with 40% horizontal shear



(d) Shear distribution perpendicular to axle for vertical load with 40% horizontal shear

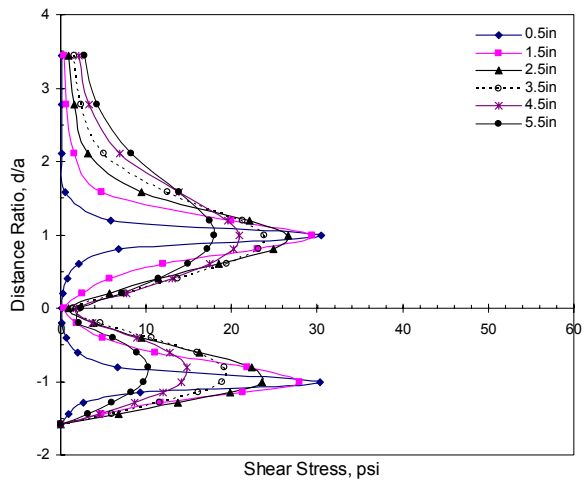


(e) Shear distribution along axle for vertical load with 70% horizontal shear

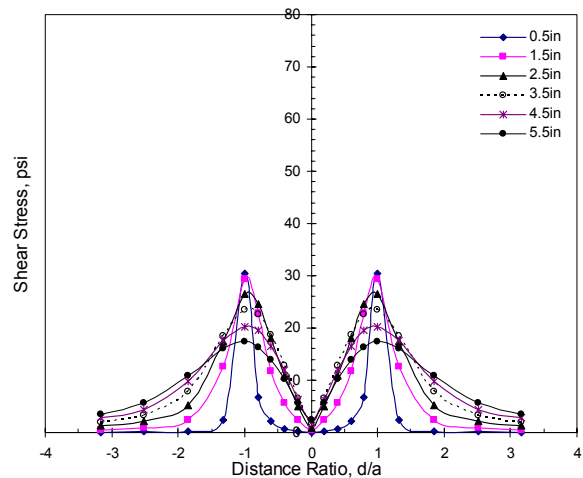


(f) Shear distribution perpendicular to axle for vertical load with 70% horizontal shear

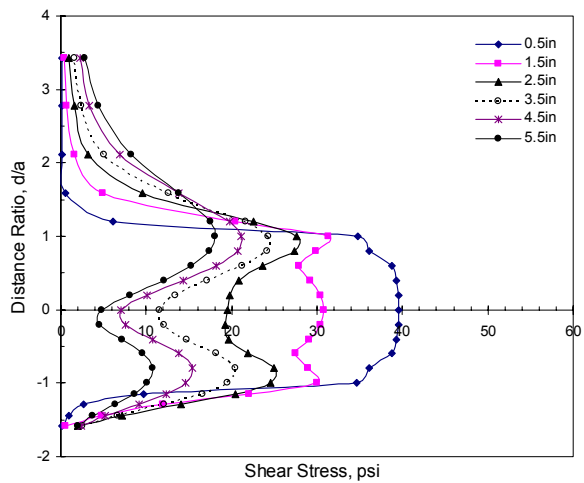
Figure F-3(a-f) Mobilized interfacial shear stresses for PCC-AC, 20 °C



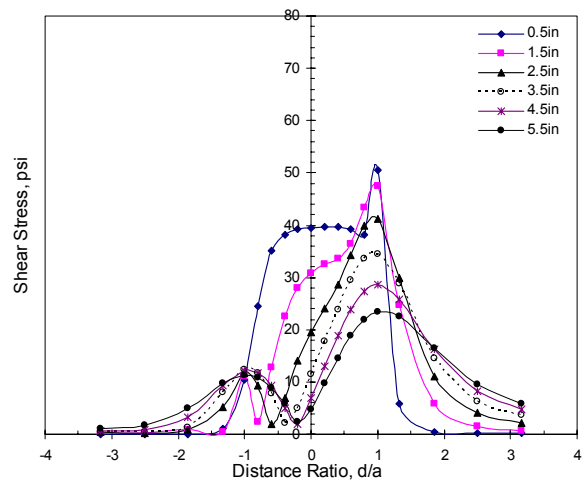
(a) Shear distribution along axle for vertical load with zero horizontal shear



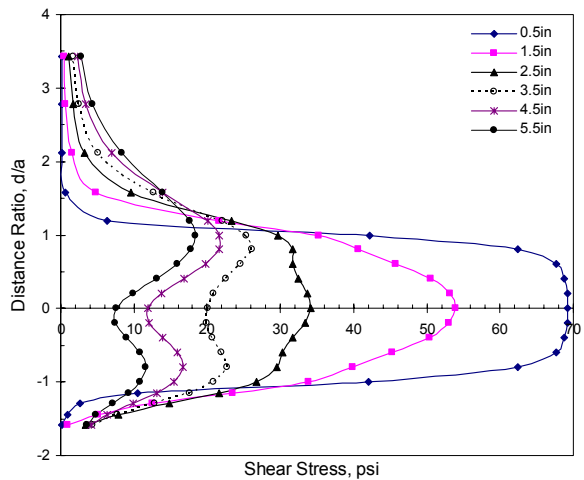
(b) Shear distribution perpendicular to axle for vertical load with zero horizontal shear



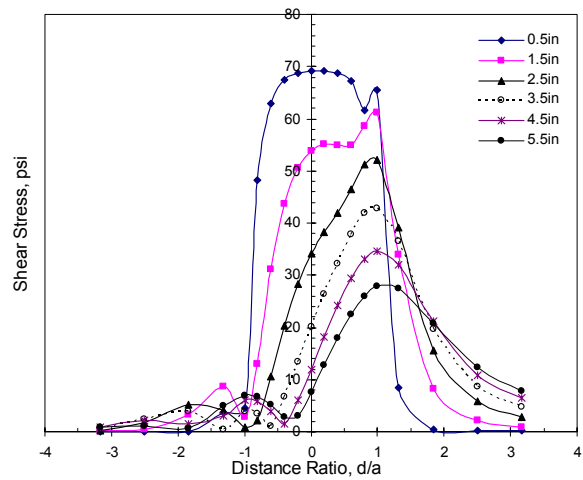
(c) Shear distribution along axle for vertical load with 40% horizontal shear



(d) Shear distribution perpendicular to axle for vertical load with 40% horizontal shear

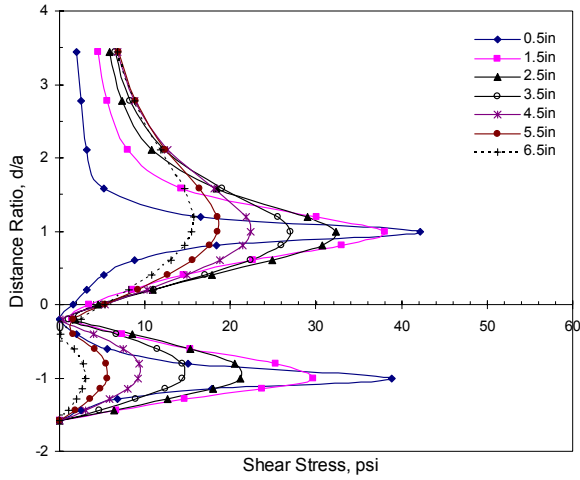


(e) Shear distribution along axle for vertical load with 70% horizontal shear

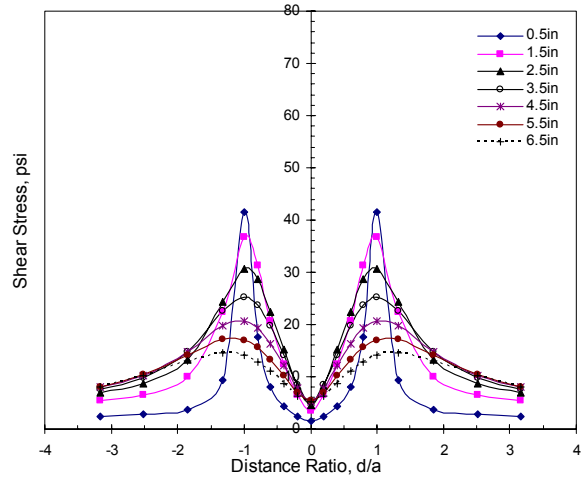


(f) Shear distribution perpendicular to axle for vertical load with 70% horizontal shear

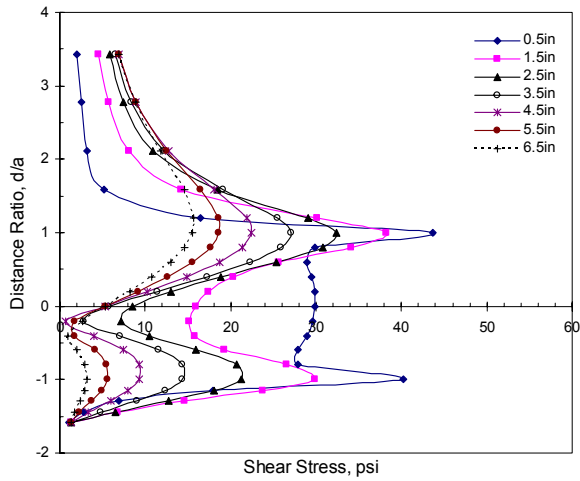
Figure F-4 (a-f) Mobilized interfacial shear stresses for PCC-AC, high temp.



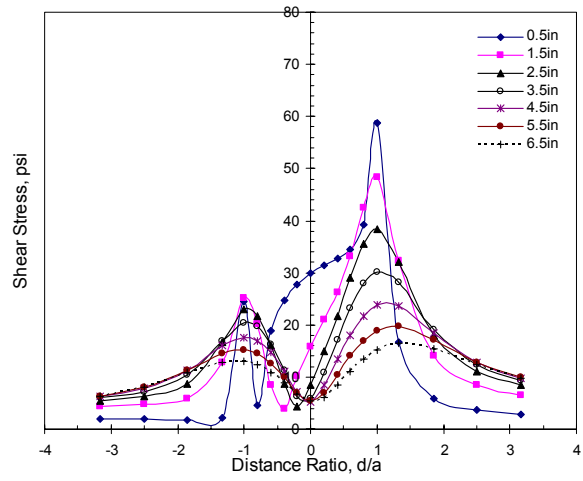
(a) Shear distribution along axle for vertical load with zero horizontal shear



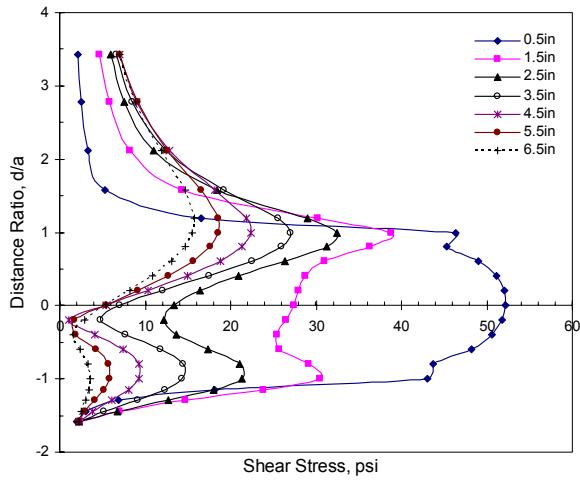
(b) Shear distribution perpendicular to axle for vertical load with zero horizontal shear



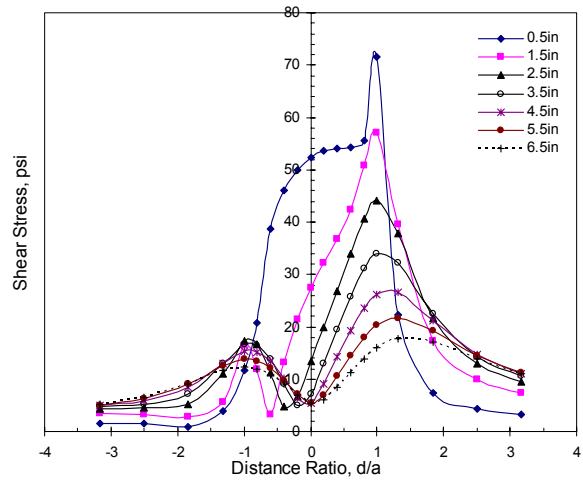
(c) Shear distribution along axle for vertical load with 40% horizontal shear



(d) Shear distribution perpendicular to axle for vertical load with 40% horizontal shear

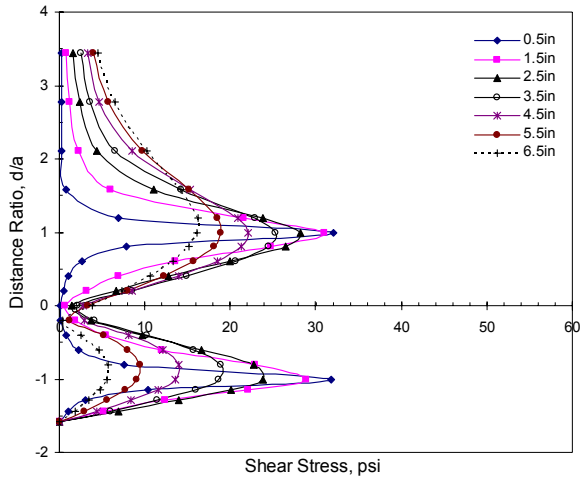


(e) Shear distribution along axle for vertical load with 70% horizontal shear

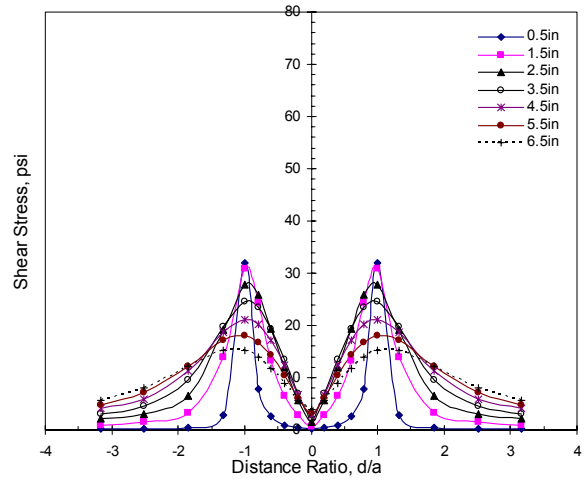


(f) Shear distribution perpendicular to axle for vertical load with 70% horizontal shear

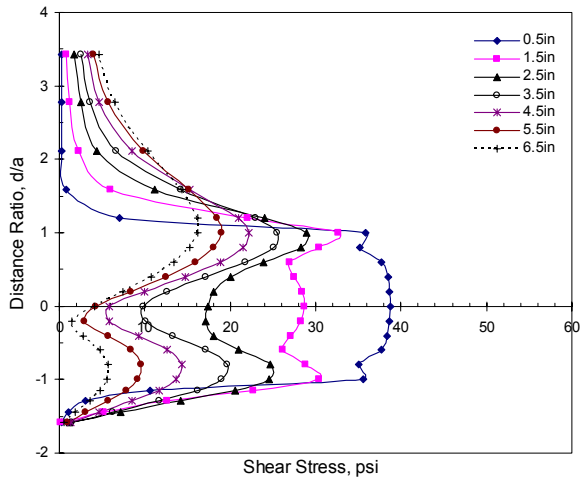
Figure F-5(a-f) Mobilized interfacial shear stresses for CTB-AC, 20 °C



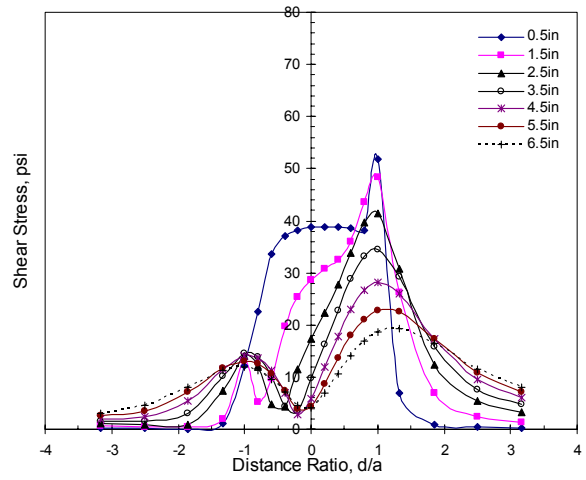
(a) Shear distribution along axle for vertical load with zero horizontal shear



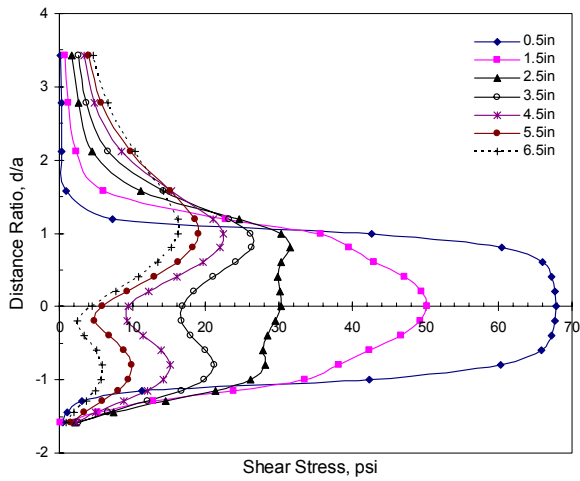
(b) Shear distribution perpendicular to axle for vertical load with zero horizontal shear



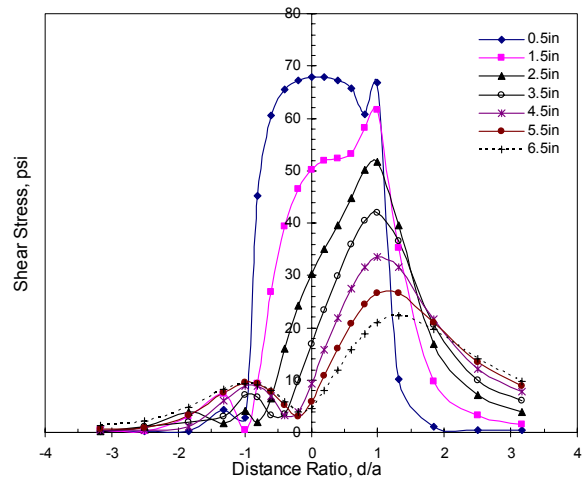
(c) Shear distribution along axle for vertical load with 40% horizontal shear



(d) Shear distribution perpendicular to axle for vertical load with 40% horizontal shear



(e) Shear distribution along axle for vertical load with 70% horizontal shear



(f) Shear distribution perpendicular to axle for vertical load with 70% horizontal shear

Figure F-6(a-f) Mobilized interfacial shear stresses for CTB-AC, high temp.